# Investigating the expression and function of aldehyde dehydrogenases in prostate cancer

Probing the expression and function of ALDHs using chemical probes, drugs and siRNA

**Maria SADIQ**

Submitted for the Degree of Doctor of Philosophy

Faculty of Life Sciences

University of Bradford

2017

## Abstract

Maria Sadiq

**Title:** Investigating the expression and function of aldehyde dehydrogenases in prostate cancer

**Sub-title:** Probing the expression and function of ALDHs using chemical probes, drugs and siRNA



**Keywords:** Aldehyde dehydrogenase (ALDH), ALDH1A3, ALDH7A1, prostate cancer, hypoxia, epigenetics, ALDH inhibitor, drug resistance, retinoic acid, cancer stem cells



Castration-resistant prostate cancer (CRPC) remains an aggressive incurable disease in men mainly due to treatment resistance. Current treatments do not effectively eradicate cancer stem cells (CSCs), which play a pivotal role in tumour maintenance, progression and drug resistance. Aldehyde dehydrogenases (ALDHs) have been used in some tumour types as CSC markers. Their high expression and high functional activity found in CSCs is also associated with drug resistance. Emerging evidence suggests deregulation of certain ALDH isoforms have implications in cancer. The role of ALDHs in prostate cancer as potential biomarkers and therapeutic targets has not been fully explored yet. Accordingly, this study investigated the expression, regulation and function of selected ALDH isoforms in prostate cancer.

This study showed that ALDH1A3, ALDH1B1, ALDH2 and ALDH7A1 are highly expressed in primary prostate cancer cells (n=9) compared to benign (n=9) prostate cells. The expression of ALDH1A3 was high in the stem cells (SCs) (n=3) as well as the more differentiated counterparts (n=16). Treatment of both benign and malignant primary prostate cancer cells with all-*trans* retinoic acid (atRA) also resulted in increased expression of ALDH1A3 and ALDH3A1, supporting a feedback loop between atRA and ALDHs. Furthermore, SerBob, Bob and LNCaP cells were sensitive to treatment with epigenetic drugs and led to significantly higher expression of ALDH1A2, ALDH3A1 and ALDH7A1 respectively.

Importantly, siRNA suppression of ALDH1A3 and ALDH7A1 led to reduced SC properties of primary prostate cultures including reduced cell viability, migration and colony formation, and increased differentiation of transit amplifying (TA) cells to committed basal (CB) cells. Novel ALDH-affinic probes showed reduced cell viability of primary prostate epithelial cultures as a single agent and also when used in combination with docetaxel. The results indicate the potential of using ALDH-affinic compounds as single agents for therapeutic intervention or in combination with docetaxel to sensitise resistant cells to this anticancer drug.

The data in this thesis provides novel findings, which supports ALDH1A2, -1A3 and -7A1 as potential biomarkers and/or therapeutic targets for drug intervention. Although, a study analysing a larger number of samples is necessary to fully understand ALDH isoform expression in CSC, TA and CB

cells it is envisaged that an ALDH-targeted therapy have potential in future treatment strategies for prostate cancer.

## Acknowledgements

I would like to begin with truly thanking God for giving me the opportunity and strength to complete this journey.

I also express my gratitude and thanks to Prostate Cancer UK for providing me the funding for this project.

A sincere thanks to my supervisors Dr. Klaus Pors, Prof Norman J. Maitland and Prof. Roger M. Phillips for their guidance, support and encouragement throughout the course of my PhD. I am very grateful to my supervisors for giving me the opportunity to be part of their research teams at both the Institute of Cancer Therapeutics (University of Bradford) and Cancer Research Unit (University of York). I would like to earnestly thank my supervisors for always sharing their knowledge and wisdom with me, and always being friendly.

A special thanks must go to Dr. Fiona M. Frame whose expertise, support and advice made this project possible. I find myself very fortunate to have your unconditional support. You have been a great help with your caring, considerate and friendly nature. I would like to deeply express my gratitude for your patience and love. I would like to extend my sincere thanks and appreciation to Dr. Simon J. Allison who trained me on various molecular techniques, advised me on my project and gave unconditional support and guidance. I am also very grateful to Dr. Mark Sutherland for his continuous advice and support throughout my project, and for always offering technical

assistance with experiments. Thanks to the friends at both universities who have made this PhD journey enjoyable.

In the end, I would like to say a heartfelt thanks to my family and friends for their endless support and faith in me throughout this project. In particular Mum, Dad, Rabbia, Omair and Asma for their endless love, support and confidence in me. I am also thankful to Tahir for his tireless efforts and help, my dearest nephew Raihaan and niece Ariana for their constant love and antics that keep me sane. A special thanks to my husband Omar for his believe in me, his unconditional love, support and patience with me whilst working on his own PhD. My family helped me to keep going when things got tough, they inspired me to be ambitious and believe in myself. I am indebted to them for everything I have achieved and the drive to face challenges. Finally, the deepest and sincerest thanks to my late cat Simba whom I lost during my write up. It was your unconditional and pure love that encouraged me and kept me strong during my PhD. Sadly, I lost Simba in his battle against cancer and I therefore dedicate this work to my beloved cat Simba who forever remains in my heart.

**This work has been presented at the following scientific meetings:**

| | | |
|---|---|---|
| March 2014 | Postgraduate Research Mini Conference, University of Bradford, UK | Oral |
| November 2014 | From target to disease: modelling stratified approaches in oncology, Royal Society of Medicine, London, UK | Poster |
| March 2015 | Research and Development Open Day, University of Bradford, UK | Poster |
| March 2015 | Postgraduate Research Mini Conference, University of Bradford, UK | Oral |
| May 2015 | Seminar, University of Bradford, UK | Oral |
| November 2015 | NCRI conference, Liverpool, UK | Poster |
| April 2016 | AACR annual meeting, New Orleans, USA | Poster |

| | | |
|---|---|---|
| October 2016 | Researcher's Networking Day, Prostate Cancer UK, Royal college of physicians, London, UK | Oral |
| February 2017 | Prostate cancer and tumour microenvironment workshop, University of Cardiff, UK | Oral |
| April 2017 | AACR annual meeting, Washington D.C., USA | Poster |

## Published review article from this thesis:

Ali I. M. Ibrahim, **Maria Sadiq**, Fiona M. Frame, Norman J. Maitland, Klaus Pors. Expression and regulation of aldehyde dehydrogenases in prostate cancer. Journal of Cancer Metastasis & Treatment.

## Published work from other projects:

M. Ahmadi, Z. Ahmadihosseini, S. J. Allison, S. Begum, K. Rockley, **M Sadiq**, S. Chintamaneni, R. Lokwani, N. Hughes, R. M. Phillips. Hypoxia modulates the activity of a series of clinically approved tyrosine kinase inhibitors. *British Journal of Pharmacology, **2013**, 171(1)*

V. Vinader, **M. Sadiq**, M. Sutherland, M. Huang, P. M. Loadman, L. Elsalem, S. Shnyder, H. Cui, K. Afarinkia, M. Searcey, L. H. Patterson, K. Pors. Probing cytochrome P450-mediated activation with a truncated azinomycin analogue. *Medicinal Chemistry Communication, **2014**, 6(1)*

Sara M. Elkashef, Simon J. Allison, **Maria Sadiq**, Haneen A. Basheer, Goreti Ribeiro Morais, Paul M. Loadman, Klaus Pors, Robert A. Falconer. Polysialic acid sustains cancer cell survival and migratory capacity in a hypoxic environment. *Scientific Reports*, ***2016**, 6*

Simon J. Allison, **Maria Sadiq**, Efstathia Baronou, Patricia A. Cooper, Chris Dunnill, Nikolaos T. Georgopoulos, Ayse Latif, Samantha Shepherd, Steve D. Shnyder, Ian J. Stratford, Richard T. Wheelhouse, Charlotte E. Willans, Roger M. Phillips. Preclinical anti-cancer activity and multiple mechanisms of action of a cationic silver complex bearing *N*-heterocyclic carbene ligands. *Cancer Letters, **2017**, 403*

Pippione AC, Giraudo A, Bonanni D, Carnovale IM, Marini E, Cena C, Costale A, Zonari D, Pors K, **Sadiq M**, Boschi D, Oliaro-Bosso S, Lolli ML. Hydroxytriazole derivatives as potent and selective aldo-keto reductase 1C3 (AKR1C3) inhibitors discovered by bioisosteric scaffold hopping approach. Eur J Med Chem. **2017**

## List of Contents

## List of Figures

## List of Tables

## Abbreviations

3-(4,5-Dimethylthiazol-2-yl)-2,5-diphenyltetrazolium bromide (MTT)

3,3-diaminobenzidine (DAB)

3-aminopropyltriethoxysilane (APES)

4′,6-diamidino-2-phenylindole (DAPI)

4-hydroperoxycyclophosphamide (4-HCPA)

5' AMP-activated protein kinase (AMPK)

5α-Reductase Inhibitor (5ARI)

Alcohol Dehydrogenase (ADH)

Aldehyde Dehydrogenase (ALDH)

All-*trans* Retinoic Acid (atRA)

Alpha-Methylacyl-CoA Racemase (AMACR)

American Joint Committee on Cancer (AJCC)

American Type Culture Collection (ATCC)

Androgen Deprivation Therapy (ADT)

Androgen Receptor (AR)

Androgen Response Elements (AREs)

Anterior Zone (AZ)

Antigen-Presenting Cells (APCs)

Area Under the Curve (AUC)

Argonaute-2 (Ago-2)

ATP Binding Cassette (ABC)

Basic Fibroblast Growth Factor (bFGF)

Benign Prostatic Hyperplasia (BPH)

Bicinchoninic Acid Assay Kit (BCA)

BODIPY aminoacetaldehyde (BAAA)

BODIPY aminoacetate (BAA)

Bovine Pituitary Extract (BPE)

Bovine Serum Albumin (BSA)

Cancer Stem Cells (CSCs)

Cancer-Associated Fibroblasts (CAFs)

Carbonic Anhydrase IX (CA9)

Castration-Resistant Adenocarcinoma (CRPC-Adeno)

Castration-resistant prostate cancer (CRPC)

CD133 (prominin)

Cell-Cycle Progression (CCP)

Cellular Retinoid-Binding Proteins (CRBP)

central zone (CZ)

Chromatin Immunoprecipitation (ChIP)

Chronic Prostatitis/Chronic Pelvic Pain Syndrome (CP/CPPS)

Colony Forming Efficiency (CFE)

Committed Basal (CB)

Complete Keratinocyte Serum-Free Medium (cKSFM)

Component 3 Promoter of RISC (C3PO)

Co-repressors Nuclear Receptor Corepressor (N-CoR)

Cyclin-dependent kinase 5 (Cdk5)

Cyclophosphamide (CP)

Cytokeratins (CK)

Decitabine (DAC)

Diethylaminobenzaldehyde (DEAB)

Diethylstilbestrol (DES)

Digital Rectal Examination (DRE)

Dihydrotestosterone (DHT)

Dimethyl sulfoxide (DMSO)

Diphenylxylene (DPX)

Disabled Homolog 2-Interacting Protein (DAB2IP)

Drug Metabolising Enzymes (DMEs)

Dulbecco's Modified Eagle Medium (DMEM)

E-26 Transformation-Specific (ETS)

Entinostat (MS275)

Epidermal Growth Factor (EGF)

Epithelial-to-Mesenchymal Transition (EMT)

Erythroblastosis Virus E26 Oncogene Homolog (ERG)

Ethylenediaminetetraacetic Acid (EDTA)

Family History (FH)

Fetal Calf Serum (FCS)

Forkhead Box A1 (FOXA1)

Free and Complexed PSA (fPSA and cPSA)

Friend Leukaemia Integration 1 (FLI1)

GATA Binding Protein 2 (GATA2)

Genome-Wide Association Studies (GWASs)

Genomic Prostate Score (GPS)

Glucose Transporter 1 (GLUT1)

Gonadotropin-Releasing Hormone (GnRH)

Granulocyte Macrophage Colony Stimulating Factor (GM-CSF)

Haematopoietic SCs (HSCs)

HAN00316 (HAN)

Head and Neck Squamous Cell Carcinoma (HNSCC)

Heat-Induced Epitope Retrieval (HIER)

Hematoxylin and Eosin (H&E)

Histone Acetyltransferase (HAT)

Histone Deacetylases (HDACs)

Homeobox B13 (HOXB13)

Homeobox Protein NKx-3.1 (NKX3.1)

Hypoxia Inducible Factor (HIF)

Hypoxia Response Element (HRE)

Hypoxic Region (HR)

Immunohistochemistry (IHC)

Insulin-Like Growth Factor (IGF)

International Union Against Cancer (UICC)

Isocitrate Dehydrogenase 1 (IDH1)

Kallikrein (KLK)

Keratinocyte Growth Factor (kGF)

Lactate Dehydrogenase (LDH)

Latexin (LXN)

Leukaemia Inhibitory Factor (LIF)

Luteinising Hormone-Releasing Hormone (LHRH)

Magnetic-Activated Cell Sorting (MACS)

Metastatic Castration Sensitive Prostate Cancer (mCSPC).

Metastatic CRPC (mCRPC)

Michigan Prostate Score (MiPS)

Microtubule-Associated Protein 1 Light Chain 3 Beta (LC3B)

Mitogen-Activated Protein Kinase (MAPK)

Multi-Parametric Magnetic Resonance Imaging (mpMRI)

Multicellular Spheroid (MCS)

Multidrug Resistance (MDR)

Necrotic core (NC)

Neuroblastoma (NB)

Neuroendocrine (CRPC-NE) Tumours

Neuroendocrine (NE)

Neuron Specific Enolase (NSE)

Non-Metastatic Prostate Cancer (nmPC)

Non-Small Cell Lung Cancer (NSCLC)

Normal Prostate Fibroblasts (NPFs)

Nuclear Factor-Kappa B (NF-$_K$B)

Octamer Transcription Factor (OCT1)

PC3 Resistant Cell Line (D8)

PC3 Wild-Type Parental Cell Line (Ag)

Peripheral Zone (PZ)

Peroxisome Proliferator-Activated Receptor γ (PPARγ)

Phosphatase and Tensin Homolog (PTEN)

Phosphatidylinositol 3-Kinase (PIK3)/AKT

Poly-ADP Ribose Polymerase (PARP)

Primary Transcript (pri-shRNA)

Propidium Iodide (PI)

Prostate Cancer Antigen 3 (PCA3)

Prostate Intraepithelial Neoplasia (PIN)

Prostate MRI Imaging Study (PROMIS)

Prostate Testing for Cancer and Treatment (ProtecT) trial

Prostate-Specific Antigen (PSA)

Prostatic Acid Phosphatase (PAP)

Protein Activator of PKR (PACT)

PSA Doubling Time (PSADT)

PSA Velocity (PSAV)

RA Response Elements (RARES)

RA-Binding Proteins (CRABP)

Radical Prostatectomy (RP)

Retinoic Acid (RA)

Retinoic Acid Receptor (RAR)

Retinoic Acid Receptor Responder 1 (RARRES1)

Retinoid X Receptor (RXR)

RNA Induced Silencing Complex (RISC)

RNA Interference (RNAi)

Short Hairpin RNA (shRNA)

Silencing Mediator of Retinoid and Thyroid Receptors (SMRT)

Single Nucleotide Polymorphisms (SNPs)

Small Interfering RNA (siRNA)

Sodium Dodecyl Sulphate (SDS)

Speckle-Type POZ Protein (SPOP)

Stem Cell Factor (SCF)

Stem Cell Media (SCM)

Stem Cells (SCs)

Stockholm 3 (STHLM3)

Surface Layer (SL)

T Cell Receptor Alpha Locus (TRA-1-60)

TAR-RNA-Binding Protein (TRBP)

Template Prostate Mapping Biopsy (TPM-biopsy)

Tetramethylethylenediamine (TEMED)

Thioguanine- and Ouabain Resistant (STO)

Transcription Factor (TF)

Transcriptional Co-Repressor 1 (RB1)

Transforming Growth Factor-β (TGFβ)

Transit Amplifying (TA)

Transitional Zone (TZ)

Transmembrane Protease, Serine 2-ETS-Related Gene (TMPRSS2-ERG)

Transmembrane Serine Protease 2 (*TMPRSS2)*

Transrectal Ultrasonography (TRUS)

Transrectal Ultrasound Guided Biopsy (TRUS-biopsy)

Transurethral Resection of the Prostate (TURP)

Trichostatin A (TSA)

Tumour Suppressor Genes (TSG)

Tumour, Node and Metastasis (TNM)

Viable Rim (VR)

Vorinostat (SAHA)

Whole Genome Sequencing (WGS)

α-1-antichymotrypsin (ACT)

γ-aminobutyric acid (GABA)

# Chapter 1

## Introduction

## 1.1 Prostate Anatomy, Function and Development

The human prostate gland is a slightly larger than walnut-sized organ surrounded by an integral fibromuscular band [1]. The prostate surrounds the urethra and sits at the base of the bladder. There are four distinct glandular regions (Figure 1) as first proposed by John E. McNeal [2, 3] (i) the peripheral zone (PZ) which makes up to ~70% of the fraction of the gland and surrounds the distal urethra, (ii) the central zone (CZ) comprises ~25% of the gland and surrounds the ejaculatory ducts, (iii) the transitional zone (TZ) represents ~5% of the prostatic volume and surrounds the proximal urethra (TZ is the region responsible for lifetime growth and also for benign prostatic enlargement) and (iv) the anterior zone (AZ) makes ~5% of the organ and is a fibro-muscular zone lacking glandular components [4].

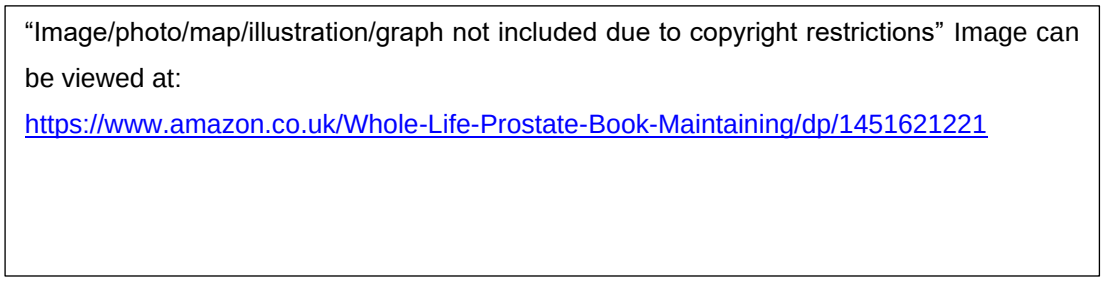


**Figure 1. The human prostate gland anatomical zones**

The human adult prostate gland consisting of the peripheral zone (PZ), central zone (CZ), transitional zone (TZ) and the anterior zone (AZ). Image taken from The Whole Life Prostate Book, Carter, H. Ballentine and Couzens, Gerald Secor, 2012, http://wholelifeprostate.com/prostate.html [5].

The prostate is an important part of the male reproductive system. It produces slightly alkaline secretions that are essential for sperm function including proteolytic enzymes, prostatic acid phosphatase (PAP), beta-microseminoprotein and prostate-specific antigen (PSA) [2]. Androgens are required for prostate development, growth and function of the prostate, and male sex characteristics such as muscle mass, spermatogenesis and hair pattern [6, 7]. Testosterone is the main male hormone; dihydrotestosterone (DHT) is a metabolite of testosterone which is predominantly involved in the regulation of the prostate [8].

The prostate develops from the urogenital sinus in an embryo forming a multi-layered epithelium surrounded by stroma upon testosterone and DHT stimulation [9, 10]. DHT has a ten-fold greater affinity for the androgen receptor (AR) as compared to testosterone [11], and is converted from testosterone by 5α-reductase, which exists in two forms; type I, mainly found in the skin, liver and prostate, and type II, which is the predominant isozyme contained in the prostate [12]. During initial prostate development proliferating epithelial cells enter stromal regions producing ducts, which then form the immature acini. Through puberty, the multi-layered prostate epithelium undergoes cellular differentiation in response to a testosterone surge to form a mature highly organised bi-layered prostate epithelium [13].

### 1.2 The AR Signalling Pathway in Prostatic Development

The development and function of normal prostate (and its cancerous counterpart) depends on the regulation of androgens, growth factors and transcriptional factors (TFs). The AR is a crucial regulator of normal prostatic function and maintenance, however it can be aberrantly expressed in the

disease state, such as over expression in prostate cancer [14]. AR is a steroidal receptor sequestered within the cytoplasm with heat-shock proteins 90, 70 and 56, and co-chaperones in the absence of its ligand DHT. Upon DHT binding, the chaperones are dissociated allowing the AR to dimerise and translocate to the nucleus where it binds to the androgen response elements (AREs), resulting in transcription of essential genes such as *PSA* and transmembrane serine protease 2 (*TMPRSS2)* that are involved in maintenance and survival of the prostate (Figure 2) [15].

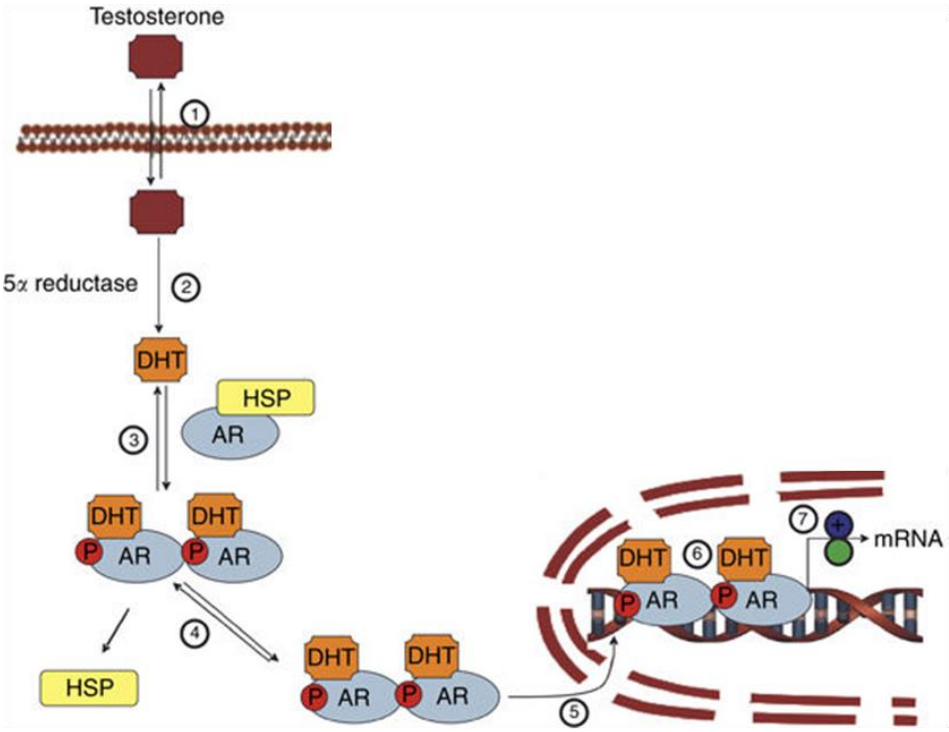


**Figure 2. Signalling pathway of AR activation**

Exracellular testosterone crosses the plasma membrane by diffusion and once inside the cell, it is metabolised by 5α-reductase to generate dihydrotestosterone. Dihydrotestosterone binds to androgen receptor causing its dissociation from heat-shock proteins, receptor dimerisation, phosphorylation and translocation to the nucleus where it binds to androgen response element leading to recruitment of co-activators or co-repressors to ultimately maintain prostate homeostasis by transcription of vital genes. Modified from [16]. Re-used image with permission from: License: http://creativecommons.org/licenses/by-nc-sa/3.0/

## 1.3 Cellular Organisation of the Normal Human Prostate Epithelium

The prostate is composed of an epithelial and a stromal compartment, separated by a strong basement membrane [17]. The mature prostate displays a high degree of cellular organisation with two distinct cellular compartments within the epithelial bilayer [18]: the terminally differentiated luminal cells that have an exocrine phenotype and the relatively undifferentiated basal cells. Within the epithelium bilayer is also the rare, scattered population of neuroendocrine (NE) cells [19]. The basal cell compartment also harbours stem cells (SCs) (Figure 3) [20].

Although the prostate is predominantly androgen-dependent for proliferation [21], the basal cellular layer is androgen-independent, however it is androgen-responsive. Thereby, survival of basal cells does not require androgens [22].

### 1.3.1 Basal and Luminal Epithelial Cells

The differentiation patterns in prostate epithelium have been established, on the basis of keratin staining [23, 24], the polarised expression of several adhesion molecules [25], and the expression of proteins responsible for AR response and cell proliferation [26].

Discrimination between luminal and basal cell types is also based on the expression of cytokeratins (CK). Keratins belong to the group of intermediate filament proteins that form part of the cytoskeleton by heterodimeric interaction and polymerisation [27]. Luminal cells primarily express CK8 and CK18 [28-30].

High columnar luminal cells constitute the secretory compartment of the prostate epithelium and overlie the basal layer of cells extending into the

acinar lumen [31]. Luminal cells exhibit relatively low proliferative capacity and a higher apoptotic index [31] than the basal compartment. These terminally differentiated cells express high levels of AR and are androgen-dependent for their function and survival [32]. They express CD57, secretory fluids containing PSA, PAP and prostaglandins, and homeobox protein NKx-3.1 (NKX3.1) luminal nuclear marker [33, 34].

The basal layer of undifferentiated cells sits firmly on the basement membrane providing a structural separation between the epithelium and the surrounding stroma. Basal cells possess the most proliferative activity and lack any secretory function [35]. CK5 and CK14 are expressed by basal cells [29, 36-38] with low levels of CK8 and CK18 [23]. The basal compartment also expresses CD44 [39] and p63 [40]. It does not express AR, however, shows focal expression of mitosis suppressors such as $p27^{kip}$ and the cell proliferation marker c-Met [41].

The basal layer comprises few, poorly differentiated SCs, and intermediate cells between the undifferentiated SCs and terminally differentiated secretory and NE cells [17, 31, 42]. Intermediate cells, which are described as transit amplifying cells (TA) and committed basal cells (CB), display moderate renewal capacity and enhanced mitotic index. These cells only have low levels of AR, are largely androgen-independent, but are androgen-sensitive and thereby rely on androgens for expansion and growth. In contrast, SCs possess an extensive renewal capacity, low mitotic index and are androgen-independent for self-renewal with no expression of AR [43].

### 1.3.2 Neuroendocrine Cells

NE cells are dispersed within the prostate epithelium bilayer. The function of terminally differentiated NE cells is largely unknown, although it is speculated that this rare population of cells induces proliferation of adjacent cells modulated by paracrine secretion of neuropeptides such as chromogranin A and synaptophysin [44]. NE cell markers include chromogranin, synaptophysin and also neuron specific enolase (NSE). Chromogranin is found in NE cell secretory granules [45]. Synaptophysin is a well-established marker for neuroendocrine differentiation [46]. NSE is a common marker for both neurons and NE cells [47]. NE cells are characterised by a lack of AR or PSA expression, making their regulatory function androgen-independent [48].

### 1.3.3 Stromal Cells

The stromal compartment of cells lies beneath the basement membrane, which separates it from the epithelial compartment. Stroma is comprised of extracellular matrix with fibroblasts, endothelial cells, smooth muscle cells, nerves, and infiltrating cells such as lymphocytes and mast cells. A proportion of stromal cells express AR and are androgen-responsive. Soluble growth factors including basic fibroblast growth factor (bFGF), epidermal growth factor (EGF), keratinocyte growth factor (kGF), transforming growth factor-β (TGFβ) and insulin-like growth factor (IGF) are responsible for crosstalk between the stromal and epithelial compartments [43], and paracrine stimulation and inhibition of epithelial growth, maintenance and differentiation.

**Figure 3 . Cellular organisation of normal prostate**

The normal prostate comprises an epithelial compartment comprising of luminal cells, basal cells, neuroendocrine cells and rare stem cells, and a stromal compartment comprising stromal cells and matrix separated by a basement membrane. Modified from [49].

### 1.3.4 Normal Stem Cells

Conventionally, SCs have been widely studied in tissues with rapid cell turnover, such as gastrointestinal tract [50], bone marrow [51] and skin [51]. Discovery and isolation of the first adult SCs were demonstrated in haematopoietic SCs (HSCs) [52], which later led to discovery of putative SCs in other tissues with limited regeneration/turnover, including the prostate [53, 54]. The existence of normal prostate SCs is generally accepted, however prostate cancer stem cells (CSCs) are more controversial, as discussed later.

The theory of putative prostate SCs was first demonstrated using a rodent model in which castration (androgen removal) caused rapid involution of the prostate gland due to increased apoptosis of androgen-dependent luminal cells. However, following restoration of androgen levels, the gland was fully regenerated by a proportion of surviving basal cells [55-57]. Repeated cycles of involution/regeneration suggested a population of long-lived androgen-

independent prostatic epithelial putative SCs may exist [58] and consequently, a SC model was proposed (Figure 4) [59].

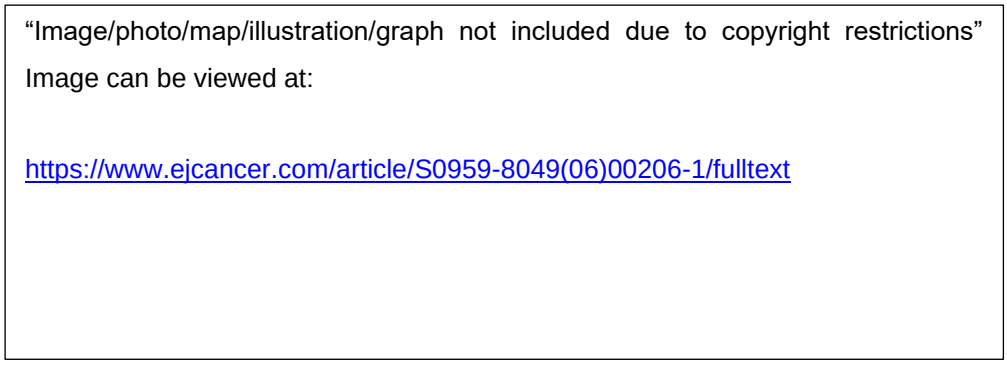


**Figure 4. Illustration of androgen context dependency of prostate epithelium**
Putative SCs in the basal compartment producing transit amplifying cells in an androgen-independent manner, which subsequently undergo differentiation by androgen stimuli giving rise to differentiated luminal cells. Image modified from [60].

In human prostatic epithelium, SCs and TA cells have high surface expression of α2β1-integrin [54] and CB cells have low surface expression of α2β1-integrin, thus enrichment of SC and TA cells can be carried out using rapid adherence to collagen I [23, 54]. Putative SCs can be further enriched by the use of an additional cell surface marker. Based on haematopoietic lineage in which the cell surface marker CD133 (prominin) was first used to isolate HSCs [61], CD133 was used as a marker for the isolation of a small subset of basal α2β1-integrin$^{high}$ prostate basal cells. CD133$^{+}$ cells have enhanced expansion in culture and generate acini with evidence of prostatic specific differentiation when grafted in athymic nude mice, with characteristics in line with a SC origin and a primary indication of "stemness" (Figure 5) [26, 27, 39, 62]. Stemness is

commonly used to refer to properties such as self-renewal, differentiation, and proliferative potential [63].

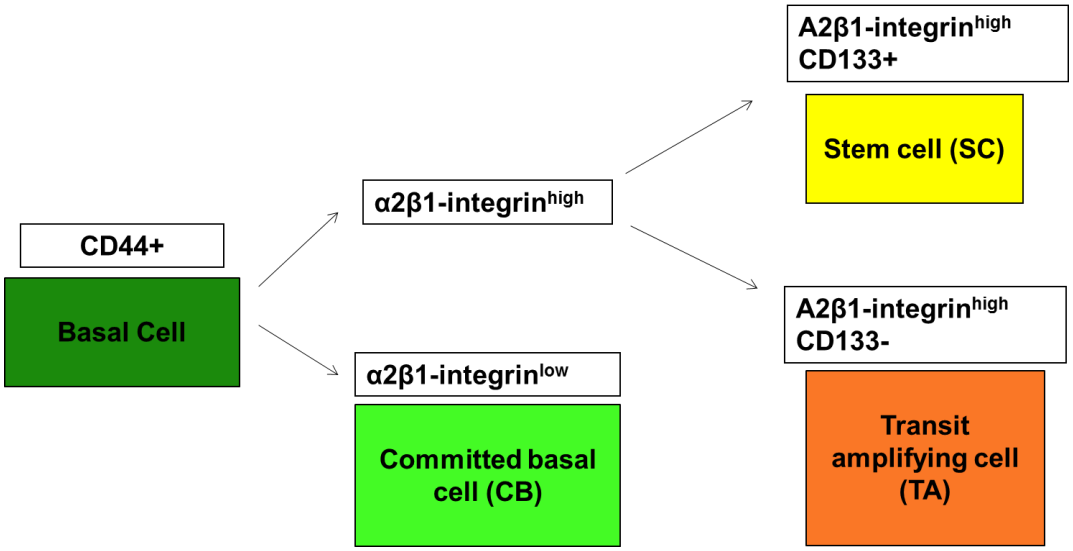


**Figure 5. Fractionation of prostatic basal cells**
The basal compartment of cells consists of different cell types which can be identified using markers. A CD44 expressing basal cell can be further categorised into a committed basal cell under low α2β1-integrin expression, a transit amplifying cell under high α2β1-integrin expression or a stem cell based on high expression of α2β1-integrin and presence of CD133.

These few α2β1-integrin$^{high}$ and CD133$^{+}$ expressing human prostate basal cells constituted less than 0.1% of the cell population and displayed SC properties. Following characterisation, the SCs were primarily in a quiescent state, exhibited high proliferative potential in culture and regenerated structured and functional acini in immunocompromised mice [39].

These cells are androgen-independent for survival and androgen-irresponsive as AR is not expressed at the mRNA level in these subpopulation of cells [64]. The SCs reside in a privileged SC niche within the basal layer of supporting cells receiving signals for continued maintenance [26, 51]. The SC niche is a microenvironment composed of mesenchymal cells and extracellular matrix molecules that support the presence and function of SCs through cross-talks

between epithelial cells and surrounding stroma [65]. The SC niche is responsible for controlling the balance between quiescence, proliferation, or differentiation [66].

SCs are defined by two essential properties, the first is self-renewal which is the ability to maintain an undifferentiated state through numerous cell divisions and the second is multi-potency, the potential to differentiate into various other cell types (Figure 6) [67]. Unlike totipotent embryonic SCs, multi-potent adult SCs commit to differentiation within the specific lineage of the tissues in which they reside due to limited differentiation potential. Accumulating evidence suggests further heterogeneity of the basal compartment of cells with varying proliferative capacity, differentiation ability and co-localisation of CK markers demonstrating intermediate cell types [27, 68-71]. Therefore, it is more appropriate to consider the prostate epithelial hierarchy as a continuum of cell differentiation.

**Figure 6. Hierarchy within the prostate epithelium lineage of cells**
A stem cell can generate a transit amplifying cell through asymmetric division, renewing the stem cell population. Transit amplifying cell can work as a repopulating cell by either directly generating luminal cells or by another intermediate population of cell, the committed basal cell. Unclear lineage relationships are illustrated with dotted arrows, SC=stem cell, TA=transit amplifying cell, CB=committed basal cell, NE=neuroendocrine cell. Figure modified from [72].

Putative SCs exhibit distinctive features, on the basis of which they can be recognised. They are slow cycling and often maintained in a quiescent state for prolonged periods. They are a small population of less than 0.1% cells with a larger nucleus compared to cytoplasm. They have high proliferative potential based on stimuli from their niche and soluble factors, and can give rise to rapidly proliferating TA cells [51, 73]. Following entry into the active cell cycle from G0 phase, a SC can either undergo symmetric or asymmetric cell division to maintain tissue homeostasis by maintaining, depleting or increasing the SC population (Figure 7) [67].

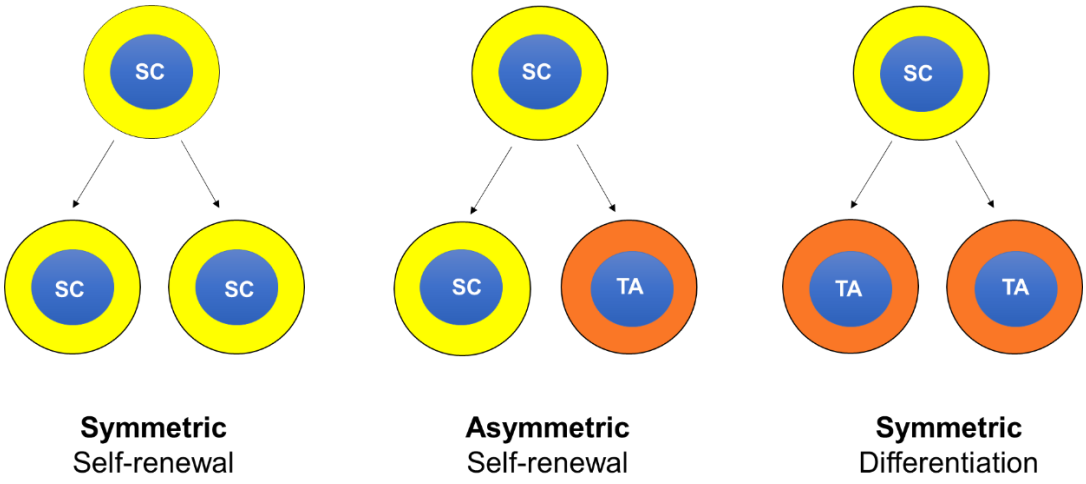


**Figure 7. Division patterns of stem cells**
A stem cell can undergo symmetric division to give rise to two daughter stem cells increasing the stem cell pool, asymmetric division to generate a daughter stem cell and a transit amplifying progenitor cell to maintain the stem cell pool and symmetric division giving rise to two identical transit amplifying cells depleting the stem cell pool.

## 1.4 Disorders of the Prostate

### 1.4.1 Prostatitis

Inflammation of the prostate gland caused by bacterial infection, stress, autoimmunity or physical injury can result in prostatitis which primarily occurs in the CZ of the prostate. Prostatitis syndromes are common, with 2-10% of adult men suffering from symptoms such as pain and distress that are associated with chronic prostatitis (not caused by infection) at any time [74]. There is increasing evidence that suggests chronic prostatitis/chronic pelvic pain syndrome (CP/CPPS) is associated with depression and catastrophizing [75], which negatively impacts the health-related quality of life [76]. However, the etiology of CP/CPPS is uncertain. Furthermore, stress has also been suggested as a potent factor in the development and perpetuation of the symptoms [77].

### 1.4.2 Benign Prostatic Hyperplasia

Benign prostatic hyperplasia (BPH) can also arise from inflammation of the prostate in older men [78-81]. BPH is a non-malignant enlargement of the prostate occurring exclusively in the TZ [82]. The enlargement of the prostate involves hyperplasia of prostatic epithelial and stromal cells [82]. BPH occurs from unregulated proliferation of connective tissue, smooth muscle and glandular epithelium [83]. BPH can be characterised as a progressive hyperplasia of both the stromal cells and glandular epithelial cells resulting in the expansion of the prostate gland [84]. Inflammatory and wound repair processes are also key components of BPH which cause altered expression of chemokines, cytokines, matrix remodelling factors and immune surveillance leading to the formation of a prototypical reactive stroma. A retrospective study

demonstrated raised cell proliferation in BPH tissue compared to normal tissue, with epithelial cell proliferation to be 9-fold higher and stromal cell proliferation to be 37-fold higher [85]. Prostate epithelial proliferation leads to enlarged glandular nodules, whereas stromal proliferation generates a more diffuse hyperplasia with increased matrix production including collagen type 1 [86]. BPH causes narrowing of the urethra resulting in restricted flow of urine from the bladder. Transurethral resection of the prostate (TURP) is commonly performed in BPH patients to overcome onset symptoms and remains the gold standard for BPH treatment [87]. Finasteride, a 5α-reductase inhibitor (5ARI) is also commonly used to treat BPH symptoms, by blocking the conversion of testosterone to DHT resulting in the reduction of prostate size [88].

### 1.4.3 Prostate Intraepithelial Neoplasia

Prostate intraepithelial neoplasia (PIN) is frequently found in the PZ of the prostate and its incidence increases with age [88-90]. In the continuum of cellular proliferation in prostate epithelium, PIN is characterised as being at the pre-invasive end of the continuum of cellular proliferation within the prostate epithelium [91]. Abnormal cellular proliferation occurs within the prostatic ducts and acini leading to cellular dysplasia and carcinoma in situ without stromal invasion [92-94]. Phenotypic description of PIN can be identified at low magnification by the appearance of a darker lining of the ductal structures, a lining thicker than the surrounding normal ducts and acini, and a complex intraluminal pattern of growth. At high magnification, there is varying degrees of nuclear enlargement with nuclear stratification, hyperchromasia and nucleolar prominence [95]. The frequency of high grade PIN found on needle

biopsies ranges from only 5 – 16% and may not lead to cancer when present as a small lesion within the biopsy [95].

### 1.4.4 Prostate cancer

Prostate cancer can occur in the CZ, TZ or the PZ with most malignant adenocarcinomas initiating in the PZ [96]. It is largely a slow developing proliferative disease occurring mainly in men over the age of 50. Bone metastasis occurs commonly with malignant prostate cancer. More details on prostate cancer follow.

## 1.5 Prostate Cancer Epidemiology

Prostate cancer is the most common type of cancer in men in the UK with over 47,000 new cases diagnosed every year and more than 11,000 cancer related deaths in the UK (Prostate Cancer UK, 2016). Prostate cancer is the second leading cause of cancer mortality in men after lung cancer (Cancer Research UK, 2014). Risk of prostate cancer significantly increases with age and it mostly affects men over the age of 50. A higher incidence of prostate cancer is apparent in black men followed by in white men, and is least common in Asian men. Men of an African descent with non-metastatic prostate cancer (nmPC) present higher PSA values at diagnosis when compared to Caucasian men with nmPC [97]. Genetic variations may play a role in the higher incidence of prostate cancer in black men. A single nucleotide polymorphism (SNP) is a DNA sequence variation which occurs when a single nucleotide in the genome differs from the normally expected nucleotide [98]. This may alter the function of the resultant protein by enhancing or reducing its activity. SNPs are therefore known to underlie differences in individuals' susceptibility to disease [98]. It has been reported that 17 out of 20 SNPs investigated in a

study, were more common in African American men and two of the 17 SNPs were associated with a high risk of developing prostate cancer [99]. Another group noted the presence of a 3.8 MB interval on chromosome 8q24 which is linked with an elevated risk of prostate cancer. The chromosome interval is mostly found in African American men [100]. Men with a family history of allelic variants in this region are 9.46 times more likely to develop the disease compared to men without allelic variants [100]. These factors among others such as environment, diet and migration can predispose men of African descent to prostate cancer. Men with a first degree relative (father, brother, son) with prostate cancer are at a higher risk of getting prostate cancer compared to men with no affected relatives (Prostate Cancer UK, 2016), [101].

## 1.6 Prostate Cancer Diagnosis

Digital rectal examination (DRE) and serum PSA are the most commonly used initial diagnostic tools for the detection of prostate cancer [102].

### 1.6.1 Digital Rectal Examination

DRE remains the main test for the initial clinical assessment of the prostate. It is routinely used and has the advantage of detecting other non-PSA secreting tumours. The accuracy of DRE has been tested by many studies suggesting the positive predictive value is about 50% [103-105]. Positive predictive values are used to indicate the likelihood of prostate cancer in patients. One such study reviewed a cohort of 806 men who underwent a prostate needle biopsy based on results obtained from DRE and PSA. 516 patients (64%) had a normal DRE and 290 patients (36%) had an abnormal DRE. 306 (38%) men were diagnosed with prostate cancer of which 136 (44%) had an abnormal DRE. In this abnormal DRE stratified cohort of patients undergoing prostate

biopsy, an abnormal DRE had a sensitivity of 44%, specificity of 68% and a positive predictive value of 46% for detecting prostate cancer on biopsy [106]. DRE has limited clinical applicability as it is only useful in identifying larger prostates [107]. This can result in missed diagnosis of smaller prostate cancers that are still clinically relevant [107]. Compared with PSA, DRE detects cancers at a more advanced pathological stage [105]. Before the discovery of PSA-based diagnosis, 75% of men diagnosed with prostate cancer by DRE eventually died of their disease and no studies to date have been reported on reduction in mortality [108].

### 1.6.2 Prostate-Specific Antigen

PSA was first described as a serine protease in 1979 [109]. It is generated by the prostate epithelium and peri-urethral glands, and is found in abundance in prostatic secretions. As a diagnostic marker, it is organ-specific but not cancer-specific, with evidence of its use as a marker for BPH [110, 111]. PSA screening involves quantification of serum PSA levels [112], which in prostate cancer are elevated [113]. However, PSA screening can give unreliable results with false positives and false negatives [114]. There is no definitive value of PSA below which there is negligible risk as studies have shown approximately 15% of men with a PSA below the traditional cut-off of 4ng/ml were still at risk for prostate cancer, and 15% of these men had high-grade disease [115]. However, given a threshold of less than 1ng/ml, the risk of high-grade cancer was very low. Furthermore, PSA levels above 4ng/ml showed the presence of cancer on biopsies in only 25%-30% of patients [116].

Elevated PSA levels may be due to other conditions such as BPH or inflammation [117]. Likewise, patients with false negative results with low PSA values may actually have the disease.

It remains uncertain how frequently PSA should be tested, but it has been suggested every 2-4 years. One study concluded that men should be screened at the age of 40 and 45 years and then every 2 years from 50 to 75, while still using the 4ng/ml cut-off as a criterion for biopsy referral [118]. However, PSA screening does not occur in the UK as standard due to no proven benefit that outweighs the risks of over diagnosis and over treatment. Others have also suggested less frequent retesting in men with lower initial PSA levels (less than or equal to 1.0, 1.5 or 2.0ng/ml) while still testing annually in those with higher PSA levels (but still below a cut-off for biopsy) [119, 120]. A large study tested the ability of PSA screening in reducing prostate cancer mortality and the risk of over diagnosis between organised and opportunistic screening every 2 years since 1995 up to 18 years in a cohort of 10 000 men in Goteborg. It was shown that the organised screening reduced the prostate cancer mortality but was associated with over diagnosis. In contrast, opportunistic testing had little effect on prostate cancer mortality and resulted in even more over diagnosis, with almost twice the number of men needed to be diagnosed to save one man from dying from prostate cancer. PSA screening was found more effective within an organised framework than unorganised screening [121]. Such studies on PSA screening take a long time with anticipated waiting for more than 10 years.

### 1.6.3 The Gleason Grading System

A number of transrectal ultrasound guided (TRUS) biopsies (usually 12 to 16) are taken from patients presenting with high serum PSA levels, and are given a Gleason score based on the Gleason grading system (Figure 8) [114, 122-124]. The histological pattern made by glands is graded on a score from 1 (least aggressive) to 5 (most aggressive) on the specimen tissue. The two most common Gleason patterns are added to give a total score ranging from 2 (1+1) to 10 (5+5) [125]. The Gleason grading system has been updated over the years to facilitate a more refined grading system. The upgraded Gleason system proposed that adenocarcinomas of Gleason grades two to five should not be detected on needle biopsy, and all cribriform tumours and poorly formed glands should be designated as Gleason grade four [126, 127].

Gleason scoring is based on two areas that make up most of the cancer. Assignment of the first number represents the grade that is most common in the tumour. In the case of 3+4=7, majority of the tumour is grade 3 rather than 4, and vice versa for 4+3=7. If the tumour shows same grade, such as 3, then the Gleason score is 3+3=6. Since grades 1 and 2 are usually not used for biopsies and are well differentiated, the lowest score of a cancer found on a biopsy is 6. Grade 6 cancers are usually well differentiated as well and are likely to be less aggressive. The higher the Gleason score, the less differentiated the cancer with poor prognosis [125]. Figure 8 illustrates the Gleason grading system.

### 1.6.4 The Grade Group System

The grade group system was derived in 2013 [128] and later validated by a large study [129], which included over 20000 men treated by radical

prostatectomy (RP) and over 5000 men who had radiotherapy, using biochemical recurrence (BCR) as the end point. The study by Berney et al. [130] is the first to demonstrate that the 5 grade groups further correlate well with prostate cancer-related death, additionally validating reliability of the new grading system [131]. The new simplified grade group system for prostate cancer has two key advantages. Firstly, it has higher accuracy for grade stratification compared to the Gleason system. Secondly, the new system is simple and intuitive having a range from 1-5 as compared to the currently used Gleason system which under practice ranges from 6-10. The new grading system of grade group 1-5 along with the conventional Gleason grade have both been agreed upon to be included in pathology reports [132].

Grade groups were introduced to address certain issues with the Gleason grading system. Although the Gleason scores from 2-10, the lowest score given is a 6 which may lead to confusion in patients often regarding their biopsy to be in the middle of the grade scale causing worry about their diagnosis and urgency in treatment [129]. In addition, Gleason scores are usually split into 3 groups including 6, 7, and 8-10. Interpretation of such a split may not be accurate as Gleason 7 can be made up from either 3+4=7 or 4+3=7, the latter with a much worse prognosis. Furthermore, Gleason scores 9 or 10 have a worse prognosis than Gleason score 8. Due to such uncertainties, the grade groups are now used in combination with Gleason score. They range from 1 (most favourable) to 5 (least favourable). Grade group 1 is equivalent to Gleason score 6 or less, grade group 2 is equivalent to Gleason 3+4=7, grade group 3 is equivalent to 4+3+7, grade group 4 is

equivalent to Gleason 8, and grade group 5 is equivalent to Gleason 9-10 [129, 132, 133].

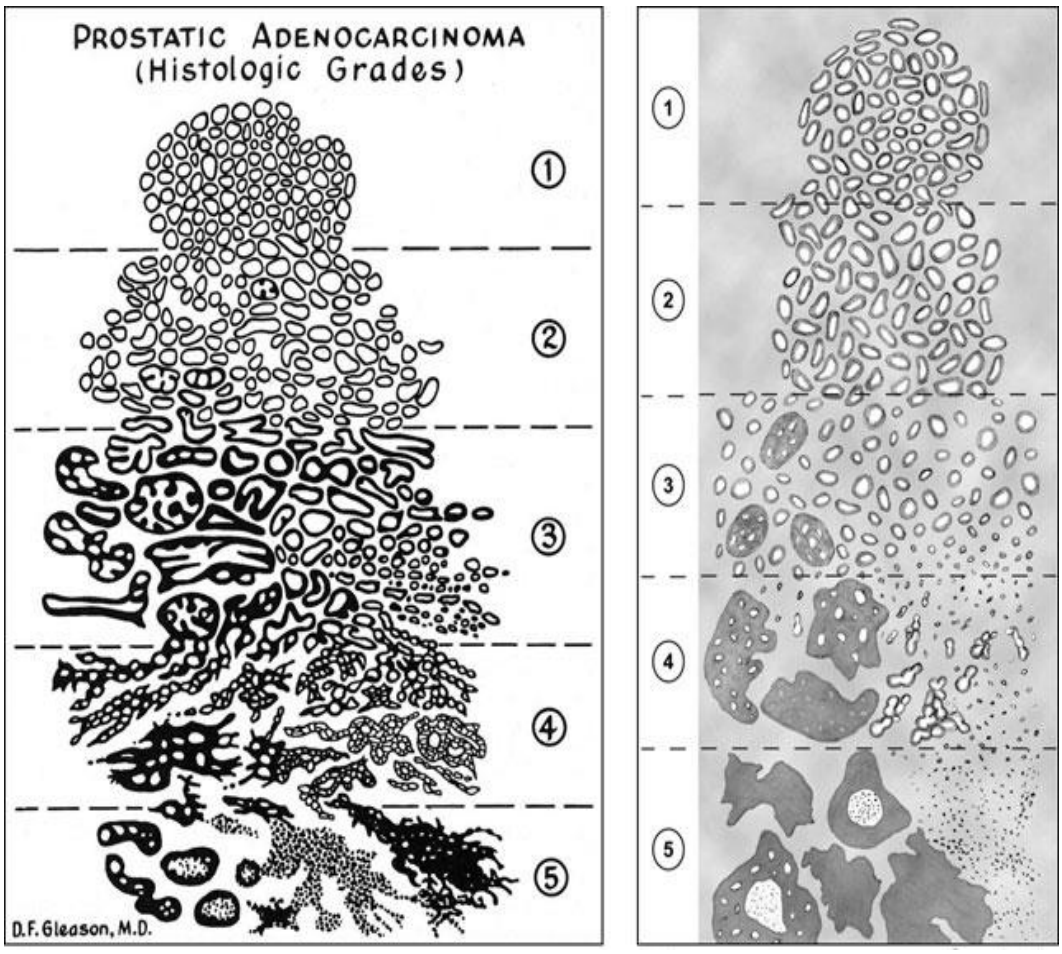


**Figure 8. The Gleason grading system**
Left: The first grading system of prostatic adenocarcinoma, right: the upgraded system showing grade 3 according to the modification is essentially grade 4 [123, 124, 127]. Grades 1 and 2 show well differentiated cells with small uniform glands. Grade 2 shows more stromal space between glands. Grade 3 is moderately differentiated with distinct infiltration of cells from glands at margins. Grade 4 shows irregular masses of neoplastic cells with few glands and is poorly differentiated. Grade 5 shows a lack of or occasional glands with sheets of cells and they are very poorly differentiated. Re-used image with permission from the Creative Commons CC-BY-NC-SA license.

### 1.6.5 Prostate Cancer Staging

Accurate prostate cancer staging is critical for prognosis assessment and planning treatment for prostate cancer. The tumour, node and metastasis (TNM) staging system for prostate cancer was first introduced in 1992, by the American Joint Committee on Cancer (AJCC) and the International Union

Against Cancer (UICC) [134], and has since been repeatedly revised to optimise the prognostic accuracy [135]. Staging of the disease is vital to enable the categorisation of the severity of prostate cancer, allow an estimation of prognosis, and recommend suitable treatment. The AJCC defines staging as T for tumour extent, N for invasion to the lymph nodes, and M for metastasis, which allows classifications to group patients. The TNM staging, used in conjunction with tumour grade and PSA score is viewed as a well-accepted practice standard for prostate cancer and is used as the basis for guiding treatment decision making [135]. Staging is sub-divided into clinical and pathological staging to examine extent of tumour spread and to predict patient prognosis. Clinical staging is based on information gained before the first definite treatment determined by DRE, transrectal ultrasonography (TRUS), or other imaging techniques. Pathological staging requires histological identification of the extent of tumour within the prostate and in surrounding tissues. While the assessment criteria for clinical staging is well defined, ambiguity exists in translating the criteria into routine surgical pathology practice after RP due to anatomically distinct lobes not being completely or histologically definable in the prostate. Furthermore, there are no defined methods for pathological staging of multifocal disease [136]. Table 1 and 2 show the most updated TNM staging according to the AJCC eighth edition due to its superior prognostic value [135]. Table 3 shows the updated AJCC eighth edition prognostic stage group. The Gleason score (seventh edition criteria) and the grade group (eighth edition criteria) should both be reported according to the latest AJCC eighth edition [135].

| Clinical Stage (cT) | Criteria |
|---|---|
| **Category T** | **Primary tumour** |
| TX | Primary tumour cannot be assessed |
| T0 | No evidence of primary tumour |
| T1 | Clinically inapparent tumour that is not palpable |
| T1a | Tumour incidental histologic finding in 5% or less of tissue resected |
| T1b | Tumour incidental histologic finding in more Than 5% of tissue resected |
| T1c | Tumour identified by needle biopsy found in one or both sides, but not palpable |
| T2 | Tumour is palpable and confined within prostate |
| T2a | Tumour involves one-half of one side or less |
| T2b | Tumour involves more than one-half of one side but not both sides |
| T2c | Tumour involves both sides |
| T3 | Extraprostatic tumour that is not fixed or does not invade adjacent structures |
| T3a | Extraprostatic extension (unilateral or bilateral) |
| T3b | Tumour invades seminal vesicle(s) |
| T4 | Tumour is fixed or invades adjacent structures other than seminal vesicles, such as external sphincter, rectum, bladder, levator muscles, and/or pelvic wall |
| **Category N** | **Regional lymph nodes** |
| NX | Regional lymph nodes were not assessed |
| N0 | No regional lymph node metastasis |
| N1 | Metastases in regional lymph nodes |
| **Category M** | **Distant metastasis** |
| M0 | No distant metastasis |
| M1 | Distant metastasis |
| M1a | Non-regional lymph nodes |
| M1b | Bones |
| M1c | Other sites with or without bone disease |

**Table 1. Eighth edition of the American Joint Committee on Cancer- TNM clinical staging [135].**

| Pathologic stage (pT) | Criteria |
|---|---|
| **Category T** | Primary tumour |
| T2 | Organ confined |
| T3 | Extraprostatic extension |
| T3a | T3a Extraprostatic extension (unilateral or bilateral) or microscopic invasion of bladder neck |
| T3b | Tumour invades seminal vesicle(s) |
| T4 | Tumour is fixed or invades adjacent structures other than seminal vesicles, such as external sphincter, rectum, bladder, levator muscles, and/or pelvic wall |
| **Category N** | **Regional lymph nodes** |
| NX | Regional lymph nodes were not assessed |
| N0 | No positive regional lymph nodes |
| N1 | Metastases in regional lymph node(s) |
| **Category M** | **Distant metastasis** |
| M0 | No distant metastasis |
| M1 | Distant metastasis |
| M1a | Non-regional lymph node(s) |
| M1b | Bone(s) |
| M1c | Other site(s) with or without bone disease |

**Table 2. Eighth edition of the American Joint Committee on Cancer- TNM pathologic staging [135].**

| Stage | T | N | M | PSA (ng/ml) | Grade group |
|---|---|---|---|---|---|
| I | cT1a-c,Ct2a | N0 | M0 | <10 | 1 |
| I | PT2 | N0 | M0 | <10 | 1 |
| IIA | Ct1a-c, Ct2a | N0 | M0 | >/=10, <20 | 1 |
| IIA | PT2 | N0 | M0 | >/=10, <20 | 1 |
| IIA | Ct2b-c | N0 | M0 | <20 | 1 |
| IIB | T1-2 | N0 | M0 | <20 | 2 |
| IIC | T1-2 | N0 | M0 | <20 | 3 |
| IIC | T1-2 | N0 | M0 | <20 | 4 |
| IIIA | T1-2 | N0 | M0 | <20 | 1-4 |
| IIIB | T3-4 | N0 | M0 | Any | 1-4 |
| IIIC | Any T | N0 | M0 | Any | 5 |
| IVA | Any T | N1 | M0 | Any | Any |
| IVB | Any T | Any | M1 | Any | Any |

**Table 3. Eighth edition of the American Joint Committee on Cancer- prognostic stage group [135].**

## 1.7 Biomarkers for Prostate Cancer

Based on the National Institutes of Health, a biomarker can be defined as a characteristic that is objectively measured and assessed as an indicator of normal biological processes, pathogenic processes, or pharmaceutical responses to a therapeutic intervention [137]. The term biomarker can range from simple examples such as hair colour, cholesterol levels or blood pressure to more complicated examples, such as mRNA profiles of tumour, proteins [138], metabolites, DNA, or epigenetic modifications of DNA, amongst other alterations [139]. Biomarkers can be detected in patient tissue samples, blood or urine [139]. In cancer, biomarkers can either be generated by the tumour or by the body in response to the tumour [138]. Cancer biomarkers can be grouped into different types including risk, diagnostic, prognostic and predictive markers.

- Risk biomarkers are used to evaluate disease disposition identifying the patient's risk factors of developing cancer in the future [139]. Several SNPs have shown correlation with risk of developing prostate cancer [140]. Other risk factors such as rarer variants may be linked with higher relative prostate cancer risk [141]. Coding variants in the homeobox B13 (HOXB13) have been observed in less than 0.1% of control, with 1.4% of men with a strong family history of early onset prostate cancer [142].
- Diagnostic biomarkers are used to identify classical histopathological characteristics in examining presence or absence of cancer such as the use of alpha-methylacyl-CoA racemase (AMACR) [138].
- Prognostic biomarkers are used to assess the outcome of patients into different prognostic risk groups thus allowing individualised management. They can predict the course of a disease and help understand tumour behaviour, thus enabling the identification of aggressive phenotype through methods such as survival probability. These markers such as PSA are used for providing information regarding the likely clinical course of a disease thus help guide therapeutic decisions [143].
- Predictive biomarkers are used to predict the effectiveness of treatment and they allow the identification of the most appropriate treatment modality [138].

## 1.8 Current Clinical Biomarkers for Prostate Cancer

### 1.8.1 PSA (diagnostic and prognostic biomarker)

PSA is encoded by the prostate-specific gene kallikrein (KLK) KLK3, a member of the tissue kallikrein family that also includes KLK2 and KLK4 [144]. The kallikrein gene family of serine proteases are located on chromosome 19q13.4. PSA is used as a diagnostic and prognostic marker and is measured in patient serum [145].

Although it has the convenience of being a non-invasive test, PSA has limitations as a biomarker with specificity and sensitivity ranges from 20-40% and 70-90%, respectively, based on the PSA cut off values used (for example 3ng/ml vs 4ng/ml) [146]. The area under the curve (AUC) metric of the receiver operating characteristic (ROC) curve is between 0.55-0.70 for the ability of PSA in identifying patients with cancer, in which a score of 1.0 is optimal discrimination and 0.5 is 50% uncertainty [146]. The poor specificity of PSA for cancer diagnosis can be due to elevated levels of serum PSA in other non-cancer-related conditions including trauma, infection, inflammation and BPH [144, 146, 147]. The presence of increased levels of PSA in over 50% of men more than 50 years old confounds PSA as a cancer biomarker [144, 148]. It is no surprise that PSA-based screening for prostate cancer is plagued by false positives with a positive predictive value of only 25-40% [149]. On the contrary, approximately 15% of men with low PSA levels (< 4.0ng/ml) have the disease, and 15% of these present a high Gleason score [115, 150].

Numerous efforts have been made to improve the performance of the PSA test including the normalising of PSA to the gland size (the PSA density) [151], and to monitor the dynamics of PSA change in serum (PSA velocity and

doubling time) [152, 153]. Furthermore, tests measuring other forms of PSA such as free and complexed PSA (fPSA and cPSA), and isoforms of the PSA protein (e.g. proPSA) have gained much interest [139].

Rather than replacement tests, fPSA and cPSA are considered adjunctive assays to total serum PSA. cPSA assay measures the molecular interaction of PSA primarily with α-1-antichymotrypsin (ACT) in the blood [154], whereas, fPSA measures the percentage of total serum PSA not bound to ACT. In prostate cancer the fPSA percentages decrease which enables to distinguish men with BPH from men with cancer. A percentage fPSA of less than 25% displayed improved sensitivity and specificity of a total PSA test and thereby reduced unnecessary biopsies [155, 156]. This test gained FDA approval for use when patients have a total PSA in the 4 to 10ng/ml grey zone [157]. In addition, combination of fPSA with (-2) pro-PSA measurement may enable the diagnosis of early prostate cancers with a PSA of 2-10ng/ml [157].

The use of fPSA also comes with limitations including, the potential instability of the fPSA measurement if the sample is processed 24 hours after collection [158], and the possible elevation in percentage fPSA following DRE or biopsy [159], again confounding its use in such settings [139].

PSA velocity (PSAV) and PSA doubling time (PSADT) dynamics have prognostic value [160]. PSAV is the change in PSA concentration each year in which a high PSAV is strongly linked with prostate cancer and a 9-fold increased risk of cancer-related death following prostatectomy [161]. PSADT is the time required for the serum PSA level to double, and is used to monitor disease progression after curative treatment for organ-confined disease, in

which an increase of PSA level following radiotherapy or prostatectomy indicates the presence of residual tumour cells. Several studies have shown that a faster PSADT (less than 10 months) is linked with reduced survival [162, 163]. In some rare cases, cancer may recur even if there was absence of an increased PSA [164]. Nonetheless, none of these tests have shown improvement over a standard PSA test [153], with same issues confounding PSA itself.

### 1.8.2 PCA3 (diagnostic biomarker)

Prostate cancer antigen 3 (PCA3) is a long non-coding RNA, which has emerged as a prominent non-PSA based diagnostic biomarker for prostate cancer. PCA3 levels are increased in more than 90% of cancer tissues, but not normal or BPH tissues, an essential difference to serum PSA [165]. The high sensitivity and specificity of PCA3 in tissues led to studies of it as a non-invasive biomarker detectable in patient urine samples [166]. The use of urine PCA3 levels have steadily added to the diagnostic information obtained from the PSA test, giving higher AUC values of 0.66-0.72 as compared to 0.54-0.63 for serum PSA alone [167]. An important feature of PCA3 is that unlike PSA, urine PCA3 levels are independent of prostate size [168], and they are not elevated in acute inflammation or infectious states [169]. Sensitivity of PCA3 levels range from 47-69%, with most between 58-69%, while a direct comparison between studies is difficult due to different analysis platforms using different criteria for patient selection and relatively small cohorts of patients (several hundred men) [167]. Furthermore, the PCA3 test maintains its predictive power in men with BPH who are on long-term treatment with 5ARI with almost no loss of specificity over 4 years [170]. Where some studies

have reported the expression level of PCA3 to be independently correlated with the outcome of the biopsy and tumour aggressiveness by a measure of the tumour volume, grade and Gleason score[171], other studies have shown no significant correlation between PCA3 score and Gleason grade from biopsy [172]. One such study demonstrated a very high PCA3 level with no evidence of malignancy in a group of men [173].

Combination of serum PSA value with urine PCA3 analysis improves both measures, with a combined AUC of 0.71-0.75 [174]. PCA3 gained FDA approval as a diagnostic test for use in patients who had a prior negative prostate biopsy [139]. However, it is not a routinely used clinical test as it is relatively more expensive than a PSA test and is only available in some private clinics. Furthermore, apart from its use as a diagnostic marker, its use as a prognostic marker remains debatable in more aggressive tumours (Gleason pattern 4 and 5) with studies suggesting a biopsy is still required to differentiate low grade from high grade tumours [175].

Studies have also investigated the RNA of the transmembrane protease, serine 2, E-26 transformation-specific (ETS)-related gene erythroblastosis virus E26 oncogene homolog (ERG), (TMPRSS2-ERG) fusion gene in patient urine [176]. The TMPRSS2-ERG fusion is only found in about 50% of prostate cancers, limiting its use as a single biomarker and thereby necessitating its use in multiplexed assays with other biomarkers. One study demonstrated a higher sensitivity (0.73) of TMPRSS2-ERG when used in conjunction with PCA3 as compared to either assay alone [176]. Another large study of more than 1300 men revealed the combination of PCA3 and TMPRSS2-ERG

measured in urine out-performed serum PSA in a diagnostic setting (AUC of 0.71 to 0.77 and AUC of 0.61 respectively) [177].

However, the PCA3 and TMPRSS2-ERG assay also has limitations as this test is currently adjunctive to PSA, and trials to determine if this assay will perform well in the absence of PSA screening are lacking. Moreover, urine expression of PCA3 or TMPRSS2-ERG is determined relative to urine PSA mRNA [176, 177], as PSA transcript abundance is indicative of the relative yield of prostate cells in the urine sample, thereby if the PSA transcript levels are too low, the test will be uninformative [139].

### 1.8.3 Michigan Prostate Score (diagnostic biomarker)

The Michigan Prostate Score (MiPS) test emerged in 2013 and it incorporates the use of serum PSA level, and urine PCA3 and TMPRSS2-ERG mRNA detection. The TMPRSS2-ERG fusion is more common in younger men with early stage cancer and in patients with low serum PSA levels [178, 179]. The MiPS test is designed for use in patients with an increased PSA level who are likely to have initial biopsies, or in patients with a previously negative biopsy outcome who want a repeat biopsy. Scoring is from 1 to 100 reflecting the percent chance of finding any cancer on the biopsy with the results also providing information on a risk estimate for detecting prostate cancer of Gleason score 7 or more [177]. Together with a very high specificity of TMPRSS2-ERG (at 93.2%) [180], a study demonstrated an improved discriminatory ability for the combined test of PSA, PCA3 and TMPRSS2-ERG, an AUC of 0.88, as compared to each test alone with an AUC of 0.72 for PSA, 0.65 for PCA3 and 0.77 for TMPRSS2-ERG [181]. With the knowledge

of MiPS score before biopsy, 35-47% can be avoided, while this can delay diagnosis in 1.0-2.3% of high grade cancers [180, 182].

### 1.9 Novel Biomarkers for Prostate Cancer

Several potential biomarkers are under investigation for use in prostate cancer. These risk stratification biomarker tests are designed for guiding management decisions and appropriate counsel post-biopsy for patients regarding active surveillance versus intervention.

#### 1.9.1 Stockholm 3 (diagnostic biomarker)

The Stockholm 3 (STHLM3) susceptibility biomarker model is a personalised risk-based tool for diagnosis that combines plasma protein biomarkers such as PSA and fPSA amongst others, genetic polymorphisms (232 SNPs) and clinical variables such as age and history. STHLM3 has been produced and validated in a Swedish population without prostate cancer [183]. The STHLM3 model was developed and validated to identify high-risk prostate cancer (Gleason score of at least 7) with better test characteristics than that provided by PSA screening alone. This prospective, population-based, paired, screen-positive, diagnostic study of men without prostate cancer aged 50-69 years was primarily designed to increase the specificity compared to PSA without decreasing the sensitivity to diagnose high-risk prostate cancer. The main outcomes were number of detected high-risk cancers (sensitivity) and the number of performed biopsies (specificity). The STHLM3 training cohort was used to train the STHLM3 model, which was prospectively tested in the STHLM3 validation cohort. This combined model has shown an increased ability to identify high risk disease (Gleason score of 7 or more) with an AUC of 0.74 as compared to PSA with an AUC of 0.56, lowering the number of

biopsies by 32% using a PSA cut-off of 3ng/ml or more for recommending biopsy [184]. STHLM3 has demonstrated the potential to reduce over-detection and considerably reduce the number of biopsies whilst retaining the same sensitivity for Gleason score 7 or more cancers.

### 1.9.2 Prolaris (prognostic biomarker)

The Prolaris score is a quantitative measure of a 46-gene expression profile, which includes 31 cell-cycle progression (CCP) genes and 15 housekeeping genes determined from qPCR using RNA from prostate cancer tumour samples [185]. This test is used to stratify the risk of disease progression in prostate cancer patients serving as a prognostic marker and it requires either a biopsy or RP sample to predict tumour aggressiveness and recurrence [169]. It is recommended for men with very low to low risk disease on biopsy and a life expectancy of 10 years [186], allowing decision making for active surveillance verses surgery or radiation.

The CCP score is an independent predictor of BCR for RP patients and is strongly linked with time to death from prostate cancer. In addition, CCP is a stronger prognostic marker over other measured variables including PSA [187]. This test scores from 0-10, with an increase of each unit reflecting a doubled risk of disease progression. This combined with other factors such as PSA and Gleason score provides a report of 10 years' prostate cancer-specific mortality risk [169].

Another similar study also reported that CCP score (reflective of proliferative index) was predictive of BCR [188]. A further study demonstrated that in a

combined cohort with 582 patients, CCP score was linked with both BCR and metastatic disease [189].

The expression of CCP genes is directly correlated with tumour aggression and recurrence, with the ability to provide information on the risk of prostate cancer-related death using the Prolaris test. It can serve as a prognostic tool in patients considering definitive treatment for their cancer and in patients who are considering adjuvant therapy [169].

However, this test is expensive and is criticised for lack of cost-effectiveness [190]. Furthermore, the clinical utility of Prolaris test awaits evaluation by prospective, randomised clinical trials, which remain unlikely to be conducted [191]. In addition, the test still requires a biopsy to be taken.

### 1.9.3 Oncotype DX (prognostic biomarker)

The Oncotype DX is a tissue based assay that analyses a 17-gene expression panel by qPCR (12 cancer-associated genes and 5 housekeeping genes). It was discovered based on 441 RP samples from low to intermediate risk patients. From 732 candidate genes involved in multiple biological pathways, 288 were predictive of clinical recurrence and tumour multifocality, and 198 predicted aggressive disease following adjustment for PSA, Gleason score and clinical stage [192]. This test was further confirmed in 167 biopsies taken before RP to generate a multiple gene expression-based signature known as the Genomic Prostate Score (GPS). The GPS scores from 0-100. Further validation of this test in 395 needle biopsies from men who were candidates for active surveillance determined its ability to predict clinical recurrence,

cancer-associated death and adverse pathological features at the time of RP [192].

The Oncotype DX test was validated by another group which included patients with very low, low or intermediate risk of prostate cancer in which GPS scores showed correlation with BCR, adverse pathology (primary Gleason 4 pattern or any pattern of 5, pT3 disease) and metastatic recurrence [193], supporting an independent predictive role of GPS scores.

The use of Oncotype DX on an initial needle biopsy may thereby predict prostate cancer aggressiveness, and guide patients in decision-making with regards to active surveillance versus treatment [194]. According to the National Comprehensive Cancer Network guidelines, this assay may be used post-biopsy for very low to low risk prostate cancer patients with a 10 to 20-year life expectancy [186].

The lack of large and prospective assessments of GPS correlation with oncological outcome may limit the actual clinical benefit of this assay [184]. Furthermore, this test also requires a biopsy and therefore once again relies on accurate targeting of biopsies.

Taken together, the use of PSA may be enhanced by other biomarkers, which combine evaluation of protein, DNA and RNA in addition to DRE. Ultimately, this may reduce unnecessary biopsies and treatments, and allow earlier detection of the disease.

## 1.10 Single Nucleotide Polymorphisms (SNPs)

Over-treatment of prostate cancer necessitates the identification of individuals most at risk of developing the disease. At present, it is recommended that early and selective screening should be carried out in men with a positive family history (FH) [195]. Currently, the use of FH is the most common method for determining whether a man has increased risk of developing prostate cancer with 1.5 to 2.5-fold raised risk if there is an affected relative [196]. The use of FH for risk assessment in the general population only proves beneficial for men who are confident about their FH of prostate cancer [195]. Several genomic studies offer a promising method to stratify men in the general population who harbour increased risk for prostate cancer. Various genome-wide association studies (GWASs) comparing the germline genotypes of men with prostate cancer to controls without known disease have identified SNPs that are associated with increased susceptibility to the disease, known as prostate cancer risk-associated SNPs [197]. SNPs are a simple form of DNA variation within individuals and can occur throughout the genome. Over 100 prostate cancer risk-associated SNPs have been described with an estimation that such genetic loci increase the estimated proportion of the familial risk to 33% [198]. These risk predictor SNPs at present are a better measure of the genetic component of prostate cancer susceptibility. Studies have demonstrated that the combination of FH with SNPs provide essential information to better identify men who are at risk of developing the disease [195]. Although individual SNPs are only modestly linked with disease risk, their combination shows a greater association [199]. Only a subset of SNPs show association with aggressive metastatic disease [200]. Furthermore,

certain risk alleles affect PSA level, which could impact prostate cancer screening. Amongst the SNPs identified, at least 5 distinct loci within chromosomal region 8q24 harbour germline variants associated with prostate cancer. GWAS has further demonstrated an association between certain SNPs and disease risk including chromosomes 2p15, 3p12, 6q25, 7p15, 7p21, 8q24, 9q33, 10q11, 10q26, 11q13, 17q12, 17q24.3, 19q13, and Xp11 [201, 202].

### 1.11 D'Amico

The D'Amico classification model developed in 1998 is used for prostate cancer patient risk stratification, which is categorised into three risk-based recurrence groups including low, intermediate, or high-risk of BCR following surgery. It is a measure based on the clinical TNM stage, biopsy Gleason score and pre-operative PSA level [202]. It is a widely used approach to assess prostate cancer risk post localised treatment allowing a more informed decision regarding patient treatment [202].

The categorisation of risk is based upon a D'Amico risk score of 0-12 as follows:

Low risk is a result of a PSA of 10ng/ml or less, a Gleason score of 6 or less, and a clinical stage T1-2a with 0 points and risk of prostate cancer recurrence of less than 25% at 5 years post treatment. Intermediate risk is based on a PSA between 10-20ng/ml, a Gleason score of 7, and a clinical stage of T2b with 1 to 3 points and risk of 25-50% at 5 years post treatment. High risk is a result of a PSA more than 20ng/ml, a Gleason score of 8 or more, and a

clinical stage ofT2c-3a with 4 to 12 points and risk of more than 50% at 5 years post treatment.

Two groups investigated over 14,000 prostate cancer patients for the ability to predict cancer-specific and overall survival rates along with the clinical relevance of D'Amico classification in contemporary medicine. It was shown that patients with additional information available to them by D'Amico classification had a higher overall survival rate post treatment for their prostate cancer, mostly the patients with a high risk of recurrence [202, 203].

The original study demonstrated the test to be more useful in intermediate and high-risk patients compared to low-risk patients [204]. A validation study a few years later showed the overall 5-year BCR-free survival rate to be 84.6%, with 94.5% for low, 76.6% for intermediate and 54.6% for high-risk group [202]. Another study showed the hazard ratio of death (chance of death occurring in the intermediate and high-risk group/chance of death occurring in the low-risk group) from prostate cancer after surgery in patients with high or intermediate disease was 11.5 and 6.3, respectively, as compared to patients with low risk [203]. Another group reported D'Amico low-risk criteria not safe enough to identify candidates for active surveillance [205]. Due to the rise in multiple risk factors in prostate cancer, the D'Amico classification system may not be the most appropriate tool for evaluation of risk recurrence in those cases in low-risk cases.

### 1.12 mpMRI and PROMIS study

The diagnostic pathway for prostate cancer involves TRUS-biopsy in patients presenting with raised PSA levels. The disadvantages of TRUS-biopsy include

unnecessary biopsies of men without cancer, detection of clinically insignificant cancers, missed detection of clinically significant cancers, development of morbidity, bleeding, pain, and may cause serious sepsis. [206, 207]. A recent prospective study Prostate MRI Imaging Study (PROMIS) used multi-parametric magnetic resonance imaging (mpMRI) as a triage test to investigate its utility in avoiding unnecessary TRUS-biopsies and improved diagnostic accuracy in men against a reference test template prostate mapping biopsy (TPM-biopsy). TPM-biopsy is able to accurately characterise disease status in men at risk by sampling the entire prostate every 5 mm. Subjects with no previous biopsies and PSA concentrations of up to 15ng/ml were employed. They undertook mpMRI, which was followed by both TRUS-biopsy and TPM-biopsy. The test taking and reporting of each test was done blind to other test results. Of the 740 men, 576 underwent mpMRI before TRUS-biopsy and TPM-biopsy. On TPM-biopsy of 576 men, 71% had cancer with 40% having clinically significant cancer. For clinically significant cancer, mpMRI was more sensitive (93%) than TRUS-biopsy (48%) and less specific (41% for mpMRI compared to 96% for TRUS-biopsy). The study suggested that using mpMRI to triage men may allow 27% of patients to avoid a primary biopsy and diagnosis of 5% fewer clinically insignificant cancers. If subsequent TRUS-biopsies were directed by mpMRI findings, up to 18% more cases of clinically significant cancer might be detected as compared with the standard pathway of TRUS-biopsy for all. mpMRI used before initial biopsy, may reduce unnecessary biopsies by 25%. mpMRI may also reduce over-diagnosis of clinically insignificant disease and improve detection of clinically significant cancer [206].

## 1.13 Prostate Cancer Development

Prostate cancer is usually a relatively slow developing proliferative disease with no apparent symptoms for years. Only when the prostate becomes large enough to pressurise the urethra is when symptoms begin to appear. Symptoms include frequent urge to urinate, strain during urination, and bladder often seeming not fully emptied. Prostate cancer is an adenocarcinoma (glandular cancer) and its aggressive form commonly metastasises to the bone.

Prostate cancer is characterised by an imbalance in cellular differentiation [208]. With disease progression, a number of features are altered; the tissue architecture degrades [123], there is destruction of the basement membrane and glandular structure, there is a significant reduction in the number of basal cells (<1%) and a considerable increase in luminal cells (>99%) making up the tumour bulk [209]. Aberrantly differentiated luminal cells are highly proliferative and therefore actively cycling in the disease [210].

## 1.14 Genetic Basis of Prostate Cancer

Gene mutations can frequently occur in tumour suppressor genes and oncogenes altering their gene expression in cancer. Phosphatase and tensin homolog (PTEN), a commonly studied tumour suppressor gene is frequently deleted in prostate cancer [211]. The PTEN homologue deleted on chromosome 10 on 10q23.3 locus is a negative regulator of the phosphatidylinositol 3-kinase (PIK3)/AKT survival pathway [212], the signal transduction pathway contributing to cancer growth and survival in a number of human cancers including prostate cancer [213]. PTEN genomic deletion has been found in human tissues representing all stages of prostate cancer

development and progression including high grade PIN, primary prostate cancer and with a higher incidence in metastatic disease and castrate-resistant prostate cancer (CRPC) [211]. It has also been reported that PTEN deletion associated with early disease recurrence concurrently showed reduced AR expression in human prostate cancer tissue [211].

The gene fusion product resulting from the translocation of the promoter region of the androgen-induced TMPRSS2 gene with the TF ERG is one of the most common genetic events in prostate cancer, present in approximately 50% of all cases and accounting for 90% of prostate cancer fusions [214]. The TMPRSS2-ERG fusion is specific to prostate cancer, and is also detectable in precursor lesions, such as PIN, if these lesions are proximal to, or contiguous with, regions of cancer [215].

Primary prostate cancer can be sub-classified as a result of a recurrent set of mutually exclusive genomic alterations that are found early in cancer development [216]. The Cancer Genome Atlas project identified seven mutually exclusive genetic subtypes including ERG, Speckle-Type POZ Protein (SPOP), ETV1, ETV4, Friend Leukaemia integration 1 (FLI1), Forkhead box A1 (FOXA1) and Isocitrate dehydrogenase 1 (IDH1) [216], with about 75% of prostate cancers falling into one of the listed genetic subtypes, and about 25% remaining uncharacterised of the total 333 tumours analysed [216].

Whole genome sequencing (WGS) studies have identified additional genetic alterations providing evidence that primary tumours display multiclonality in parallel with multifocal disease. A WGS study demonstrated extensive

genomic heterogeneity within prostate tumours from a cohort of 5 patients with Gleason scores of 7-8 [217]. The same study demonstrated multiclonality in the tumour of a patient that was dissected into 4 regions, each of which harboured disease foci. The index lesion shared SPOP mutations and chromosomal deletions on chromosome 8 and 16 with one focus, however not in the remaining 2 dissected foci, which shared a deletion on chromosome 19 [217]. The study also found a previously unidentified recurrent amplification of MYCL associated with TP53 loss [217]. Likewise, morphologically normal prostate tissues have shown high levels of mutations and distinct ERG fusions that are present in malignant tissues [218], reflecting clonal expansions and the underlying mutational events present in both normal tissue and cancer [218]. This causes extensive branching evolution and cancer clone mixing as a result of the co-existence of several cancer lineages harbouring distinct ERG fusions within a single cancer nodule. It was shown that this subset of mutations was common in morphologically normal and malignant tissue or between different ERG-lineages, highlighting earlier or separate clonal cell expansions [218]. However, whether the clones of cells in normal tissue are produced by a pathological process or are a result of somatic mosaicism involving unexpectedly high mutation rates remains to be understood. The consequential clonal fields of cells may influence cancer development and/or contribute to multifocality and the existence of multiple cancer lineages in a single cancer mass [218].

Where gradual acquisition of genomic alterations is commonly thought to be the primary driver of tumourigenesis, other events that accelerate the process could include chromothripsis and chromoplexy [219]. Chromothripsis, a huge

and catastrophic reshuffling of entire chromosomes or regions of chromosomes, and chromoplexy, the complex rearrangements that could arise from numerous rounds of DNA repair, may account for the rapid tumourigenesis and metastasis [220, 221].

Patterns of consistent allelic loss reflects the reduction or loss-of-function of putative tumour suppressor genes in prostate cancer. Frequent events include loss of heterozygosity at chromosomes 8p, 10q, 13q and 17p affecting genes such as NKX3.1, PTEN, Rb and p53 [222].

### 1.15 Castration-Resistant Prostate Cancer

There is consensus that the initial stage of prostate cancer depends on androgens for growth and thereby can be effectively treated by androgen deprivation therapy (ADT) [223, 224]. However, almost all cases invariably recur within 2-3 years with a more advanced and aggressive form of prostate cancer known as CRPC whereby the cancer acquires an androgen deprivation-resistant phenotype for which there is currently no effective treatment [223, 225]. The prevailing model suggests that CRPC development is initiated by adaptation of previously androgen dependent cells [226].

In CRPC, the AR is constitutively expressed by a number of mechanisms resulting in the expression of AR target genes indicating the vital interplay between AR and its signalling pathway (Figure 9) [227].

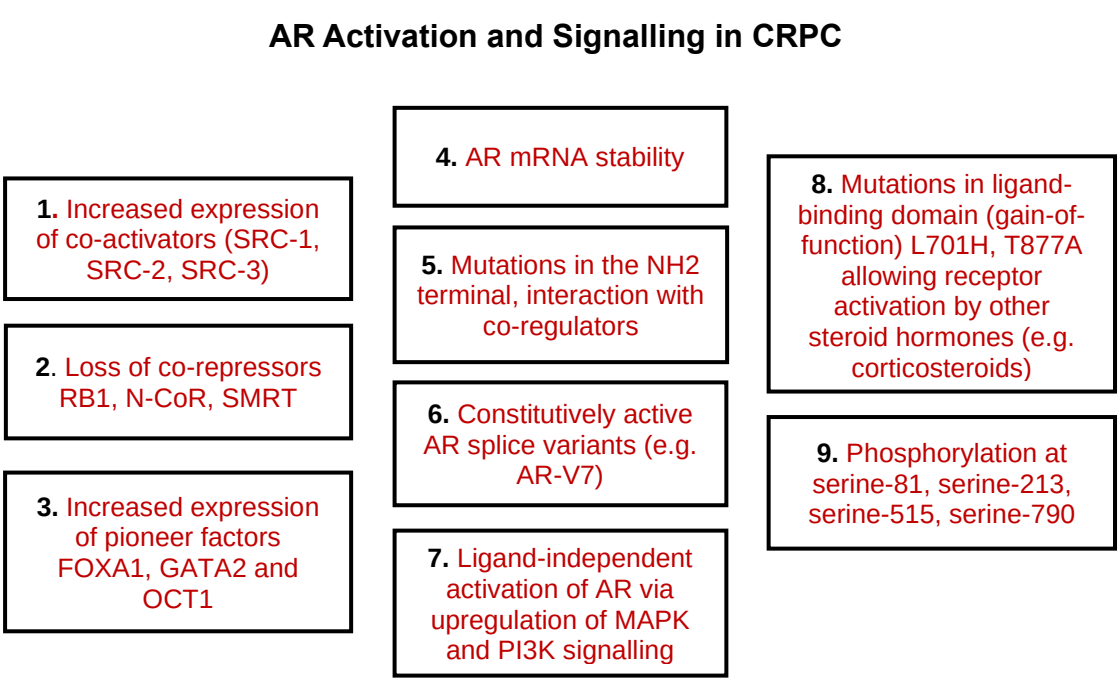


**Figure 9. Various mechanisms of androgen receptor (AR) activation in castration resistant prostate cancer (CRPC).**
1. Increased expression of steroid receptor co-activator (SRC 1,2 and 3) has poor prognosis [228]. 2. Loss of tumour suppressor gene RB transcriptional co-repressor 1 (RB1) enhances AR activity via E2F1 transcription factor activation to induce resistance [229], decreased expression of co-repressors nuclear receptor corepressor (N-CoR) and silencing mediator of retinoid and thyroid receptors (SMRT) may lead to resistance [230]. 3. Increased expression of pioneer factors Forkhead box A1 (FOXA1), GATA binding protein 2 (GATA2) and Octamer transcription factor (OCT1) has shown poor prognosis may be due to hyper-sensitising cells [231]. 4. Increased AR mRNA expression due to gene amplification [230]. 5. Mutations in the N terminal of AR influences downstream interactions with co-regulators [232, 233]. 6. Constitutive activity of AR splice variants such as AR-V7 promote therapy resistance [234]. 7. Upregulation of growth factor signalling pathways mitogen-activated protein kinase (MAPK) and phosphatidylinositide 3-kinase (PI3K) induces ligand-independent activation of AR [235, 236]. 8. Ligand binding domain mutations allow AR activation by other steroid hormones [237, 238]. 9. Increased AR phosphorylation at different amino acid sites may occur under low androgen levels which sensitises the AR [239].

## 1.16 The CSC Hypothesis

At present, two conflicting schools of thought of carcinogenesis exists [240] (Figure 10); the conventional stochastic model suggests that all cells in a heterogeneous tumour have an equal probability of acquiring mutations and initiating a tumour. Conversely, the hierarchical model upon which the CSC hypothesis is based, suggests only a minor distinctive subset of cancer cells in the population have the capacity to initiate a tumour, whereas the majority of tumour cells are differentiated with limited replicative ability [241]. Currently, anti-cancer therapies are based on the conventional model and have not had success with curing cancer, which compels attention to be directed to the hierarchical model of CSCs [240], however, the CSC perception remains a controversial area.

**Figure 10. Two carcinogenesis models of prostate cancer**
The classic stochastic model (A) depicts all cells in a heterogeneous tumour can acquire mutations and can equally initiate a tumour. The cancer stem cell (CSC) model (B) suggests that only a small number of CSCs have the ability to generate a tumour, whereas other population of tumour cells are differentiated with only limited replicative ability [242].

CSCs with tumour-initiating ability were initially hypothesised based on transplant experiments showing a heterogeneous cell population with differences in self-renewing ability and reconstitution of the original tumour following transplantation [243, 244]. The CSC model is emerging as the more widely accepted model for cancer initiation with a subset of cancer cells possessing CSC characteristics discovered in a number of cancer tissues such as haematopoietic system [245], breast [246], prostate [247] [248, 249],

lung [250], melanoma [251], colon [252], pancreas [253] and bladder [254]. Most of these putative CSCs have been identified using normal SC markers as they are analogues of normal SC and therefore share common markers and behaviours, including high proliferative potential, self-renewal and ability to generate new tissue and undergo symmetric or asymmetric cell division [240].

### 1.17 CSC Characteristics

Aponte and Caicedo recently reviewed the SC properties as the ability to self-renew, ability to give rise to progeny capable of differentiating into diverse cell types, and the existence of a SC niche in which the SCs reside. The term “stemness” is used to refer to such aforementioned properties and correspond to cells devoid of differentiation markers [255]. Malignant cells undergo all aspects of stemness, but instead of sustaining tissue homeostasis, they promote progression of cancer [255].

### 1.18 Prostate CSCs

A study by Collins et al. was first to identify prospective prostate cancer cells [247]. Whilst this study showed the replicative potential, colony forming ability and differentiation capacity of the putative CSCs, it did not show the gold standard at the time, which is the ability of a CSC to form a tumour in mice. Since this publication other groups have also worked on prostate SCs. A study by Heer et al. used the same markers as Collins et al, α2β1 integrin and CD133, to subdivide prostate basal cells into SC ($\alpha2\beta1^{hi}/CD133^{+}$) and TA cells ($\alpha2\beta1^{hi}/CD133^{-}$) [248].

A further study using the same markers showed low detectable levels of AR in the SCs and TA cells, which was in contrast to the original papers. Activity

of AR was shown by the expression of low levels of AR regulated genes PSA, KLK2 and TMPRSS2 [249].

Contradictory evidence suggests that (i) prostate CSC can originate from the luminal compartment [256, 257], (ii) prostate cancer is derived from intermediate progenitor cells with acquired ability to self-renew [27], or (iii) CSC residing in the basal compartment initiates the disease [247].

It has been reported that hyperplastic and tumour cells in *PTEN* knockout mouse model of prostate cancer have a phenotype of luminal epithelial progenitor cells, including the overexpression of CK8, CK19 and Sca-1 luminal cell and progenitor cell markers. However, tumour cells were negative for the expression of basal epithelial cell cytokeratins. Furthermore, AR expression was detected at all stages of tumour development [256, 257].

Unlike studies that solely report on luminal phenotype of prostatic carcinoma, an early study indicated co-localisation of basal and luminal cell cytokeratins expression in human prostatic tumour tissue of primary and hormone-independent prostatic carcinoma. Cells positive for K14 (basal cell marker) and $K_{basal}$ (stain for basal cell compartment in human prostate including CK5) were not detected in the tumours which indicated a stem cell phenotype was not present, however $K_{basal}$ and K18 (luminal cell marker) were detected in both primary and hormone-independent prostate cancer tissue postulating the presence of transit amplifying cells responsible for the neoplastic transformation [27].

Growing evidence strongly supports initiation of prostate cancer from a CSC residing within a basal niche [247, 258-260]. Xenotransplantation experiments

have further shown that less than 100 cells of tumour initiating fraction of human cells from prostate biopsies are needed to generate a new tumour in mice and that these cells exhibit a basal phenotype [64].

Rajasekhar et al. identified a small subset of stem-like human prostate tumour initiating cells (TICs) that did not express AR or PSA. These cells exhibited SC characteristics and multi-potency as shown by *in vitro* sphere formation and *in vivo* tumour initiation, respectively. The putative prostate CSCs represented an undifferentiated subtype of basal cells that were purified from prostate tumours using the co-expression of the human pluripotent SC marker T cell receptor alpha locus (TRA-1-60), CD151 and CD166. The triple marker positive cells demonstrated high capacity for self-renewal and differentiation, and were able to recapitulate the original tumour heterogeneity in serial xenotransplantations, suggesting a tumour cell hierarchy in prostate cancer development. These cells also exhibited high nuclear factor-kappa B (NF-$_K$B) activity pointing to a potential mechanism involved in the CSC biology [261]. This study suggests the triple markers as driver of stemness for sphere formation and tumour initiation. This study did not test for the presence of the CD133 marker in the same population of cells.

Studies have also investigated the hedgehog pathway to target CSCs. One such study used an inhibitor erismodegib to investigate the mechanisms that regulate SC characteristics and tumour growth in prostate cancer. Prostate CSCs were isolated from human tumours based on positive expression of CD44 and CD133. Use of the inhibitor demonstrated reduced cell viability by suppressing miR-21 and reduced spheroid formation, and induction of apoptosis by activating caspase-3 and cleaving poly-ADP ribose polymerase

(PARP). The hedgehog pathway was also inhibited by inhibiting Gli transcriptional activity and Gli nuclear translocation in the CSCs. In addition, erismodegib inhibited pluripotency maintaining factors Nanog, Oct-4, c-Myc and Sox-2. The inhibition of polycomb-group gene Bmi-1, which is overexpressed in prostate CSCs by the inhibitor was regulated by upregulation of miR-128. The inhibitor also suppressed epithelial-to-mesenchymal transition (EMT) by upregulating E-cadherin and inhibiting N-cadherin, Snail, Slug and Zeb1 through regulation of the miR-200 family. It also inhibited motility, invasion and migration of the CSCs. The study also showed the inhibitor inhibited tumour growth in vivo. The study highlighted targeting the hedgehog pathway may result in the depletion of CSCs and suggested the CSCs to be drivers of the processes studied [262].

A recent study demonstrated the knockdown of disabled homolog 2-interacting protein (DAB2IP), a novel tumour suppressor, led to the transformation of immortalised normal human prostate epithelial cells derived from androgen receptor negative basal cell population into tumorigenic cells that acquired stem cell phenotype. These included increased formation of spheroid prostaspheres, increased exclusion of Hoechst dye, and increased *in vitro* migration and invasion. The stem-like cells showed increased chemo-resistance to docetaxel. DAB2IP has previously been shown to play a crucial role in suppressing stemness through modulating CD117 transcription [263]. These cells exhibited $CD44^{+}/CD24^{-}$ instead of $CD177^{+}$ indicating existence of another regulation mechanism. It was shown that CD44 alongside being a SC marker is also a driver for prostate CSC formation in which CD44 expression is modulated by the Wnt pathway via direct interaction with the promoter. The

use of Wnt inhibitor and docetaxel synergistically to target CSCs and their progeny non-CSCs enhanced the therapeutic efficacy of CRPC both *in vitro* and *in vivo* models showing reduction in chemo-resistance of knock down cells. The study suggested driver roles of the CSCs in Wnt signalling [264].

The aforementioned studies indicate that the stemness features of the putative prostate CSCs are drivers of tumourigenesis, metastases and therapy resistance.

### 1.19 Prostate CSC Markers

Alongside using $CD44^{+}$, $\alpha2\beta1\text{-integrin}^{high}$ and $CD133^{+}$ as CSC marker, are other important markers that have been used to identify and isolate prostate CSCs.

For example, ATP binding cassette (ABC) transporters, which are proteins that play a vital role in the efflux of drugs have also been used to enrich CSCs, however they are also expressed in normal SCs [265, 266]. The use of a unique phenotype of CSCs, including at least two markers that are only present in CSCs and not normal SCs is more desirable for isolation of CSCs [265].

Recently, it is becoming more evident that certain aldehyde dehydrogenase (ALDH) isoenzymes may fit this purpose as a marker for CSCs, and may also have functional roles in differentiation, self-protection and expansion [267]. The family member ALDH1 is a marker for normal and malignant mammary SCs in humans and is also a predictor of poor clinical outcome [268]. The functional activity of ALDHs has been extensively used to identify and purify CSCs in the breast [269], ovaries [270], bone marrow [271], lungs [272],

prostate [273], colon [268] and pancreas [274]. Prostate cancer cell lines PC-3M-Pro4luc and C4-2B with high ALDH activity have shown both increased clonogenicity and migratory capacity *in vitro* and furthermore, the PC-3M-Pro4luc cell line has enhanced tumourigenicity and increased metastatic ability *in vivo* [273].

The self-renewal and regeneration characteristics of CSCs allow their prolonged survival in tumours, which makes them potential candidates for acquisition of genetic and epigenetic alterations leading to a more aggressive cancer and therapy resistance. In short-lived differentiated cells however, the opportunity to accumulate mutations becomes reduced [275].

## 1.20 Treatments for Prostate Cancer

Treatment for prostate cancer is currently based on the stage of the disease (Figure 11). Once a Gleason score is assigned, the cancer can be separated into either low-grade organ-confined disease, locally advanced or high grade metastatic disease. Localised prostate cancer can be separated into low risk (PSA 10ng/ml or less, Gleason score of 6 or less, clinical stage T1-2a) [202].

### 1.20.1 Treatments for Low Risk Prostate Cancer

Low risk localised prostate cancer is generally defined as PSA less than 10ng/ml, Gleason score 6 or less, clinical stage T1-2. The National Comprehensive Cancer Network guidelines [276] have further divided low risk disease into very low and low risk groups. The very low risk group is characterised as PSA less than 10ng/ml, Gleason score 6 or less, clinical stage T1c, presence of disease in fewer than 3 biopsy cores, 50% or less

prostate cancer involvement in any core and PSA density less than 0.15ng/ml/g [277].

In low-grade non-malignant tumours, the cancer cells are well differentiated forming intact glands, thus the treatment option can be active surveillance.

Active surveillance involves the deferral of treatment initially for a proportion of patients detected with low risk disease. Men are followed carefully with serial PSA monitoring and repeat biopsies [278]. Serial mp-MRI is also recently being used in diagnosis to identify patients with clinically significant cancer and larger disease burden who would most likely benefit from intervention [279].

Prostate Testing for Cancer and Treatment (ProtecT) trial is a large UK based randomised trial that provided the first evidence comparing the long-term impacts of active surveillance, surgery (RP) and radiation on outcomes such as prostate cancer-specific mortality, all-cause mortality, quality of life, incidence of metastases and disease progression of patients aged from 50 to 69 with localised prostate cancer, at a median of 10 years of follow-up. Results showed that all 3 treatments resulted in similar, very low rates of prostate cancer related death. Surgery and radiotherapy reduced the risk of cancer progression over time as compared to active surveillance, but caused more side effects. Some men in the surgery group experienced urine leakage and problems with sex life, whereas some men in the radiation group experienced bowel problems. Overall quality of life such as anxiety and depression, was not affected by any treatment at any time [280].

No significant difference was observed in prostate cancer-related death among the active monitoring group (8 deaths overall), surgery group (5 deaths

overall) and radiation group (4 deaths overall) from a total of 1643 men that participated in the trial. In addition, no significant difference was observed in the number of deaths from any cause (169 deaths overall) among the 3 groups. Furthermore, development of metastases was significantly higher in the active monitoring group (33 men), than in the surgery (13 men) or the radiotherapy group (16 men). Significantly higher rates of prostate cancer progression were found in the active monitoring group (112 men), than in the surgery group (46 men) or the radiotherapy group (46 men).

Radiotherapy is another option for the treatment of organ-confined disease in which ionising radiation is exposed to the tumour to limit its growth. There are two methods by which radiation can be delivered, the first method is the external beam radiation therapy which utilises external source of radiation to target the tumour. The second method is the brachytherapy in which several radioactive seeds are implanted into the prostate next to the tumour through which radiation can be emitted. A low dose rate permanent implant of radioactive seeds using isotopes such as iodine 125, palladium 103 or cesium 137, delivers a high intraprostatic radiation dose over an extended 6-month treatment interval. The average dose rate is about 10 cGy per hour. A high dose rate brachytherapy involves the temporary implantation of hollow source-carrier needles (or catheters) delivering a high activity iridium 192 source at about 100 Gy per hour with a treatment of 6-8 minutes [281].

The first method of external beam radiation offers treatment which is less invasive but with more side effects, whereas the second method of brachytherapy limits radiation dose to surrounding tissues minimising undesirable side effects [282].

More recently, the use of cyberknife, a non-invasive method of delivering high radiation dose at a more accurate tumour location, has shown improved patient tolerance and treatment outcome in comparison to brachytherapy [283].

### 1.20.2 Treatments for Intermediate and Advanced Prostate Cancer

Intermediate risk is defined as a PSA between 10-20ng/ml, Gleason score of 7, clinical stage T2b, and high risk is defined as a PSA more than 20ng/ml, Gleason score of 8 or more, clinical stage T2c [202]. In locally advanced prostate cancer, the tumour cells break through the capsule of the prostate gland and may spread to nearby tissues or lymph nodes (PSA higher than 20ng/ml, Gleason score between 8-10, T3, N0, M0/T4, N0, M0/any T, N1, M0). In advanced/metastatic prostate cancer, tumour cells spread to other parts of the body (any T, any N, M1). The status of the primary tumour is assigned from organ-confined to fully invasive (T1-4), with or without lymph node involvement (N0 or 1), and the presence and degree of distant metastases (M0 and 1a-c) [284].

In high grade malignant prostate cancer, the cells are poorly differentiated with compromised tissue architecture indicating spread outside of the prostate. Current treatments for metastatic prostate cancer are mainly ineffective resulting in poor prognosis.

ADT is usually recommended as a treatment option in metastatic prostate cancer [285]. It exploits the dependency of tumours on androgens for development by either removing circulating androgens or by blocking their binding to the AR. The following are some of the main hormone ablation

therapies, which are often used in the following order, however the exact treatment plan may differ depending on other factors that a patient may present.

1. Finasteride is a gonadotropin-releasing hormone (GnRH) antagonist that blocks 5α-reductase activity by binding to the GnRH receptor [286]. It is used to treat patients with BPH before any signs of prostate cancer [88].
2. Zoladex is a synthetic decapeptide analogue of luteinising hormone-releasing hormone (LHRH) used as a potent inhibitor of pituitary gonadotropin secretion [287]. It removes testosterones from testes and is used as medical castration. It is approved for use in combination with antiandrogens (to minimise side effects such as flare) for locally advanced prostate cancer. This combination treatment starts 8 weeks before radiation and continues during radiation. Zoladex is also approved to lessen or relieve symptoms of advanced prostate cancer [288].
3. Hydroxyflutamide/flutamide is a non-steroidal AR antagonist that is involved in the inhibition of androgen mediated transcription [289]. It is a 1$^{st}$ generation antiandrogen approved in 1989. It is used to treat locally advanced prostate cancer or metastatic castration sensitive prostate cancer (mCSPC). It is used with a LHRH agonist to provide combined androgen blockade [290]. Due to significant gastrointestinal toxicity, it has been mostly replaced by the antiandrogen bicalutamide.
4. Bicalutamide is a non-steroidal AR antagonist, an anti-androgen that binds to the AR thereby preventing ligand binding [291]. Bicalutamide is

a 1st generation antiandrogen approved in 1995 for the treatment of locally advanced and metastatic prostate cancer. It is used with LHRH agonist and has a 4-fold greater affinity for AR compared to flutamide [292].

5. Stilbestrol/diethylstilbestrol (DES) binds strongly to estrogen receptors alpha and beta, inhibiting 5α-reductase inactivating testosterone [293]. It was the first endocrine treatment for prostate cancer as shown by Huggins et al [294]. Surgical castration (orchidectomy) and DES were used as first line treatment options for CRPC over the next two decades with reported efficacy [295, 296]. However, increased mortality from cardiovascular and thromboembolic toxicities were reported [297]. The discovery of LHRH agonists, which showed similar efficacy to that of orchiectomy and DES as first line therapy, but without the concerning toxicities, led to a loss of interest in DES [298]. DES has significant activity in CRPC and remains a palliative option for symptomatic CRPC in patients that are not fit for chemotherapy [299]. DES has an acceptable toxicity profile in the management of patients with symptomatic CRPC when used at a dose of 1-3mg [299].
6. Abiraterone – used to block the action of the enzyme CYP17, thereby blocking the androgen biosynthesis [300]. Abiraterone is approved to be used with prednisone to treat high-risk **mCSPC** and metastatic CRPC **(mCRPC**) [301]. In 2011, abiraterone was approved for use with prednisone following docetaxel treatment for mCRPC. In 2012, it was approved for use with prednisone before docetaxel treatment for mCRPC [302].

7. Enzalutamide – a nonsteroidal antiandrogen directly binds to the AR and inhibits the binding of androgens, AR nuclear translocation, and AR-mediated DNA binding [303]. Enzalutamide is a 2nd generation anti-androgen designed to overcome resistance to 1st generation antiandrogens, and avoid antagonist-to-agonist conversion, which is often seen in the 1st generation anti-androgens [302]. It is more potent with a 5 to 8-fold higher binding affinity for AR than bicalutamide [304]. Enzalutamide is used with flutamide and radiation therapy in localised prostate cancer, it is also approved to treat non-metastatic CRPC following findings from the PROSPER trial [305]. It has also shown significantly improved progression-free survival compared to bicalutamide in metastatic prostate cancer [306]. In 2012, enzalutamide was approved for use following docetaxel treatment for mCRPC. In 2014, it was approved for use before docetaxel treatment for mCRPC [302].

Chemotherapy is an important treatment modality in metastatic CRPC that is hormone-refractory upon ineffectiveness of ADT. FDA approved drugs generally used to treat CRPC include docetaxel, cabazitaxel and mitoxantrone. These drugs mainly function by targeting dividing cells, causing disruption of microtubule function by stabilising tubulins, and thereby hindering mitosis through prevention of depolymerisation [307]. Before the approval of docetaxel with prednisone in 2004, treatment for mCRPC was limited to agents with no evidence of survival benefit such as mitoxantrone [302]. Since the approval of docetaxel, other agents such as cabazitaxel have been

approved by FDA for treatment of mCRPC with established survival benefit [302]. Docetaxel is the most common chemotherapy used to treat mCRPC, however, in certain circumstances if side effects are too severe, mitoxantrone may be offered as first-line treatment to improve quality of life. Cabazitaxel with prednisone was approved in 2010 as a second-line treatment after docetaxel treatment in mCRPC [302].

However, in almost all cases, the tumour ultimately acquires a chemotherapy resistant phenotype making chemotherapy largely ineffective, thus development of novel therapies for CRPC is required.

Immunotherapy is also used to treat asymptomatic or minimally symptomatic mCRPC that no longer responds to ADT. Sipuleucel-T comprises of autologous peripheral blood-derived mononuclear cells that are cultured with a PAP and granulocyte-macrophage colony-stimulating factor (GM-CSF) fusion protein. Sipuleucel-T, approved in 2010, is the only FDA approved immunotherapy to date based on the results of 3 trials that showed its clinical efficacy [308].

Sipuleucel-T has shown robust activation of antigen-presenting cells (APCs), T-cell responses specific to the antigens, and increased cytokine association with T-cell activation. The number of activated APCs, which is measured by CD54 upregulation showed positive correlation with improved overall survival [309].

A combined analysis of two of the trials showed an improved overall survival (over 4 months) in patients treated with sipuleucel-T compared to placebo control. However, the primary endpoint of improved progression-free survival

was not met [310]. The third trial (IMPACT) further showed a 4.1 month increase in overall survival in patients with mCRPC treated with sipuleucel-T compared the control, however with no difference in time to progression [311].

Despite the approval of sipuleucel-T, subsequent progress in the field of prostate cancer immunotherapy development has been limited by unsatisfactory results with novel vaccination approaches and by the development of resistance to immune checkpoint blockade [308].

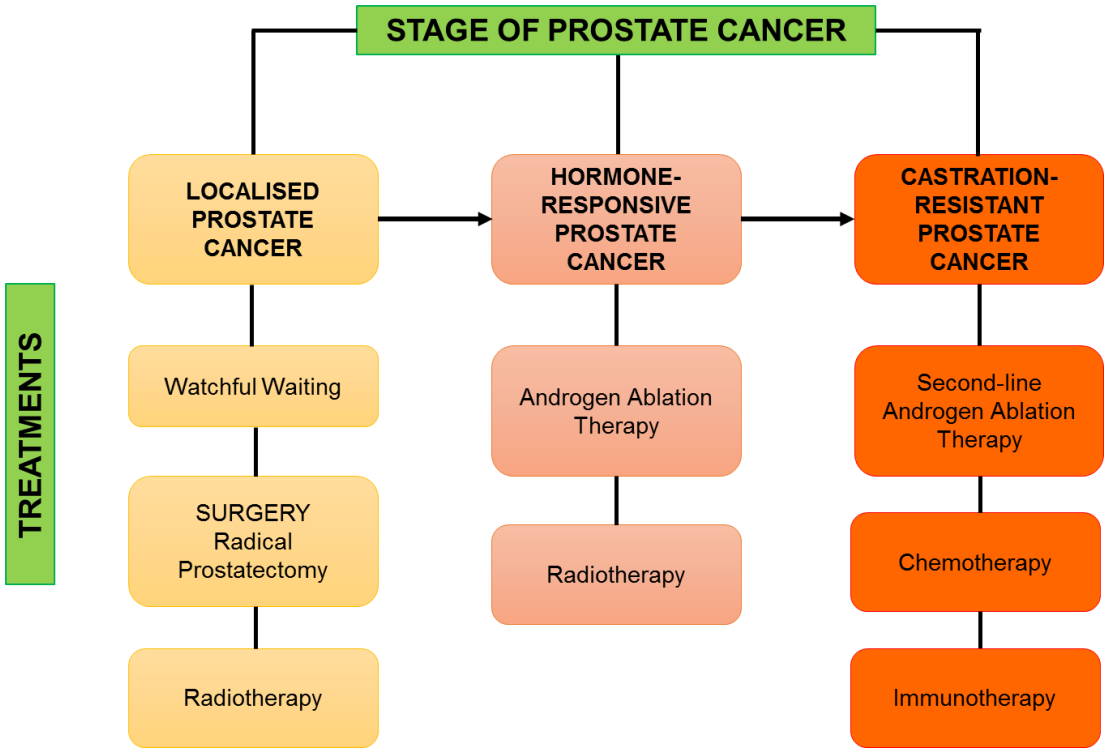


**Figure 11. Stages of prostate cancer and treatment options.**
Localised cancer is managed with either active surveillance, radical prostatectomy or radiotherapy. Hormone responsive cancer is treated with androgen deprivation therapy or radiotherapy. Castration resistant cancer can be treated with second-line androgen deprivation therapies, chemotherapy or immunotherapy.

## 1.21 CSC Differentiation Therapy

Current treatment strategies using monotherapy or combined therapy such as ADT and chemotherapy, have largely failed due to the heterogeneous nature of prostate cancer, in which ADT therapy fails to target AR negative cancer cells, and the capacity of chemotherapy to only target proliferating cancer cells and not quiescent cells, both resulting in resistance. This could lead to an enrichment of the therapy resistant CSC population resulting in tumour relapse. However, the challenge of targeting CSCs cannot be underestimated and can be attributed to the protected niche in which they reside and their quiescent phenotype. An exploitation of the phenotypic differences between CSCs and their differentiated counterparts through differentiation therapy could potentially enable elimination of CSCs [312]. Promoting differentiation of CSCs involves stimulating a quiescent CSC to undergo cycling and the use of drugs to push the cells to differentiate into proliferative progenitor cells [313]. In general, CSCs display a more chemotherapy-resistant phenotype, due to multidrug resistance (MDR), and increased expression of ABC transporters [314]. Moreover, CSCs have an enhanced DNA repair mechanism in glioma [315], anti-apoptotic pathway in glioblastoma [316], and slower cell-cycle kinetics in atypical teratoid/rhabdoid tumors [317]. Some studies have demonstrated the potential of differentiation therapy in leukaemia, however any potential use in prostate cancer has yet to be realised [313].

### 1.22 Clonal Evolution of Prostate Cancer

Recent studies have highlighted the complexity of prostate cancer and new techniques have allowed the tracking of prostate cancer within individual patients. Clonal populations of cancer cells undergo persistent evolution due to environmental conditions [219]. The concept of tumour evolution was proposed by Nowell in 1976, based on cytogenetic data [318]. According to this early model, a cell of origin acquires genetic alterations promoting neoplasia. Further genetic instability fuels clonal expansion of “fit” clones that ultimately results in advanced malignancy, metastasis, and emergence of therapy resistance [318].

Compared to advanced disease, primary tumours display lower mutational events and genomic instability [216, 319]. Upon disease progression to metastatic and castration resistant phases, there is increased mutations, structural rearrangements, and genomic instability. Such genomic alterations suggest clonal evolution and sub-clonal selection against environmental pressures. Alterations in AR signalling following metastatic spread occurs in more than 50% of metastases, and remains a key target for therapies [319]. Frequently observed genomic alterations in metastatic CRPC include TP53 mutations or loss, PTEN loss and associated PI3K pathway defects, DNA repair pathway deficiencies, and amplification or mutation of AR [319-323]. Differentiation between alterations that promote metastasis and alterations that promote treatment resistance has been difficult due to the use of tissues that are from extensively treated CRPC patients to study metastasis. Where some studies have pointed to genomic AR mutations as a driver of metastasis

[216], others have indicated it to be a driver of treatment resistance [321, 324-326].

One investigation of sub-clonal structure within CRPC metastases showed that different AR gene alterations can occur in different metastatic foci within a single patient, an indication that the alterations occurred in response to treatment, following metastatic spread [325]. Furthermore, it was indicated that TP53 loss, PTEN loss, and DNA repair pathway alterations occurred prior to metastatic spread [325]. In addition, the TP53 and PTEN inactivation was more frequent in mCRPC as compared to primary tumour, indicative of driver roles in metastasis [216].

Early studies using rapid autopsy demonstrated varied PSA immunostaining across and within metastatic foci, indicating that multiple sub-clonal populations existed with metastases [327, 328]. Studies investigating genome wide copy number and targeted sequencing have shown that metastases within a patient shared common mutations and thus shared clonal origins [329, 330]. However, it was also revealed that these tumours harboured sets of divergent mutations, highlighting that sub-clonality existed between individual tumour foci.

Robbins et al, showed shared amplifications at chromosomes 5p and 14q along with a set of shared somatic mutations in 3 spatially distinct metastases from a single autopsy subject [330], which indicated a clonal progenitor cell likely from the primary tumour. This study was limited by the absence of the availability of primary tumour tissue from the same patient [330]. Likewise, Liu et al, demonstrated that 80 anatomically distinct metastatic foci isolated from 24 patients with CRPC shared a clonal origin in most patients [329]. Notably,

metastases shared clonal copy number variations with the primary tumour in 5 patients with tissue availability [329].

A generally accepted model of metastasis depicts sub-clonal populations colonising metastatic sites in waves originating from the primary tumour [331]. Sub-clonal populations within the primary tumour compete for dominance and are selected for survival and growth by environmental selection pressures [332]. A recent longitudinal study performed on 4 patients revealed that metastases were seeded in temporally separated waves originating from the primary tumour [321]. It was presumed that as the primary tumour acquired more mutations, structure variations, and alterations in copy number, new metastatic sub-clonal populations were released to seed and re-seed organ sites [321]. Another similar study, which investigated a single case, demonstrated that anatomically different metastatic sites of a patient with CRPC shared several genetic alterations which included high level amplification of the AR locus, *TP53* loss, *PTEN* loss, and *SPOP* mutation reflecting the clones to be monoclonal in origin [333]. Furthermore, investigation of the micro-dissected primary tumour exhibited that a small well-differentiated Gleason pattern 3 lesion displayed PTEN negative immunohistological staining. In addition, DNA sequencing of the lesion showed the same 4 base pair deletion in *PTEN* found in the metastatic clones concurrent with *TP53* mutation, indicating that this lesion harboured the progenitor cell that seeded distant metastases [333]. Interestingly, the surrounding higher grade Gleason pattern 4 tumour tissue did not contain the same underlying mutations as the metastases [333]. These studies suggest

that the primary index lesion is not always responsible for harbouring the lethal cell clone that is accountable for seeding distant metastasis [219].

Along with monoclonal metastatic evolution, polyclonal patterns have also been defined. It was shown that 50% of the subjects in a rapid autopsy study displayed polyclonal seeding of multiple metastatic sites [325]. Herein, polyclonal seeding was described as multiple genetically distinct sub-clones colonising a single metastatic site. Interestingly, all cases of polyclonal seeding involved genetic mutations with known association in treatment resistance, suggesting that polyclonal seeding and inter-clonal cooperation may be needed for therapy evasion. Together, these studies have highlighted that the initiation of metastatic seeding may be by monoclonal or polyclonal population of tumour cells that originate in both the primary tumour and metastases in other sites [321, 325].

ADT confers a selection pressure upon tumour foci, such that cell clones that harbour genomic alterations including AR point mutations promote ADT derived resistance by seeding and reseeding multiple sites [325]. Such rare sub-population of cells within tumour foci promote ADT escape by reactivating AR through acquired mutations, copy number alterations, or induce constitutively active AR splice variants [334]. A targeted sequencing study by Carreira et al, further demonstrated this concept by showing AR amplification and the appearance of AR point mutations in response to treatment with abiraterone acetate or enzalutamide in tumour samples obtained from ERG positive patients prior to, during and following treatment [324].

### 1.23 Treatment Resistance

Epithelial plasticity may enable cancer cells to adapt in response to treatment resulting in tumour cells exhibiting reduced to no expression of AR and the frequent display of neuroendocrine features, both of which are recognised mechanisms of resistance to AR-directed therapy [335]. However, the molecular basis of such resistant cell types remains largely unknown. The prognostic outcome of neuroendocrine (CRPC-NE) tumours is poor as a result of late recognition, heterogeneous clinical features, and a shortage of effective systemic therapies [336, 337]. A recent study demonstrated significant genomic similarities between castration-resistant adenocarcinoma (CRPC-Adeno) and CRPC-NE histologies by whole exome sequencing data of metastatic biopsies from patients, wherein, analysis of serial progression samples pointed to a model most consistent with divergent clonal evolution. Unlike the genomic landscape, epigenomic analysis of genome-wide DNA methylation showed marked epigenetic differences between CRPC-NE and CRPC-Adeno which also designated cases of CRPC-Adeno with clinical features of AR-independence as CRPC-NE, indicating that epigenetic modifiers may play a role in the treatment resistance state. This study supported divergent evolution of CRPC-NE from one or more CRPC-Adeno cells by adaptation as compared to linear or independent clonal evolution, with selective pressure of AR-wild type sub-clonal population and acquisition of new genetic and epigenetic drivers linked with reduced AR signalling and epithelial plasticity [335].

## 1.24 Factors Contributing to Prostate Cancer Progression

A complex interplay of prostate cancer cells with the surrounding stroma, AR signalling, EMT and other signalling pathways lead to progression of the disease.

### 1.24.1 Role of the Stroma in Prostate Cancer Progression

Stromal cells such as fibroblasts and myofibroblasts are involved in hormone signalling and thereby control the stromal-epithelial interactions in the primary tumour setting [338]. Similar to epithelial cancer cells, the surrounding stromal cells undergo progressive histopathological, molecular and functional alterations in prostate cancer [339]. While the main focus of most prostate cancer studies involves the use of epithelial cancer cells, tissue recombination assays have been used to demonstrate the significance of the stroma. It has been demonstrated that cancer-associated fibroblasts (CAFs) isolated from human prostate cancer tissue induce the benign prostate epithelial cell line BPH-1 to form tumours [18, 340]. However, normal prostate fibroblasts (NPFs) derived from benign prostate specimens did not [340]. These findings emphasise the role of CAFs in prostate cancer, highlighting the importance of the stromal microenvironment of prostate cancer.

### 1.24.2 Role of EMT in Prostate Cancer Progression

The cancer cells acquire a more invasive and migratory phenotype through the EMT process [341]. Cell adhesion is reduced in early metastatic prostate cancer by downregulation of E-cadherin and b-catenin expression (characteristically expressed in normal epithelial cells) [342]. In contrast, the expression of N-cadherin (characteristically expressed in mesenchymal cells) is upregulated [343]. Clinical studies have shown lower E-cadherin and b-

catenin expression and higher N-cadherin expression in tumour specimens from patients with higher grade prostate cancer than lower grade specimens [344, 345]. Overexpression of E-cadherin and b-catenin were also associated with the metastatic prostate cancer cells in bone, indicating their involvement in the intercellular adhesion of the metastatic cells in bone [346].

### 1.24.3 Role of PTEN in Prostate Cancer Progression

SC maintenance requires the expression of the *PTEN* gene as demonstrated in mouse models of leukaemia [347] and prostate cancer [348]. Studies have demonstrated approximately 2-14% of prostate cancer specimens harbour PTEN mutations, and 12-41% have copy number loss [349]. Mutations in PIK3CA have been observed in 3-4% of patients, and amplifications have been reported in 4-10% of cases [349]. *PTEN* is a negative regulator of the PI3K/AKT signalling pathway [350]. Deficiency of *PTEN* and *TP53* together in prostate cancer results in increased hexokinase-2 expression, which promotes aggressive prostate cancer growth *in vivo* [351]. The absence of *PTEN* in prostate cancer is linked to a poor prognosis [352].

## 1.25 The Role of ALDHs in Prostate Cancer

Failure of current therapies in the treatment of CRPC necessitates the need to develop new therapeutic strategies to circumvent the current clinical challenge. As a consequence, it is important to further understand the underlying biology of the disease and identify prostate cancer markers and markers unique to the putative CSC population. It is hypothesised that ALDHs may have an important role in prostate cancer, and so they were the focus of this study.

### 1.25.1 ALDHs

Enhanced ALDH activity confers resistance to chemotherapy. Early studies in 1984 first demonstrated a chemo-resistant role of ALDHs in a cyclophosphamide (CP) resistant L1210 leukaemia cell line [353]. There were high levels of ALDH activity in L1210 cells and treatment with disulfiram (ALDH inhibitor) reversed the resistance phenotype of the cells to CP. A subsequent study confirmed the role of ALDH-mediated CP resistance in medulloblastoma [354]. Similar studies later demonstrated that high ALDH activity does confer CP resistance in cancer and CSCs [355]. Therefore, inhibiting ALDH activity can serve to sensitise CSCs to drugs such as CP [356]. ALDH1A1 and ALDH3A1 were found to inactivate CP [357]. Moreover, ALDH appears to confer resistance to other drugs such as cisplatin, doxorubicin, temozolomide and taxanes [357].

A recent study revealed sphere forming cells from the sarcoma cell line MG63 with strong resistance to doxorubicin and cisplatin compared with their monolayer adherent counterparts. The sarcosphere cells with high ALDH1 activity were proposed as a candidate for sarcoma SCs, with strong chemo-resistant capacities. The efficient detoxification may contribute to the chemo-resistant phenotype of the stem-like sphere cells [358]. Furthermore, high ALDH expression in CSCs conferred chemo-resistance in breast cancer SCs and head and neck squamous cell carcinoma (HNSCC) SCs [359]. The ALDH expression in HNSCC SCs was associated with high Snail expression, since knockdown of Snail expression significantly decreased the expression of ALDH1, inhibited cancer stem-like properties and blocked the tumorigenic abilities of $CD44^+$ $CD24^-$ $ALDH1^+$ cells [359].

## 1.26 The Human Aldehyde Dehydrogenase Superfamily

The human ALDH superfamily consists of 19 putatively functional genes in 11 families and 4 subfamilies [267] with distinct chromosomal locations [360] (Figure 12). In 1998, a standardised gene nomenclature classification, based on divergent evolution and amino acid identity of the ALDH family was established [361], such that families within the superfamily shared more than 40% sequence identity and members of the same subfamily shared more than 60% sequence identity. ALDHs are found in the cytoplasm, mitochondria, nucleus, and endoplasmic reticulum, with several found in more than one compartment [267, 362]. The enzyme levels and tissue and organ distribution varies with different ALDHs [363-365] and they display distinct substrate specificity [366] . Highest levels are found in the liver, followed by the kidney, uterus and brain [367]. ALDHs are involved in several normal physiological processes including protection of SCs and are therefore used as a SC marker (Table 4) [241].

**Figure 12. The human aldehyde dehydrogenase superfamily of enzymes**
Clustering dendrogram depicting the evolution of mammalian aldehyde dehydrogenases (ALDHs) and their chromosomal location. The nomenclature is referred as the following: ALDH identifies the root symbol, the first number identifies the family, the following letter identifies the subfamily and the last number identifies the individual gene. Figure modified from [368].

| ALDH | Subcellular location | Tissue/Organ distribution | Preferred aldehyde substrate | Additional functions and characteristics |
|---|---|---|---|---|
| ALDH1A1 | Cytosol | Liver, kidney, erythrocytes, skeletal muscle, lung, breast, lens, stomach mucosa, brain, pancreas, testis, prostate, ovary | Retinal | Ester hydrolysis; binds androgen, cholesterol, thyroid, daunorubicin, and flavopiridol; corneal and lens crystallin; |
| ALDH1A2 | Cytosol | Testis, small amounts in liver, kidney | Retinal | High affinity for LPO-derived aldehydes |
| ALDH1A3 | Cytosol | Kidney, skeletal muscle, lung, breast, testis, stomach mucosa, salivary, glands | Retinal | High affinity for LPO-derived aldehydes |
| ALDH1B1 | Mitochondria | Liver, kidney, heart, skeletal muscle, brain, prostate, lung, testis, placenta, more | Acetaldehyde | May protect the cornea from UV-light |
| ALDH1L1 | Cytosol | Liver, kidney, skeletal muscle | 10-Formyltetrahydrofolate | Binds acetaminophen |
| ALDH1L2 | Mitochondria | Pancreas, heart, brain | 10-Formyltetrahydrofolate | Induced by the anti-inflammatory agent indomethacin |
| ALDH2 | Mitochondria | Liver, kidney, heart, skeletal muscle, lung, lens, brain, pancreas, prostate, spleen | Acetaldehyde | Ester hydrolysis; nitroglycerin bioactivation, oxidizes LPO-derived aldehydes; binds acetaminophen; oxidizes DOPAL and DOPEGAL |
| ALDH3A1 | Cytosol, nucleus | Stomach mucosa, cornea, breast, lung, lens, esophagus, salivary glands, skin | Aromatic, aliphatic aldehydes | Ester hydrolysis; scavenges ROS; UVfilter corneal crystallin; oxidizes LPOderived aldehydes; regulation of cellcycle; inducted by PAHs |
| ALDH3A2 | Microsomes, peroxisomes | Liver, kidney, heart, skeletal muscle, lung, brain, pancreas, placenta, most tissues | Fatty aldehydes | Insulin regulates gene expression |
| ALDH3B1 | Cytosol, Endoplasmic reticulum | Kidney, lung, pancreas, placenta | Lipid peroxidation-derived aldehydes | Oxidizes LPO-derived aldehydes |
| ALDH3B2 | Cytosol, Endoplasmic reticulum | Parotid gland | Unknown | Unknown |
| ALDH4A1 | Mitochondria | Liver, kidney, heart, skeletal muscle, brain, placenta, lung, pancreas, spleen | Glutamate γ-semialdehyde | Ester hydrolysis; may mitigate oxidative stress |
| ALDH5A1 | Mitochondria | Liver, kidney, heart, skeletal muscle, brain | Succinate semialdehyde | Neurotransmission efficiency |

Continued

| | | | | |
|---|---|---|---|---|
| ALDH6A1 | Mitochondria | Liver, kidney, heart, skeletal muscle | Malonate semialdehyde | Esterase activity; only known human CoA-dependent ALDH |
| ALDH7A1 | Cytosol, nucleus, mitochondria | Fetal liver, kidney, heart, lung, brain, ovary, eye, cochlea, spleen, adult spiral cord | α –Aminoadipic semialdehyde | Closely related to plant osmoregulatory protein; may regulate cel cycle |
| ALDH8A1 | Cytosol | Liver, kidney, brain, breast, testis | Retinal | Oxidizes LPO-derived aldehydes and acetaldehyde |
| ALDH9A1 | Cytosol | Liver, kidney, heart, skeletal muscle, brain, pancreas, adrenal gland, spinal cord | γ-Aminobutyraldehyde | Oxidises betaine, acetaldehyde and DOPAL; involved in carnitine biosysnthesis; esterase activity |
| ALDH16A1 | Unknown | Neuronal cells | Unknown | Unknown |
| ALDH18A1 | Mitochondria | Kidney, heart, skeletal muscle pancreas, testis, prostate, spleen, ovary, thymus | Glutamic γ-semialdehyde | Unknown |

**Table 4. The aldehyde dehydrogenase superfamily**
The table shows 19 different aldehyde dehydrogenase (ALDH) cellular localisation, tissue/organ distribution, preferred aldehyde substrate and associated additional functions. Modified from [241, 369, 370].

## 1.27 Principal Function of ALDHs

ALDHs are NAD(P)+ dependent multi-functional enzymes that play a major role in a detoxification process and belong to phase 1 drug metabolising enzymes (DMEs). Specifically, they catalyse the irreversible oxidation of aldehyde substrates to their corresponding less reactive forms of carboxylic acids, a process which enables ALDHs to protect cells from the harmful effects of highly reactive aldehydes and maintain cellular homeostasis [362, 371, 372] (Figure 13). The most convincing evidence relies on the observation that mutations and polymorphisms in *ALDH* genes which results in loss-of-function are associated with various human pathologies (Table 5) [373].

**Figure 13. ALDH driven oxidisation of aldehydes**
Illustration of highly toxic sources of aldehydes irreversibly oxidised to their corresponding carboxylic acid that are involved in normal cellular processes to maintain homeostasis. Unconverted aldehydes can harm the cell by several mechanisms including causing DNA and protein damage, membrane destruction and oxidative stress leading to cellular toxicity and/or disease (Figure exemplifies retinoic acid generation) [374].

| Gene | Chromosome | Mutation/LOH/SNP | Mutational phenotype | Reference |
|---|---|---|---|---|
| ALDH4A1 | 1p36.13 | A 1 bp deletion (G) at nucleotide 21 (A7fs (-1)), 1 bp insertion of a T following nucleotide 1563 (G521fs (+1)) cause a frameshift. Missense mutations (S352L and P16L) | Type II hyerprolinemia | [375] |
| ALDH7A1 | 5q31 | missense mutation P169S | Pyridoxine-dependent seizures | [376] |
| ALDH1A1 | 9q21.13 | 17-base-pair deletion, ALDH1A1*2 allele | Alcohol sensitivity;(?) *Aldh1a1*$^{-/-}$ mice develop cataracts | [377] |
| ALDH1A2 | 15q22.1 | Silent change A151A (c. 453A>G), 2 intronic polymorphisms rs3784259 and rs3784260 | ↑ Risk of spina bifida; (?) *Aldh1a2*$^{-/-}$ mice are embryonic lethal | [378] |
| ALDH1A3 | 15q26.3 | Transgenic knock out mice | (?) *Aldh1a3*$^{-/-}$ mice are embryonic lethal | [379] |
| ALDH1B1 | 9p11.1 | Unknown | Unknown | - |
| ALDH2 | 12q24.2 | ALDH2*2 allele (single base pair mutation G/C → A/T), which results in an E487K substitution | ↓ Risk for alcoholism; ↑ risk for cancer, AD, myocardial infarction and cirrhosis | [380-382] |
| ALDH1L1 | 3q21.2 | Knockout | (?) *Aldh1l1*$^{-/-}$ mice have decreased hepatic folate and low fertility | [383] |
| ALDH1L2 | 12q23.3 | Unknown | Unknown | - |
| ALDH9A1 | 1q23.1 | Unknown | Suggested candidate gene for human non-alcoholic steatohepatitis | [384] |
| ALDH5A1 | 6p22.2 | *Aldh5a1*$^{-/-}$ knockout mice | γ - Hyroxybutyic aciduria | [385] |
| ALDH8A1 | 6q23.2 | Unknown | Unknown | - |
| ALDH6A1 | 14q24.3 | a transversion (1336G > A) in *ALDH6A1* leading to the replacement of a highly conserved glycine with an arginine (G446R) | Developmental delay, metabolic abnormalities, methylmalonic aciduria | [386] |
| ALDH3A1 | 17p11.2 | Transgenic knockout mice | (?) *Aldh3a1*$^{-/-}$ mice develop cataracts | [387] |
| ALDH3A2 | 17p11.2 | c.943C>T mutation, c.1297_1298delGA allele | Sjögren-Larsson syndrome | [388] |
| ALDH3B1 | 11q13.2 | A SNP in intron 2 (rs581105; T/G) | Locus linked to paranoid schizophrenia | [389] |
| ALDH3B2 | 11q13.2 | Unknown | Unknown | - |
| ALDH18A1 | 10q24.3 | a missense mutation resulting in the replacement of a highly conserved leucine with a serine (L396S), and an arginine to glutamine substitution (R84Q) at a conserved residue within the γ-glutamyl kinase domain | Hyperammonemia; hypoprolinemia; neurodegeneration; cataracts | [390, 391] |
| ALDH16A1 | 19q13.33 | Unknown | Unknown | - |

**Table 5. Mutational phenotypes of the human aldehyde dehydrogenase (ALDHs)**
Illustration of the evolutionary relationship of the 19 human *ALDH* genes. Different mutational events of *ALDH* genes leading to several disease states. Question mark (?) indicates phenotype demonstrated in animal only [373].

Other catalytic functions of ALDHs include ester hydrolysis and nitrate reductase activity [362, 371]. ALDHs are also involved in the generation of RA which is required for several cellular processes [392]. Non-catalytic functions include antioxidant roles (production of NAD(P)H, and the absorption of UV light. Furthermore, several ALDHs act as binding proteins for various endogenous (androgen, thyroid hormone and cholesterol) and exogenous (acetaminophen) compounds [373].

### 1.28 Sources of Aldehydes

Aldehydes are highly reactive electrophilic species that play an important role in normal physiological processes such as embryonic development, vision and neurotransmission, however, most are highly cytotoxic and carcinogenic, and therefore effectively removed by ALDHs [241, 360].

Aldehydes are produced from a range of endogenous and exogenous precursors during several physiological processes. Endogenous precursors include biotransformation of amino acids, neurotransmitters, carbohydrates and lipids [373]. Over 200 aldehyde species are generated from oxidative degradation of lipid peroxidation such as malondialdehyde [373]. Catabolism of amino acids produces numerous aldehyde intermediates such as glutamate γ-semialdehyde, whilst neurotransmitters, such as γ-aminobutyric acid (GABA), dopamine, noradrenaline and serotonin also generate aldehyde metabolites [373]. Aldehydes are also generated by the metabolism of vitamins (retinal to retinoic acid (RA)) [241] and steroids [371, 372].

Exogenous sources of aldehydes derive from xenobiotics and drugs such as ethanol, which produces acetaldehyde, and the anti-cancer drugs CP and

ifosfamide, involved in producing acrolein, are essential aldehyde precursors. Other forms of aldehydes are generated from the environment (smog), industrial processes (polyester plastics) and exist as dietary aldehydes added as food additives [373].

### 1.29 Association of ALDHs with SCs

ALDH1 has been primarily used as a SC marker for identification and isolation of SCs and CSCs. The isoforms 1A1 and 3A1 have essential functional roles in SCs in the context of differentiation, self-protection and expansion of their population [267].

### 1.30 Role of ALDH as a SC Marker

SCs from adult tissues have become attractive therapeutic targets due to the expression of cell surface molecules which are used to isolate them allowing efficient expansion in culture [393]. The expression of a broad range of cell surface molecules such as CD73, CD90, CD105, CD34, CD14, CD45, and HLA-DR are used to identify SCs in tissues such as liver, mesenchymal cells, and hematopoietic cells [267]. Due to the negligible level of extracellular MHC class I and II determinants, these markers exhibit no proliferative response from allo-reactive lymphocytes [394]. SCs also function in innate and adaptive immune responses [394]. Different types of SCs can be isolated using specific SC markers either as a single marker or in combination with other markers. HSCs are usually identified by CD34 and/or CD133 [395], whereas neural SCs are identified by CD133 or the surface antigen Lewis X [396].

High ALDH1 activity combined with the presence of ABC transporter G2 and high telomerase activity may potentially be a universal SC marker due to their

presence in SCs isolated from most tissues [396]. SCs purified using the aldefluor assay have been used in the field of regenerative medicine [397].

ALDH isoforms 1A1, 1A2, 1A3 and 3A1 play an important role in drug resistance and RA generation and are also crucial for the protection of SCs from reactive forms of aldehydes and for SCs to differentiate [267]. It is still unclear which ALDH isoforms are responsible for the ALDH activity used for identification of SC progenitors [398].

ALDH1A1 has been identified as an established SC marker for haematopoietic progenitors for several years [267]. RA function in granulocyte differentiation of HSCs led to the discovery of ALDH isoform 1A1 and 1B1's role in the catalysation of cellular RA synthesis as well as their expression in $CD34^+$ haematopoietic progenitors [399, 400]. ALDH2 and ALDH7A1 have also been identified as markers in different SC populations [267].

### 1.31 Role of ALDH as a CSC Marker

For the first time in 2003 the existence of CSCs in solid tumours was reported in tumour-initiating breast cancer cells upon their identification and isolation from primary tumours and pleural effusions of breast cancer patients based on a $CD44^+CD24^-$ phenotype [401]. These cells demonstrated high tumorigenic properties in mouse models [401]. Further studies demonstrated $CD44^+CD24^-$ breast cancer cells exhibited high expression of SC markers, their ability of self-renewal, increased capacity for *in vitro* mammosphere formation and invasion, expressing high levels of anti-apoptotic proteins, and their ability to recapitulate a heterogeneous tumour population [401-404]. CSCs and putative CSCs have now been further identified in many other cancer types such as

liver, brain, pancreas, colon, and prostate depending on their surface antigens [267, 401].

Soon after the isolation of leukaemia SCs based on the increased activity of ALDH through the use of the aldefluor assay [405], $ALDH^+$ cells from breast cancer which exhibited tumourigenic and self-renewal properties of CSCs were successfully isolated [406]. This research enabled further studies to quantify the activity of ALDHs in solid tumours. Alongside other CSC markers, ALDH activity is used as marker for CSCs in cancers such as lung [407], colon [408], bone [409], pancreatic [410] and prostate [273]. High ALDH activity was used to identify tumour-initiating as well as metastasis-initiating cells in human prostate cancer [273].

Recently, studies have demonstrated the activity of cytosolic ALDH1 as a reliable CSC marker in various solid tumours including lung, head and neck, liver, cervix, pancreas, breast, ovaries, bladder, colon and prostate [267]. High ALDH1 is also linked with poor prognosis in breast, bladder and prostate cancer patients [267, 269].

The expression of ALDH1 has been shown as a marker for normal and malignant human mammary and colon SCs [268, 269]. Interestingly, it was observed that the number of SCs expressing high levels of ALDH1 increased from normal epithelium of colon to the mutant epithelium to adenoma progression [268].

It has been reported in a study that breast cancer patients with ALDH1 positive tumours showed a lower overall survival than patients with ALDH low tumours [267, 269]. Decreased survival may be due to the ability of $ALDH1A1^+$ breast

cancer cells to promote tumour invasion *in vitro* and tumour metastasis in mouse xenografts. Furthermore, ALDH1A1 expression has shown to be independent predictor factor for early metastasis and decreased survival in inflammatory breast cancer [411].

Likewise, two different studies showed high expression of ALDH1A1 in primary prostate cancer patient samples which were correlated with lower overall survival, pathological stage and Gleason score [412, 413].

Studies have revealed that highly expressing ALDH1 CSCs in adenoid cystic carcinoma [414], head and neck squamous cell carcinoma [267], pancreatic adenocarcinoma [413], lung cancer [272], bladder cancer [415], cervical carcinoma [416], and prostate cancer [412, 417] are greatly tumourigenic and exhibit enhanced SC characteristics *in vitro* and *in vivo* when compared to low ALDH1 activity cells.

An *in vivo* study showed that when $1x10^4$ breast cancer cells expressing low levels of ALDH1 were transplanted into a mouse model, no tumour formation was observed. In contrast, injection of only 500 cells expressing high levels of ALDH1 generated tumours within 40 days, suggesting the $ALDH^+$ breast cancer stem-like cells are greatly tumorigenic [269]. Other studies have indicated that an $ALDH1^{hi}CD44^+$ phenotype can be used for the identification of stem-like breast cancer cells and that these cells display a significant increase in the metastatic potential as compared to $ALDH1^{low}$ $CD44^-$ cells both *in vitro* and *in vivo* [418]. Several other studies have shown that breast, bladder, and prostate CSCs expressing elevated levels of ALDH1 activity

seem to exhibit more aggressive features, which may facilitate metastasis as well as linked to poor prognosis [267].

Suitability of ALDH1 as a CSC marker comes down to specific tumour types. A recent study showed that ALDH1-high cells are clearly distinguished as they are found in regions in which epithelial stem/progenitor cells are commonly located [267]. Moreover, normal tissue distribution of ALDH1 was classified into 3 main categories: tissues with no or limited ALDH1 expression such as lung and breast, tissues with relatively weak ALDH1 expression such as gastric epithelium and colon, and tissues with relatively elevated ALDH1 expression such as pancreas and liver [267]. This lead to the conclusion that ALDH1 may be effectively used as a CSC marker only in tissue types that express relatively low levels of ALDH1 including lung, breast, gastric and colon and not in tissues that have high expression of ALDH1 such as pancreas and liver [270].

As various ALDH isoforms including -1A1, -1A2, -1A3 and 8A1 function in RA production by oxidation of all-trans-retinal and 9-cis-retinal in RA cell signalling, ALDHs may potentially also have a role in CSC biology other than just as CSC markers [392].

### 1.32 The Aldefluor Assay

The activity of ALDHs especially ALDH1 in live cells can be efficiently measured using flow cytometry and/or fluorescent microscopy using fluorescent substrates for ALDH1 [267, 419]. ALDH bright cell populations from adult tissue are isolated through flow sorting. The aldefluor assay was originally used to isolate primitive HSCs by the use of the fluorescent substrate

BODIPY aminoacetaldehyde (BAAA) [267-269], however, it is now commonly used to measure the activity of ALDHs from adult tissue cells, primary cancer cells and cultured cells. In theory, cells that express ALDH1 can uptake uncharged ALDH substrate BAAA (non-toxic fluorescent substrate) through passive diffusion after which they convert BAAA into negatively charged BODIPY aminoacetate (BAA). BAA stays retained within the cells and causes fluorescence of cells ($ALDH^{high}$) with high ALDH activity. Addition of a cold assay buffer prevents the ABC transporters from pumping out the BAA substrate from the cells. 4-(diethylamino)benzaldehyde (DEAB) quenches the activity of $ALDH^{high}$ cells, preventing their fluorescent (Figure 14). Populations of $ALDH^{high}$ and $ALDH^{low}$ cells can be determined by sorting gates. $ALDH^{high}$ cells can be distinguished by comparing them to DEAB used as a negative control which is a pan-ALDH inhibitor [267, 420]. Commonly, 100,000-1,000,000 cells are suspended in the aldefluor assay buffer which contains BODIPY aminoacetaldehyde with or without DEAB. Fluorescence excitation is at 488nm and emission is detected at 530nm [417]. This assay can be used to isolate viable HSCs and more recently $ALDH^{high}$ CSCs. However, care must be employed as studies have reported that ALDH1A1 deficient haematopoietic cells demonstrated aldefluor activity due to the presence of other isoforms including ALDH1A3, -2, -3A1 and -9A1 [392].

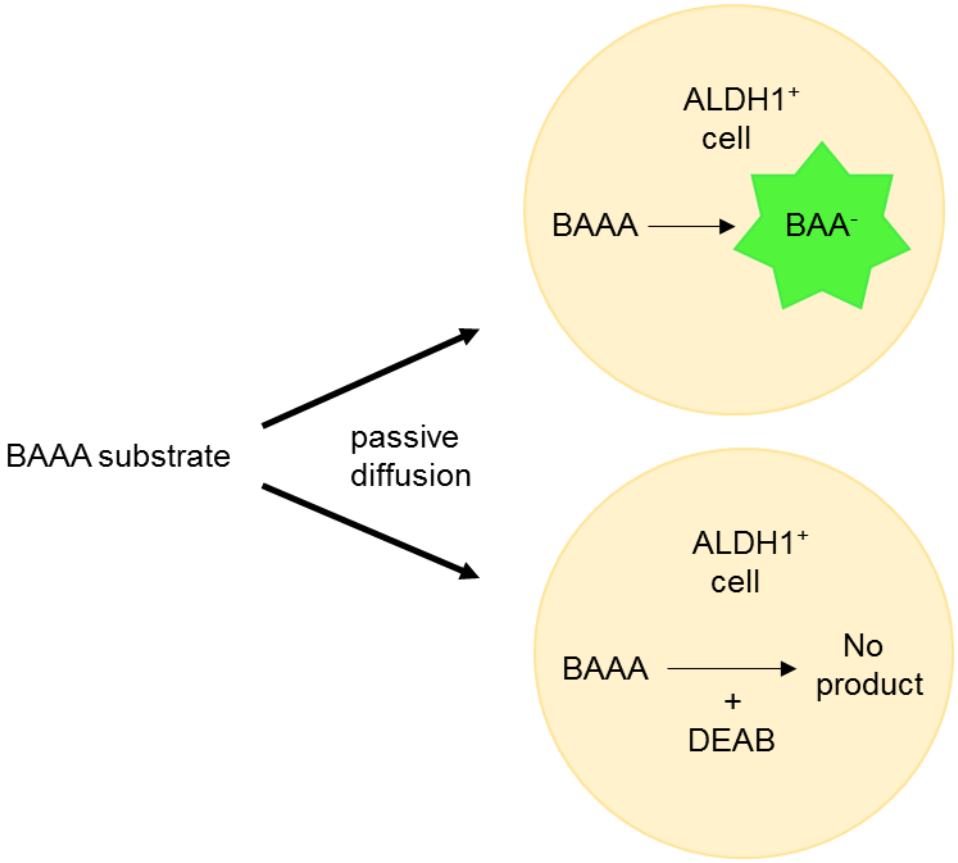


**Figure 14. The Aldefluor assay**
Aldehyde dehydrogenase (ALDH) positive cells uptake uncharged fluorescent substrate BODIPY aminoacetaldehyde (BAAA) by passive diffusion and convert it to negatively charged BODIPY aminoacetate (BAA) fluorescent product which is retained inside the cell and causes the ALDH high cells to become fluorescent. The intensity of fluorescent signal is proportional to the ALDH activity in the cells as measured by flow cytometer. The addition of an ALDH inhibitor 4-(diethylamino)benzaldehyde (DEAB) acts as a negative control by quenching the activity of ALDH. This allows sorting cells into ALDH high or low population of cells. Modified from [241].

Despite the successful use of this assay in several human models [267, 269, 421], there are controversies for its use in murine HSC models [421]. A study on breast cancer patient tumour samples showed the expression of ALDH1A3 to be best correlated with the activity of ALDH in cell lines. Knockdown of ALDH1A3 decreased ALDH activity in the aldefluor high breast cancer cell lines [422]. Van den Hoogen et al. identified prostate CSCs using the aldefluor assay and reported that higher level of expression of other ALDH

isoforms such as ALDH7A1 but low expression of ALDH1A1 was observed in prostate cancer cell lines, prostate cancer tissue and matched bone metastasis samples, [417].

### 1.33 AldeRed-588-Assay

Only recently has a new assay emerged which allows fluorescence signal detection in the red channel using the ALDH substrate AldeRed-588-A (532nm excitation and 615nm emission) as compared to the conventional Aldefluor assay which offered signal in the green fluorescence (488nm excitation and 530nm emission) channel for labelling viable $ALDH^+$ cells. However, both assays provide the same efficacy and efficiency based on sharing acetaldehyde as a common substrate moiety. However, lack of selectivity of this assay is similar to that of Aldefluor [423, 424].

### 1.34 ALDH1 and the Retinoid Signalling Pathway

The retinoid signalling pathway has been implicated in normal SCs [425] and cancer cells [426-429]. RA plays a role in several vital physiological processes such as the regulation of gene expression, morphogenesis and development in a wide range of tissues, including prostate, through regulating numerous genes involved in proliferation, differentiation and homeostasis [430-432]. RA also stimulates apoptosis through upregulation of the expression of caspase 7 and 9 [433]. RA can both positively and negatively affect prostate gland development depending on the stage of prostate development suggesting that RA is crucial for the development and differentiation of the prostate epithelium [434, 435]. There are four different families of retinoid dehydrogenases which are involved in the conversion of retinol (vitamin A) to RA (Figure 15). These include alcohol dehydrogenase (ADH), aldoketo reductase, short chain

dehydrogenase and ALDH [430]. ADH first reversibly oxidises retinol to retinaldehyde, cytosolic human ALDH1 (-1A1, 1A2, and 1A3) then irreversibly oxidises retinaldehyde to RA [267]. The second reaction is a highly regulated event which is also tissue specific [267]. The second step is tissue specific because the oxidation of retinaldehyde to RA is an irreversible reaction, with RA having a potent biological activity. All ALDHs identified are tissue-specific, therefore they specifically metabolise retinaldehyde to RA in the tissues in which they are present. The selective expression of ALDHs (1A1, 1A2 and 1A3) catalysing the second step is what limits the tissues that can completely metabolise retinol to RA to initiate retinoid signalling [436].

*In situ* synthesised RA then binds to nuclear retinoic acid receptor (RAR) and retinoid X receptor (RXR) forming a heterodimer complex that binds to RA response elements (RARES) in the DNA sequence and leads to downstream regulation of gene expression and cell differentiation [430-432, 437]. All-trans retinoic acid (atRA) and 9-cis-RA bind to RARs, whereas only 9-cis-RA can bind to RXRs [267]. Upon synthesis of RA, the RA signalling pathway is initiated and can be inhibited by degradation of RA [430]. In the absence of ligand, RARs are found in the nucleus predominantly bound to RAREs located in the promoter of target genes repressing transcription through their association with HDAC-containing complexes and corepressors [438].

Retinoids are hydrophobic and are therefore stored and transported in complex with either cellular retinoid-binding proteins (CRBP) or cellular RA-binding proteins (CRABP) [439]. CRABP shuttles RA to the nucleus where it binds to the RAR/RXR heterodimer [440]. This subsequently leads to the dissociation of co-repressors NCoR, SMRT and HDAC complex and allows co-

activators SRC/p160 family, creb-binding protein (p300/CBP) and co-activator-associated arginine methyltransferase 1 (CARM-1) to bind [441]. The chromatin structure is modified by histone acetyltransferase (HAT) or methyltransferase activity causing the chromatin structure to relax [442] facilitating the recruitment of transcriptional machinery and for gene transcription to initiate [443] (Figure 15).

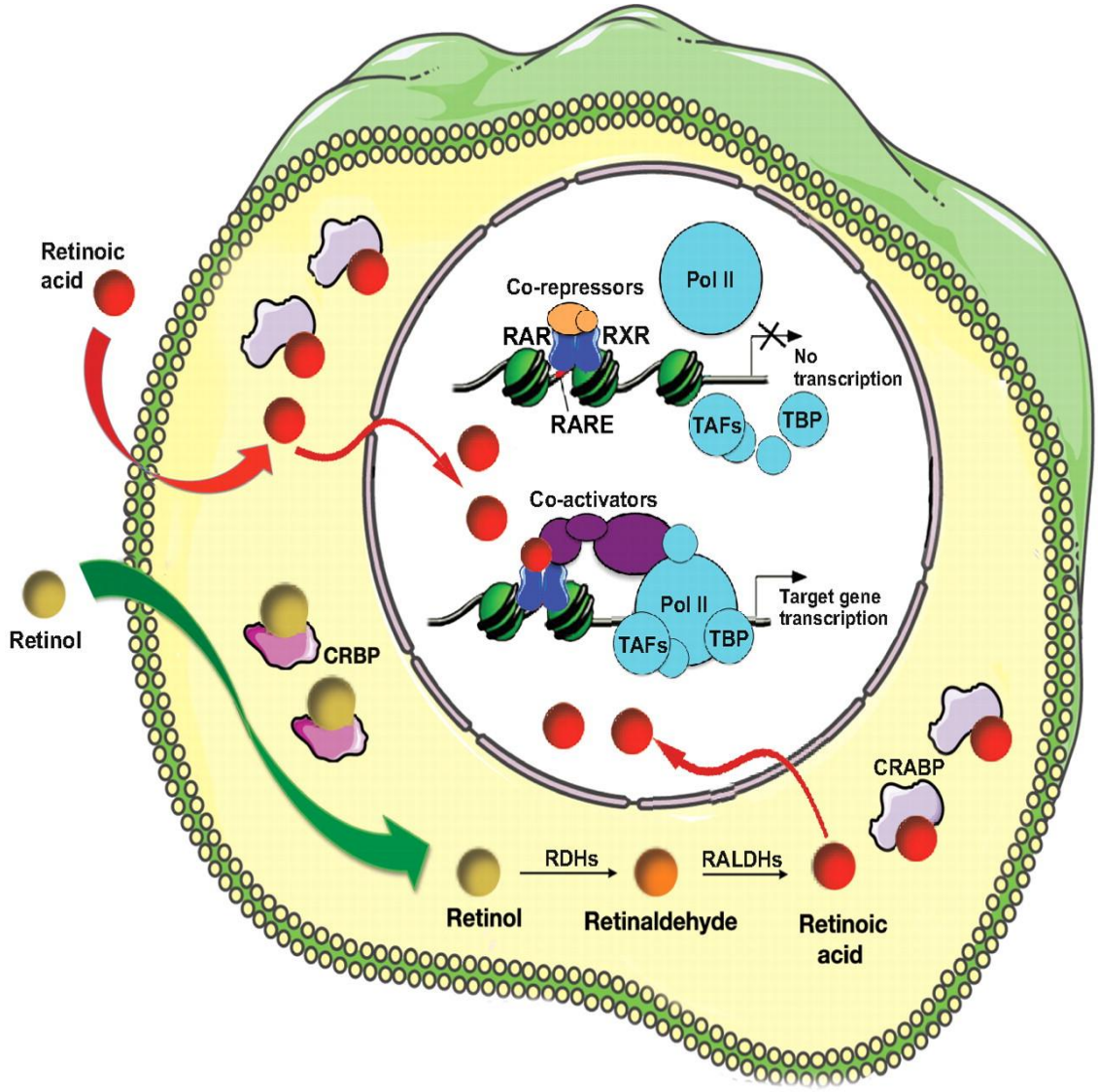


**Figure 15. RA signalling pathway**
Retinol is first converted to retinaldehyde and then irreversibly oxidised to RA which binds onto cellular RA-binding proteins (CRABP). Upon translocating to the nucleus, RA binds to retinoic acid receptor (RAR) and retinoid X receptor (RXR) forming a heterodimer which binds onto the RA response elements (RAREs) releasing co-repressors and recruiting co-activator complexes that destabilise the nucleosomes and facilitate assembly of the transcription machinery. In the absence of RA, RAR/RXR bind to RAREs in their target genes interacting with co-repressors to stabilise the chromatin nucleosomal structure and prevent access to the promotor. Adapted from [444]. Image re-used with permission from license: 'Development' is an Open Access journal and According to SHERPA/RoMEO

ALDH isoforms 1A1, 1A2, 1A3 and 8A1 function in the RA signalling pathway [431, 445-447] which is associated with the "stemness" characteristics of CSCs [427]. RA signalling has an important role in prostate development and

function as transgenic mice lacking RAR-G develop prostate squamous metaplasia which also renders them sterile [448, 449].

In prostate cancer it has been reported that there is aberrant retinoid signalling with prostate carcinoma tissues containing significantly less RA than normal prostate or BPH tissues [450]. Evidence from clinical trials using atRA for hormone-refractory prostate cancer showed no or minimal response among patients potentially due to enhanced clearance of atRA [451].

Studies have shown RA represses invasion and SC phenotype by inducing metastasis suppressors retinoic acid receptor responder 1 (RARRES1) and latexin (LXN) in prostate cancer [452]. RA also induces apoptosis in androgen-independent prostate cancer cells through the non-cyclin regulator p35 cleavage and cyclin-dependent kinase 5 (Cdk5) over activation [453].

Retinoids are used as cancer treatment, in part due to their ability to induce differentiation and arrest proliferation. However, delivery of retinoids presents a challenge because of the rapid metabolism of some retinoids and the epigenetic alterations that can render cells retinoid resistant [454].

### 1.35 Tumour Microenvironment and Hypoxia

Microenvironment-related mechanisms may also contribute to drug resistance of CSCs. Hypoxia is a major feature of the tumour microenvironment and a potential contributor to MDR and enhanced tumourigenicity of CSCs [455]. Within this niche, hypoxic cells are surrounded by an acidic microenvironment which activates a subset of proteases that contribute to metastasis [456]. As a consequence of poor angiogenesis and the inaccessible location, hypoxic cells do not receive sufficient therapeutic concentrations of chemotherapeutics

thereby contributing to patient relapse. Furthermore, certain drugs require oxygen to function and so all these factors lead to MDR [359].

Hypoxia is a common feature of solid tumours which occurs as a result of limited oxygen diffusion in avascular primary tumours or their distant metastases. Continuous hypoxia causes significant reduction in the efficacy of radiation and chemotherapy leading to therapy-resistance and therefore the acquisition of a more aggressive cancer phenotype. Hypoxia leads to an increased expression of genes involved in the suppression of apoptosis such as c-myc, 5' AMP-activated protein kinase (AMPK) and glucose transporter 1 (GLUT1), and it promotes tumour angiogenesis, EMT, invasion and metastasis [457]. Hypoxia inducible factor (HIF) is known as the master regulator of several transcriptional targets. HIF is a heterodimeric TF that is comprised of an oxygen-regulated α subunit and a constitutively expressed β subunit [457]. HIF1α is an oxygen-responsive TF that mediates adaptation to hypoxia. During low oxygen concentration, HIF1α is stabilised and is translocated to the nucleus where it leads to specific target gene expression through binding of HIF1β to a hypoxia response element (HRE). HIF1α is involved in the regulation of several genes that contribute to tumour progression [457]. A recent study showed breast cancer SCs with $ALDH^{high}$ activity had a greater hypoxic response and subsequent induction of HIF1α expression compared to the $ALDH^{low}$ cells, and silencing of HIF1α in these $ALDH^{high}$ cells resulted in significant reduction of the SC properties [458]. Other studies have demonstrated increased expression levels and transcriptional activity of HIF1α in prostate cancer during progression and bone metastases and is associated with therapy-resistance and poor clinical outcome [459].

## 1.36 ALDH Associated Drug Resistance

The elevated levels of ALDHs in cancer has been associated with drug resistance and cancer relapse [460, 461]. For drugs that are aldehyde based or releases aldehyde-containing metabolites from drugs or prodrugs, it is proposed that resistance potentially occurs due to metabolic inactivation of the drugs as a consequence of ALDH activity linked with detoxifying capacity. A number of studies focused on oxazaphosphorines exemplify this as shown in Table 6.

It is well established that ALDHs are involved in chemotherapy resistance potentially due to the CSC niche and the quiescent characteristic of the putative CSCs, rendering these cells more drug-resistant and aggressive (see Table 6).

ALDHs play a critical role in acquiring drug resistance with a variety of different mechanisms and confer resistance to aldehyde-based drugs, conventional chemotherapeutics and targeted therapeutics.

| Drug | ALDH-Associated Resistance | Reference |
|---|---|---|
| **ALDH based drugs/metabolites from prodrugs** | | |
| CP | Breast cancer patients with low levels of ALDH1 had enhanced response to CP based treatment in comparison to patients with high ALDH1A1 | [462] |
| Oxazaphosphorines | Resistance to oxazaphosphorines was directly correlated with ALDH3A1 activity in breast cancer | [305] |
| CP and its metabolite, 4-hydroperoxycyclophosphamide (4-HCPA) | RNA interference mediated knockdown of ALDH1A1 and ALDH3A1 effectively sensitised lung cancer cell lines to CP and 4-HCPA reflecting their levels as predictors of therapeutic response to oxazaphosphorines | [306] |
| Mafosfamide | Lung adenocarcinoma and glioblastoma cells have re-sensitivity towards mafosfamide upon ALDH3A1 inhibition | [307] |
| **Cytotoxic drugs lacking ALDHs** | | |
| Paclitaxel/Cisplatin | ALDH1 was upregulated in paclitaxel-resistant and cisplatin-resistant lung cancer cells compared to their parental cell lines | [308, 309] |
| Paclitaxel/Doxorubicin | Over expression of ALDH1 led to resistance against paclitaxel, doxorubicin and radiotherapy in breast cancer cell lines which was reversed following treatment with DEAB or RA | [310] |
| 1-β-D-Arabinofuranosylcytosine | There is an association of ALDH1A2 with drug resistance in leukaemia cells, which was overcome by knocking down ALDH1A2 expression leading to sensitisation of cells to 1-β-D-arabinofuranosylcytosine | [311] |
| 5-Fluorouracil | Upregulated levels of ALDH1A3 were found in 5-fluorouracil-resistant colon cancer cells in contrast to the parental cell line HT29 | [312] |
| **Resistance to molecularly-targeted therapy** | | |
| Crizotinib | A MET kinase inhibitor-resistant gastric carcinoma displayed high ALDH1 expression | [313] |
| Zoledronic acid | Proteomics analysis exhibited high ALDH7A1 expression in prostate cancer cells DU145 resistant to zoledronic acid, a nitrogen-containing bisphosphonate | [314] |

**Table 6. ALDH associated resistance**

The table exemplifies ALDH-linked resistance to ALDH-based drugs, chemotherapeutics and targeted therapeutics in which different ALDH isoforms have been identified to confer resistance.

## 1.37 Chromatin Remodelling of ALDHs in Prostate Cancer

Chromatin remodelling consists of a number of covalent modifications of the histones including acetylation, phosphorylation and methylation [463]. Acetylation is mediated by HATS and deacetylation is mediated by histone deacetylases (HDACs). Acetylation of conserved lysine residues in histone tails neutralises the positively charged histones and thereby loosens their interaction with negatively charged DNA which leads to the opening of the chromatin structure. This facilitates binding of transcription factors and initiation of gene transcription. Whereas, deacetylation of histones is involved in the tightening of their interaction with DNA, leading to a closed chromatin structure and the inhibition of gene transcription (Figure 16) [464]. Aberrant transcriptional regulation by histone acetylation or deacetylation has implications in a variety of diseases including cancer and is the most studied histone modification [465].

"Image/photo/map/illustration/graph not included due to copyright restrictions" Image can be viewed at: https://www.ahajournals.org/doi/full/10.1161/01.RES.0000197782.21444.8f?url_ver=Z39.88-2003&rfr_id=ori%3Arid%3Acrossref.org&rfr_dat=cr_pub%3Dpubmed

**Figure 16. Histone modification by acetylation/deacetylation**
DNA/chromatin assembly into nucleosomes can either by stimulated in an open structure by histone acetyltransferases (HATs) allowing the transcription of genes or a closed structure by histone deacetylases inhibiting gene transcription (HDACs) [466].

Methylation of DNA in the promoter region of tumour suppressor genes (TSG) seems to take place at early stages of cancer progression [467]. Other epigenetic alterations of such genes also includes histone modification [467]. CpG islands are regions rich of CpG of 200bp to many kilobases in length, commonly located near the promoter of highly expressed genes [467]. These sites are commonly methylated in human tumours [468], including prostate cancer. Hypermethylation of cytosine 5' to guanosine (CpG) in the regulatory area [467, 469] results in 5-methyl cytosine which is unstable and thus mutated to thymine and methylated CpG sites are degraded to TpG [467]. Hypermethylation of TSGs in prostate cancer plays a significant role in the carcinogenesis and progression of the disease [470].

Prostate cancer exhibits low prostatic RA levels and altered retinoid metabolism [471, 472]. It has been demonstrated that ALDH1A2 promoter regions in primary prostate tumours are densely hypermethylated in comparison to normal prostate tissues [473]. This is further shown by Touma et al., who detected lower ALDH1A2 expression in all prostate tumour formalin-fixed paraffin embedded sections as compared to normal prostate tissue [472]. Thus, it is suggested that ALDH1A2 is a TSG in prostate cancer, and its epigenetic changes may potentially occur in the early stages of prostate cancer [467]. In addition, ALDH1A2 is a RA synthesis gene with pro-differentiation properties. A study showed that re-expression of methylated ALDH1A2 in the prostate cancer cell line DU145 lead to reduced colony growth in culture which was comparable to treatment with a demethylating agent or RA [474].

Another study showed ALDH1A3 as androgen responsive [475], and up regulation of it can increase the conversion of retinal to RA [467]. Studies have also shown hypermethylation of ALDH1A3 promoter region in prostate cancer [476].

Therefore, methylation of the promoter regions of ALDH1A2 and ALDH1A3 may be used as potential markers for prostate cancer detection and prevention [467], but further exploration is required to establish clinical potential.

## 1.38 Aims and Objectives

Aggressive prostate cancer remains a challenge to treat perhaps due to a small number of cancer cells that are multidrug resistant with tumour-initiating and metastasising properties. ALDHs are gaining recognition as enzymes with implications in a number of solid tumours, with high activity found in CSCs, however their exact role is yet to be elucidated. A better understanding of the role of ALDHs in prostate cancer may lead to identification of a potential biomarker or therapeutic target.

The main aim of this project was to investigate the expression and function of selected ALDH isoforms in prostate cancer.

More specifically, the objectives of the study were to:

i. Investigate the gene and protein expression of isoforms from ALDH1-3 families (ALDH1A1, ALDH1A2, ALDH1A3, ALDH1B1, ALDH2, ALDH3A1) and additionally ALDH7A1 in prostate cell lines, primary prostate epithelial cultures, SCs, TA cells and CB cells.
ii. Explore potential regulatory roles of selected ALDH isoforms in primary prostate epithelial cultures.
iii. Investigate ALDH expression in docetaxel-resistant cells and examine a library of small molecules to identify potential hit compounds, which could serve as starting points for discovery of more potent and selective ALDH inhibitors.

# Chapter 2

## Materials and Methods

## 2.1 Culturing of mammalian cells

PNT2C2, LNCaP, DU145 and PC3 cells were obtained from American Type Culture Collection (ATCC) and were routinely cultured in RPMI 1640 (Sigma) medium supplemented with 10% v/v fetal calf serum (FCS) (Gibco), 2mM L-glutamine (Sigma) and 1mM sodium pyruvate (Sigma). Bob and SerBob cells were cultured in complete keratinocyte serum-free medium (cKSFM) consisting of KSFM with 5ng/ml EGF, 50µg/ml bovine pituitary extract (BPE) (Invitrogen), 2ng/ml leukaemia inhibitory factor (LIF) (Millipore), 0.05µg/ml cholera toxin (CT) (Sigma), 1ng/ml granulocyte macrophage colony stimulating factor (GM-CSF), and 2ng/ml stem cell factor (SCF). 10% v/v FCS was added to the culture medium of SerBob cells only. SerBob and Bob cell lines are spontaneously immortalised, with Bob cells cultured in the absence of serum which presents a basal phenotype of the cell line, whereas SerBob cells are cultured in the presence of serum with limited differentiation [477]. Cells were maintained at 37$^{o}$C with 5% $CO_2$ in a humidified incubator. Cells were routinely passaged for sub-culture in T75 flasks when 70-80% confluent and medium was changed every 2 days (Table 7).

| Cell line | Origin | Culture media | Reference |
|---|---|---|---|
| **PNT2C2** | Normal prostate cells originating from young male organ donors | RPMI 1640 | [478] |
| **Bob** | TURP of CRPC tissue | cKSFM | [477] |
| **SerBob** | TURP of CRPC tissue | cKSFM | [477] |
| **LNCaP** | Left supraclavicular lymph node metastasis | RPMI 1640 | [479] |
| **DU145** | Isolated from the brain of a patient with prostate cancer metastasis | RPMI 1640 | [480] |
| **PC3** | Bone metastasis from grade 4 prostate adenocarcinoma | RPMI 1640 | [481] |

**Table 7. Details of cell lines used.**
The table lists the benign cell line PNT2C2 and the cancer cell lines Bob, SerBob, LNCaP, DU145 and PC3 used in the present study, with their origin and culture media used. Transurethral resection of the prostate (TURP), castration resistant prostate cancer (CRPC), complete keratinocyte serum-free medium (cKSFM).

## 2.2 Determination of cell number

A 10µl cell suspension was diluted 1:1 with 10µl 0.4% trypan blue solution (Sigma) and loaded onto each chamber of a haemocytometer. Cells were counted using standard methods. Cells stained blue were not counted.

## 2.3 Epigenetic drug treatment of prostate cell lines

Stock solutions for drugs were first prepared at 20mM in dimethyl sulfoxide (DMSO) (Fisher Scientific) and aliquoted to smaller volumes which were stored at -20$^{o}$C. Working concentrations of the drugs were prepared fresh in complete culture medium. In all cases, DMSO concentration was always below 0.1% to minimise effect on cells. Same volume of DMSO was used in the control to account for any effects of the carrier on the cells.

Cells were seeded at a density of 1 x $10^5$ cells per T75 flask 24 hours prior to treatment. On the day of treatment, cell confluence was about 60%, and cells were either treated with demethylating drug decitabine (DAC) or HDAC

inhibitors trichostatin A (TSA), entinostat (MS275) or vorinostat (SAHA). Cell treatments included 1µM DAC for 6 days (replacing media containing drug every other day due to the short 8-12 hours half-live of DAC in culture), 0.1µM TSA for 48 hours, 0.5µM MS275 or SAHA for 48 hours for RNA and protein extraction. Due to the longer treatment of cells with DAC, the confluence was about 80% prior to harvesting for RNA and protein extraction and this may have impacted on results as cells are towards the end of their exponential phase of growth before entering plateau.

### 2.4 Treatment of primary prostate cultures with TSA

Cells were either treated with DMSO or TSA at 0.6µM concentration for 24 hours. This was performed by Prof. Norman J. Maitland's team in the University of York.

### 2.4 Treatment of primary prostate cultures with atRA

Cells were treated with atRA for 72 hours at 100nM. Primary samples used included BPH, BPH containing prostatic intraepithelial neoplasia (BPH-PIN) and cancer samples. atRA treatment was performed by Prof. Norman J. Maitland's team in the University of York.

### 2.5 Exposure of prostate cell lines to hypoxia

A seeding density of 2 x $10^5$ cells / T75 flask was used for all cell lines followed by incubation in either the hypoxic chamber (Don Whitley Scientific) containing hypoxic conditions of 0.1% $O_2$, 95% $N_2$, 5% $CO_2$, 37ºC and 80-100% humidity or in normoxic condition incubator containing 20% $O_2$, 5% $CO_2$, 37ºC and 80-100% humidity for control samples. Cells were incubated either in normoxic or hypoxic conditions for 24 and 48 hours before being harvested for RNA and

protein extraction. For hypoxic conditions, culture media was kept in the hypoxic chamber at least 24 hours before use to allow it to equilibrate to the hypoxic conditions. Cell harvesting was performed in the hypoxic chamber.

### 2.6 Real-time quantitative PCR

Cells were harvested using trypsin/ethylenediaminetetraacetic acid (EDTA) and the cell pellet washed in phosphate buffered saline (PBS). PBS was completely removed from the cell pellet and the pellets were stored in -20$^{o}$C until analysis. Trypsin/EDTA can have an impact on cell surface proteins if incubated for a long period of time as it cleaves the junctions between cells including amino acids. Therefore, cells were only briefly (about a minute) treated with trypsin/EDTA to avoid damage to cell surface proteins and quickly resuspended in culture media containing serum which includes protease inhibitors such as α1-antitrypsin that inhibits trypsin activity. Since ALDHs are not cell surface proteins, this study used trypsin/EDTA for cell-cell and cell-dish detachment. Another method which may be used is to scrape off the cells from the culture dish to avoid any usage of trypsin for cell harvesting, thus reducing an impact on expression of targets.

#### 2.6.1 RNA extraction, purification and quantification

The RNA of all primary samples used in chapter 3 only were kindly provided by Prof. Norman J. Maitland. Sample details are outlined in appendix. Cell lines and primary cells used in chapter 4 were processed for RNA extraction in this study.

Cells were washed with 10ml PBS after drug treatment, trypsinised with 1ml trypsin/EDTA for a minute, re-suspended in 10ml complete medium, and centrifuged at 1000rpm for 5 minutes. The supernatant was removed, and

cells resuspended in 10ml PBS. The cells were then centrifuged at 1000 rpm for 5 minutes, supernatant removed, and the resultant dry pellet (no PBS) was stored at -20$^{o}$C. RNA extraction was carried out using the RNeasy Mini Kit (Qiagen). Cells were resuspended in 350µl buffer RLT and thoroughly vortexed to allow disruption and homogenization. Equal volume of 70% ethanol was added to the lysate and mixed well by pipetting and the 700µl cell lysate was transferred to a QIAgen RNeasy Mini spin column placed in a 2ml collection tube and centrifuged for 15s at 10000rpm. The flow-through was discarded. 350µl of buffer RW1 was then added to the column and centrifuged for 15s at 10000rpm, and the flow-through was discarded. 80µl of DNase I was added directly to the RNeasy column membrane and incubated for 15 min at room temperature. 350µl buffer RW1 was then added to the RNeasy column and centrifuged for 15s at 10000rpm and the flow-through was discarded. 500µl of buffer RPE was then added to the spin column and centrifuged for 15s at 10000rpm and the flow-through was discarded. 500µl buffer RPE was again added to the spin column and centrifuged for 2 min at 10000rpm. Next, the RNeasy spin column was placed in a new 2ml collection tube and centrifuged at full speed for 1 min to dry the membrane. The RNeasy spin column was then placed in a new 1.5ml collection tube and 30µl of RNase-free water was added to the spin column membrane and centrifuged for 1 min at 10000rpm to elute the RNA. The concentration and quality of the eluted RNA was determined by measuring the absorbance of UV light using Nanodrop$^{TM}$2000 (Thermo Fisher Scientific) spectrophotometer and measuring the 260/280 ratio. The RNA samples were stored at -80$^{o}$C until further use.

### 2.6.2 cDNA synthesis

Total RNA of 50-2000ng was reverse transcribed into single-stranded cDNA using the High Capacity cDNA Reverse Transcription Kit (Life technologies). The components of the kit were allowed to thaw on ice and the reaction mix was also prepared on ice. A 2X RT master mix was created by adding 2µl of 10X RT buffer, 0.8µl of 25X dNTP Mix (100mM), 2µl of 10X RT Random Primers, 1µl of Multiscribe reverse transcriptase, 1µl of RNase inhibitor and 3.2µl of nuclease-free $H_2O$. The reaction mix was mixed well by pipetting. 10µl of total RNA sample was added to each reaction mix to obtain a 1X mix giving a final reaction volume of 20µl to be reverse transcribed. The reaction tubes were then briefly spun down and kept on ice. The conditions of the ML Research PTC-200 Peltier thermal cycler were set as listed in Table 8 below and reverse transcription was started. Once the reaction finished, samples were either stored at -20$^{o}$C or purified using the QIAquick PCR Purification Kit (Qiagen).

| | Step 1 | Step 2 | Step 3 | Step 4 |
|---|---|---|---|---|
| Temperature ($^{o}$C) | 25 | 37 | 85 | 4 |
| Time (min) | 10 | 120 | 5 | ∞ |

**Table 8. Thermal cycling conditions for cDNA synthesis**

### 2.6.3 cDNA purification and determination of concentration

The QIAquick PCR Purification Kit was used to purify DNA prior to determining cDNA concentration after cDNA synthesis from RNA of primary cells kindly provided by Prof. Norman J. Maitland (Cancer Research Unit, University of York). All centrifugation steps were carried out at 13000rpm at room temperature. Briefly, 100µl of buffer PB was added to the cDNA sample and mixed by pipetting. If the colour of the mixture was orange, 10µl of 3M sodium

acetate pH5.0 was added upon which the colour of the mixture turned yellow. The contents were transferred to a QIAquick column to bind DNA and centrifuged for 60s after which the flow-through was discarded. To wash, 750µl of buffer PE was added to the QIAquick column and centrifuged for 60s followed by discarding the flow-through. The QIAquick column was placed in a new 2ml collection tube and centrifuged for 1 min to remove residual wash buffer before being placed in a clean 1.5ml microcentrifuge tube. To elute the purified cDNA, 30µl $H_2O$ was added to the centre of the QIAquick membrane and left to stand for 1 min followed by centrifuging the column for 1 min. The concentration and quality of the cDNA was measured by using Nanodrop spectrophotometer and the samples were stored at -20$^oC$.

### 2.6.4 Real-time quantitative PCR

qPCR was carried out in 25µl total PCR reaction using the TaqMan Universal PCR Master Mix (Applied Biosystems). The PCR reaction consisted of 12.5µl of 2X master mix, 1.25µl of 20X TaqMan Gene Expression Assay Mix, and 11.25µl cDNA diluted in $dH_2O$. The cDNA samples were diluted 1:5 and 2µl of diluted cDNA was used. A 96-well MicroAmp Optical plate (Applied Biosystems) was used and all reactions were run in triplicates. Primers used were obtained from TaqMan Gene Expression Assays as listed below in Table 9 and validated by the company before release. The PCR reactions were centrifuged and then run on 7500 Real time PCR system and analysis was carried out using the 7500 software v2.3 (Applied Biosystems). The thermal cycling conditions consisted of an initial setup of a hot start of 10min at 95$^oC$ which was followed by 40 cycles of 15s at 95$^oC$ for denaturing and 1min at 60$^oC$ for annealing/extending. The gene expression level relative to internal

control RPLP0 was calculated using the formula $2^{-dCT}$ and the fold change in gene expression was worked out using the $2^{-ddCT}$ method.

| Target gene | TaqMan gene expression assay | Amplicon context Sequence containing probe sequence |
|---|---|---|
| **ALDH1A1** | Hs00946916_m1 | 5'-gcc gac ttg gac aat gct gtt gaa t-3' |
| **ALDH1A2** | Hs00180254_m1 | 5'-gat cat ccc atg gaa ctt ccc cct g-3' |
| **ALDH1A3** | Hs00167476_m1 | 5'-agg aga taa gcc cga cgt gga caa g-3' |
| **ALDH1B1** | Hs00377718_m1 | 5'-cct gct gca gag tgt cag cat gct g-3' |
| **ALDH2** | Hs01007998_m1 | 5'-agc agc ccg agg tct tct gca acc a-3' |
| **ALDH3A1** | Hs00964880_m1 | 5'-aag tca ctg aaa gag ttc tac ggg g-3' |
| **ALDH7A1** | Hs00609622_m1 | 5'-aaa atc tgg gca gat att cct gct c-3' |
| **RPLP0** | Hs04189669_g1 | 5'-gtc ctc gtg gaa ggc ccg gga ccg c-3' |
| **CA9** | Hs00154208_m1 | 5'-atc gct gag gaa ggc tca gag act c-3' |

**Table 9. TaqMan Gene Expression Assays.**
The sequence of each Taqman gene expression assay is not provided as standard since they are proprietary. The sequence was identified by the method advised by ThermoFisher Scientific; the reference sequences are provided and the assay location is provided. The 25bp probe sequences surround this assay location (12bp upstream and downstream). All Taqman probes adhere to the MIQE Guidelines (Minimum Information for Publication of QRT-PCR Experiments). In addition, TaqMan probes are accompanied by the TaqMan guarantee, where reproducibility and specificity are rigorously tested before the product is released (see white paper on this guarantee - https://www.thermofisher.com/content/dam/LifeTech/Documents/PDFs/PG1500-PJ9167-CO017361-TaqMan-Guarantee-WhitePaper-Global-FHR.pdf)

## 2.7 Analysis of protein expression in prostate cell lines by Western blot

Cells were treated as before and the cell pellet washed with PBS and stored at -20$^{o}$C until further analysis. All steps were carried out on ice and cell pellets were kept on ice throughout the procedure. RIPA buffer (50mM Tris-HCl pH 8.0, 150mM NaCl, 1% Nonidet P-40, 0.5% sodium deoxycholate, 0.1% sodium dodecyl sulphate (SDS), 10µl/ml protease inhibitor) was prepared and 300µl

was added to the cell pellet and mixed well by pipetting and left to stand on ice for 20min to obtain whole cell lysates. For samples that appeared viscous, sonication was carried out to allow further lysis. Since the high energy produced by sonication can heat up the samples and generate free radicals, samples were placed on ice during the process and sonication was applied in short bursts only. Samples from all the cell lines in this study appeared viscous and were therefore subjected to sonication. The samples were then centrifuged at 16000 rpm in a pre-cooled centrifuge for 20min at 4$^{o}$C. The supernatant was transferred to a fresh pre-chilled eppendorf tube and stored at -20$^{o}$C. The protein concentration was then determined using the Bicinchoninic acid assay kit (BCA).

### 2.7.1 BCA protein assay

The concentration of whole cell protein lysates was measured using the BCA assay (Thermo Scientific) which is a colorimetric assay. According to the manufacturers' guide, briefly a series of standards were prepared using 2mg/ml BSA and 10µl of each concentration was added to 4 wells in a 96-well plate. 2µl of unknown samples were also added to 4 wells. 200µl of the BCA working solution was then added to each well at a ratio of 10:0.2 of reagent A and reagent B respectively, and mixed by pipetting. The plate was left to stand at room temperature for 30min. The absorbance was measured at 562nm on a spectrophotometer. A graph of absorbance with bovine serum albumin (BSA) standards was plotted to give a line of best fit from which the concentration of the unknown samples was extrapolated. The final concentration of the unknown samples was worked out by taking into account the difference of volume input between standards and unknowns. The BCA protein assay was

used as it was a standard method in our laboratory for quantifying protein concentrations and it offers the convenience of using a 96-well plate in which smaller volumes can be used as compared to other methods such as the Bradford assay.

### 2.7.2 SDS-PAGE gel electrophoresis

20µg of protein lysate for each sample was prepared by mixing with 2X laemmli buffer (4% SDS, 10% 2-mercaptoethanol, 20% glycerol, 0.004% bromophenol blue, 0.125M Tris-HCl and adjusted to pH 6.8) which was vortexed and spun down before incubating at 95$^{o}$C for 5 min in a heating block. The samples were then vortexed again followed by a quick spin before loading on the gel. A 12% resolving gel (30% acrylamide mix, 1.5M Tris pH 8.8, 10% SDS, 10% ammonium persulfate, tetramethylethylenediamine (TEMED) and $H_2O$) was poured into the glass slides before a layer of butanol was added to obtain a levelled surface of the gel, which was allowed to set for 25min. A 12% gel was suitable for the size of the ALDHs to be separated ranging from 50-65kDa according to Abcam's western blot protocol. The layer of butanol was discarded once the gel was set and the surface of the gel washed twice with $dH_2O$ and carefully blotted off to dry. A 5% stacking gel (30% acrylamide, 1.0M Tris pH 6.8, 10% SDS, 10% ammonium persulfate, TEMED, $H_2O$) was then poured over the resolving gel and allowed to set. The glass assembly containing the gel was transferred to a Bio-Rad electrophoresis tank and running buffer (25mM Tris pH 8.3, 190mM glycine, 0.1% SDS) was poured into the tank. 20µg of the denatured protein samples were loaded into the wells alongside of protein ladder (Thermo Scientific, Pierce) for protein size determination and enable visualisation of protein

transfer. The samples were subjected to a run at 70V for 5 min followed by 150V until they reached 1cm before the end of the gel.

### 2.7.3 Western blot

A wet transfer of the protein onto a nitrocellulose transfer membrane (Whatman, Protran) was carried out by first immersing the membrane in $dH_2O$ for 5 min and then equilibrating in transfer buffer (25mM Tris pH8.3, 190mM glycine, 20% methanol) for 5 min. Associated sponges and filter papers were also immersed in $dH_2O$ for 10 min and subsequently in transfer buffer for 15 min. Gels were then assembled into a sandwich cassette with the membrane and transferred at either 300mA for 2 hours on ice or overnight at 35mA.

Following transfer, membranes were washed in either TBST (20mM Tris pH7.5, 150mM NaCl, 0.1% Tween 20) or PBST (PBS with 0.1% tween) for 5 min to remove any residual gel. TBST was initially used to wash the membranes in early experiments, however due to faint signals detected upon visualisation of the bands it was changed to PBST as a less harsh treatment for the membrane. Membranes were then blocked in 5% (w/v) Marvel milk prepared in PBST for one hour at room temperature on a shaker. Next, membranes were incubated with unconjugated primary antibodies (Table 10) prepared in blocking buffer overnight at 4$^{o}$C on a shaker. Membranes were washed 4 times for 10 min in PBST followed by one-hour incubation with peroxidase-labelled secondary antibodies diluted in blocking buffer at room temperature (Table 11). The membranes were washed four times again for 10 min in PBST. These were coated in HRP substrate chemiluminescent (Roche) for 1-2min before exposure to films. Finally, the membranes were exposed to

hyperfilm ECL (GE Healthcare) for 1-15 minutes depending on the target protein and processed in Kodak GBX developer and fixer solutions.

| 1º Ab | Species | Supplier | Working dilution | Incubation time | Incubation temperature (ºC) |
|---|---|---|---|---|---|
| **ALDH1A1** | Goat | Santa Cruz | 1:250 | Overnight | 4 |
| **ALDH1A2** | Rabbit | Abcam | 1:250 | Overnight | 4 |
| **ALDH1A3** | Goat | Santa Cruz | 1:250 | Overnight | 4 |
| **ALDH1B1** | Rabbit | Abcam | 1:1000 | Overnight | 4 |
| **ALDH2** | Rabbit | Abcam | 1:250 | Overnight | 4 |
| **ALDH3A1** | Mouse | Santa Cruz | 1:50 | Overnight | 4 |
| **ALDH7A1** | Rabbit | Abcam | 1:3500 | Overnight | 4 |
| **LDH** | Rabbit | Abcam | 1:5000 | Overnight | 4 |
| **B-actin** | Mouse | Merk Millipore | 1:20000 | Overnight | 4 |

**Table 10. Primary antibodies for western blots**

| 2ºAb | Host species | Dilution | Supplier |
|---|---|---|---|
| **Anti-Mouse** | Polyclonal rabbit | 1:3500 | Dako |
| **Anti-Rabbit** | Polyclonal goat | 1:3500 | Dako |
| **Anti-goat** | Polyclonal rabbit | 1:3500 | Dako |

**Table 11. Secondary antibodies for western blots**

### 2.7.4 Data analysis

The detected protein band densities were measured using Image J software. Data was normalised by dividing treated samples with control sample for each target. The ratio of protein expression was then calculated by dividing target protein with control protein.

## 2.8 Analysis of protein expression of primary cultures by immunofluorescence

Cells were seeded at a density of 10,000 cells per well in 8-well chamber slides and allowed to adhere overnight in 37$^{o}$C incubator. Media was removed and the cells washed twice in PBS. Cells were then fixed with 200µl of freshly prepared 4% paraformaldehyde for 15 minutes. Following removal of fixing agent, cells were washed three times in PBS for 5 minutes with each wash. 200µl of 0.3% Triton X-100 in PBS was then added to each well for 15 minutes followed by three PBS washes for 5 minutes each. Cells were then blocked with 200µl of 10% FCS in PBS for 1 hour at room temperature. Primary antibodies were diluted in 0.1% Triton X-100 and added to the cells with an overnight incubation at 4$^{o}$C on a shaker. See Table 12 for antibody details. Next, cells were washed three times in PBS with 5-minute wash each and secondary antibodies (diluted in PBS) were added to the cells for one hour (Table 13). Control wells included secondary antibodies only, however, non-specific IgG control was not used. Antibody concentrations used were recommended by the supplier as well as by our group in which the concentrations had been previously titrated to reach an optimum. Cells were washed three times in PBS with 5-minute wash each. Chambers were carefully removed from the slide ensuring no glue was stuck to the slide. Three drops of vectashield mounting medium with 4′,6-diamidino-2-phenylindole (DAPI) (Vector laboratories) were added to the slides followed by a coverslip. Excess vectashield was dabbed off and the coverslip was sealed to the slide using clear nail varnish. Slides were kept in the dark and analysed using a fluorescent microscope.

| 1ºAb | Species | Supplier | Dilution |
|---|---|---|---|
| **ALDH1A3** | Goat | Santa Cruz | 1:250 |
| **ALDH1A3** | Rabbit | GeneTex | 1:250 |
| **ALDH1B1** | Rabbit | Abcam | 1:250 |
| **ALDH2** | Rabbit | Abcam | 1:250 |
| **ALDH7A1** | Rabbit | Abcam | 1:250 |
| **CK5** | Rabbit | Abcam | 1:500 |
| **CK14** | Mouse | Serotec | 1:500 |

**Table 12. Primary antibodies used for immunofluorescence**

| 2ºAb | Species | Supplier | Dilution |
|---|---|---|---|
| **Alexa Fluor 568 (red) Anti-rabbit IgG** | Goat | Life technologies | 1:1000 |
| **Alexa Fluor 488 (green) Anti-goat IgG** | Rabbit | Invitrogen | 1:1000 |
| **Alexa Fluor 568 (red) Anti-mouse IgG** | Goat | Invitrogen | 1:1000 |

**Table 13. Secondary antibodies used for immunofluorescence**

## 2.9 Analysis of protein expression and localisation in primary prostate BPH tissue by immunohistochemistry

### 2.9.1 Generation of BPH tissue slides

BPH samples were collected from patients undergoing TURP procedure. Patient consent was obtained and patients were anonymised. Several tissue chips were collected, following the procedure, by a dedicated tissue procurement officer. Follow-up pathology results were obtained from the pathologist based at Castle Hill Hospital (Dr. Greta Rodriguez) to confirm BPH diagnosis. Following paraffin-embedding and tissue slicing, every tenth slide

was stained for hemotoxylin and eosin. In this way, pieces of tissue that showed areas of epithelial glands can be picked for staining i-e. areas of tissue that showed only stroma would not be chosen. This procedure was performed by Prof. Norman J. Maitland's team in the University of York. The dewaxing, rehydration, antigen retrieval and IHC was performed in this study.

### 2.9.2 Dewaxing and rehydration

Sections were dewaxed in four different xylenes troughs for 2x 10 minutes and 2x 1 minute. Sections were then immersed in three different 100% ethanol glass troughs for 1 minute each, followed by 1 minute in 70% ethanol. Slides were then washed under running tap water for 5 minutes.

### 2.9.3 Antigen retrieval

Sections were immersed in sodium citrate buffer (2.94g trisodium citrate/1L, pH 6.0, 0.05% tween 20) and left in a pressure cooker for at least 24 hours ensuring the sections stay immersed to protect from drying out. The pressure cooker was used for heat-induced epitope retrieval (HIER). This can be done using a pressure cooker or microwave or a steamer. Some optimization is required for each method in terms of buffers and time of incubations. The cycle time in the pressure cooker is 20 minutes then the slides are left to cool from 2 hours to overnight. This is according to the manufacturer's instructions. Slides were then washed in running tap water for 5 minutes and ready to be stained using the ImmPRESS Excel peroxidase Staining Kit containing anti-rabbit Ig (Vector laboratories).

### 2.9.4 Immunohistochemistry (IHC)

Circles were drawn around each tissue section (Table 14) using a grease marker to separate out each section. Sections were first incubated in 70-100µl BLOXALL blocking solution to quench endogenous peroxidase activity for 10 minutes. Slides were then washed in running water for 10 minutes. Each section was incubated with 70µl of 2.5% normal horse serum for 20 minutes. Next, sections were incubated with rabbit primary antibody diluted in 2.5% normal horse serum overnight at 4$^{o}$C in a moist container (Table 15) before the slides were washed in TBST three times for 5 minutes on a shaker. Control sections included incubation with Amplifier antibody (2$^{o}$ antibody) without the primary antibody. The primary antibodies were selected based on supplier's recommendation for use in IHC and from our group in which the antibodies have been used previously. Sections were then incubated for 15 minutes with Amplifier antibody and washed twice in TBST for 5 minutes on a shaker. Each section was incubated with ImPRESS Excel Reagent for 30 minutes before washed once in TBST and d$H_2O$ for 5 minutes each. 3,3-diaminobenzidine (DAB) was prepared by combining equal volumes of ImmPACT DAB EqV reagent 1 and reagent 2 and added to sections until they turned brown (2-5 minutes). Slides were rinsed in dH2O followed by tap water. Each slide was counterstained with haematoxylin for up to 30 seconds. Finally, the slides were rinsed in running tap water and coverslip mounted with diphenylxylene (DPX). Slides were allowed to air dry before visualised using the OLYMPUS light microscope. Sections used are listed in Table 14. NKX-3.1 was used as a positive control to label luminal cells in BPH tissue. Antibodies used are listed in Table 15.

| BPH tissue |
|---|
| 039108 11 |
| 039108 13 |

**Table 14. BPH tissue samples used for IHC.**
BPH samples collected following TURP procedure. The codes of BPH tissue are related to sample 039108, with 391 being the patient number, 08 means year 2008, and the 11 and 13 refer to the number of slide as the tissue was sectioned.

| Primary antibody | Species | Supplier | Dilution |
|---|---|---|---|
| ALDH1A3 | Rabbit | Santa Cruz | 1:250 |
| ALDH1B1 | Rabbit | Abcam | 1:250 |
| ALDH2 | Rabbit | Abcam | 1:250 |
| ALDH7A1 | Rabbit | Abcam | 1:250 |
| NKX 3.1 | Rabbit | MenaPath | 1:500 |

**Table 15. Primary antibodies used for IHC**

## 2.10 Multicellular Spheroids generation

### 2.10.1 Spheroid formation using the hanging-drop method

MCS were generated from LNCaP prostate cancer cell line. Cells were seeded at a density of 10,000 cells per 30µl drop of culture medium containing 20% methylcellulose as a drop on the flip side of the lid of a 10cm petri dish. A series of drops were seeded onto the cover of the petri dish. The petri dish itself was filled with 10ml PBS to allow for humidity. After seeding the cells as drops, the lid containing the drops was inverted in one smooth movement allowing the drops to hang over the petri dish containing PBS. The dish was incubated at 37ºC over a week. Images were taken using an inverted light microscope (Leica Lumascope) with a 10x objective lens. The diameter of the

spheroids was measured every day. Medium was carefully changed by removing 15µl of old medium and replenishing with 15µl of fresh medium.

### 2.10.2 Determination of spheroid diameter

The diameter of LNCaP spheroids was measured in µm every day using a calibrated graticule with a measuring scale fixed to the eye piece of the light microscope. A minimum of 20 spheroids were measured and an average diameter taken. The measured diameter was multiplied by 25 if the x4 objective was used and by 10 if the x10 objective was used.

### 2.10.3 Spheroid formation using the 96-well plate method

Cells were seeded at a density of 5000 cells in 200µl of medium containing 20% methylcellulose in a non-treated round bottom 96-well plate. Following cell seeding, plates were centrifuged at 1000rpm for 20 minutes to allow the cells to form a cluster at the bottom of each well and incubated at 37$^{o}$C and 5% $CO_2$ incubator to allow the spheroid to form and grow over a number of days. Diameter of the spheroids was measured using an inverted light microscope.

### 2.10.4 Preparation of culture medium with methylcellulose

Methylcellulose was dissolved in 250ml Dulbecco's Modified Eagle Medium (DMEM) medium (Sigma) in a sterile bottle and stirred with a magnetic stirrer for 30 minutes at 100$^{o}$C. Then, fresh 250ml medium was added to the bottle and stirred for 2 hours at 4$^{o}$C. Next, 50ml aliquots were prepared and centrifuged at 3700 rcf for 2 hours at room temperature. Finally, the supernatant was transferred to a fresh 50ml tube carefully leaving at least a 2-

3ml residual behind and the methylcellulose containing media was finally stored at 4$^{o}$C.

### 2.10.5 Harvesting and fixing spheroids

LNCaP spheroids were carefully collected using a P1000 pipette with the tip slightly snipped off with scissors to allow ease of drawing up the 30µl drop or 200µl medium containing the compact spheroid. All spheroids were subsequently harvested and pooled into a 25ml tube where they settled/sedimented at the bottom of the tube. Medium was carefully removed and the spheroids washed once in PBS and then fixed in a 3ml yellow Bouin's solution (Sigma), which contains formaldehyde as a fixing agent and picric acid that stains it yellow. The spheroids were incubated in bouin's solution for 75 minutes at room temperature before the Bouin's solution was carefully poured off and the spheroids washed 3 times in 70% ethanol. Finally, the spheroids were stored in 70% ethanol in the final wash at room temperature until further processing.

### 2.10.6 Spheroid embedding

The 70% ethanol was carefully removed from the spheroids and 90% ethanol was added for 1 hour and incubated at room temperature. After 1 hour, the 90% ethanol was removed and 100% ethanol added for 30 minutes followed by another 100% ethanol for 30 minutes. Ethanol was discarded after dehydrating the spheroids and replaced by xylene for 30 minutes followed by another xylene wash for 30 minutes. The spheroids were then transferred to an embedding mould and excess xylene removed. Xylene is miscible with both ethanol and molten paraffin wax, and clears out the ethanol, as ethanol cannot

mix with paraffin. The mould containing the spheroids was filled with hot paraffin wax and the mould was gently tapped to allow the spheroids to sit at the bottom of the paraffin and incubated at 68$^{o}$C for 30 minutes. This was to ensure that the spheroids are positioned in the centre of the mould. The paraffin wax was carefully removed using a pre-warmed pipette and replaced with fresh paraffin wax and the mould returned to the incubator for a further 5 minutes (this step was repeated twice). These multiple steps of fresh wax ensured gradual addition of molten wax to the spheroids and complete removal of xylene. The mould was then immediately placed on a cold stage to allow the wax containing the spheroids to set for 30 minutes before storing the mould in -20$^{o}$C. Storage at -20$^{o}$C hardens the wax compared to a softer texture at room temperature, and thus allows an easier removal from the mould.

### 2.10.7 Spheroid sectioning

The paraffin wax blocks containing the spheroids were removed from -20$^{o}$C and placed on a microtome to cut a series of 5µm thick sections. The sections were first placed on room temperature d$H_2O$ to allow straightening out of any paraffin folds followed by 30$^{o}$C d$H_2O$. The sections were then mounted on superfrost plus slides (BDH, Poole, UK) and left to dry on a heated stage of 37$^{o}$C for 2 hours or overnight to allow attachment of section to the slide.

### 2.10.8 Hematoxylin and Eosin (H&E) Staining

Spheroid sections were first de-paraffinised by immersing the slides in xylene I for 5 minutes, xylene II for 5 minutes, and 50% xylene/ethanol for 5 minutes and subsequently rehydrated by immersing in 100% ethanol for 5 minutes

followed by 100% ethanol for 2 minutes, 90% ethanol for 2 minutes and finally 70% ethanol for 2 minutes. For histological visualisation of the spheroids, H&E staining was performed by first immersing the sections in Harris' hematoxylin for 10 minutes before these were washed in running tap water for 5 minutes. Removal of excess blue stain was achieved by immersing the slides in acidic alcohol (0.5% HCl in 70% ethanol) for 3-5 seconds and washing in running tap water for 5 minutes. Next, the slides were immersed in Scott's tap water for 1-2 minutes for blue colour development. Spheroid sections were subsequently counterstained with 1% aqueous Eosin dye for 1 minute followed by washing in running tap water. Sections were drained for 1 minute to remove excess water. The sections were then dehydrated by immersing in absolute alcohol for 1 minute, absolute alcohol for 3 minutes, 50% xylene/ethanol for 3 minutes, xylene II for 3 minutes and clear xylene for 5 minutes. Coverslips were then mounted on the slide using DPX medium (BDH, Dorset) and left to air dry overnight. Once dried, the sections were visualised using a light microscope.

### 2.10.9 APES coated slides

For immunofluorescence detection of hypoxia in spheroids, slides were first immersed in acetone for 2 minutes and then coated in a freshly prepared 4% (v/v) solution of 3-aminopropyltriethoxysilane (APES) in acetone for 2 minutes. Excess APES solution was drained off the slides and the slides washed in running tap water twice for 2 minutes. APES coated slides were air-dried overnight and stored at room temperature. APES makes the slides more adhesive to the tissue. The APES makes the slides positively charged, which binds to negative charges in the tissue. Without it there is the possibility of the tissue floating off the slide during further processing.

## 2.11 Detection of hypoxia in MCS

Following culturing of spheroids using either the hanging-drop or 96-well plate method, spheroids were harvested and pooled into a 1ml eppendorf tube. Old medium was removed and spheroids treated with 1ml fresh medium containing 100µM of pimonidazole (Hypoxyprobe-Green kit) for 2 hours at 37$^{o}$C incubator. Negative samples with no treatment were also included. The tubes were gently shaken every 30 minutes. Following incubation, medium was removed and the spheroids fixed, embedded and sectioned respectively. The sections were mounted on APES coated slides for immunofluorescence detection of hypoxia marker pimonidazole and the proliferation marker Ki67.

### 2.11.1 Immunofluorescence staining of hypoxia and Ki67

Paraffin embedded 5µm thick spheroid sections were baked for 20 minutes at 45$^{o}$C on a slide dryer followed by rehydration. For antigen retrieval, slides were then microwaved for 3 x 10 minutes on full power in freshly prepared sodium citrate solution (2.94g trisodium citrate in 1L, pH6.0, 0.05% tween 20) ensuring topping up of the buffer to avoid sections drying out in between. 3 x 10 minutes of microwaving was selected as this allowed gradual heating rather than rapid heating. The stopping after 10 minutes between each run was done to monitor liquid levels ensuring slides are not dried out by evaporation. By the last 10-minute run, the buffer reached its boiling point upon which the slides were removed from the microwave. The company Cell Signaling Technology recommends microwave or pressure cooker methods for antigen retrieval, suggesting to get the buffer to the point of boiling and then letting it cool. The slides were left to cool in the buffer for 20-30 minutes before washed 3x for 5

minutes in PBS on a circular rocker at medium speed. A PAP pen was used to draw a water repellent circle around each tissue section to prevent the waste of valuable reagents by keeping the liquid pooled in a small droplet. For blocking, 10% FCS in PBS and 5% BSA in PBS was added to each section for hypoxia and Ki67 detection respectively and incubated for 1 hour in a dark moist box at room temperature.

For hypoxia detection, the block was removed and pimonidazole adducts were detected by incubation of sections with FITC conjugated (mouse) Mab1 (Hypoxyprobe$^{TM}$-1 Green kit) at a 1:150 dilution in 10% FCS in PBS for 2 hours at 37$^{o}$C.

Ki67 stains nuclear protein and it is used as a marker for cell proliferation. Ki67 staining was used to observe cell proliferation in the LNCaP spheroid model. For Ki67 detection, the block was removed and Ki67 expression was detected using primary rabbit monoclonal anti-Ki67 antibody (Abcam) at a dilution of 1:150 in 5% BSA in PBS with overnight incubation at 4$^{o}$C. Primary antibody was removed and sections washed 3x for 5 minutes in PBS on a circular rocker at medium speed. Secondary antibody donkey anti-rabbit IgG Alexa Fluor 546 (Molecular Probes) diluted at 1:200 in PBS was then added to the section and incubated for 1 hour in a dark moist box at room temperature.

Finally, sections were washed 4x for 5 minutes in PBS on a circular rocker at medium speed in the dark. Slides were mounted with a coverslip using vectashield with DAPI and sealed with clear nail varnish. Slides were allowed to dry before analysis using a fluorescent microscope (Leica).

## 2.12 Isolation of primary prostate epithelial cultures

Primary prostate epithelial cells were initially cultured from patient tissue by Prof. Norman Maitland's group. Cancer samples were obtained by targeted needle biopsy from radical prostatectomies and benign samples were obtained from TURP. Patient consent and approval was received before biopsies were taken and all samples were anonymised. Tissue processing was kindly performed by Prof. Norman Maitland's team in the University of York. Once the cells were initially plated from tissue processing, subsequence sub-culturing of the primary cells was performed in the present study. Limitations of cells derived from RP and TURP samples include the inability to grow as luminal cells in culture, resulting in a population of only basal cells. Furthermore, primary cells have a short life-span, limiting their sub-culturing.

## 2.13 Primary prostate epithelial cultures derived from patient tissue

The pathology details of the samples used in chapter 4 are outlined in Table 16. The cancer samples were derived from patients aged 60-68 with a Gleason scores of 7. The Gleason score 7 was mainly from (3+4) cancers, with the exception of sample H488/14 RM which was from (4+3) cancer. Interestingly, this sample was from the youngest patient in the cancer group with 4+3 cancer which is more aggressive than 3+4. This exemplifies patient variability in the samples used in this study.

| Patient sample code | Operation | Diagnosis | Gleason score | Patient age | PSA score (ng/ml) |
|---|---|---|---|---|---|
| **H398/14** | TURP | BPH | N/A | 66 | 2.7 |
| **H405/14** | TURP | BPH | N/A | 82 | 8.7 |
| **H415/15** | TURP | BPH | N/A | 74 | 0.61 |
| **H507/14 LM** | RP | PCa | Gl7 (3+4) | 68 | 9.9 |
| **H507/14 RB** | RP | PCa | Gl7 (3+4) | 68 | 9.9 |
| **H488/14 RM** | RP | PCa | Gl7 (4+3) | 60 | 12.6 |
| **H568/15 RM** | RP | PCa | Gl7 (3+4) | 69 | 8.5 |
| **H431/14 LM** | RP | PCa | Gl7 (3+4) | 66 | 14 |
| **H517/15 RM** | RP | PCa | Gl7 (3+4) | 65 | 4.4 |

**Table 16. Pathology of patient samples used.**

The table lists the primary prostate epithelial samples used in this chapter. Diagnosis is based on the most up-to-date pathology. Patient information includes sample code, operation type, diagnosis, Gleason score, patient age and PSA score. PCa- prostate cancer, BPH- benign prostatic hyperplasia, Gl- Gleason, TURP- transurethral resection of the prostate, RP- radical prostatectomy, PSA- prostate-specific antigen.

## 2.14 Maintenance of primary epithelial cultures

Cells were maintained in stem cell media (SCM) [482], which is KSFM (Gibco) supplemented with 5ng/ml of human recombinant EGF protein EGF, 50µg/ml of BPE, 1ng/ml GM-CSF (Milteny Biotec), 2ng/ml SCF (First Link UK Ltd), 100ng/ml CT (Sigma), 2ng/ml LIF (Chemicon) and 1% L-glutamine. Cells were grown and sub-cultured with irradiated Sandoz inbred mouse, Thioguanine- and Ouabain resistant (STO) fibroblast feeder cells in SCM to retain an

undifferentiated basal cell population and to aid in structuring of primary epithelial cells. With each subsequent sub-culture, the fibroblast population diminishes. Cells were grown on BioCoat$^{TM}$ type I collagen-coated 100mm dishes (BD Biosciences). Cells were passaged using 0.05% trypsin-EDTA once 80% confluence and were passaged to a maximum of passage 5. Fresh medium was added every 2 days.

### 2.15 Irradiation of STO fibroblasts

Mouse fibroblasts were inactivated using irradiation to interfere with mitosis. Cells were trypsinised when 80% confluent and subsequently centrifuged to collect a cell pellet. The cell pellet was resuspended in 10ml KSFM and exposed to a radiation dose of 60Gy. Fibroblasts were stored at 4$^{o}$C for a maximum of 4 days before use. This procedure was kindly performed by Dr. Fiona Frame and Dr. Robert Seed.

### 2.16 Preparation of siRNA reagent against ALDHs

20nmol of each siRNA was reconstituted in 1ml of 1X Dharmacon siRNA resuspension buffer to make up a stock solution of 20µM. A working stock solution was further prepared at 2 and 4µM and aliquots were stored at -80$^{o}$C.

#### 2.16.1 siRNA transfection of cells

Cells from passage 2-3 were seeded in a T-25 flask at a density of 1.5 x $10^5$ cells/flask ensuring they were roughly at 20-30% confluence and thoroughly mixed followed by overnight incubation at 37$^{o}$C. Transfection reagents were prepared as shown in Table 17. 30 µl of either 2µM or 4µM siRNA working stock solutions (Ambion) against ALDH1A3, ALDH1B1, ALDH2 and ALDH7A1 were added to the tubes containing Optimem to obtain a final concentration of

siRNA at either 20nM or 40nM respectively. Stock oligofectamine (Invitrogen) was then thoroughly vortexed and a 1:5 dilution was prepared with Optimem to obtain a diluted oligofectamine solution which was incubated for 20-30 minutes at room temperature to allow formation of complexes. Following incubation, 45µl of the diluted oligofectamine was added to the relevant tubes and left for 45-minute incubation at room temperature. Cells were washed with 5ml optimem after removing old media to ensure all serum traces are removed (in the case of cell lines). 2ml optimem was then added to each flask followed by 500ul of the siRNA mixture which was added drop-wise. The flasks were gently mixed and returned to the incubator. Following 4 hours of incubation, 2.5ml of normal complete media was added to the flasks and flasks returned to the incubator for a further 48 or 72 hr before harvesting for downstream applications. Images of cells were taken using a light microscope before harvesting to see any phenotypic changes of cells post transfection. A mock (media only) and liposomal only (media and oligofectamine only) control were used to check for any non-specific effects given by the reagents. A non-sense or scrambled control was not included as a negative control due to cost restrictions. This is further explained in the discussion section.

| | Optimem | siRNA | Diluted Oligofectamine | Final volume of mixture | Final volume added to cells |
|---|---|---|---|---|---|
| **Mock control** | 500µl | - | - | 500µl | 500µl |
| **Liposome only control** | 555µl | - | 45µl | 600µl | 500µl |
| **siRNA transfected** | 525µl | 30µl | 45µl | 600µl | 500µl |
| **siRNA co-transfected** | 495µl | 30µl (each) | 45µl | 600µl | 500µl |

**Table 17. siRNA transfection reagents**

## 2.17 Cell proliferation using trypan blue assay

Primary cells were seeded at a density of 3 x $10^4$ cells/ml and counted 48hr after siRNA transfection (72hr post seeding) using a hemocytometer. Briefly, cells were harvested and resuspended in complete media. 10µl of cell suspension was mixed with 10µl of 0.4% Trypan blue solution (Sigma) and loaded on each side of the chamber. Cells were counted in 5 grids and an average was taken which was multiplied by 2. Cells that stained blue were not included in the cell count as they are indicative of dead cells.

## 2.18 Colony forming assay

Primary cells were harvested 48hr post transfection using trypsin/EDTA and 500 cells were seeded per well in a 12-well collagen-I coated plate in 1ml SCM with about 200,000 - 250,000 feeder STO cells. Cells were incubated at 37$^o$C in 5% $CO_2$. Medium was replenished every two days and STOs added when they appeared sparse. STOs were primarily added during the establishment of the primary cultures to get the cells from single cells to forming colonies and then filling the plate. As the primary epithelial cells grew out, the irradiated STOs gradually died off. At the point of plating primary cells for colony forming

or viability assays the plate was predominantly primary cells with very few STOs. The density of STOs and the volume they were resuspended in were consistent.

Following 7-14 days of growth, old medium was removed and cells washed once with PBS. Cells were fixed with 1ml crystal violet solution (dissolve 0.3g crystal violet in 3ml 100% ethanol and add 27ml PBS) for 15 min followed by removal of crystal violet solution and a single wash with PBS. Colonies were then counted using a Leica DM IL LED microscope by Dr. Fiona Frame and percentage colony forming efficiency (CFE) was worked out using the number of colonies counted and dividing it by the cell seeding density and finally multiplying it by 100.

### 2.19 Wound healing assay (Migration assay)

Primary cells were seeded at a density of 90,000 cells per well in a 12-well plate 48hr post siRNA transfection in 1ml SCM and allowed to attach for 24 hours at 37$^{o}$C and 5% $CO_2$. A scratch was introduced vertically in the monolayer of cells along the centre of the well using the tip of a 1ml pipette tip. PBS was used to wash the cells once and fresh SCM was added to the cells. Images were taken using Evos XL transmitted light microscope (AMG) at 0 hours of scratch and subsequent images were taken at different time points of 3hr, 6hr and 24hr to assess cell migration. Image J software was used to measure wound widths at three different areas and the migratory rate was calculated using:

(width at 0 hour) - (width at $x$ hours) / time ($x$)

## 2.20 Cell cycle analysis

Media was removed from the cells 48hr post siRNA transfection and collected in a 20ml tube. The cells were washed with PBS and the PBS was pooled with media. Trypsin/EDTA was then added to the cells to allow detachment. Trypsin/EDTA was neutralised with media and the cell suspension was pooled with the old media and PBS wash. Cells were centrifuged at 1000x rpm for 3 minutes and the cell pellet was resuspended in 0.5ml PBS. The cells were then fixed by adding 2ml ice cold 70% ethanol dropwise whilst vortexing and left for a 30-minute incubation on ice. Cells were then centrifuged at 1000x rpm for 3 minutes and the ethanol was removed. Cells were then resuspended in 5ml PBS, centrifuged and resuspended in 0.4ml PBS. Then, 50µl of RNAse (1mg/ml) (Sigma) and 50µl of propidium iodide (PI) (1mg/ml) (Sigma) were added to the cells and incubated for 30 minutes at 37$^{o}$C. Cells were then analysed for 2N and 4N DNA content on a flow cytometer (Cyan ADP Analyser, Beckman Coulter). Fluorescence was measured in the Texas red channel and 10,000 events were measured. Data analysis was performed using the Summit software.

## 2.21 Analysis of cell differentiation

Primary cells were harvested 48hr post siRNA transfection using trypsin/EDTA and neutralised in SCM. Cells were then centrifuged at 1000 rpm for 3 minutes and washed once in PBS and re-centrifuged. Cells were then resuspended in 300µl of cold magnetic-activated cell sorting (MACS) buffer (2mM EDTA, 0.5% BSA in PBS) and split into three 5ml FACs tubes each containing 100µl cell suspension. Tubes included cells only, control antibody and CD49b antibody. 10µl of MACS FcR blocking reagent was then added to the two antibody tubes

followed by 10µl of the relevant antibodies to two antibody tubes (REA control (s)-Fitc Ab and CD49b-Fitc) (cat:130-104-610 and 130-100-337, MACS, Miltenyi Biotec). Tubes were then put on a rotator at 4$^{o}$C for 10 minutes. Cells were then washed in 2ml ice-cold MACS buffer, centrifuged at 1000 rpm for 3 minutes and resuspended in 1ml ice-cold MACS buffer. Cells were then analysed for CD49b expression using a flow cytometer. Gates were set up using cell only control samples. PI stain was added immediately before analysis at 1µl to test live/dead cells before running samples. Samples were protected from light to avoid bleaching of the fluorescence signal. CD49b expression was measured in the FITC channel (excitation 495nm / emission 519nm). 10,000 events were measured and data was analysed using the Summit software.

The median of the FITC plot was used relating to the brightness of signal and measured at a wavelength of 495nm excitation and 519nm emission. A ‘FITC log versus Violet2 log’ plot was drawn (Violet 2 is negative). The positive area was gated on one plot (CD49b positive). An area relating to high expression and therefore relating to TA cells was gated on another plot (same axes). To measure the percentage of CB cells, the cells inside the TA gate were removed from the total positive gate. The numbers were plotted as a proportion of total percentage. At least 6 biological samples were investigated (BPH n=2, cancer n=4).

There is a risk to cell surface proteins, such as CD49b, when using trypsin to harvest cells because the proteins may be cleaved off due to the proteolytic activity of trypsin [483]. Therefore, to minimise cleavage, cells were only briefly incubated with trypsin, which was neutralised by complete media. In addition,

flow cytometry was carried out on separated cells, which gave the expected high CD49b expression in TA cells and low CD49b expression in CB cells. This acted as a CD49b control ensuring that it was still present on the cells.

### 2.22 Alamar blue cell viability assay

Primary cells were seeded in 96-well plates at a density of 5000 cells/well in 100µl SCM and incubated at 37$^{o}$C, 5% $CO_2$ for 24 hours. ALDH compounds were prepared in DMSO at a stock concentration of 200mM. Cells were treated with 100µl of ALDH inhibitors at concentrations of 50µM and 200µM as single treatment. Combination treatments included 100µl of 50µM ALDH inhibitor + 1nM docetaxel and 100µl of 200µM ALDH inhibitor + 1nM docetaxel. Cells were also treated with 100µl of 1nM docetaxel only. 1nM of docetaxel was chosen since it was the IC50 when other primary samples had been analysed previously by Dr. Fiona Frame in a different study. Control wells included blank (media only) and untreated cells (DMSO only). Experiment was performed in triplicate, and cell seeding density was the same in all well, therefore changes in treated cells were compared to untreated DMSO control cells. Plates were returned to the incubator for 72-hour incubation before further processing. Alamar blue solution was added at 10% of total sample volume and plates were incubated at 37$^{o}$C for 1-4 hours before absorbance was analysed in a plate reader. Alamar blue has excitation wavelength of 530-560nm and emission wavelength of 590nm. Total % cell viability/cell survival was calculated by dividing absorbance of treated sample by absorbance of control and multiplying it by 100.

## 2.23 Cell lines tested against different compounds

The cancer cell lines used for compound testing are summarised in Table 18.

| Cell line | Cancer type | Status | Obtained from | Reference |
|---|---|---|---|---|
| H1299/mock | NSCLC | Low endogenous ALDH expression | Prof. Jan Moreb (Univeristy of Florida) | [484] |
| H1299/7A1 | NSCLC | Low endogenous ALDH expression, stable transfection with ALDH7A1 | Prof. Jan Moreb (Univeristy of Florida) | [484] |
| A549 | NSCLC | Naturally expresses ALDH1A1 and ALDH3A1 | Dr. Klaus Pors (University of Bradford) | [484] |
| PC3 Ag | Prostate | Aged alongside PC3 D8 as control | Dr. Amanda J O'Neil (University College Dublin, Ireland) | [485] |
| PC3 D8 | Prostate | Numerous docetaxel treatment cycles | Dr. Amanda J O'Neil (University College Dublin, Ireland) | [485] |

**Table 18. Cancer cell lines used for compound testing**

## 2.24 PC3 resistant cell line development

The PC3 resistant cell line (D8) and its wild-type parental cell line (Ag) were generated by Dr. Amanda J O'Neil's group (University College Dublin, Ireland). Briefly, the PC3- resistant sub-line D8 was generated by initially treating with docetaxel at 4nM (dissolved in DMSO) in T75 flasks for 48 hours. The generation of these cell lines have been described [485] but briefly involved the following: after exposure to docetaxel, the surviving cells were re-seeded into new flasks and recovery was allowed for 2-3 weeks. After 7 treatments at 4nM, the dose of docetaxel was increased to 8nM. The cells underwent a total of 18 treatment cycles at 8nM (cell passage numbers 21-55). After each treatment, the cells were allowed to fully recover prior to assessing their resistance to docetaxel. As the passage number of the treated cells increased over time, a subset of PC3 cells were aged alongside these cells as an

appropriate control to ensure that the effects seen were due to resistance rather than due to an aging effect of the PC3 Ag cells [485]. Resistance was defined as the emergence of P-gp (ABC transporter MDR-1) expression and the use of Elacridar (a potent inhibitor of P-gp).

### 2.25 H1299 mock and ALDH7A1 isogenic cell line pair development

The lung cancer cell line isogenic pair H1299/mock and H1299/7A1 was developed by Prof. Jan Moreb's group through inducing stable transfection of ALDH7A1.

### 2.26 Drug cytotoxicity testing using the MTT assay

The effect of docetaxel and ALDH inhibitors on cell viability was assessed using the 3-(4,5-Dimethylthiazol-2-yl)-2,5-diphenyltetrazolium bromide (MTT) assay. This assay is similar to the Alamar blue assay, however, since this part of the study was carried out in University of Bradford, MTT was the available method in house. Both methods are acceptable and work in similar ways such as both are metabolic and colorimetric assays, with Alamar blue previously reported as a more sensitive method [486]. MTT assay is based on the bioreduction of tetrazolium salts from pale yellow to the dark blue formazan crystals by mitochondrial dehydrogenases and is an end-point assay. Alamar blue also known as resazurin, is transformed from blue colour to a highly fluorescent resorufin (pink) within a redox reaction process. Alamar blue assay is non-toxic and allows continuous monitoring of cultures over time, with the advantage that further analytical assays can be performed on the same samples compared to the MTT assay [487].

Cells were seeded in a 96-well plate at a seeding density of 2000 cells/well in 180µl complete medium and allowed to adhere for 24 hours at 37$^{o}$C, 5% $CO_2$

and 95% humidity. Control wells included medium only to serve as the blank and cells without drug (untreated) which act as 100% cell survival control. The following day, cells were treated with 20µl of working drug solutions in complete medium added to the relevant wells at different concentrations. Control cells were treated with DMSO in complete medium with a final concentration of no more than 0.1%. Cells were then incubated for 96 hours at 37$^{o}$C and 5% $CO_2$. After incubation, 20µl of MTT dissolved in $dH_2O$ (5mg/ml) was added to each well of the plate and left for a further incubation of 4 hours. All supernatant was carefully removed from the wells leaving the resulting formazan crystals at the bottom of the wells which were dissolved with 150µl of DMSO. Formation of formazan crystals correlated with cell number as formazan is formed by metabolically viable cells. Absorbance was read in a plate reader at 540nm and percentage cell survival was calculated by first subtracting the absorbance of all the wells from the blank, then dividing treated cells by untreated control and finally multiplying by 100.

## 2.27 Statistical analysis

Statistical analyses were carried out using GraphPad Prism 6. Where experiments were carried out in triplicate, error bars represent ± standard deviation. Statistical significance is highlighted as * p = 0.01 to 0.05, ** p = 0.001 to 0.01, *** p = 0.0001 to 0.001, **** p < 0.0001. Selection criteria of statistical test was based on whether the data was parametric or non-parametric.

Comparing untreated samples with treated samples derived from same cell line or primary cells was considered paired analysis. Comparing one cell line to another, or comparing a group of primary cultures from different patients was considered unpaired. To determine whether the data had a Gaussian distribution, and subsequently whether a parametric or non-parametric test should be applied, normality tests were carried out using the GraphPad Prism 6 and SPSS software, taking into account the sample size. Normality test used included Shapiro-Wilk test, and Skewness and Kurtosis test to determine data distribution.

A student's t-test was used to compare the means of an untreated group to a treated group in which the samples were paired/unpaired and had a normal distribution with n=3 or more. A Mann Whitney U test was applied to compare two groups (paired/unpaired and non-parametric) with more than 3 samples. A one-way ANOVA test was applied to make multiple comparisons at once using a paired/unpaired group compared with 2 or more paired/unpaired groups.

# Chapter 3

## Evaluation of the expression patterns and regulation of ALDHs in prostate cancer

## Introduction

### 3.1 ALDH expression in subpopulation of human prostate primary cells

DNA microarray analysis data of SC and CB cell types isolated from BPH and prostate cancer tissue generated by Prof. Norman J. Maitland's group (data not published but kindly permitted by Prof. Norman J. Maitland to use for the purpose of this chapter), revealed differential expression of all 19 human ALDH isoforms within the selected cell populations and disease states. Analysis of the ALDH expression pattern from 12 patient samples, showed that ALDH1A3 is the highest expressing isoform in prostate tissue. ALDH1A1 is well studied but this data revealed that ALDH1A1 is not the most highly expressed isoform in prostate tissue (Figure 17).

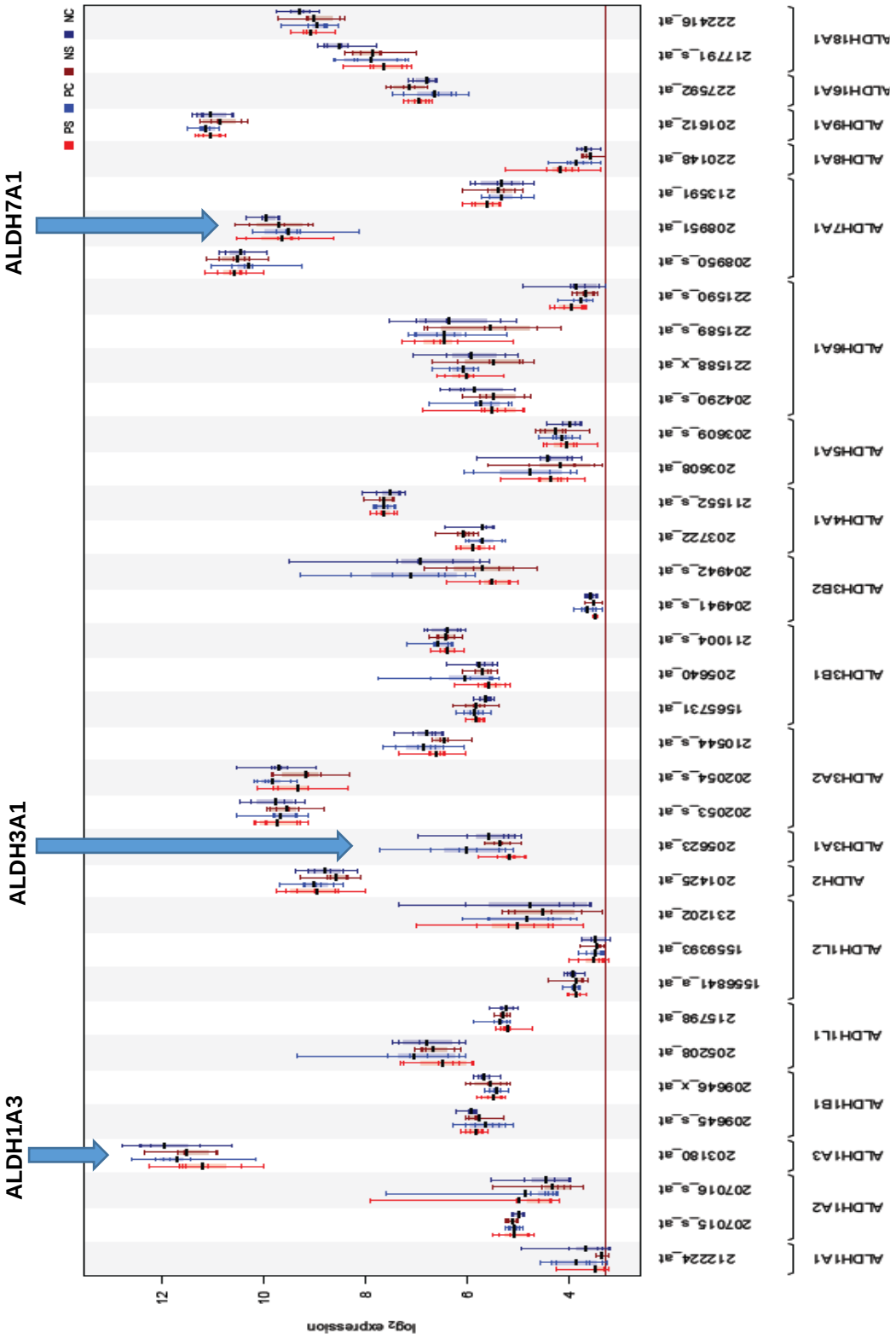


**Figure 17. Microarray analysis of selected aldehyde dehydrogenase isoform expression levels in primary prostate samples.**

Primitive stem cells (S) and their more differentiated progeny (C) from both clinical PCa (P) and benign (N) samples. (data not published but used with the permission from Prof. Norman J. Maitland, University of York), data is from the microarray reported in [488].

## 3.2 Aims and Objectives

Currently, only two studies have described the epigenetic modulation of ALDHs [474, 489], one of which demonstrated dense hypermethylation of the ALDH1A2 gene promoter and reported it as a candidate TSG in prostate cancer. Furthermore, the correlation between ALDH expression and hypoxia in prostate cancer has not yet been explored while only little is known about the influence RA has on selected ALDH isoform expression. Accordingly, this chapter will explore the expression and regulation pattern of selected ALDH isoforms including ALDH1A1, ALDH1A2, ALDH1A3, ALDH1B1, ALDH2, ALDH3A1 and ALDH7A1 in prostate cancer.

ALDH isoforms -1A1, -2 and – 3A1 were selected based on the findings of Dr. Cosentino for further investigation. ALDH1A2 was reported as a candidate TSG in prostate cancer [474], ALDH1A3 was the most highly expressed isoform from the microarray analysis from Prof. Maitland's group and ALDH1B1 was studied to include a B member of the ALDH1 family as it is a relatively unexplored member of the ALDH superfamily. Finally, ALDH7A1 was selected as it has been reported to be contributing to the aggressiveness of prostate cancer and is involved in bone metastasis [490].

Specifically, the objectives were:

- Profile gene and/or protein expression of the selected ALDHs in a benign prostate cell line, a panel of prostate cancer cell lines, primary prostate epithelial cultures, subpopulations of SC, TA and CB primary prostate cells and human benign tissue to investigate the expression pattern of the ALDHs in normal and cancer state.

- Evaluate the gene and/or protein expression of ALDHs following treatment with epigenetic drugs in prostate cell lines and primary prostate cultures.

- Investigate the ALDH gene expression upon atRA treatment in primary prostate cultures to explore ALDH regulation by RA.

- Investigate the impact hypoxia has on the gene and protein expression of ALDHs in prostate cell lines to understand if low oxygen tensions affect ALDH expression.

- Optimise a prostate cancer multicellular spheroid (MCS) model for future exploration of ALDH expression within different regions of the spheroids.

## 3.3 Results

## 3.4 ALDH gene expression investigation in prostate cell lines

Preliminary studies carried out by Dr. Laura Cosentino (previous PhD student in the Pors' group) using normal prostate cell lines and cancer cell lines to explore ALDH1A1, ALDH2 and ALDH3A1 gene expression by qPCR (data not published, but kindly provided for the purpose of this chapter by Dr. Pors), revealed low levels of ALDH1A1 in the normal PNT2C2 cells compared to higher expression in cancer cell lines PC3, DU145 and LNCaP. The expression of ALDH2 was also lower in PNT2C2 compared to PC3, DU145 and LNCaP cells. The expression of ALDH3A1 was low in PNT2C2, DU145 and LNCaP cells but high in PC3 cells (Figure 18). There was increased expression of ALDH1A1 following DAC treatment of PNT2C2, PC3, DU145 and LNCaP cells. However, ALDH3A1 expression only increased in DU145 and LNCaP cells after DAC treatment (Figure 19). Interestingly, the normal cell line PNT1A as compared to PNT2C2 and RC165, showed high expression of ALDH1A1, -2 and -3A1, with increased ALDH1A1 expression following DAC treatment. However, no further studies were undertaken to address this observation.

Although Dr. Cosentino also looked at PNT1a, RC165 and P4E6, the present study has focused on PNT2C2, PC3, DU145 and LNCaP cell lines only due to time limitations as this study further incorporated the use of primary prostate cultures as a study model. PNT2C2 was the preferred cell line as a normal model as it showed differences in ALDH expression compared to the cancer cell lines, and it was the only normal cell line available in the institute's cell

bank. The three cancer cell lines were selected because they are traditionally used in the field as standard models for prostate cancer, and a further two prostate cancer cell lines SerBob and Bob were included in the present study. The present study did not study ALDH1A1, -2, and -3A1 expression in cell lines that was shown by Dr. Laura Cosentino. Data from Figure 18 and 19 were generated by Dr. Laura Cosentino prior to the work done in the present thesis, and no statistical tests were applied by Dr. Cosentino to validate the statistical significance of these previous findings.

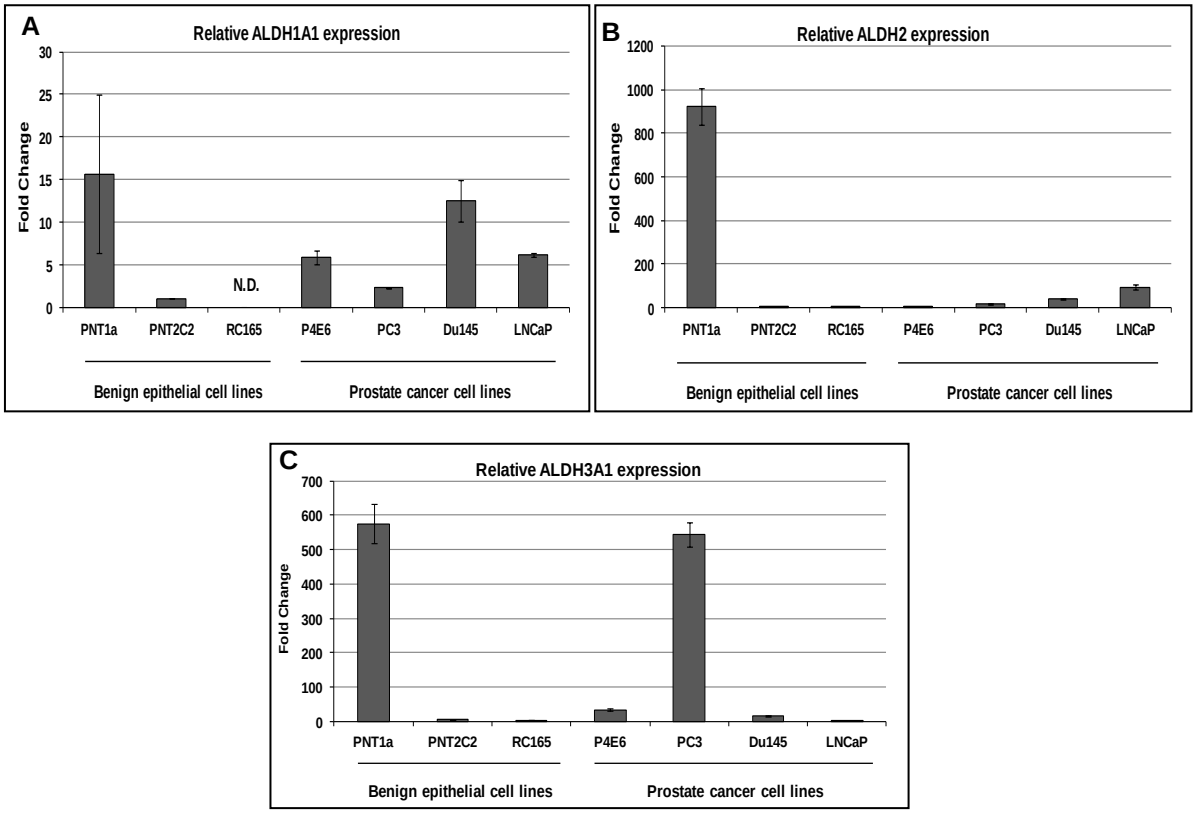


**Figure 18. Preliminary gene expression data by qPCR on selected ALDH isoforms and prostate cell lines.**
(A) ALDH1A1, (B) ALDH2 and (C) ALDH3A1 gene expression in the benign cell lines PNT1A, PNT2C2 and RC165, and in the cancer cell lines P4E6, PC3, DU145 and LNCaP. Data produced by Dr. Laura Cosention.

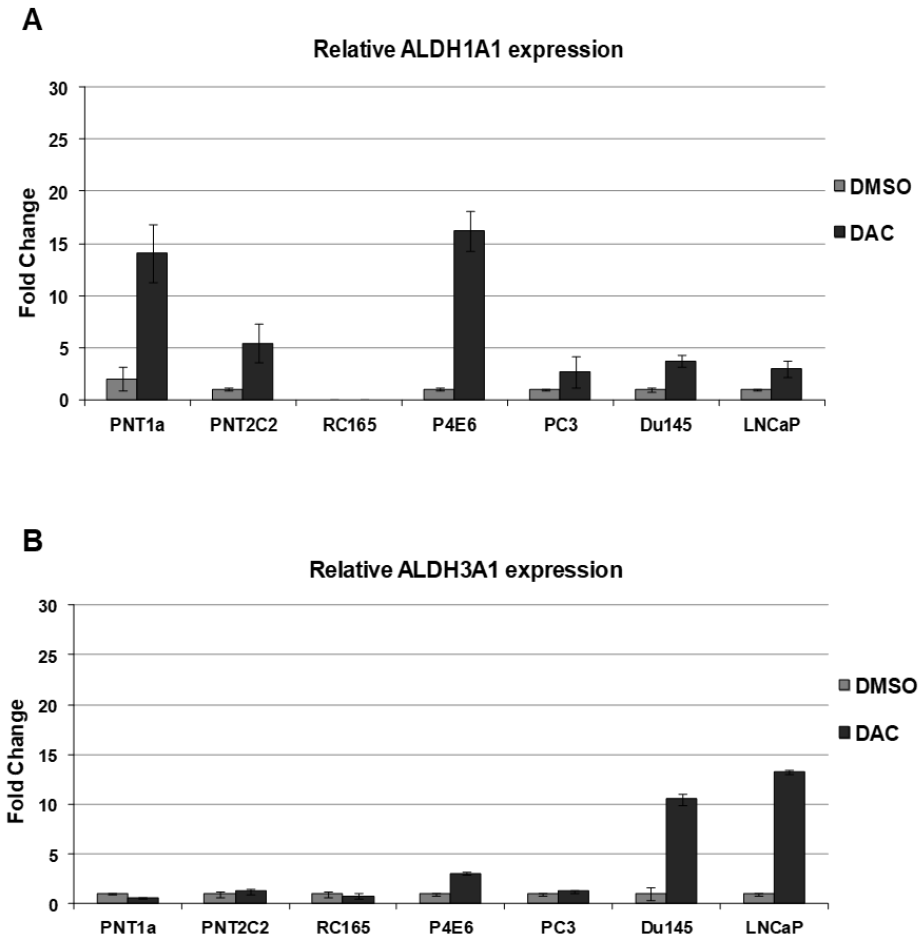


**Figure 19. Preliminary gene expression data by qPCR following treatment with decitabine (DAC) on selected ALDH isoforms and prostate cell lines**

(A) ALDH1A1 and (B) ALDH3A1 gene expression in the benign cell lines PNT1A, PNT2C2, and RC165, and in the cancer cell lines P4E6, PC3, DU145 and LNCaP. Data produced by Dr. Laura Cosentino.

## 3.5 Differential expression patterns of ALDH genes in prostate cell lines

The basal mRNA expression levels of ALDH1A1, -1A2, -1A3, -1B1, -2, -3A1 and -7A1 were quantified by qPCR in a normal prostate cell line PNT2C2 and a panel of prostate cancer cell lines including SerBob, Bob, LNCaP, DU145 and PC3. For normalisation of the target genes, the housekeeping gene RPLP0 was used as it had been optimised as a reference gene for most prostate cell lines by Professor Maitland's group at the University of York. In the case of using the SC/TA/CB selected populations from the primary cultures, previous work in the Maitland lab showed that the expression of some housekeeping genes varied between the subpopulations. Therefore, multiple housekeeping genes were not used. RPLP0 was chosen because it was the most consistently expressed between the subpopulations. The basal mRNA expression was generated using $2^{-dCT}$ method from three independent experiments, and a mean value ± SD was calculated.

Figure 20 (A) shows a significantly high expression of ALDH1A1 in prostate cancer cell line SerBob compared to PNT2C2. Figure 20 (B) shows a significantly high expression of ALDH1A2 only in PC3 cells. ALDH1A3 mRNA expression was significantly reduced in SerBob, Bob, LNCaP and DU145 cells compared to PNT2C2 as shown in Figure 20 (C). Figure 20 (D) shows significantly low mRNA expression of ALDH1B1 in SerBob, Bob DU145 and PC3 cells. ALDH2 and ALDH3A1 expression was significantly increased in SerBob cells as shown Figure 20 (E and F). ALDH7A1 expression was significantly decreased in Bob, LNCaP and PC3 cells as shown in Figure 20 (G). Taken together, ALDHs showed varied expression in the different cell

lines. ALDH1A3 showed highest expression in PNT2C2 benign cell line, however its expression was also high in the most aggressive cell line PC3. ALDH1A2 expression was not detected in most cases with the exception of PC3 cells. This correlates with the potential hypermethylation of ALDH1A2 in cells with malignant properties as reported by an earlier study [474]. The expression of ALDH1A3, ALDH1B1 and ALDH7A1 was observed in most cancer cell lines to various degrees.

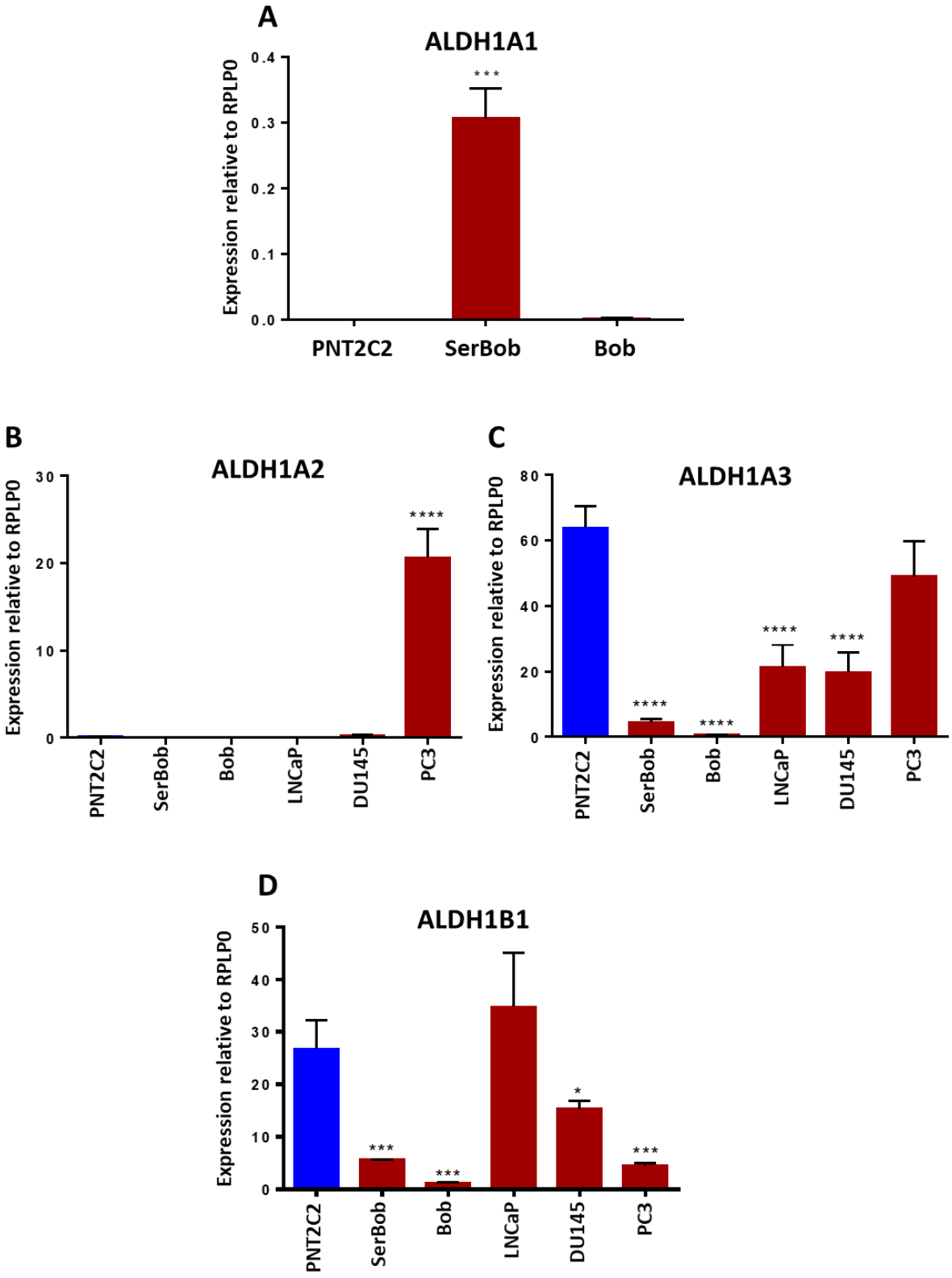
A
ALDH1A1
Expression relative to RPLP0
0.4
0.3
0.2
0.1
0.0
***
PNT2C2
SerBob
Bob
B
ALDH1A2
Expression relative to RPLP0
30
20
10
0
****
PNT2C2
SerBob
Bob
LNCaP
DU145
PC3
C
ALDH1A3
Expression relative to RPLP0
80
60
40
20
0
****
****
****
****
PNT2C2
SerBob
Bob
LNCaP
DU145
PC3
D
ALDH1B1
Expression relative to RPLP0
50
40
30
20
10
0
***
***
*
***
PNT2C2
SerBob
Bob
LNCaP
DU145
PC3

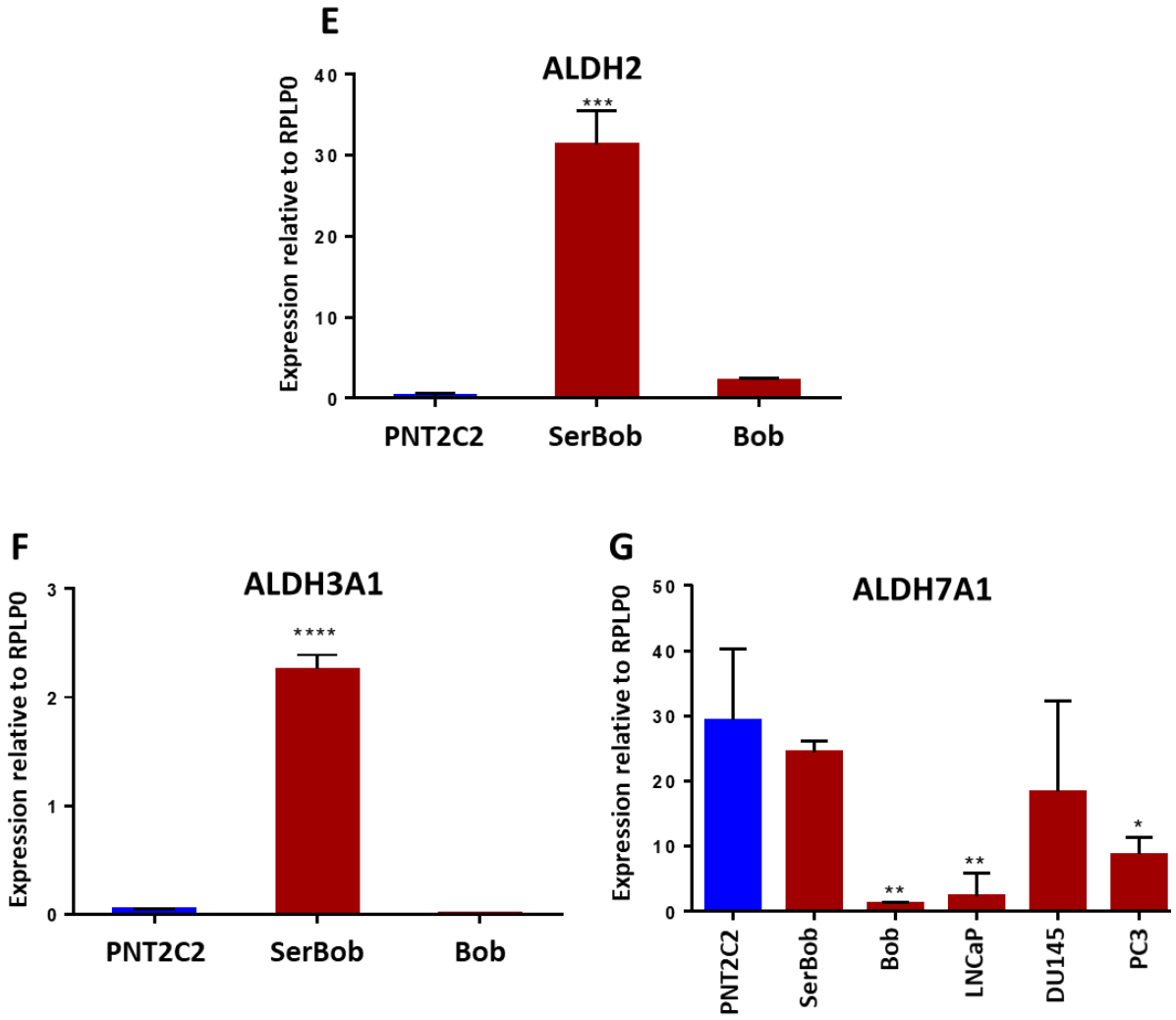


**Figure 20. qPCR analysis of ALDH gene expression relative to housekeeping gene RPLP0 in prostate cancer cell lines.**

Gene expression of (A) ALDH1A1, (B) ALDH1A2, (C) ALDH1A3, (D) ALDH1B1, (E) ALDH2, (F) ALDH3A1 and (G) ALDH7A1 was measured using $2^{-dCT}$ in a panel of selected prostate cancer cell lines. Where ALDH1A1, -2 and -3A1 had already been analysed previously by Dr. Cosentino (Por's group) in LNCaP, DU145 and PC3 cell lines, these were not investigated in this study. Note difference in scale of Y-axis. Statistical significance was measured as a comparison of each cell line to the normal PNT2C2 cell line. Data are represented as a mean of three independent experiments ± SD. Statistical significance was calculated using one-way ANOVA for unpaired groups; multiple comparisons (more than two groups); cancer cell lines (red) compared to benign cell line (blue). * p = 0.01 to 0.05, ** p = 0.001 to 0.01, *** p = 0.0001 to 0.001, **** p < 0.0001.

### 3.6 Expression profiling of ALDH genes in primary epithelial cultures derived from human prostatic benign and cancer tissues

Whole population RNA samples were kindly provided by Professor Maitland's group (University of York) with a Gleason score ranging from 6-9.

A significant difference was observed for expression of ALDH isoforms 1A3 (Figure 21 C), 1B1 (Figure 21 D) and 2 (Figure 21 E) in primary prostate samples with a higher expression in cancer than in BPH samples and this observation was more pronounced with ALDH1A3 expression (note difference in scale). ALDH1A1, 3A1 and 7A1 were found to be similarly expressed in benign and cancer samples (Figure 21 A, F, G). The expression of ALDH1A2 was low in most samples analysed (Figure 21 B).

In contrast to ALDH expression in cell lines, ALDH1A3 expression was much higher in primary cancer samples compared to primary benign samples at mRNA level. Taken together, these results exemplify the importance of using primary cells as a model to validate gene expression and suggests the correlation of ALDH1A3, ALDH1B1 and ALDH2 with prostate cancer.

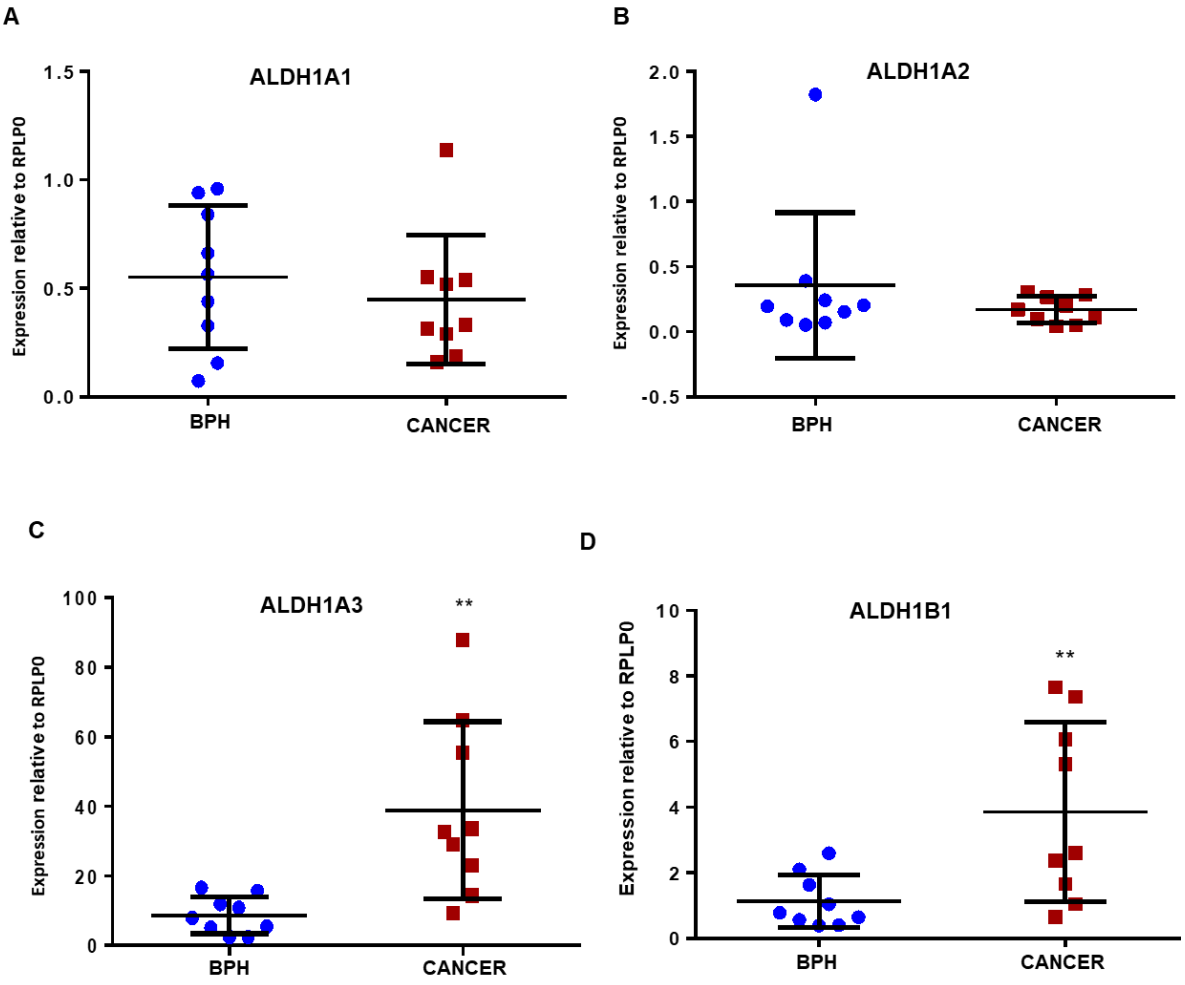
A
ALDH1A1
Expression relative to RPLP0
1.5
1.0
0.5
0.0
BPH
CANCER
B
ALDH1A2
Expression relative to RPLP0
2.0
1.5
1.0
0.5
0.0
-0.5
BPH
CANCER
C
ALDH1A3
**
Expression relative to RPLP0
100
80
60
40
20
0
BPH
CANCER
D
ALDH1B1
**
Expression relative to RPLP0
10
8
6
4
2
0
BPH
CANCER

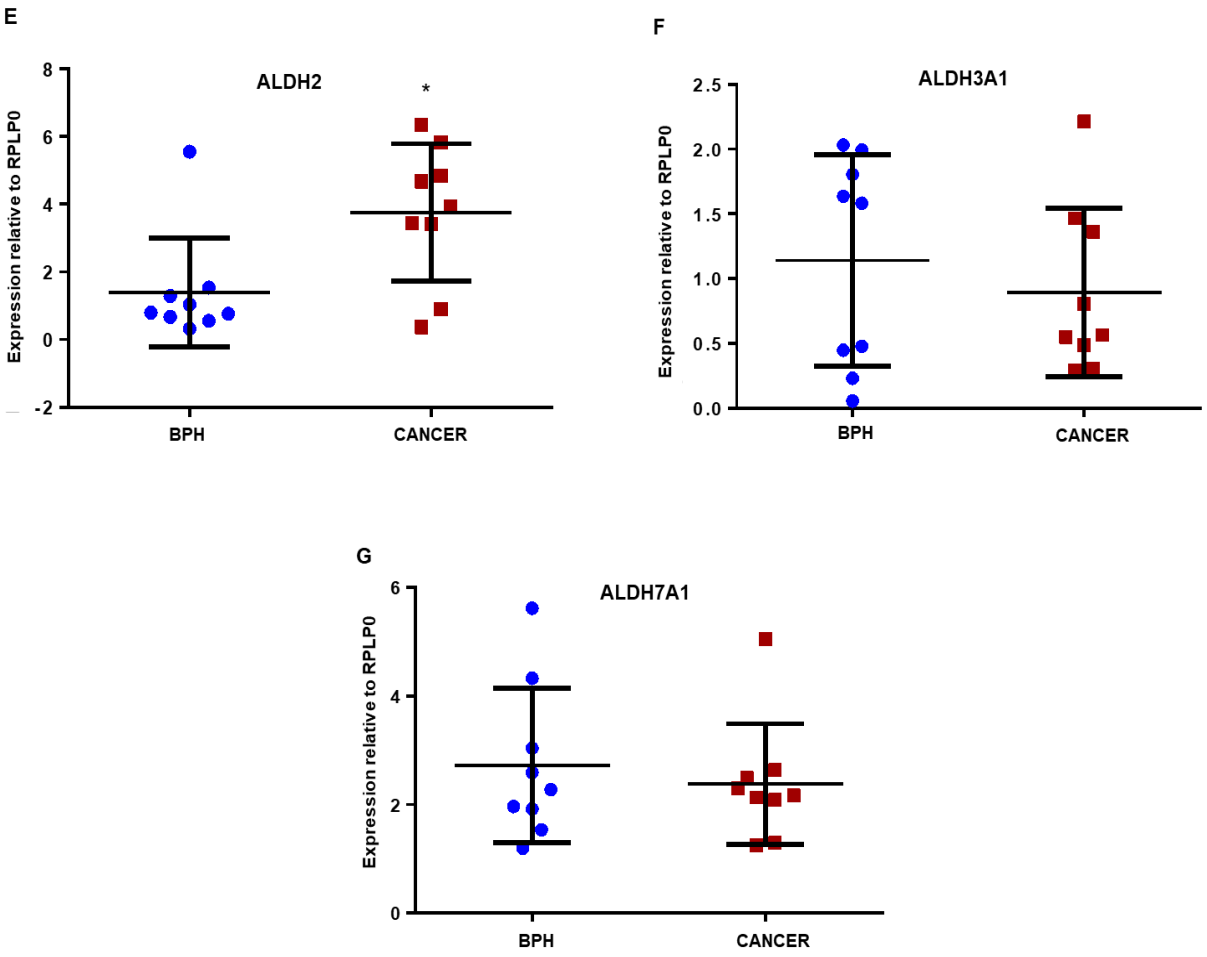


**Figure 21. qPCR analysis of ALDH gene expression relative to RPLP0 in prostate primary epithelial cultures.**

Gene expression of (A) ALDH1A1, (B) ALDH1A2, (C) ALDH1A3, (D) ALDH1B1, (E) ALDH2, (F) ALDH3A1 and (G) ALDH7A1 was measured using $2^{-dCT}$. RNA was extracted from patient-derived prostate epithelial cells from prostate cancer tissue (n=9) and BPH tissue (n=9). *Note difference in scale on Y-axis. Statistical significance was calculated using Mann Whitney U test, for unpaired groups, non-parametric distribution, comparison of only two groups. BPH samples denoted as blue circles and cancer samples as red squares. * p = 0.01 to 0.05, ** p = 0.001 to 0.01, *** p = 0.0001 to 0.001, **** p < 0.0001. See appendix I for sample details.

### 3.7 Differential expression of ALDHs in the primary prostate epithelial hierarchy

In an attempt to investigate the difference in ALDH gene expression pattern in different population of cells within the tissue, RNA from primary benign and cancer cells which had been selected into SC, TA, and CB cell populations based on their cell surface antigens was used [491]. The different cell populations were cultured, harvested and RNA extracted by Prof. Norman Maitland's group in University of York, and the RNA samples were kindly provided by them for this study. cDNA synthesis of this RNA and qPCR was performed as part of this study.

qPCR analysis of primary prostate epithelial cells showed differential ALDH gene expression between the different cell types of cells within a heterogeneous tissue. However, it did not differentiate between benign and cancer samples. Analysis of more patient samples would be required in order to determine if there is a distinction (Figure 22 A-G). In addition, the number of samples was very low for each population in particular the SC population. Since, the RNA yield was very low for the SCs, analysis was focused on ALDH1A3 and ALDH1B1 due to their high expression in cell lines and primary cells. ALDH7A1 was also focused on as it has previously been reported to be associated with prostate cancer. For these 3 isoforms, One-way ANOVA statistical test was used to compare SCs with TA and CB as unpaired groups. However, due to only 1 SC sample for the remaining ALDH isoforms (1A1, 1A2, 2, and 3A1), this comparison was not feasible, hence the TA population was compared with CB population using the Mann Whitney U test. Both tests were applied and it was shown that there was no statistical difference in ALDH

expression between any populations for all the ALDHs. The expression appeared varied in some samples within each population. This may be due to the samples being different based on patient variability, and therefore having an impact on the statistical outcomes. More samples are needed to truly see a statistical difference between the cell types.

Interestingly the expression of ALDH1A1 was higher in CB cells than SC and TA cells, contrary to previous studies using ALDH1A1 as SC marker (Figure 22 A). In accordance with cell line and whole population primary cell data, the expression of ALDH1A2 is least expressed in most samples compared to other ALDHs across the 3 population of cells, except one sample that showed high ALDH1A2 expression in TA and CB cells (Figure 22 B). It was found that ALDH1A3 expression was similar between the different cell types and the expression was higher compared to other ALDH isoforms (note difference in scale) (Figure 22 C). ALDH1B1, -2 and -3A1 showed a similar pattern of expression between SC, TA and CB cell populations with some outliers (Figure 22 D-F). The expression of ALDH7A1 was higher in the more differentiated TA and CB cells than SC (Figure 22 G).

Taken together, this data suggests that ALDH1A3 and ALDH7A1 are highly expressed in prostate tissue with the former also contributing to expression in the SC component in contrast to ALDH1A1. However, none of the difference in ALDH expression between different cell types was statistically significant and therefore, more samples would be required to make this distinction and validate the observed changes.

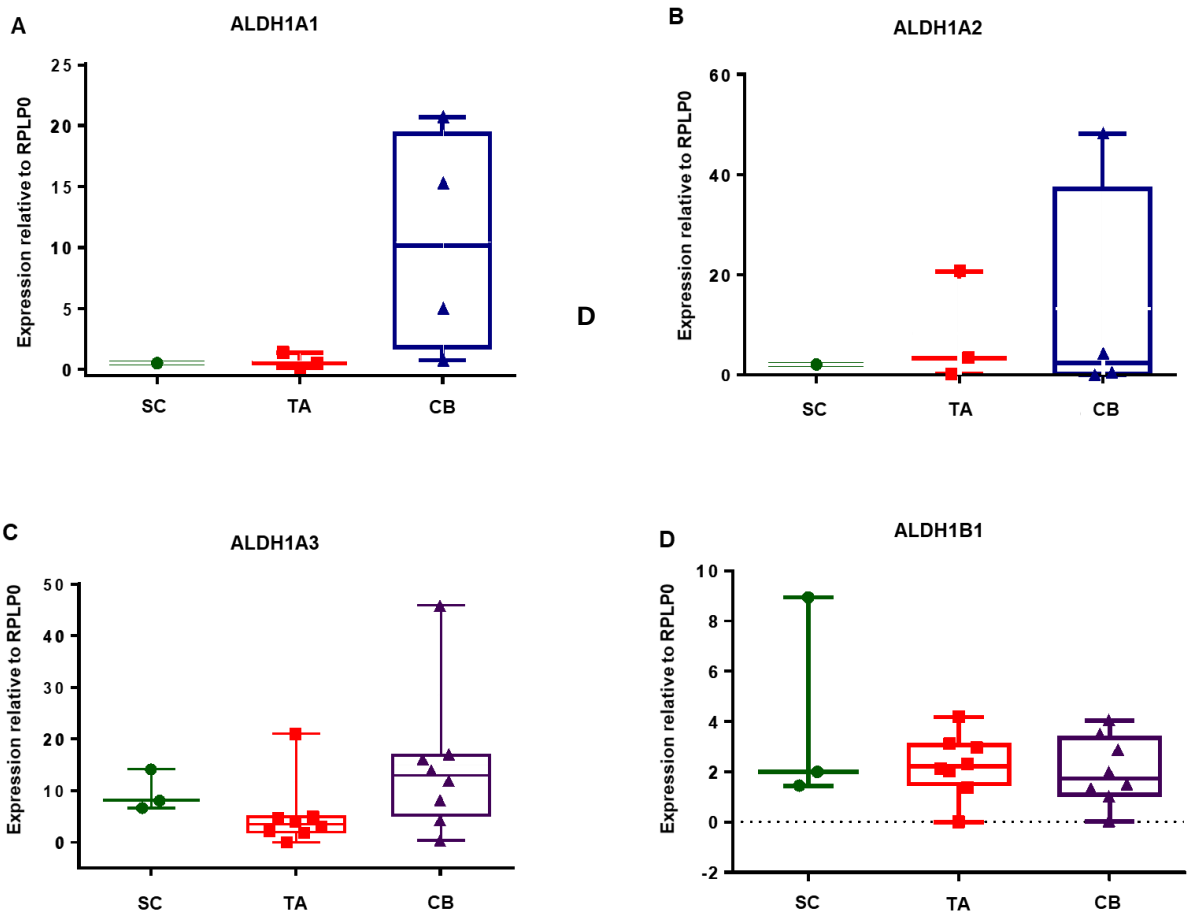
A
ALDH1A1
Expression relative to RPLP0
25
20
15
10
5
0
SC
TA
CB
B
ALDH1A2
Expression relative to RPLP0
60
40
20
0
SC
TA
CB
C
ALDH1A3
Expression relative to RPLP0
50
40
30
20
10
0
SC
TA
CB
D
ALDH1B1
Expression relative to RPLP0
10
8
6
4
2
0
-2
SC
TA
CB

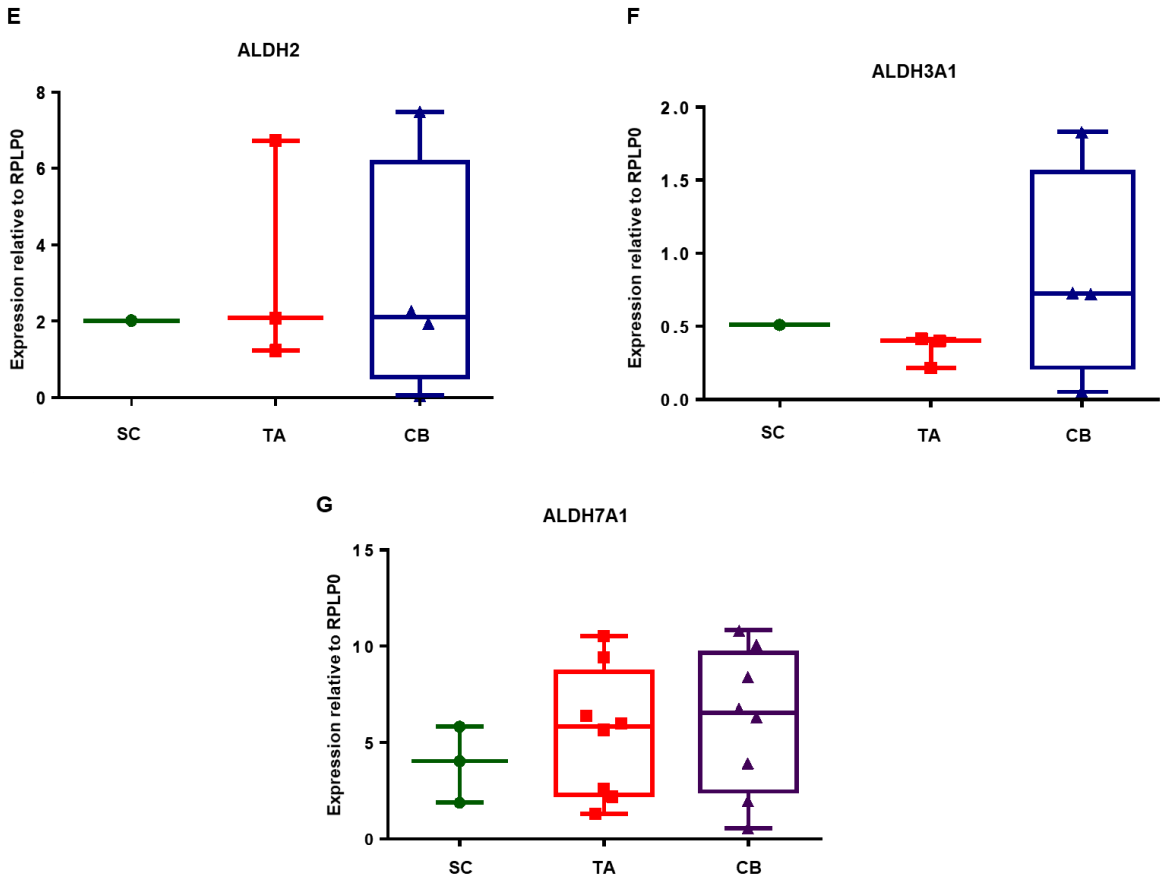


**Figure 22. qPCR analysis of ALDH expression in basal epithelial cells after subpopulation selection.**

Gene expression of (A) ALDH1A1, (B) ALDH1A2 and (C) ALDH1A3, (D) ALDH1B1, (E) ALDH2, (F) ALDH3A1 and (G) ALDH7A1 using $2^{-dCT}$. RPLP0 was used as the control gene. SC- stem cell, TA- transit amplifying cell, and CB- committed basal cells. For ALDH1A1, -1A2, -2, and -3A1 statistical significance was assessed using the Mann Whitney U test for comparing unpaired groups for TA compared with CB, herein SC (n=1), TA (n=3) and CB (n=4). Due to only one sample for SC, statistical test for this population was unobtainable. For ALDH1A3, -1B1 and -7A1 statistical significance was assessed using the one-way ANOVA for multiple comparisons of unpaired groups, TA (n=8) and CB (n=8) compared to SC (n=3), and no statistical significance was found. *Note difference in scale. See appendix II for sample details.

### 3.8 ALDH protein expression in primary prostate epithelial cultures

As the mRNA expression of ALDH1A3, -1B1, and -2 was high in cancer samples compared to benign samples, the protein expression of these selected ALDH isoforms was investigated by immunofluorescence in primary cultures. ALDH7A1 was also included due to its reported association with prostate cancer [490]. CK5 and CK14 were used as positive controls for basal epithelial cells in benign and malignant samples.

The expression pattern at protein level correlated with that of mRNA level in primary cultures. The expression of ALDH1A3 was moderate to weak in benign samples (Figure 23 A-C) with the expression of ALDH7A1, 1B1 and 2 to be weak. In cancer samples, the expression of ALDH1A3 was very strong, with weak expression of ALDH7A1, strong expression of ALDH1B1 and weak to moderate expression of ALDH2 (Figure 23 D-G). The overall ALDH protein expression is summarised in Table 19.

| | ALDH1A3 | ALDH1B1 | ALDH2 | ALDH7A1 |
|---|---|---|---|---|
| **BPH** | ++ | + | + | + |
| **Cancer** | ++++ | +++ | + | + |

**Table 19. ALDH protein expression in primary prostate epithelial cells.**
Expression is represented as very strong (++++), strong (+++), moderate (++), and weak (+). ALDH1A3 expression was very strong in the cancer samples with moderate expression in normal and BPH samples. Expression of ALDH1B1 was strong in cancer, moderate in normal and weak in BPH. Expression of ALDH2 and ALDH7A1 was weak in all different stages of prostate tissue.

Secondary antibody only controls showed no staining, suggesting any staining was specific to the primary antibody. The intensity of staining is different for each ALDH isoform across the BPH and cancer samples, supporting the specificity of the primary antibodies used, because if staining was non-specific the intensity would be the same in all the samples. However, the addition of

co-localisation controls for cytoplasm, nucleus and mitochondria staining would have been appropriate to use to identify and confirm cellular location of the ALDHs. Although DAPI was included to stain the nucleus, other dyes to stain the cytoplasm and mitochondria were not included. The use of counterstains such as phalloidins to label actin filaments [492], DRAQ5 (a modified anthraquinone) to label DNA/nuclei [493], and tetramethylrhodamine methyl ester to label mitochondria [494] would have confirmed specificity of the primary antibody binding to the subcellular location.

To confirm the observed high expression of ALDH1A3 in primary prostate cancer cultures, siRNA knockdown of ALDH1A3 was performed to validate the result. Primary prostate cancer sample H507/14 RB was used and no cell lines were used for this experiment.

Primary prostate cancer cells were either mock only treated (no oligofectamine, no siRNA-ALDH1A3), liposomal only treated (with oligofectamine but without siRNA-ALDH1A3), or siRNA-ALDH1A3 treated (with oligofectamine and siRNA for ALDH1A3). Mock and liposomal control transfected primary cells showed high expression of ALDH1A3. Knockdown of ALDH1A3 expression by siRNA reduced the ALDH1A3 expression although some expression was expected as siRNA knockdown may not have completely knocked down ALDH1A3 expression, confirming the observed ALDH1A3 expression in mock and liposomal control samples by target specificity. Furthermore, secondary antibody only control ensured no non-specific binding to ALDH1A3 (Figure 24).

Taken together, ALDH1A3 is highly expressed in cancer compared to benign and normal cells. The expression of ALDH7A1 was weak in all cell types while

the expression of ALDH1B1 was strong in cancer but weak in benign cells. The expression of ALDH2 was weak in benign with moderate expression in cancer cells.

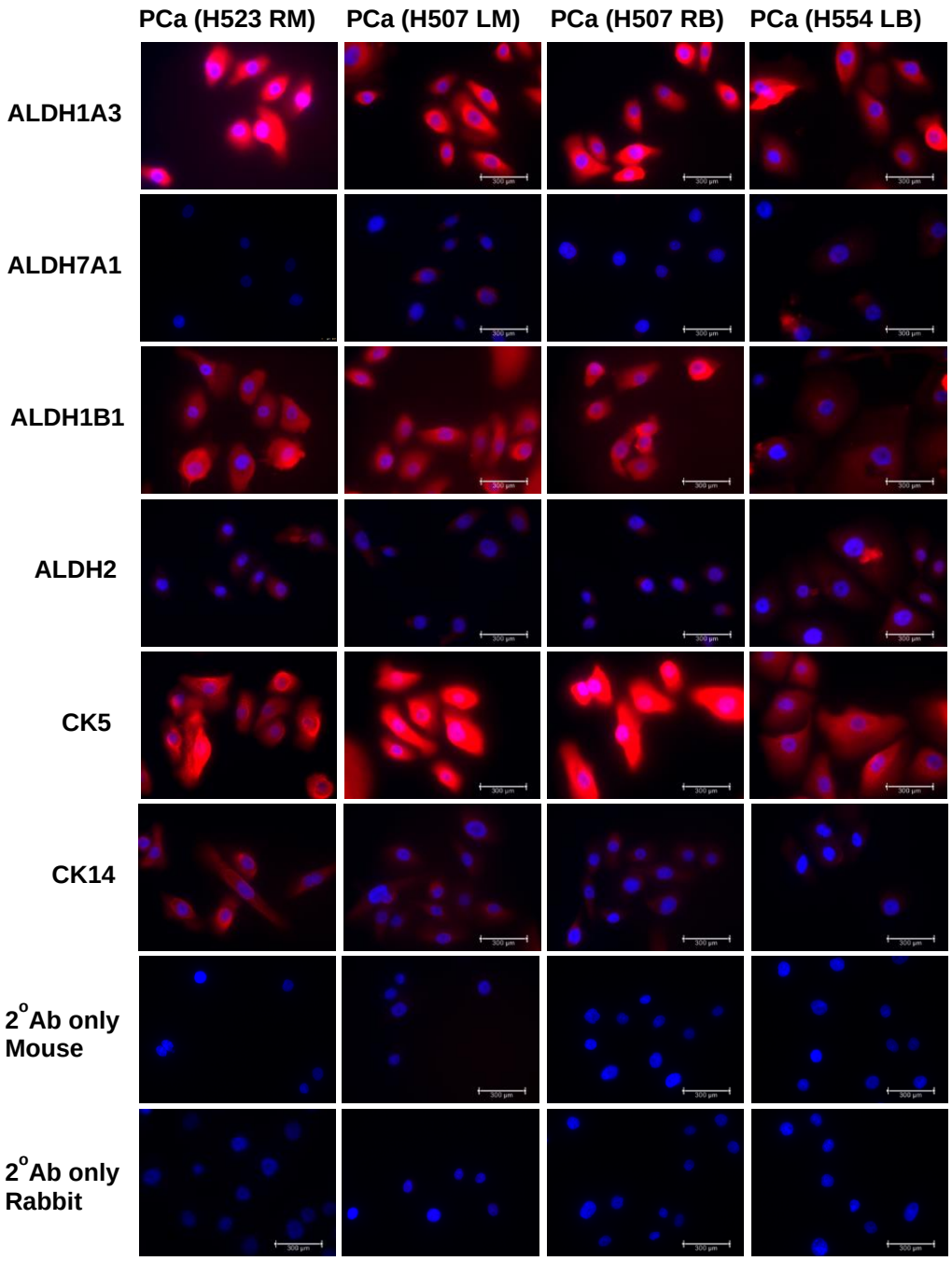
PCa (H523 RM)
PCa (H507 LM)
PCa (H507 RB)
PCa (H554 LB)
ALDH1A3
ALDH7A1
ALDH1B1
ALDH2
CK5
CK14
2°Ab only Mouse
2°Ab only Rabbit

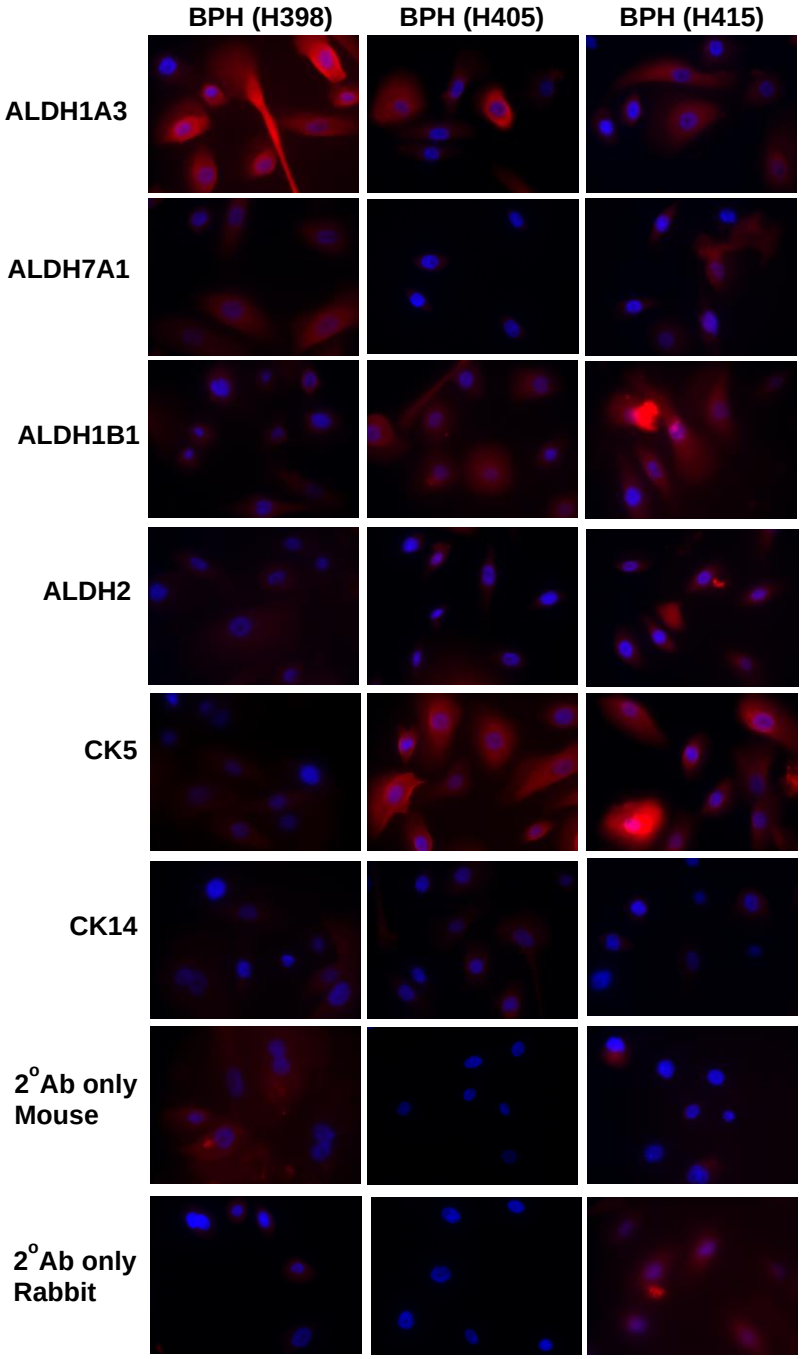


**Figure 23. Immunofluorescence analysis of protein expression in primary cultures**
Representative images show merged picture of DAPI and red staining combined. Fluorescence was measured at 358nm excitation/461 nm emission for DAPI, and 578nm excitation/600nm emission for red signal for alexaFluor568 secondary antibodies. See appendix IV for sample details.

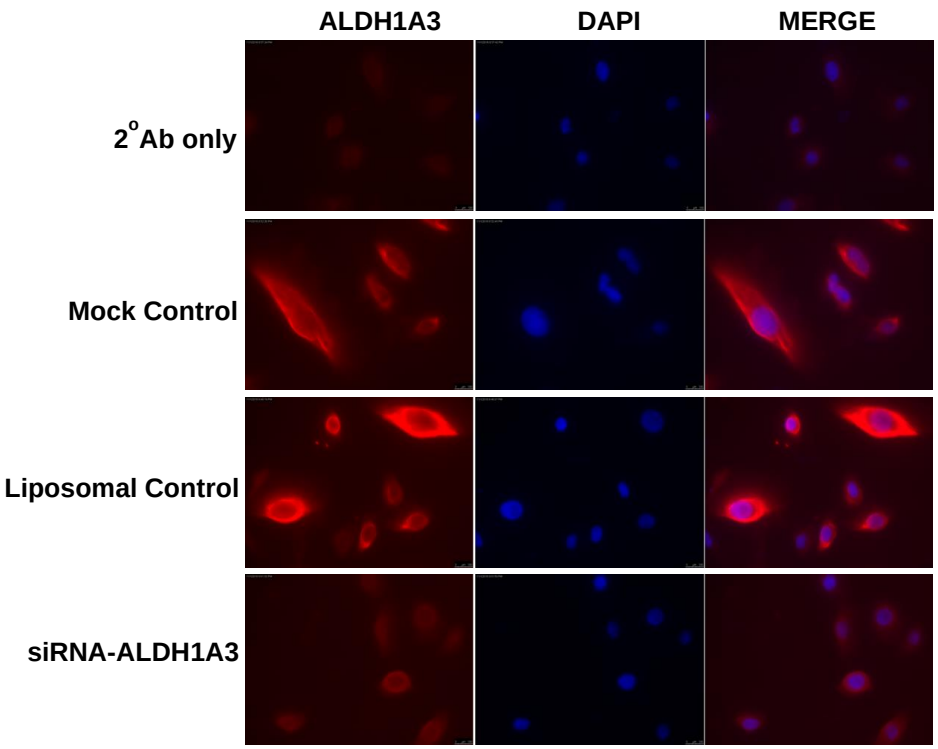


**Figure 24. Immunofluorescence analysis of ALDH1A3 expression in primary prostate epithelial cancer following knockdown of ALDH1A3 by siRNA.**
ALDH1A3 expression was assessed in primary prostate epithelial cancer sample H507/14 RB following the knockdown of ALDH1A3 by siRNA. Secondary only control was used to ensure that the secondary antibody does not non-specifically bind to ALDH1A3. Mock control did not carry any oligofectamine or siRNA for ALDH1A3, therefore observed staining is for ALDH1A3. Liposomal control only carried oligofectamine but not siRNA for ALDH1A3 to ensure staining shown is not due to presence of the vehicle oligofectamine when compared to mock control. siRNA-ALDH1A3 was used to knockdown the expression of ALDH1A3 to confirm its stainin in mock and liposomal control. Fluorescence was measured at 358nm excitation/461nm emission for DAPI, and 578nm excitation/600nm emission for red signal for alexaFluor568 secondary antibodies. See appendix IV for sample details.

### 3.9 ALDH protein expression and localisation in human BPH tissue

Tissue samples were obtained and prepared by Professor Norman J. Maitland's team in the University of York. Tissue slides were kindly provided by Dr. Fiona M. Frame for immunohistochemistry staining. Samples used for immunohistochemistry staining of ALDHs included BPH tissue from human benign tissue. BPH sample was collected from patients undergoing TURP procedure as detailed in chapter 2 Materials and Methods. Only two slides containing 3 tissue sections each (a total of 6 sections) of the same BPH tissue (successive tissue sections) were processed in this study. The 6 BPH tissue sections from the same tissue were analysed for ALDH1A3, ALDH7A1, ALDH1B1, ALDH2, NKX 3.1 (positive control, expressed in nucleus of luminal cells) and secondary antibody only (negative control). Pathology results of the BPH tissue was obtained by pathologist Dr. Greta Rodriguez from Castle Hill Hospital confirming BPH diagnosis. Hemotoxylin and eosin staining performed by Prof. Norman Maitland's group determined tissue sections that contained epithelial glands and these sections were then provided for the purpose of this study. Therefore, all the successive 6 sections used for the present study contained epithelial glands.

BPH tissue displayed some intact lumens within the tissue and a more structured prostate tissue as expected in benign disease. Although BPH tissue showed strongest staining of ALDH1A3 and ALDH1B1 (Figure 25), it appeared non-specific due to its expression throughout the tissue including stromal regions, with the intensity of staining the same across the tissue. Moderate expression of ALDH2 mostly around the lumen was shown suggesting

epithelial staining, with some stromal staining (blue stain indicating nuclei of stromal cells) (Figure 25). Only low expression of ALDH7A1 was observed in the epithelium surrounding the lumen (mostly stained blue), with ALDH7A1 staining mainly in the stromal cells (brown stain) (Figure 25).

NKX 3.1 is an androgen regulated homeodomain gene, found primarily in secretory epithelia of BPH [495] and hence used as a positive control (Figure 25). Staining of NKX 3.1 is observed in the nuclei of luminal epithelial cells (Figure 25) and no stromal staining is seen. Negative control used only included secondary antibody, and no staining was observed in the tissue indicating that the secondary antibody gave no non-specific staining (Figure 25).

Images taken with objective x40 magnification were out of focus due to a fault in the lens and therefore not included here which may have clarified the staining pattern at a higher magnification. In addition, the use of p63 as a positive marker for basal cells may have assisted in compartmentalising basal layer of epithelial cells. Furthermore, control tissue with no ALDH expression could have been tested with ALDH antibodies as a negative control. Due to the limitations of obtaining human tissue, this was not performed.

Future study could include peptide blocking of the antibodies to check for their specificity. Positive and negative control tissues could be used alongside experimental tissue to confirm specificity of staining. In addition, cancer tissue could also be analysed alongside BPH tissue, preferably using tissue microarrays, to distinguish ALDH expression between benign and cancer.

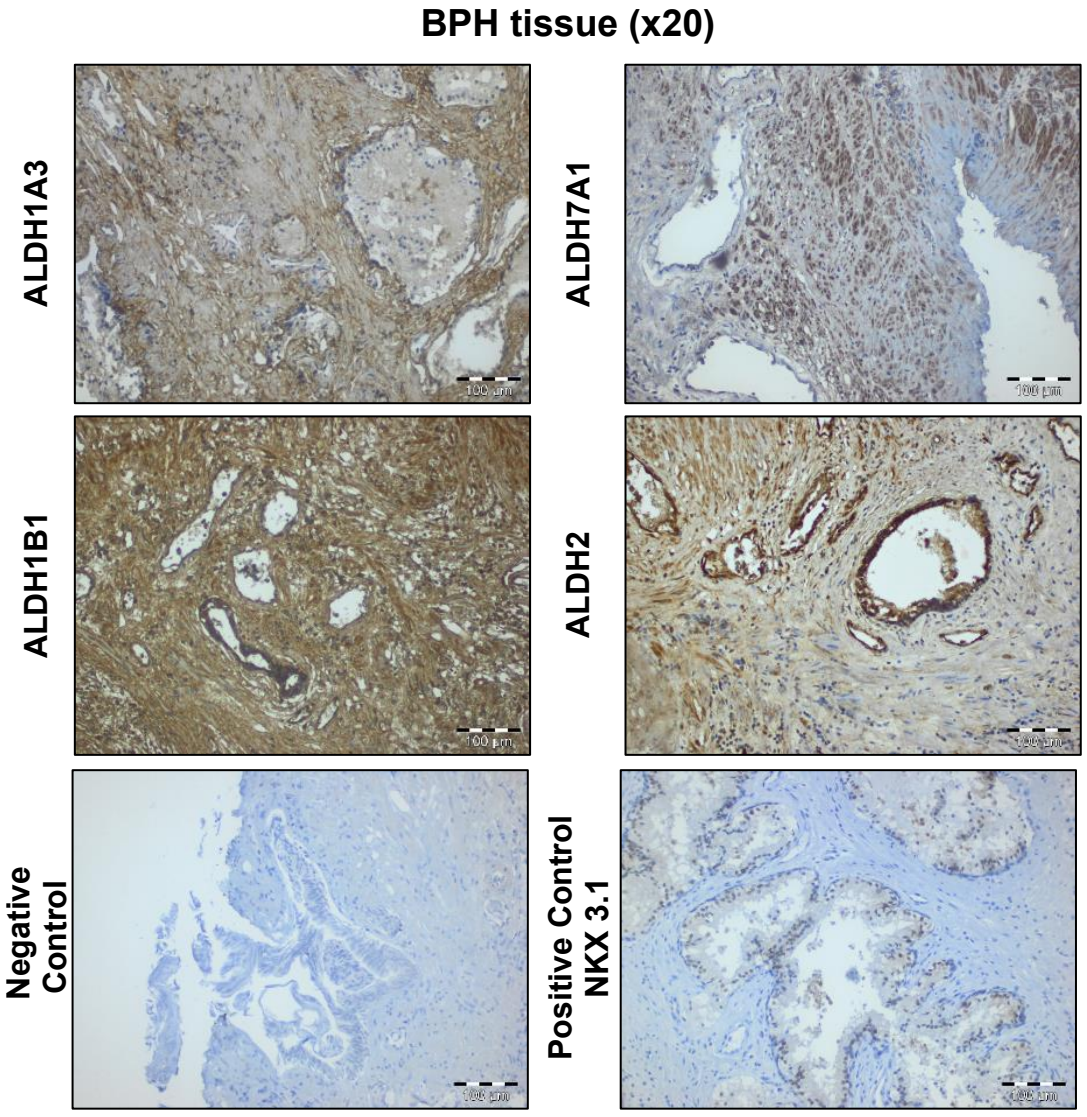


**Figure 25. Immunohistochemistry analysis of ALDH in BPH tissue.**
Magnifications at x20. BPH tissue from patient 391 (2008). Brown stain 3,3-diaminobenzidine (DAB) represents staining used to target ALDH1A3, -7A1, -1B1, -2, and NKX 3.1. DAB reacts with the HRP attached to the secondary antibody to give the brown signal. NKX 3.1 stains the nuclei of luminal epithelial cells. The slide was counterstained with hematoxylin to visualise the nuclei. Negative control included secondary antibody only. Code:03910811 and 03910813 represents 391 as the patient number, 08 as the year 2008, and 11 and 13 as successive tissue sections from the same BPH tissue.

## 3.10 Regulation of ALDH gene expression by epigenetic drugs in prostate epithelial cell lines

Gene expression profiling of the selected ALDH isoforms were also investigated following treatment of cells with epigenetic drugs DAC, TSA, MS275 and SAHA. These experiments were performed in order to understand if ALDHs may be sensitive to epigenetic control and treatment. The fold change in gene expression relative to DMSO control was calculated using the method $2^{-ddCT}$ by qPCR using three independent experiments. DAC was used as a DNA demethylation agent, whereas HDACs were used as histone deacetylation agents. The different HDAC inhibitors used are summarised in Table 20.

| HDAC inhibitor | Specificity of inhibition | Structurally grouped classes | Mechanism of action |
|---|---|---|---|
| Trichostatin A (TSA) Zinc binding inhibitor | Pan inhibitor of class I, II and IV HDACs | Hydroxamate | Induced mitotic cell death by acetylated histones which disrupts the structure and function of the centromere and the pericentric heterochromatin, with loss of binding to heterochromatin binding protein [62, 496] |
| Vorinostat (SAHA) Zinc binding inhibitor | Pan inhibitor of class I, II and IV HDACs | Hydroxamate | Induced the cyclin-dependent kinase inhibitor p21 expression, which increased acetylation of histones H3 and H4 associated with the proximal promoter of the p21 gene [62] |
| Entinostat (MS275) Zinc binding inhibitor | Selective inhibitor of HDAC class I (HDAC 1, 2 and 3) | Benzamide | Increases E-cadherin promoter activation by reducing Twist and Snail association with the promoter, and has shown to inhibit cell migration [497] |

**Table 20. Characterisation of HDAC inhibitors.**
Trichostatin A (TSA) and Vorinostat (SAHA) are both from the hydroxamate class of HDAC inhibitors which are pan inhibitors of class I, II and IV HDACs. Entinostat (MS275) belongs to the benzamide class of HDAC inhibitors which selectively inhibits class I HDACs. All these inhibitors are dependent on zinc for their inhibitory activity. Their mechanism of actions are not fully understood but studies have demonstrated their effect on cell death, cell cycle arrest and inhibition of EMT suppressing cell migration. MS275 differs from TSA and SAHA based in its selectivity for class I HDACs. TSA and SAHA share non-specificity for HDACs but have shown different mechanisms of action.

There was a 3.5-fold and 17.5-fold increase in ALDH1A2 expression in PNT2C2 cells following DAC and MS275 treatment respectively. No changes in the expression of other isoforms were observed after treatment with any of the epigenetic drugs (Figure 26 A). ALDH isoforms 1A1, 1A2 and 3A1 showed to be highly expressed after epigenetic treatment with DAC, TSA and MS275 in the Bob cell line (Figure 26 B). In the SerBob cell line, ALDH isoforms 1A1 and 1A2 were expressed by DAC and at low levels following TSA and MS275 treatment (Figure 26 C). There was about 80-fold increase in ALDH7A1 expression following DAC treatment, and a notable increase in ALDH1A2 and ALDH1A3 expression after DAC treatment in LNCaP cells (Figure 26 D). In DU145 cells, there was a 15-fold increase in ALDH1A2 expression after DAC treatment and a 4-fold increase after MS275 treatment (Figure 26 E). None of the epigenetic drugs had much effect on the expression of the ALDHs in PC3 cells (Figure 26 F). Taken together, these results suggest that ALDH expression may be regulated by DNA methylation and/or histone modification. ALDH1A2, a previously proposed TSG, was re-expressed after epigenetic drug treatment in most cases.

A

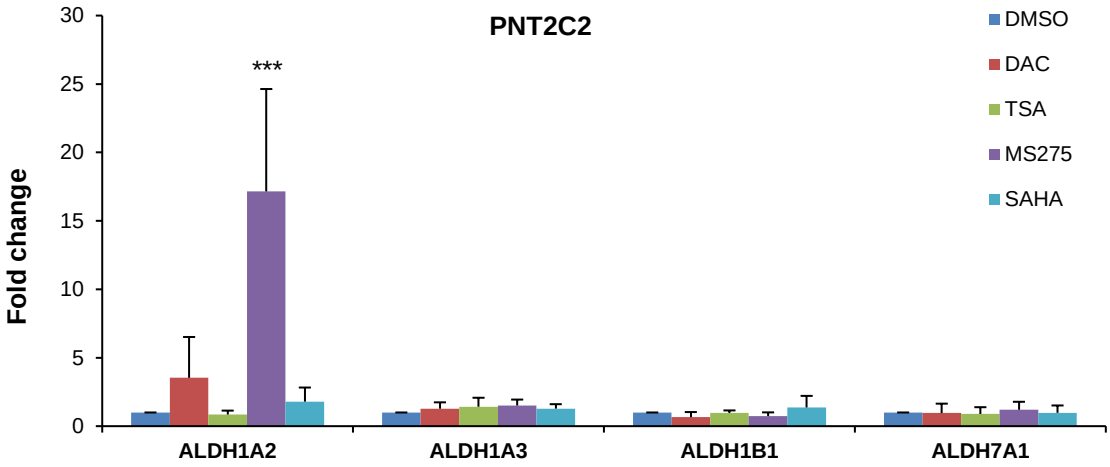
PNT2C2
Fold change
30
25
20
15
10
5
0
***
DMSO
DAC
TSA
MS275
SAHA
ALDH1A2
ALDH1A3
ALDH1B1
ALDH7A1

B

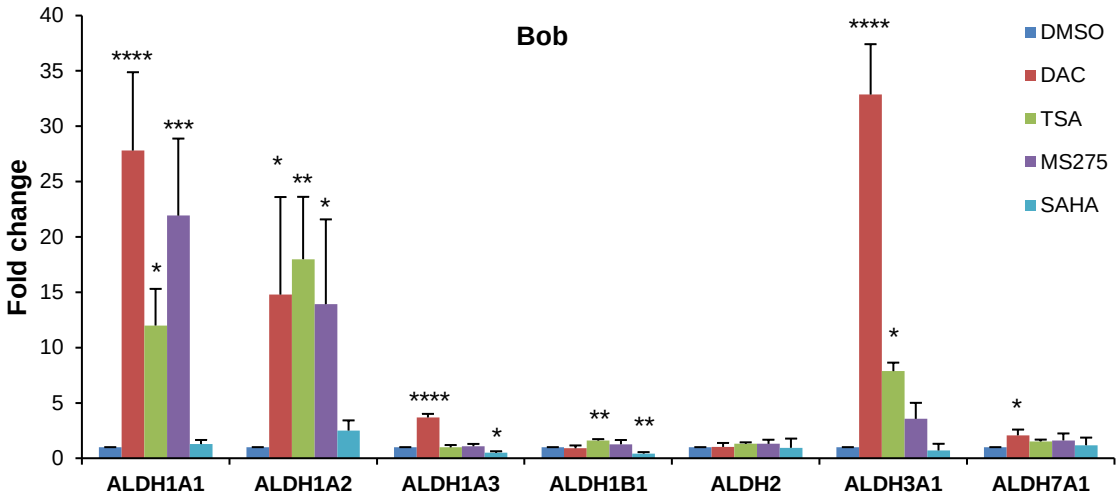
Bob
Fold change
40
35
30
25
20
15
10
5
0
****
***
*
*
**
*
****
*
**
**
****
*
*
DMSO
DAC
TSA
MS275
SAHA
ALDH1A1
ALDH1A2
ALDH1A3
ALDH1B1
ALDH2
ALDH3A1
ALDH7A1

**C**

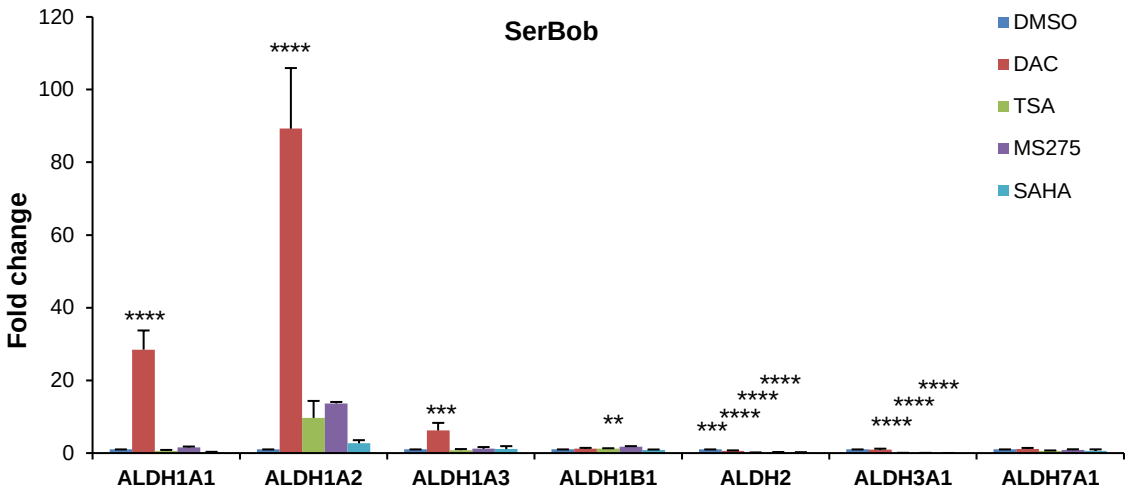
SerBob
Fold change
120
100
80
60
40
20
0
DMSO
DAC
TSA
MS275
SAHA
****
****
***
**
***
****
****
****
****
****
ALDH1A1
ALDH1A2
ALDH1A3
ALDH1B1
ALDH2
ALDH3A1
ALDH7A1

**D**

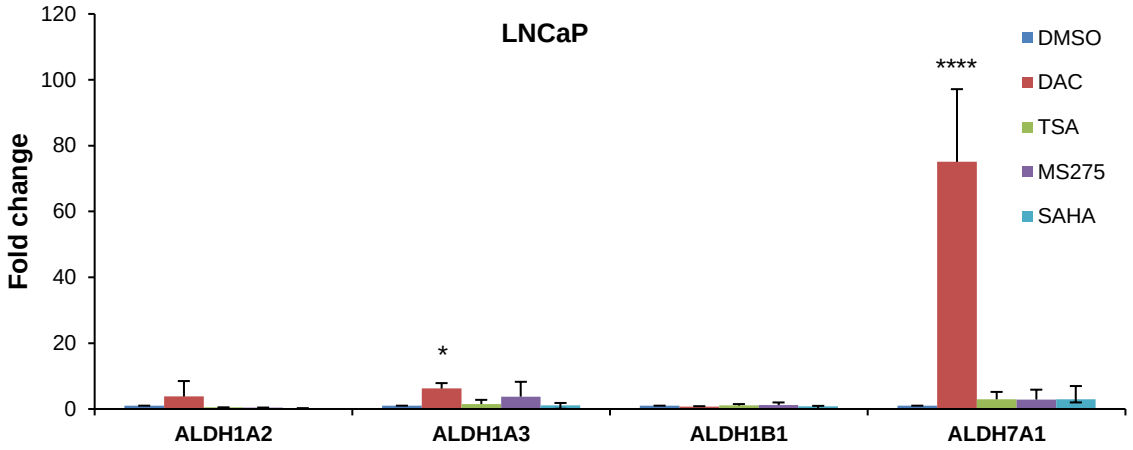
LNCaP
Fold change
120
100
80
60
40
20
0
DMSO
DAC
TSA
MS275
SAHA
*
****
ALDH1A2
ALDH1A3
ALDH1B1
ALDH7A1

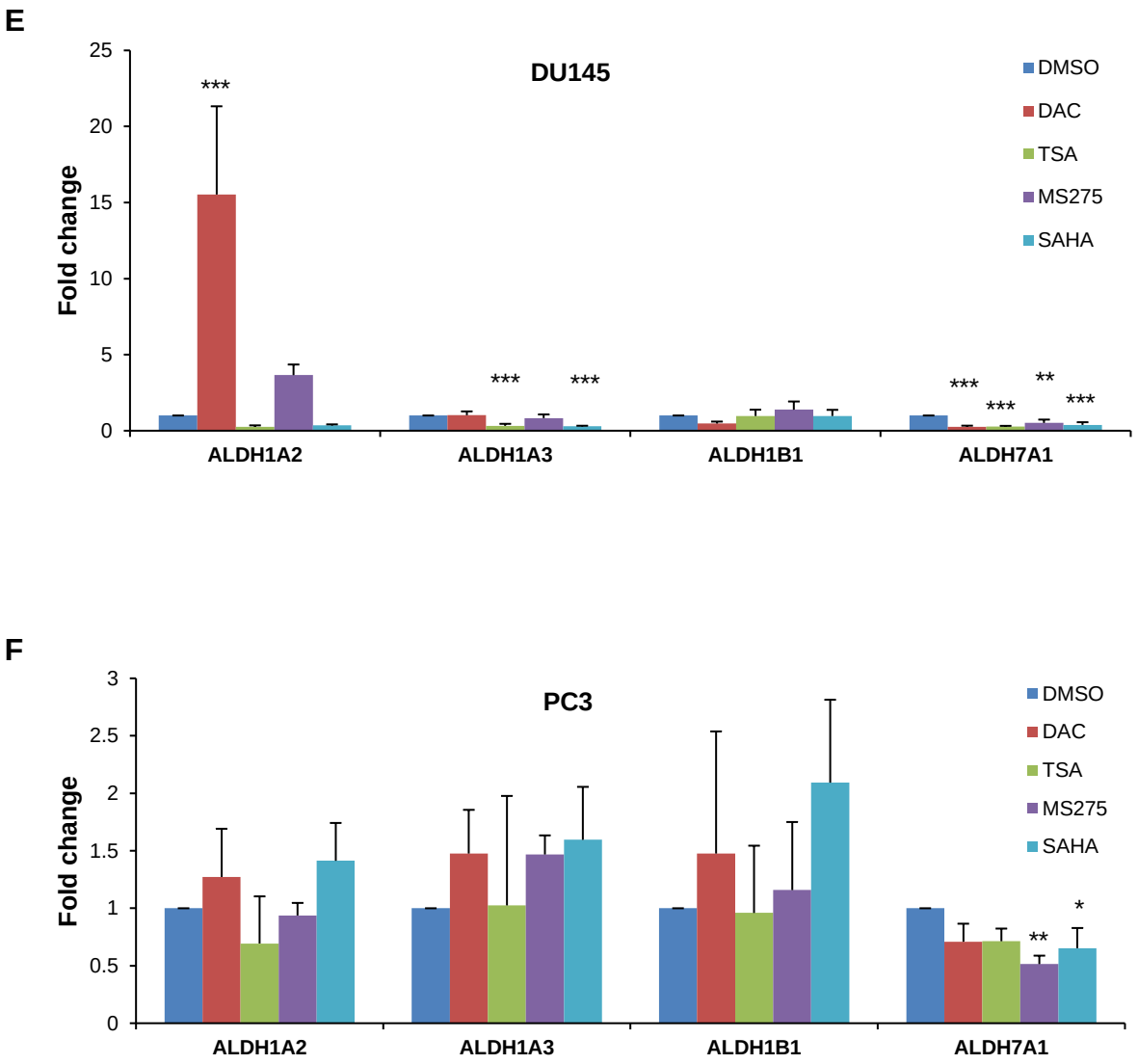


**Figure 26. Gene expression analysis in prostate cell lines before and after epigenetic treatment.**

Relative ALDH expression in (A) normal epithelial prostate cell line and (B-F) prostate cancer cell lines. DMSO control samples are set at 1 and the treatments are plotted as fold change relative to control. Data are represented as a mean of three independent experiments ± SD. Gene expression analysis was carried out by qRT-PCR and gene expression fold change of the ALDHs were worked out using $2^{-ddCT}$. RPLP0 was used as the control gene. DAC treatment of 1µM was repeated every other day for 6 days. Treatment of 0.1µM of TSA, 0.5µM of MS275 and 0.5µM of SAHA was carried out for 48 hours. DAC- decitabine, TSA- trichostatin A, MS275- entinostat, SAHA- vorinostat. Statistical significance was calculated using one-way ANOVA for paired groups; multiple comparisons (more than two groups); DMSO control compared to DAC, TSA, MS275 and SAHA. * p = 0.01 to 0.05, ** p = 0.001 to 0.01, *** p = 0.0001 to 0.001, **** p < 0.0001. * Note difference in scale. Where there are different ALDH isoforms with high expression and low expression on the same graph, the lower expressed isoforms that are significantly differently expressed compared to DMSO control are also shown with asterisks.

### 3.11 Effect of epigenetic drugs on ALDH protein expression in prostate epithelial cell lines

Based on the gene expression data, western blotting detection was carried out to study whether effects observed at the mRNA level were also observed at the protein level. Herein, focus was made on four cell lines including PNT2C2 (to include a normal prostate cell line), Bob (as it showed the upregulation of more than one ALDH isoform following epigenetic treatment, and as it is a basal cell line), SerBob (as it showed the upregulation of more than one ALDH isoform following epigenetic treatment, and it is a more differentiated cell line compared to Bob) and LNCaP (as it showed a significantly high expression of ALDH7A1 following DAC treatment). SAHA was excluded due to no effect seen at the gene level in most cell lines. For protein expression, only selected isoforms were included for different cell lines for comparison analysis. For the benign PNT2C2 cells, all the 7 ALDH isoforms were included, however ALDH1A2 and ALDH3A1 were not seen in this cell line. ALDH1B1 was included in all cell lines to include a B family member of the ALDH family. ALDH7A1 was also included in all cell lines due to its association with prostate cancer as previously shown by Hoogen et al. All isoforms were included in Bob and LNCaP cells, however ALDH1A1 and ALDH1A2 were not seen in Bob and LNCaP cells respectively. Due to time limitations only ALDH1B1 and ALDH7A1 were studied in SerBob cells.

Specificity of the antibodies were assessed with the ALDH molecular weights (MW), since the ALDH isoforms studied have different MWs. If a clear band appeared at the corresponding MW of the ALDH isoform, the antibody was

regarded specific. However, in the case of isoforms with similar MW (ALDH1A1 56.2kDa, ALDH2 56kDa, ALDH7A1 55kDa, ALDH1B1 and ALDH1A2 57kDa), a more direct way to check specificity would be to generate knockout cell lines to included wild-type (with ALDH expression) and its ALDH$^{-/-}$ pair. Antibody testing with such a model would give more accurate results for specificity, because the band would be absent in the knockout cell line. Likewise, isogenic pair of cell lines to include wild-type ALDH$^{-/-}$ cell line and an ALDH transfected cell line pair may also be used. But these experiments require time to generate such cell line pairs and therefore were not carried out within the time frame for this study. In addition, the antibody for ALDH1A3 was used to confirm its specificity by carrying out a knockdown experiment in PC3 cells. The siRNA knockdown of ALDH1A3 resulted in 74% knockdown of this isoform as shown by the immunoblot in Figure 27 (data also used in chapter 4).

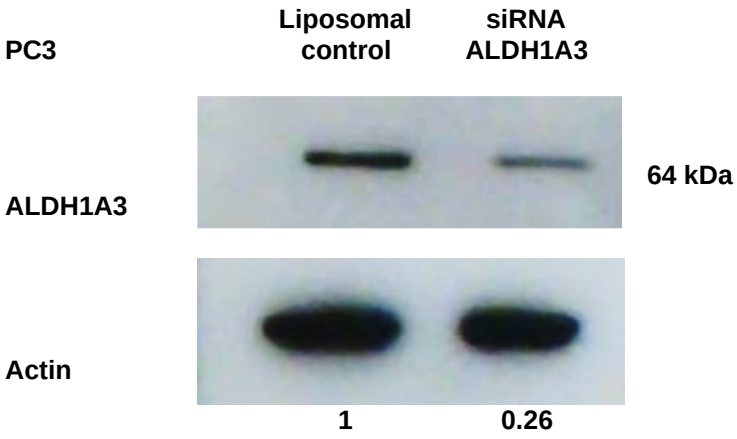


**Figure 27. Knockdown of ALDH1A3 by siRNA in PC3 cells.**
PC3 cells were treated with either oligofectamine only (vehicle) or with siRNA for ALDH1A3. Actin was used as the control gene to normalise expression. Expression of ALDH was reduced by 0.26 fold upon silencing with siRNA.

The addition of positive control cells that highly express ALDH1A1 would have been useful to test the ALDH1A1 antibody as no bands were observed in PNT2C2 or LNCaP cells. If a positive control shows ALDH1A1 bands, then the absence of ALDH1A1 expression in PNT2C2 and LNCaP cells would have been validated. Herein, Bob cells were assessed for ALDH1A1 expression but the results could not be obtained.

In PNT2C2 cells, the protein expression of ALDH1A3, -1B1, -2 and -7A1 disappeared after DAC treatment, however no change was seen at the mRNA level of these isoforms (Figure 28 A). In SerBob cells, results obtained for the isoforms 1B1 and 7A1 showed the expression to be the same in all conditions, which is in correlation with the gene expression data (Figure 28 B).

Bob cells showed a reduced expression of ALDH1A2 with DAC, TSA and MS275 treatment. ALDH1A3 expression was increased 9.84-fold with DAC, correlating with the mRNA level. ALDH1B1 was expressed in all conditions with a 10.13-fold higher expression in TSA treatment. ALDH2 and -7A1 were expressed in all treatments and this was the case at the mRNA level suggesting they are unaffected by treatments. ALDH3A1 protein expression was 25.77-fold elevated in response to DAC treatment, which is consistent with ALDH3A1 mRNA expression after DAC treatment (Figure 28 C).

In LNCaP cells there was a 4.15-fold increase in ALDH1A3 expression following DAC treatment. ALDH1B1 expression was seen in all treated cells but a slightly lower expression in DAC treated cells was observed. ALDH2 expression was increased by 4.07-fold, 2.43-fold and 3.59-fold following treatment with DAC, TSA and MS275 respectively. ALDH3A1 was also

expressed in all treated samples, with a 1.95 and 2.49-fold increase following DAC and TSA treatment. ALDH7A1 was highly expressed following DAC treatment. Herein, the protein expression data correlates with the gene expression data (Figure 28 D).

Taken together, this data further suggests that the expression of certain ALDH isoforms may be under epigenetic regulation including DNA methylation and histone modification, in particular the upregulation of ALDH1A3, ALDH1B1, ALDH2, ALDH3A1 and ALDH7A1.

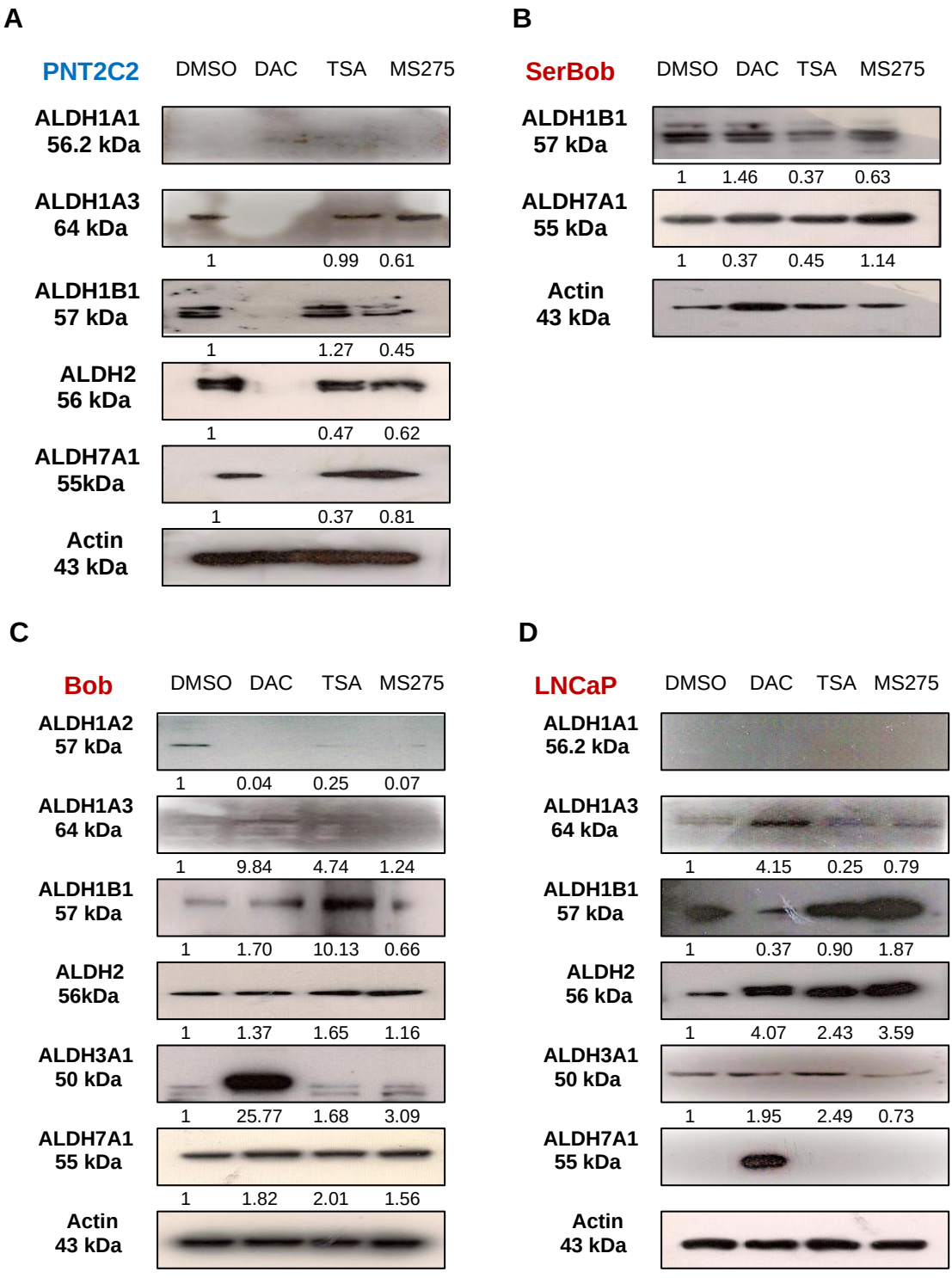


**Figure 28. Protein expression analysis by western blot in prostate cell lines before and after epigenetic treatment.**

Relative ALDH expression in (A) normal epithelial prostate cell line and (B-D) prostate cancer cell lines. Actin was used as control. DAC treatment of 1µM was repeated every other day for 6 days. Treatment of 0.1µM of TSA, 0.5µM of MS275 and 0.5µM of SAHA was carried out for 48 hours. DAC- decitabine, TSA- trichostatin A, MS275- entinostat. Numbers below each blot represents the fold change in ALDH expression. Where DMSO had no band, the fold change in ALDH expression following epigenetic treatment was not achievable.

### 3.12 ALDH expression after treatment with TSA in primary prostate epithelial cultures

To further understand whether the observed epigenetic modulation of ALDH expression in prostate cell lines showed a similar pattern in primary prostate epithelial benign and cancer cells, the gene expression of ALDHs was investigated following treatment with the HDAC inhibitor TSA. Dose establishment was previously carried out by Dr. Euan Polson and Dr Davide Pellacani [62] from Prof. Norman Maitland's group and IC50 values were obtained from which a non-toxic dose was selected. Cells were treated with either DMSO or TSA at 0.6µM for 24 hours. After treatment, cells were harvested and the RNA extraction was carried out. Prof. Norman Maitland kindly provided the RNA samples for this study. The cDNA synthesis and qPCR was performed in the present study. Specificity and off-target effects were controlled by selecting a low enough dose not to be toxic.

TSA treatment showed upregulation of ALDH1A1 (Figure 29 A), ALDH1A2 (Figure 29 B), ALDH1A3 (Figure 29 C), and ALDH2 (Figure 29 E) relative to DMSO control set at 1 as shown in the bigger scale graphs, however it was not statistically significant. Not much effect was seen in the expression of ALDH1B1 (Figure 29 D), ALDH3A1 (Figure 29 F) and ALDH7A1 (Figure 29 G) across the range of samples following TSA treatment.

Taken together, this data suggests that certain ALDH isoforms may potentially be regulated by histone modification whilst, ALDH1A2, -3A1 and -7A1 are predominantly affected by DNA methylation as previously observed in Figure

31 and 32. Some ALDHs exhibit regulation by both epigenetic mechanisms, which complicates the process of understanding their expression pattern.

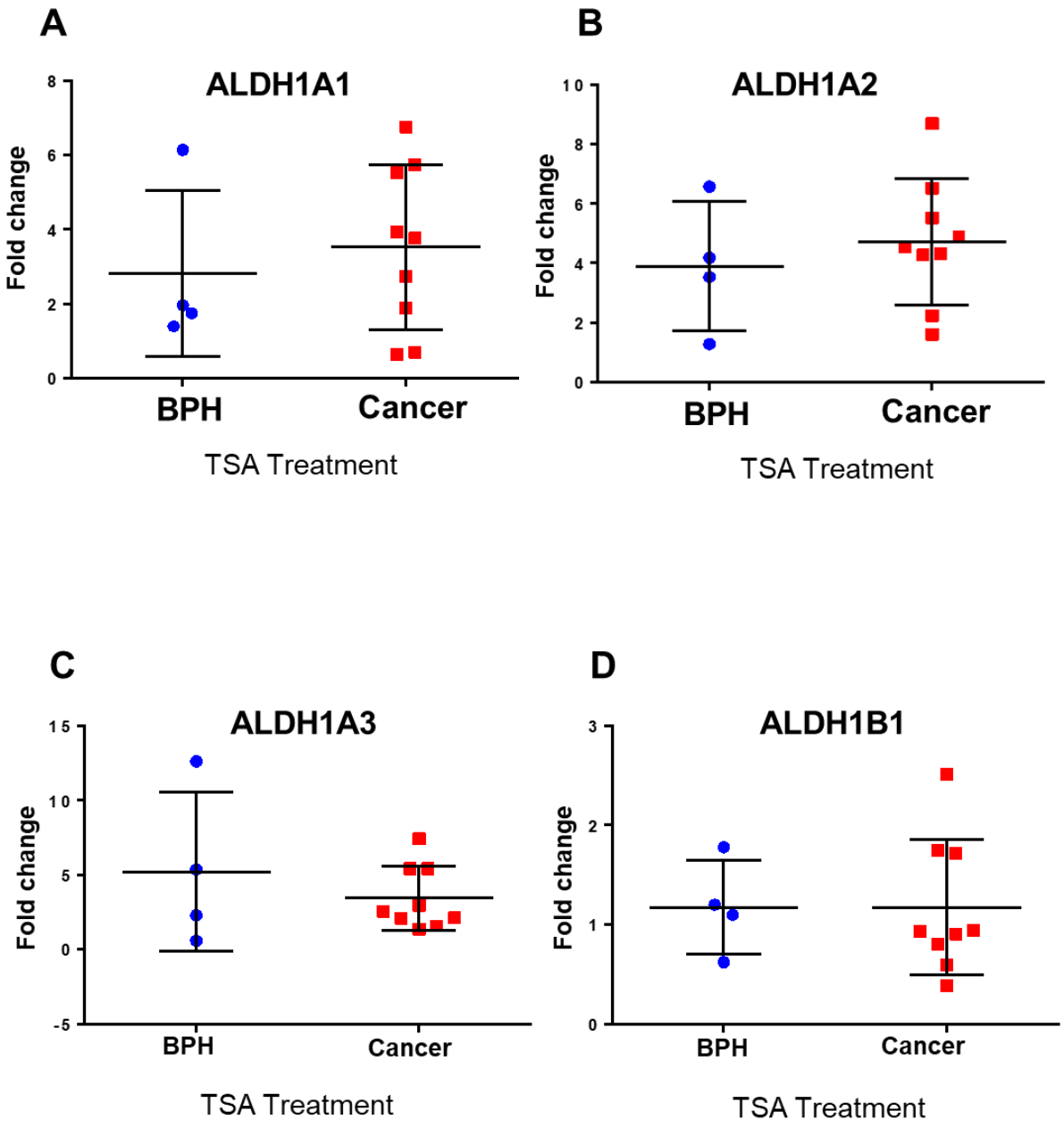
A
ALDH1A1
Fold change
8
6
4
2
0
BPH
Cancer
TSA Treatment
B
ALDH1A2
Fold change
10
8
6
4
2
0
BPH
Cancer
TSA Treatment
C
ALDH1A3
Fold change
15
10
5
0
-5
BPH
Cancer
TSA Treatment
D
ALDH1B1
Fold change
3
2
1
0
BPH
Cancer
TSA Treatment

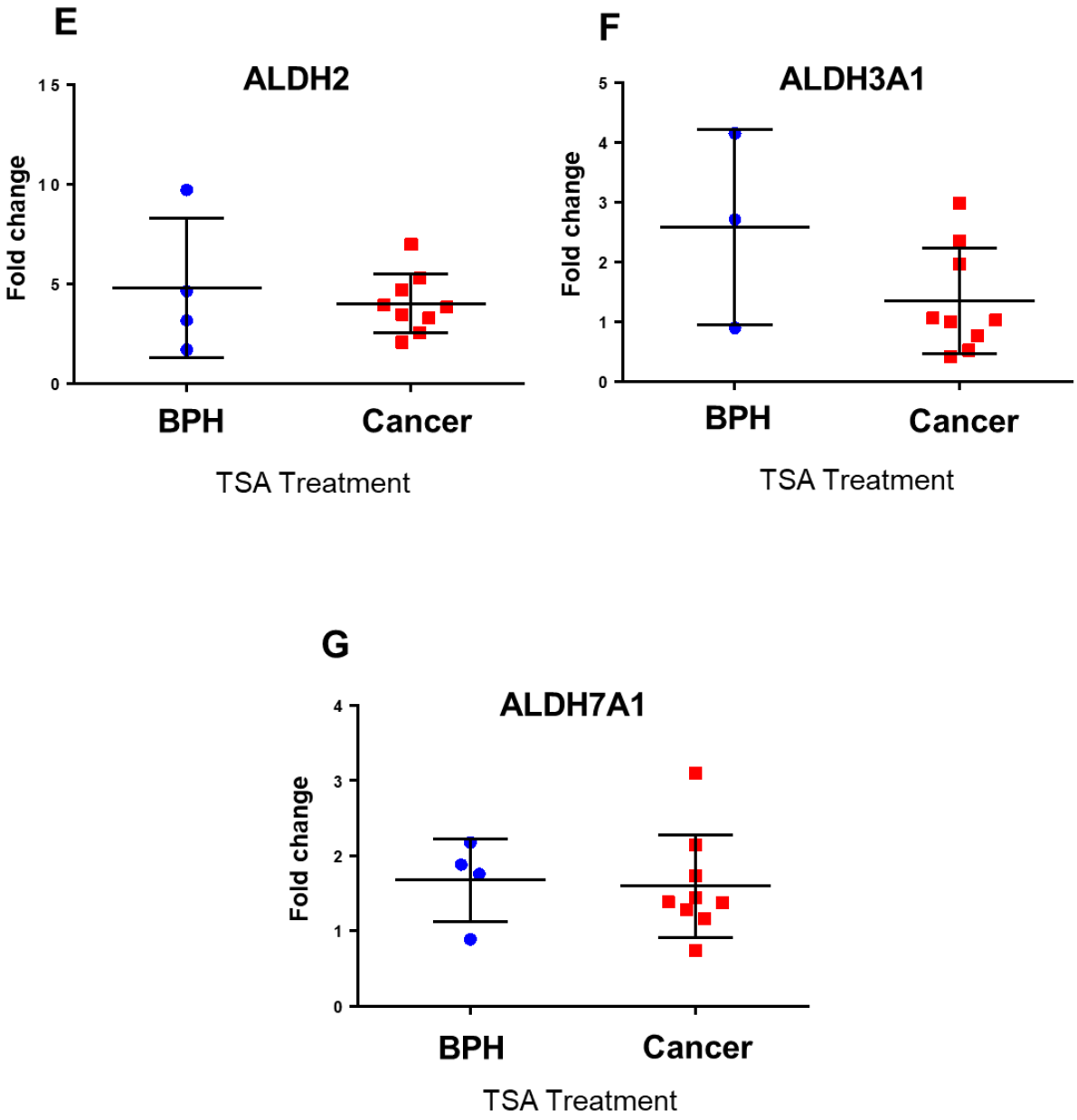


**Figure 29. qPCR analysis of ALDH expression in primary prostate epithelial cells following treatment with TSA.**

Samples were either treated with DMSO or 0.6µM TSA for 24 hours. The fold change in ALDH expression was worked out using $2^{-ddCT}$ relative to DMSO control which was set at 1. Values represented as the mean and SD of three technical repeats. Statistical test was used to compare BPH samples (n=4), except for ALDH3A1 BPH (n=3), with Cancer samples (n=9) using Mann Whitney U test which considered 2 unpaired groups, non-parametric distribution, and differences in the number of BPH and cancer samples. There was no statistical difference in ALDH expression between the two groups. *Note difference in scale. See appendix V for sample details.

### 3.13 Regulation of ALDH gene expression by retinoic acid in primary prostatic epithelial cells

The RA signalling pathway was explored as there is some indication of a potential link between ALDH expression and RA gene regulation as outlined in the Introduction. Here. the ALDH gene expression was profiled in RA treated and non-treated primary prostate epithelial samples. Benign samples (BPH) were compared with BPH-PIN (BPH with evidence of PIN) and cancer samples.

Cells were either treated with DMSO or atRA at 100nM for 72 hours; this dose was previously used and optimised by Dr. Euan Polson, Dr. Davide Pellacani and Dr. Emma Oldridge [452] in Prof. Norman Maitland's group and showed no phenotypical changes. The RNA samples were prepared and kindly provided for this study. The cDNA synthesis and qPCR was carried out as part of this study.

A small increase in ALDH1A1 expression following treatment with 100nM atRA was observed in both cancer samples relative to DMSO (Figure 30 A). No difference in ALDH1A2 expression was shown in the atRA-treated cancer samples, however a small reduction in ALDH1A2 expression in the atRA-treated BPH-PIN sample was shown (Figure 30 B). An increase of about 19-fold, 8 and 12-fold and 27-fold in the expression of ALDH1A3 following atRA treatment was shown in BPH, BPH-PIN and cancer samples respectively (Figure 30 C). ALDH1B1, -2 and -7A1 expression showed no changes upon atRA treatment (Figure 30 D, E, G). There was an increase of about 9-fold and 12-fold of ALDH3A1 expression in BPH-PIN and a cancer sample respectively

after atRA treatment (Figure 30 F). However, due to the small number of samples, a statistical test could not be applied to assess significance of change on ALDH expression upon treatment with atRA. Furthermore, the use of a positive control gene such as retinoic acid receptor responder 1 (RARRES1) for atRA induced expression [452], would have been useful to compare the observed upregulation of ALDH1A3 and ALDH3A1 following atRA treatment.

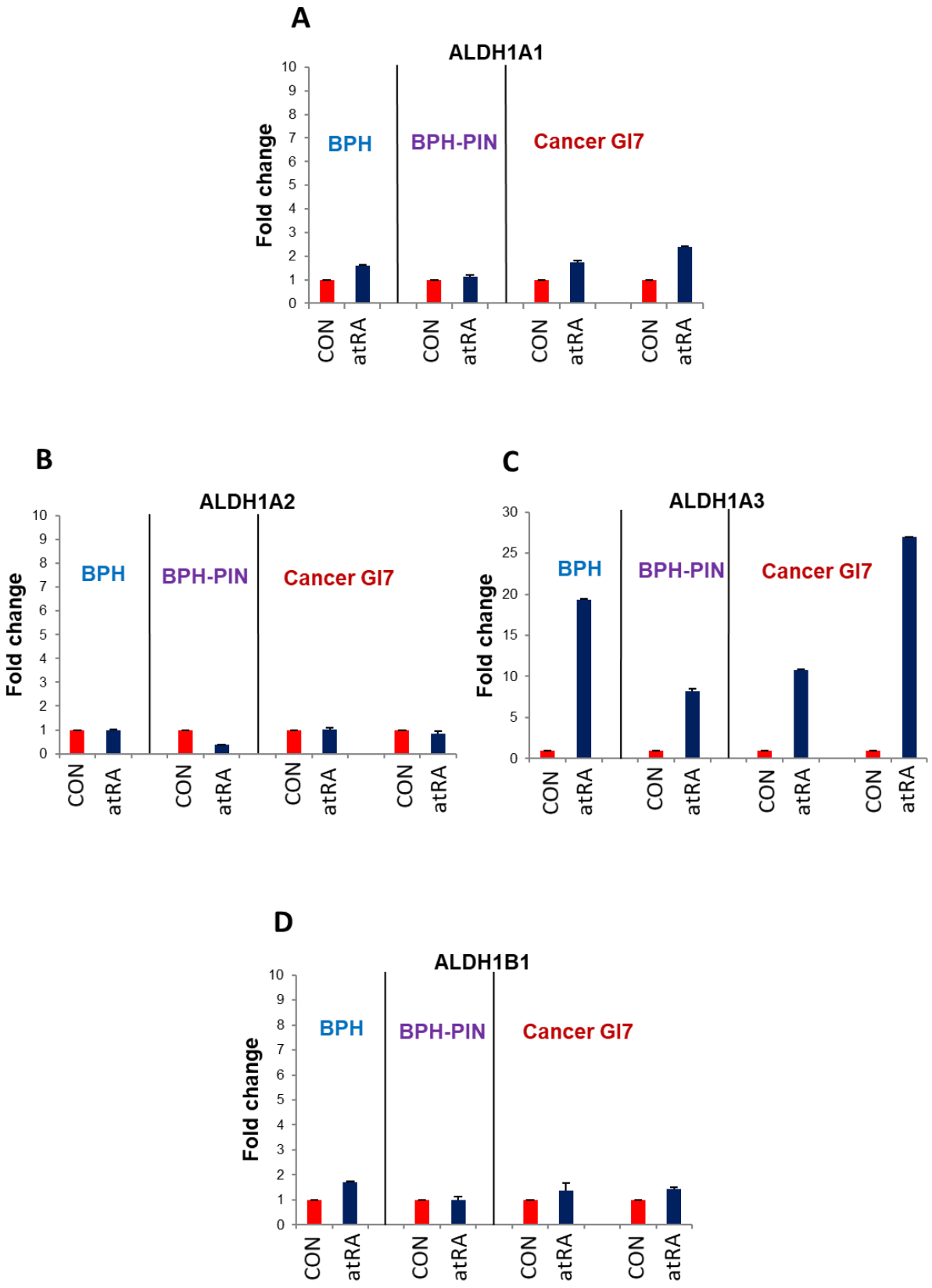
A
ALDH1A1
Fold change
BPH
BPH-PIN
Cancer GI7
CON
atRA
B
ALDH1A2
C
ALDH1A3
D
ALDH1B1

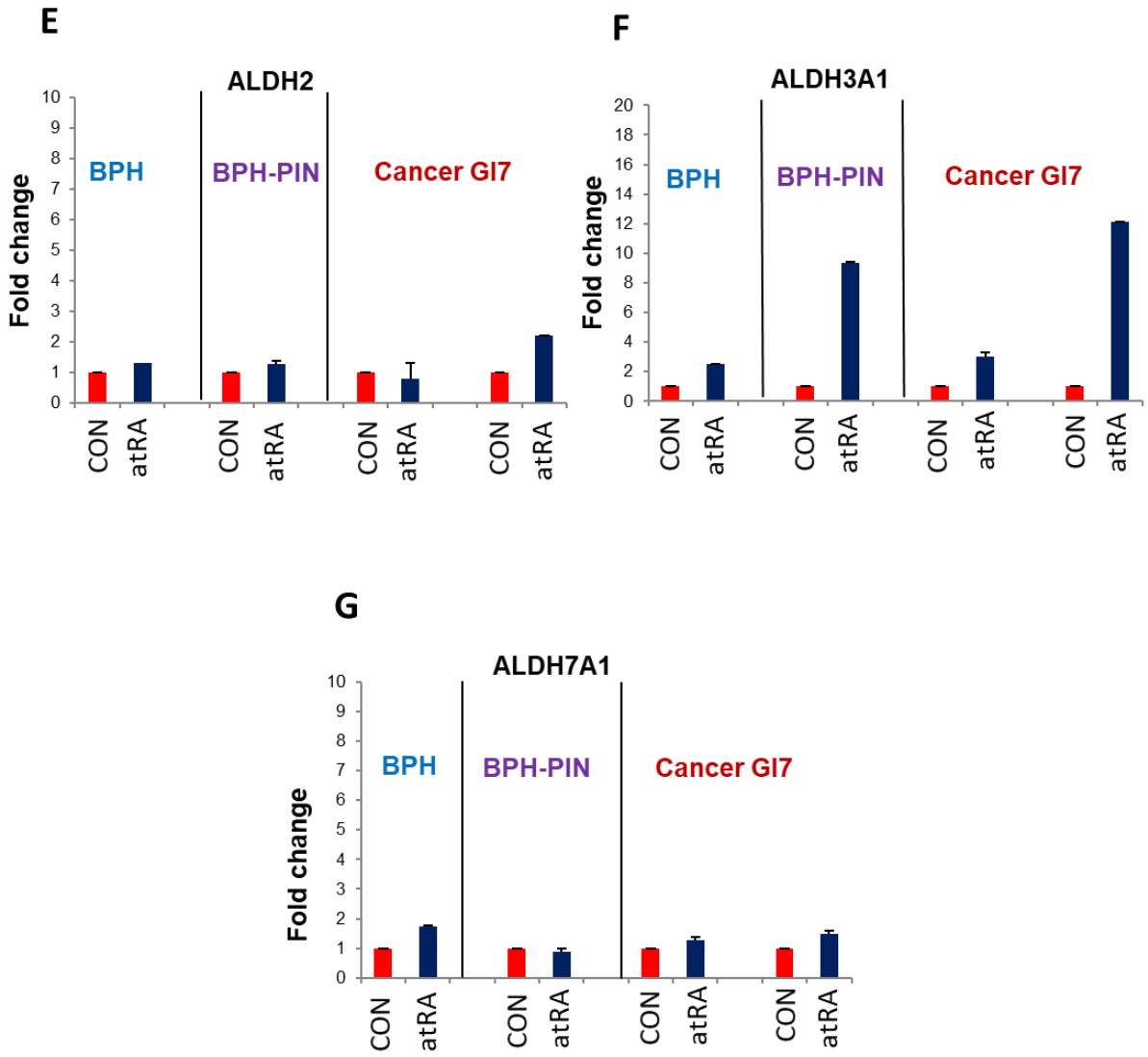


**Figure 30. ALDH gene expression analysis of primary prostatic epithelial cells after atRA treatment.**

Fold change of (A) ALDH1A2, (B) ALDH1A3, (C) ALDH7A1, (D) ALDH1A1, (E) ALDH1B1, (F) ALDH2 and (G) ALDH3A1 expression relative to untreated control. RPLP0 was used as the housekeeping gene. Analysis was performed by qPCR using $2^{-ddCT}$. Retinoic acid treatment was for 72 hours at 100nM. Samples studied were BPH, BPH-PIN (BPH sample but with signs of PIN) and cancer primary cells. Due to the requirement of a minimal of 3 repeats (n=3) to compare means of the groups, it was not possible to do apply a statistical test. Herein, BPH (n=1), BPH-PIN (n=1) and cancer (n=2) samples. See appendix VI for sample details.

### 3.14 Regulation of ALDH gene expression by hypoxia in prostate epithelial cell lines

To investigate if hypoxia had an effect on the expression of ALDH gene expression, prostate cell lines were exposed to either normoxic conditions, hypoxic conditions for 24 hours or hypoxic conditions for 48 hours before analysis by qPCR. Carbonic anhydrase IX (CA9) was used as a positive control for hypoxia.

In the PNT2C2 cells, there was a small but statistically significant increase in expression of ALDH1A1 at 24h hypoxia, ALDH2 at 48h hypoxia and ALDH3A1 at 48h hypoxia when compared to normoxia. However, the expression of ALDH1A1 decreased at 48h hypoxia (Figure 31 A). In SerBob cells, the expression of ALDH1A1 at 48h hypoxia and ALDH1B1 at 24h and 48h hypoxia were significantly reduced as compared to normoxia (Figure 31 B). In Bob cells, a significant increase in ALDH1A3 expression at 24h hypoxia was observed, but at 48h hypoxia ALDH1A3 expression was reduced. A significant decrease in ALDH2 and ALDH7A1 was observed at both 24h and 48h hypoxia as compared to normoxia (Figure 31 C). In LNCaP cells, a significant increase in ADLH2 expression at 48h hypoxia was observed, with a significant decrease in ALDH3A1 expression at both 24h and 48h hypoxia when compared to normoxia (Figure 31 D). In DU145 cells, the expression of ALDH1A2, ALDH1A3, ALDH2 and ALDH3A1 were significantly increased at 48h hypoxia, with ALDH2 expression also significantly upregulated at 24h hypoxia as compared to normoxia (Figure 31 E). In PC3 cells, there was a significant downregulation of ALDH1A1, ALDH1A3 and ALDH1B1 expression

at 24h and 48h hypoxia. The expression of ALDH1A2 and ALDH7A1 was also decreased at 48h hypoxia as compared to normoxia (Figure 31 F).

Taken together, this data showed that ALDH expression may be affected by the influence of hypoxia in prostate cell lines. Although changes observed in ALDH expression seemed small but were statistically significant. ALDH isoforms can be upregulated or downregulated under hypoxic stress in prostate cell lines which may have phenotypic consequences. However, to address this, further studies are needed to evaluate the effect of hypoxia induced changes in ALDH expression on biological processes.

**A**

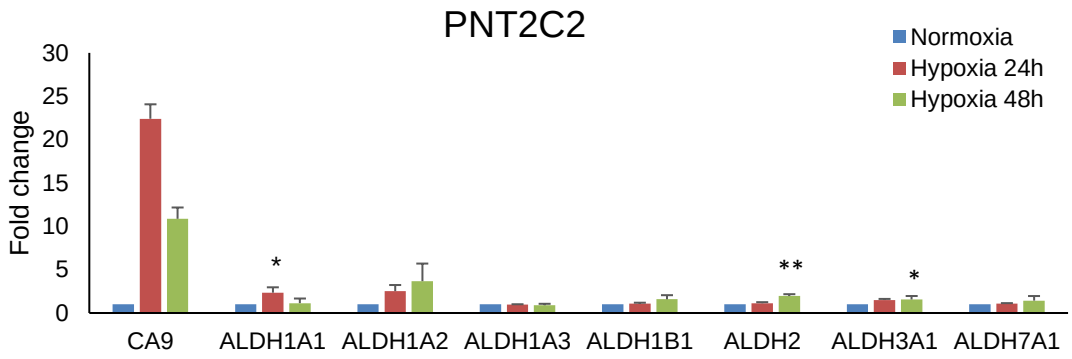
PNT2C2
Normoxia
Hypoxia 24h
Hypoxia 48h
Fold change
30
25
20
15
10
5
0
*
**
*
CA9
ALDH1A1
ALDH1A2
ALDH1A3
ALDH1B1
ALDH2
ALDH3A1
ALDH7A1

**B**

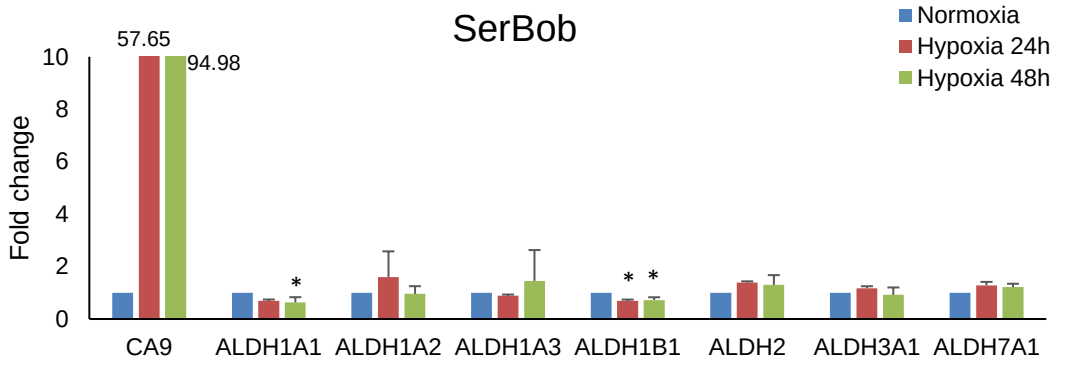
SerBob
Normoxia
Hypoxia 24h
Hypoxia 48h
Fold change
57.65
94.98
10
8
6
4
2
0
*
* *
CA9
ALDH1A1
ALDH1A2
ALDH1A3
ALDH1B1
ALDH2
ALDH3A1
ALDH7A1

**C**

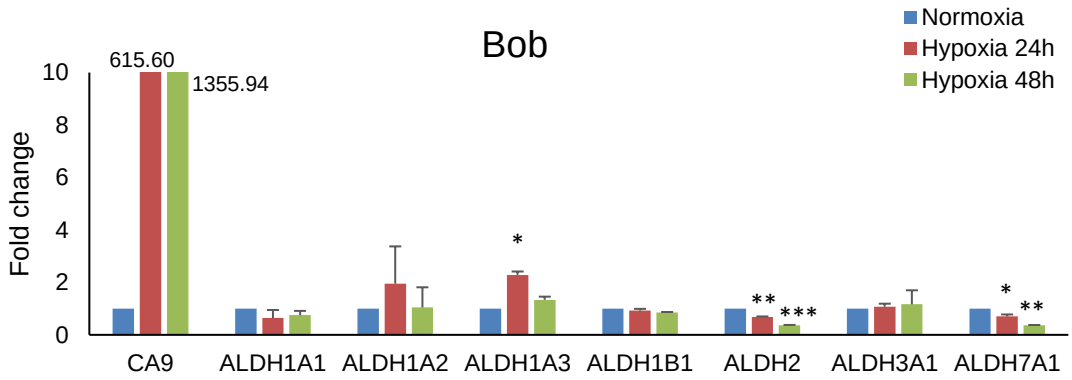
Bob
Normoxia
Hypoxia 24h
Hypoxia 48h
Fold change
615.60
1355.94
10
8
6
4
2
0
*
**
***
*
**
CA9
ALDH1A1
ALDH1A2
ALDH1A3
ALDH1B1
ALDH2
ALDH3A1
ALDH7A1

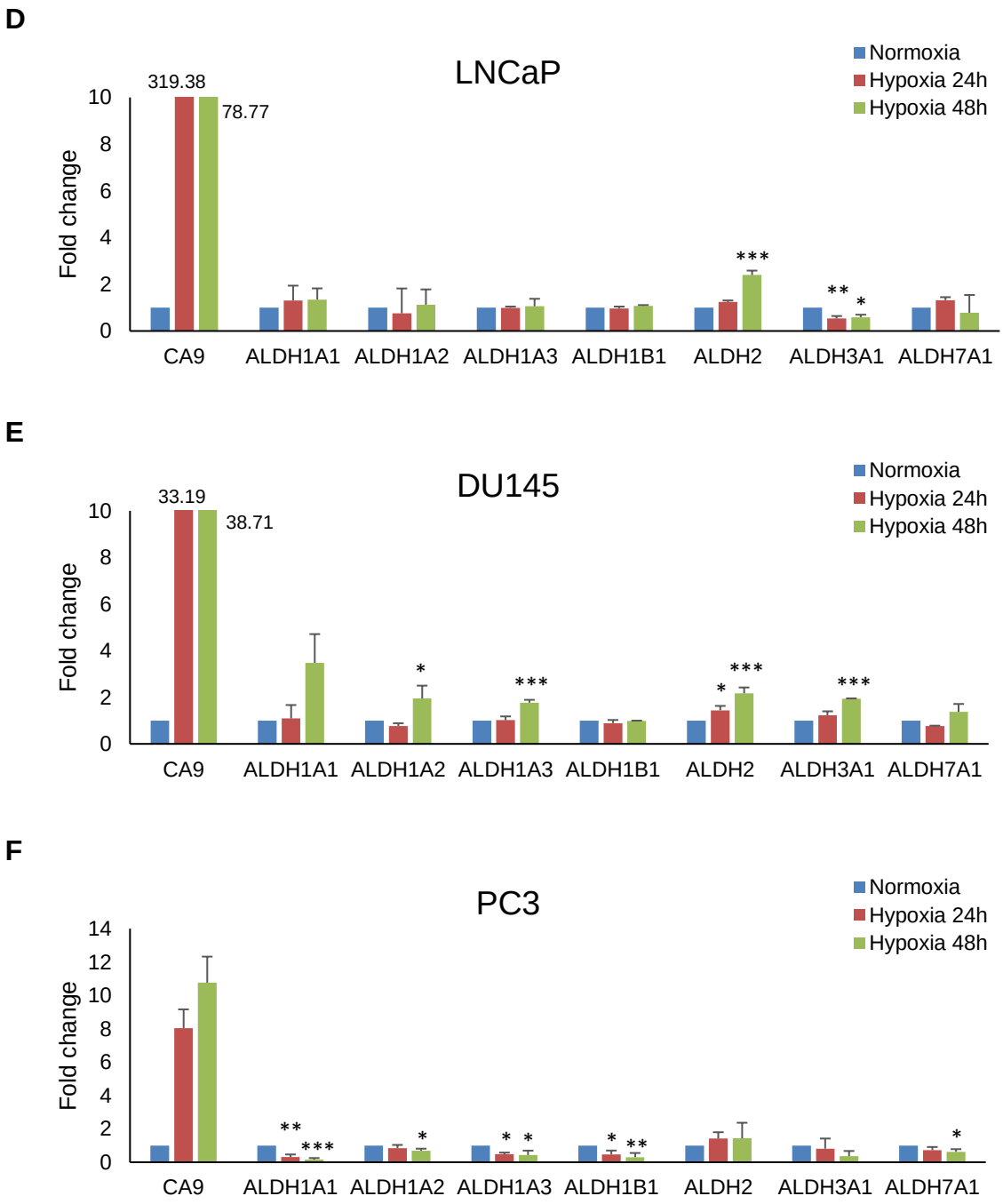


**Figure 31. Gene expression analysis in prostate cell lines under normoxic and hypoxic conditions.**

ALDH expression under hypoxia relative to normoxia in normal epithelial prostate cell line (A) and (B-F) prostate cancer cell lines at 24h and 48h exposure. Normoxic control samples are set at 1. Hypoxic conditions were maintained at 0.1% oxygen exposure. Data are represented as a mean of three independent experiments ± SD. Gene expression analysis was carried out by qRT-PCR and gene expression fold change of the ALDHs was worked out using $2^{-ddCT}$. RPLP0 was used as the internal control gene and CA9 was used as a positive control. Statistical test used was the one-way ANOVA for comparing paired groups including control (normoxia) with two hypoxic groups. * p = 0.01 to 0.05, ** p = 0.001 to 0.01, *** p = 0.0001 to 0.001, **** p < 0.0001). * Note difference in scale.

### 3.15 Effect of hypoxia on ALDH protein expression in prostate cell lines

To investigate whether hypoxia had an effect on ALDH protein level, western blot analysis was carried out on PNT2C2, SerBob, LNCaP, DU145 and PC3 cell lines. CA9 and HIF1α are often used as positive controls for hypoxia-related experiments, but in this study, lactate dehydrogenase (LDH) was used as previous experiments from Dr. Klaus Por's group suggested LDH as a stronger positive control.

In PNT2C2 cells, protein expression of ALDH1A1 was increased by 1.23-fold at 24h hypoxia which correlated with the mRNA expression data. In contrast to mRNA data, a decrease of 0.47-fold of ALDH1A3 expression was observed at 48h hypoxia. ALDH1B1 expression was increased by 1.42 and 1.53-fold at 24h and 48h hypoxia respectively, whereas no change was seen at mRNA level when compared to normoxia. The protein expression of ALDH3A1 was increased at 24h hypoxia (3.51 fold) but reduced at 48h hypoxia by 0.71-fold. Expression of ALDH7A1 reduced by 0.60-fold at 24h hypoxia (Figure 32 A).

In SerBob cells, there was an increase of 2.95-fold in ALDH1B1 expression at 24h hypoxia which correlated with mRNA expression. In contrast to mRNA expression, ALDH3A1 protein expression was reduced by 0.45-fold at 24h hypoxia (Figure 32 B).

In LNCaP cells, ALDH1A1 expression was reduced by 0.58 and 0.80-fold at 24h and 48h respectively which is in contrast to its mRNA expression. This pattern was also seen in ALDH1B1 expression. ALDH3A1 expression

decreased at 48h hypoxia which correlated with mRNA expression (Figure 32 C).

In DU145 cells, a 2.2-fold increase in ALDH3A1 expression was observed at 48h hypoxia exposure which correlated with mRNA expression (Figure 32 D).

In PC3 cells, a reduction in ALDH1A1 expression at both 24h and 48h hypoxia was observed which is in correlation with mRNA expression. The expression of ALDH1A3 is increased by 2.77-fold at 24h hypoxia but reduced by 0.47-fold at 48h hypoxia, the latter correlated with mRNA expression. ALDH1B1 expression was decreased by 0.77-fold and undetected at 24h and 48h hypoxia respectively, which correlated with mRNA expression. ALDH7A1 expression was decreased by 0.48-fold at 48h hypoxia as compared to normoxia correlating with the mRNA expression (Figure 32 E).

Taken together, gene and protein expression data suggested ALDH expression may be regulated by hypoxia. Two time points of 24 and 48-hour exposure to hypoxia identified 4 different expression patterns; changes in expression at 24h hypoxia but no changes at 48h hypoxia (temporary change in expression affected by hypoxia in a short time); no changes at 24h hypoxia but observed changes at 48h hypoxia (longer exposure to hypoxia induces changes); changes in expression at 24h also sustained at 48h (changes observed at both time points); and no changes in expression at either time point under hypoxic conditions. The ALDH expression pattern varied in the cell lines examined following exposure to hypoxia. Future studies are needed to investigate ALDH isoforms that are deregulated at 48h hypoxic exposure to

evaluate if the changes in ALDH expression have implications on biological processes in prostate cancer cells.

Where results are negative, inclusion of a positive control with high ALDH expression would have been useful to validate results. For example, the expression of ALDH1A3 was undetected in LNCaP and DU145 cells, but present in PNT2C2, SerBob and PC3 cells. Therefore, the addition of one of these cell lines in the LNCaP or DU145 blots could have served as a positive control and allowed the determination of the negative results. If there was no detection of ALDH1A3 in LNCaP and DU145 cells but a band in the PC3 cells for example, this would have validated the negative results.

The quality of blots for ALDH1A1 expression appeared poor in SerBob, DU145 and PC3 cells. This could have been improved by optimising the experimental methods in which a few variables could have been adjusted such as, blocking time, blot washing time, number of washes, duration of incubation with primary and secondary antibody, and exposure time of blots to ECL reagent. Or simply, purchasing of a better antibody, which was not available at the time but may now be available.

A

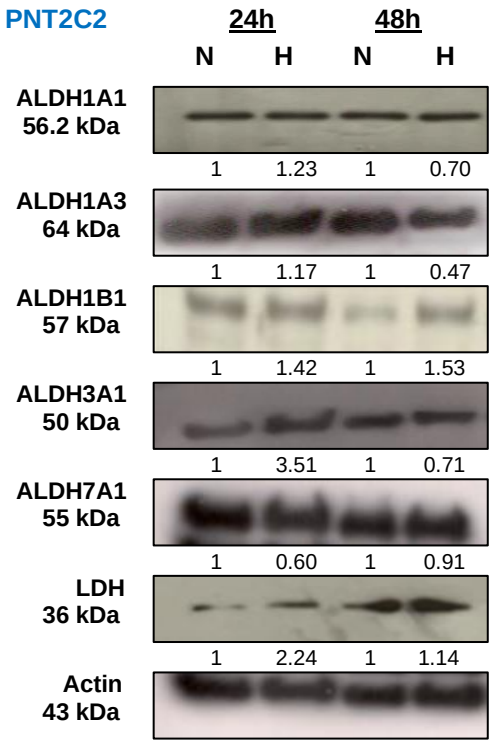
PNT2C2
24h
48h
N H N H
ALDH1A1 56.2 kDa
1 1.23 1 0.70
ALDH1A3 64 kDa
1 1.17 1 0.47
ALDH1B1 57 kDa
1 1.42 1 1.53
ALDH3A1 50 kDa
1 3.51 1 0.71
ALDH7A1 55 kDa
1 0.60 1 0.91
LDH 36 kDa
1 2.24 1 1.14
Actin 43 kDa

B

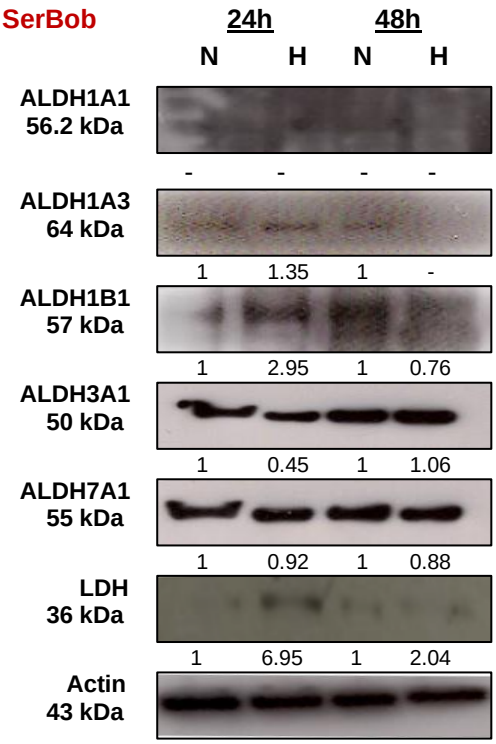
SerBob
24h
48h
N H N H
ALDH1A1 56.2 kDa
- - - -
ALDH1A3 64 kDa
1 1.35 1 -
ALDH1B1 57 kDa
1 2.95 1 0.76
ALDH3A1 50 kDa
1 0.45 1 1.06
ALDH7A1 55 kDa
1 0.92 1 0.88
LDH 36 kDa
1 6.95 1 2.04
Actin 43 kDa

C

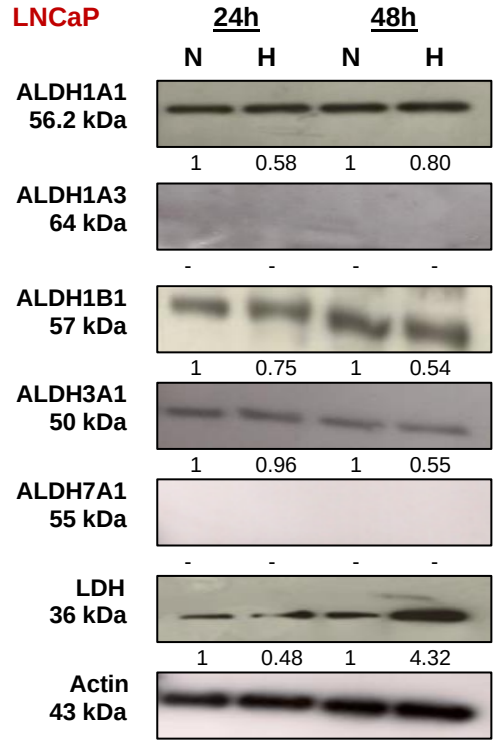
LNCaP
24h
48h
N H N H
ALDH1A1 56.2 kDa
1 0.58 1 0.80
ALDH1A3 64 kDa
- - - -
ALDH1B1 57 kDa
1 0.75 1 0.54
ALDH3A1 50 kDa
1 0.96 1 0.55
ALDH7A1 55 kDa
- - - -
LDH 36 kDa
1 0.48 1 4.32
Actin 43 kDa

D

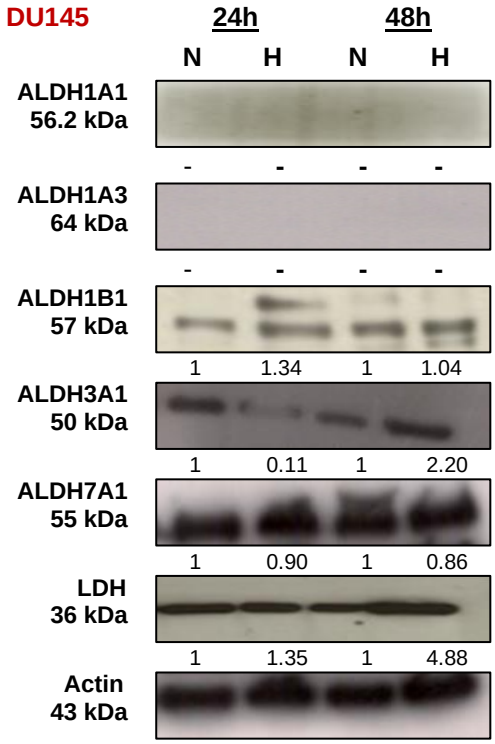
DU145
24h
48h
N H N H
ALDH1A1 56.2 kDa
- - - -
ALDH1A3 64 kDa
- - - -
ALDH1B1 57 kDa
1 1.34 1 1.04
ALDH3A1 50 kDa
1 0.11 1 2.20
ALDH7A1 55 kDa
1 0.90 1 0.86
LDH 36 kDa
1 1.35 1 4.88
Actin 43 kDa

**E**

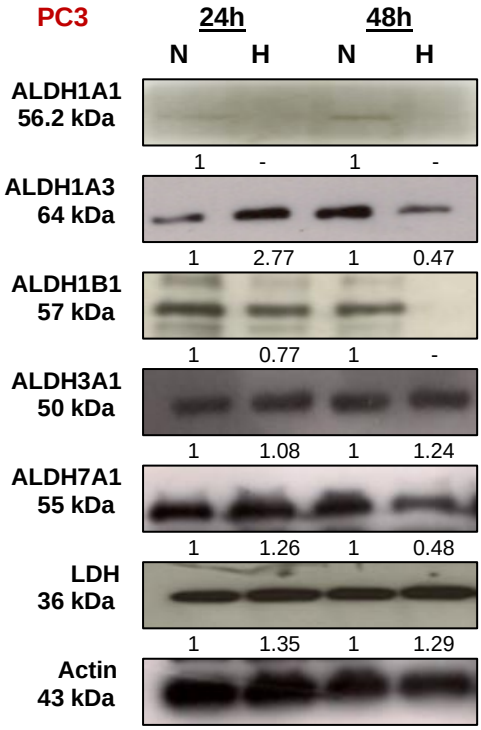


**Figure 32. Protein expression of ALDHs in prostate cell lines under normoxia and hypoxia by Western blot analysis.**

Relative ALDH expression in (A) normal epithelial prostate cell line and (B-E) prostate cancer cell lines. Actin was used as control to normalise ALDH expression. LDH was used as a positive control for hypoxia. ALDH protein expression under normoxia and hypoxia at 24h and 48h exposure. Hypoxic conditions were maintained at 0.1% oxygen exposure. Numbers below each blot represents the fold change in ALDH expression.

### 3.16 Generation of MCS using LNCaP cell line

To assess whether a MCS model of a prostate cancer cell line could be generated using LNCaP cells, two methods were investigated; the hanging-drop method and the 96-well plate method using methylcellulose as a key component in the culture media to facilitate spheroid formation. Methylcellulose, a cellulose derivative, is a polysaccharide that dissolves in aqueous solutions at temperatures below 50$^{o}$C, forming a viscous gel. It promotes cell aggregation and prevents cells from attaching to the culture surface even in serum containing media [498].

Upon seeding 1000, 2000 and 5000 cells in a petri dish for the hanging-drop method, the diameter of the spheroid was slightly reduced by day 2 and 3 of measurement due to the spheroids acquiring a more compact and round structure initially. This may be due to the broken cell-cell adhesion in the cell suspension upon seeding the cells which may have occupied a larger surface area, but by day 2 the cell-cell adhesion is re-established forming a tight aggregate, hence the reduced spheroid diameter. By day 4 the diameter increased (Figure 33 A and B). However, upon seeding 10,000 cells on day 1, the diameter reduced even at day 4 of measurement suggesting the seeding density was too high for generating spheroids possible due of cell death (Figure 33 A and B).

Cell seeding of 5000 cells was tested using the 96-well plate method and the diameter stayed similar over a growth period of 6 days which highlighted that the hanging-drop method was more suitable for spheroid formation of LNCaP cells (Figure 33 C and D). This is because in the hanging-drop method, the diameter of the spheroids increased over the number of days in culture when

seeded at 1000, 2000 and 5000 cells, facilitating the formation of a necrotic core in the centre of the spheroid surrounded by a region of hypoxic cells which are then surrounded by a periphery of a viable rim consisting of normoxic cells that are the closet to the oxygen and nutrient supply in the culture media. This method allows investigations to be carried out in the different compartments of the spheroids. In the 96-well plate method, the spheroid diameter did not change over 6 days suggesting no growth of the spheroid and perhaps no formation of the hypoxic and necrotic fraction of cells.

Figure 33 E showed H&E staining of LNCaP spheroid including the viable rim (VR) and necrotic core (NC), immunofluorescence detection of the proliferation marker Ki67 (red) sporadically across the VR and immunofluorescence detection of hypoxic region (HR) (green), surface layer (SL) (blue) and necrotic core (NC).

The empty NC observed in these spheroids by H&E and immunofluorescence suggested that the semi-adherent cell line LNCaP may not be the ideal model for a prostate cancer spheroid due to its compromised adhering ability in culture. These MCSs only represented the SL and HR as shown by H&E staining.

The LNCaP spheroids did not exhibit a perfectly round shape as not all cell lines develop spherical spheroids, however their value as a MCS model may be questionable since the SL and HR were only distinguishable but not the NC as this was lost through processing of the spheroids.

Immunofluorescence of Ki67 was used to detect proliferating cells in LNCaP spheroids. The Ki67 marker is a standard proliferation marker and the

antibody had been previously optimised in the institute where clear detection was observed. Although Ki67 detection was stronger in the VR of the spheroid, some scattered detection was also observed in the hypoxic region indicating cells may still have the ability to proliferate under hypoxic stress but at a reduced rate. It would be interesting to compare Ki67 expression in this LNCaP MCS model (with varying degrees of oxygen and nutrient supply throughout the spheroid) to monolayer LNCaP cells grown in a T75 flask (with enhanced oxygen and nutrient supply) as a control for Ki67 expression in the spheroids.

LNCaP spheroids showed hypoxic cells as indicated in green, with a viable rim of normoxic cells surrounding it in blue. Spheroids were either treated with pimonidazole for hypoxia detection or not treated. Negative controls included secondary antibody only for Ki67 detection and non-pimonidazole treated spheroids for hypoxia detection.

Perhaps a different prostate cancer cell line with better cell culture adherence may prove useful as a prostate cancer MCS model using the hanging drop method described here. However, the spherical shape may still be compromised as not all cell lines generate spherical spheroids, unlike e.g. some colon cancer cell lines [499] that are well known for their spheroid formation ability.

Taken together, this model can be further optimised using a different prostate cancer cell line to investigate ALDH expression in the different regions within a MCS.

A

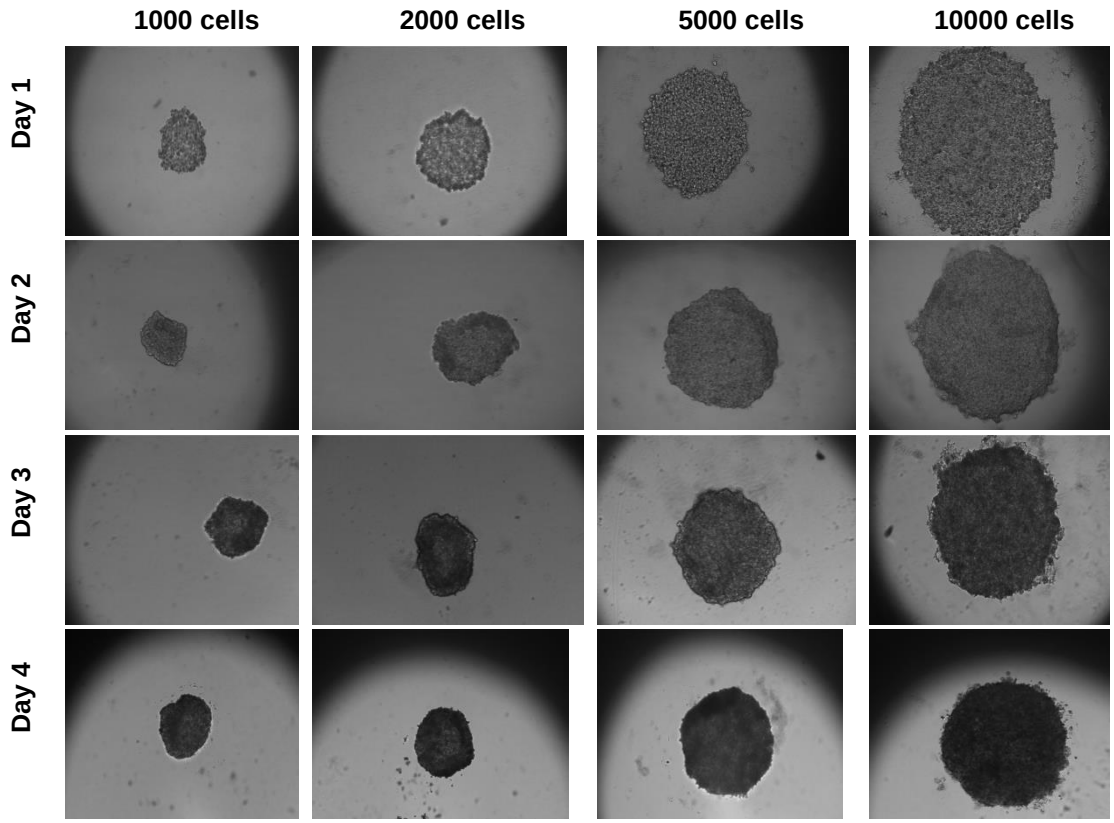
Hanging-drop method
1000 cells
2000 cells
5000 cells
10000 cells
Day 1
Day 2
Day 3
Day 4

B

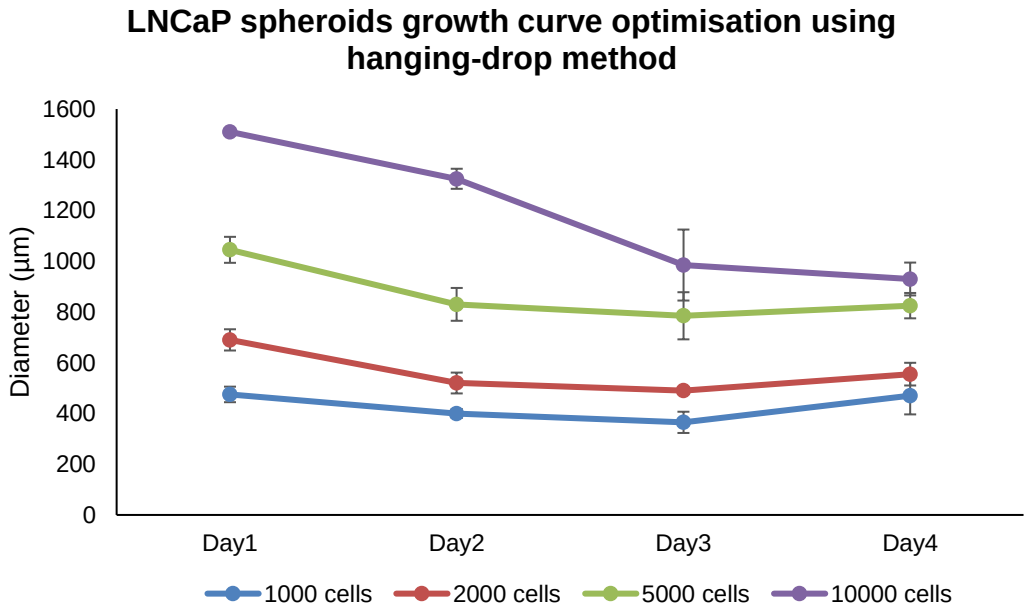
LNCaP spheroids growth curve optimisation using hanging-drop method
Diameter (µm)
1600
1400
1200
1000
800
600
400
200
0
Day1
Day2
Day3
Day4
1000 cells
2000 cells
5000 cells
10000 cells

C

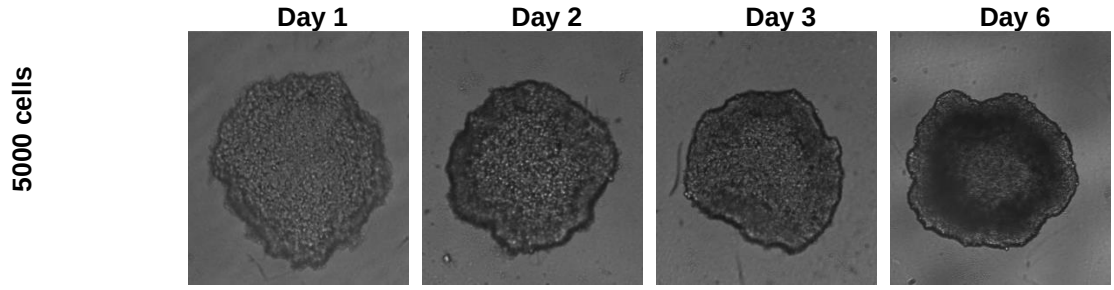
96-well plate method
Day 1
Day 2
Day 3
Day 6
5000 cells

D

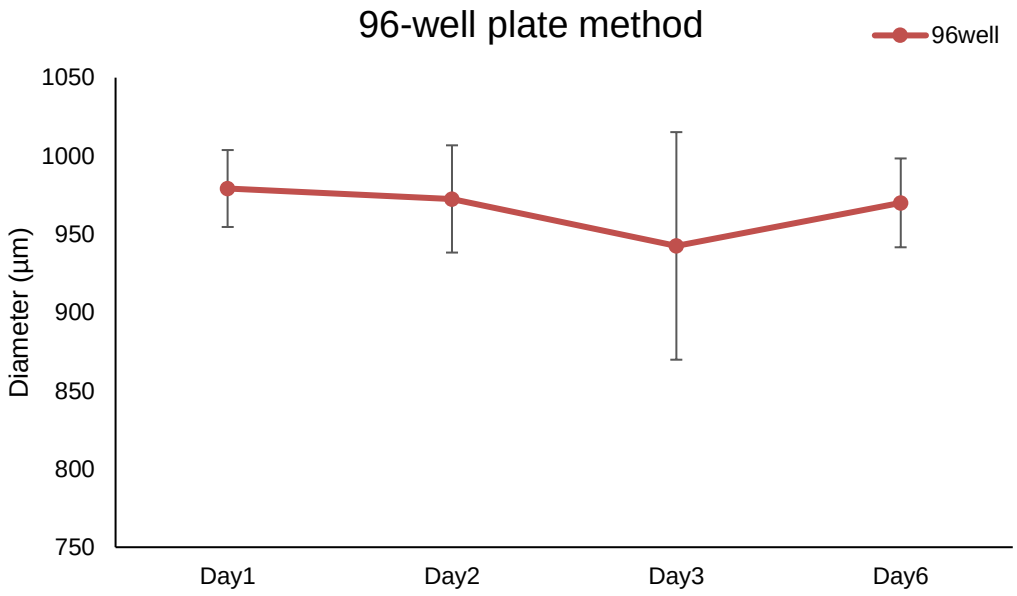
96-well plate method
96well
1050
1000
950
900
850
800
750
Diameter (µm)
Day1
Day2
Day3
Day6

**E** **Characterisation of LNCaP spheroids**

Day 4 of spheroid generation

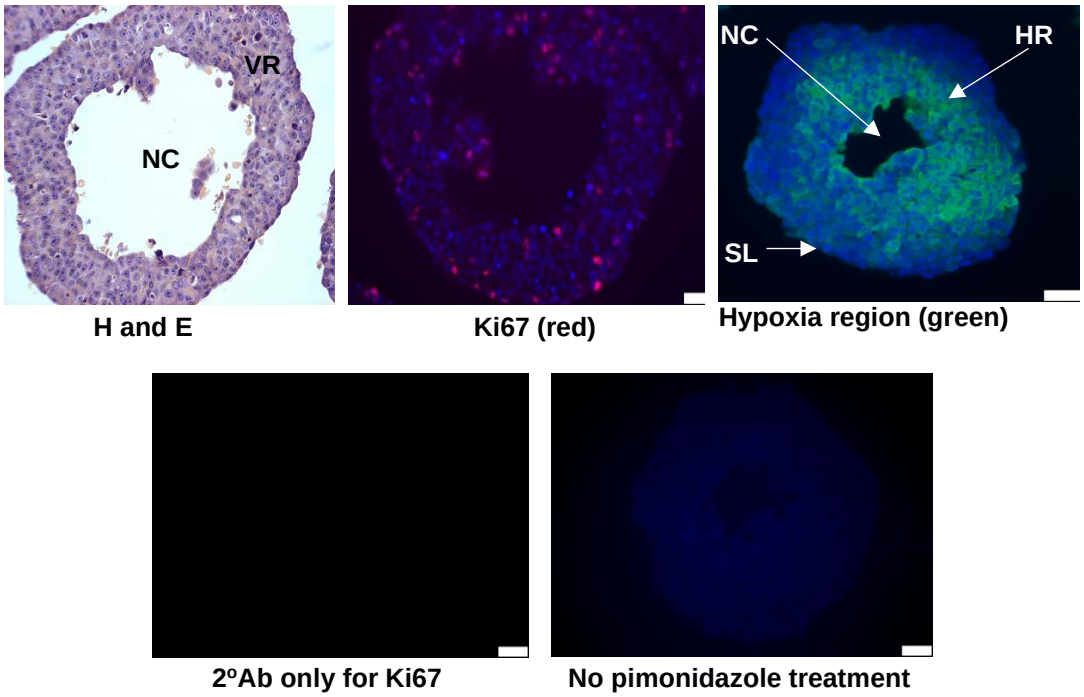


**Figure 33. LNCaP spheroid generation and characterisation.**
Hanging-drop method: (A) Illustration of spheroid development using different cell seeding densities over a period of 4 days, and (B) generation of spheroid growth curve from hanging-drop method. 96-well plate method: (C) Illustration of spheroid development over 6 days using 5000 cells, and (D) generation of spheroid growth curve from 96-well plate method. (E) H&E staining depicting the viable rim (VR) and loss of a necrotic core (NC) visualised at x20 magnification (left), Ki67 staining in red detected in tritc channel (580nm excitation/620nm emission) showing sporadic cell proliferation in VR and hypoxic region with DAPI staining (358nm excitation/461nm emission) cell nucleus (middle), secondary antibody only control for Ki67 (below middle), hypoxia detection in the hypoxic region shown in green from fitc channel (495nm excitation/519nm emission) with non-hypoxic surface layer in blue from DAPI staining (right), and no pimonidazole treated control with DAPI staining (below right).

# Chapter 4

## Investigation of the biological and therapeutic significance of ALDHs in primary prostate epithelial cultures using siRNA silencing and ALDH-affinic probes

## 4.1 Introduction

It is well established that ALDHs play a major role as a CSC marker in different cancer types. Multiple markers have been used for enriching cells with stem-like properties from human tumour primary tissue and human cancer cell lines by the use of aldefluor assay [357].

Other roles include ALDH7A1 being functionally involved in prostate cancer bone metastasis as shown by the knockdown of ALDH7A1 in a prostate cancer cell line inoculated in nude mice which resulted in decreased intra-bone growth and inhibited experimentally induced bone metastasis, while intra-prostatic growth was not affected suggesting microenvironment dependency [490]. Other ALDH isoforms include ALDH1A1 as a potential marker for malignant prostate SCs [500] while ALDH3A1 has been linked with prostate tumorigenesis [501]. A more recent study that used a proteomic approach revealed upregulation of ALDH7A1 in prostate cancer cell DU145, which is resistant to zoledronic acid, suggesting a potential role of ALDH7A1 in drug resistance [502]. Zoledronic acid is a drug known as bisphosphonate which is often used to treat bone metastases. It is a potent osteoclast inhibitor and is used to prevent skeletal related events including osteoporosis, high blood calcium and bone breakdown due to cancer, preserving quality of life in patients [503].

Furthermore, data obtained in chapter three showed ALDH1A3, ALDH1B1 and ALDH2 to be expressed at a significantly higher level in primary prostate cancer samples compared to BPH samples. In addition, ALDH7A1 was re-expressed in LNCaP cells following treatment with decitabine indicating promoter silencing of ALDH7A1 by hypermethylation. Most studies have

focused on the isolation of putative CSC using the aldefluor assay which is based on the activity of ALDHs in cells, however, only relatively few studies have highlighted functional roles of ALDHs in prostate cancer and these studies have typically used cell lines. Therefore, the aim of this study was to investigate the biological functions of ALDH isoforms related to prostate cancer using primary epithelial cells derived from patient tissue.

ALDH gene expression may be linked with increased Snail expression as studies have shown the knockdown of Snail expression significantly reduces ALDH1 expression, prevents cancer stem-like properties and inhibits the tumorigenic abilities of $CD44^{+}/CD24^{-}/ALDH1^{+}$ cells [504]. Certain agents may be effective against CSCs and result in reduced population of ALDH positive cells [504], such as treatment of breast cancer cells with dietary polyphenols, piperine and curcumin that significantly decreases mammosphere formation [505]. Furthermore, DEAB a specific ALDH inhibitor may enhance the sensitisation of $ALDH^{+}$/CD44+ cells to chemo- and radiotherapy [504]. In addition, disulfiram and atRA treatment inhibits ALDH and increases sensitisation of cancer cells to chemotherapy [241]. Accordingly, this chapter describes work that investigated novel ALDH-affinic compounds in single and combination treatments to understand whether targeting ALDH-expressing populations (potentially CSCs) can be used as a potential treatment strategy for prostate cancer.

In order to study biological function in cells, RNA interference (RNAi) technology was used.

RNAi is a process to induce silencing of gene expression by degrading RNA by either double-stranded small interfering RNA (siRNA) or the vector-based short hairpin RNA (shRNA) [506-508].

siRNAs are 21-25 nucleotides long with both a sense and an antisense polarity forming a duplex [509]. They are directly introduced to cells in culture and steadily accumulate in the cytoplasm [507-510]. Once in the cytoplasm, the siRNAs associate with an RNase complex known as RNA induced silencing complex (RISC) consisting of endoribonuclease Argonaute-2 (Ago-2), Dicer (a dsRNA-specific RNAse III enzyme) and TAR-RNA-binding protein (TRBP). The siRNA duplex is then nicked by Ago-2 and separated resulting in the passenger strand to be removed from the RISC complex by the endonuclease activity of component 3 promoter of RISC (C3PO) [511]. The guide strand with RISC is then exposed for base-pairing with its homologous mRNA target where it cleaves and degrades the mRNA by the activity of Ago-2 [511]. The siRNA mechanism is diagrammatically illustrated in Figure 34.

**Figure 34. Schematic of the siRNA mediated RNA interference pathway.**
Once inside the cell, the siRNA associates with RNA induced silencing complex (RISC), Dicer (RNase III enzyme) and TAR-RNA-binding protein (TRBP). The double-stranded siRNA gets nicked by Argonaute-2 (Ago-2) and splits into two resulting in the removal of passenger strand from RISC complex via the endonuclease component 3 promoter of RISC, leaving the guide strand to be exposed for base-pairing with target mRNA in which the target mRNA gets degraded by Ago-2 activity. Adapted from [508].

shRNA synthesis occurs in the nucleus of transfected cells upon delivery of bacterial or viral expression vectors into the cytoplasm of cells. Transcription of shRNA can be driven by either RNA polymerase II or III based on the promotor involved in the expression [512]. The resulting primary transcript (pri-shRNA) formed consists of a hairpin-like structure containing a stem like section of paired sense and antisense strands joined by a loop of unpaired nucleotides. The pri-shRNA is processed in the nucleus by a complex containing the RNase III enzyme Drosha and the double-stranded RNA-binding domain protein DGCR8 to create pre-shRNA [513] before it is

transported to the cytoplasm by exportin 5 [514]. The pre-shRNA is then taken on by a complex consisting of Dicer-TRBP-protein activator of PKR (PACT) causing the loop of the hairpin to be cleaved off to form a double stranded siRNA [515]. The resultant siRNA is then taken up by Ago-2 protein consisting RISC. Herein, the cleaving and degradation process is the same as described for siRNA [508]. The shRNA mechanism is diagrammatically illustrated in Figure 35.

"Image/photo/map/illustration/graph not included due to copyright restrictions" Image can be viewed at:
https://www.sciencedirect.com/science/article/pii/S0169409X09000969?via%3Dihub

**Figure 35. Schematic of the shRNA mediated RNA interference pathway.**
The shRNA once in the nucleus is processed by a complex containing the RNase III enzyme Drosha and the double-stranded RNA-binding domain protein (DGCR8) to generate a pre-shRNA prior to its transportation to the cytoplasm by exportin 5. Once in the cytoplasm, pre-shRNA binds to a Dicer complex containing TAR-RNA-binding protein (TRBP) and protein activator of PKR (PACT) in which the hairpin loop is cleaved forming a double-stranded siRNA. The process is then the same as siRNA mediated RNA interference. Adapted from [508].

## 4.2 Aims and Objectives:

- To optimise the siRNA transfection protocol using siRNAs against ALDH1A3, ALDH1B1, ALDH2, and ALDH7A1 in prostate cancer cell lines PC3 and Serbob.
- To evaluate siRNA knockdown of ALDH1A3, ALDH1B1, ALDH2 and ALDH7A1 in primary prostate epithelial cultures.
- To evaluate the effect of silencing selected ALDHs in primary cultures on:
    1. Cell proliferation using trypan blue exclusion assay
    2. Cell cycle analysis using flow cytometry
    3. Cell migration using the wound healing assay
    4. Colony formation using the colony forming assay
    5. Cell differentiation using CD49b as a marker
- To evaluate the effect novel ALDH-affinic compounds have on cell viability of primary prostate epithelial cells when used as a single treatment vs combination treatment with docetaxel.

## 4.3 Results

## 4.4 Preliminary data for optimisation of siRNA concentration

siRNA knockdown efficiency was first tested in prostate cancer cell lines SerBob and PC3 for method optimisation before starting knockdown experiments in primary prostate epithelial cultures. siRNA knockdown against ALDH1A3, ALDH7A1, ALDH1B1 and ALDH2 at 20nM was first investigated in SerBob cells seeded at 2.75 x $10^5$cells/T25 flask seeding density and cells harvested 48 and 72 hours post transfection. Figure 36 and Table 21 show qPCR analysis of target knockdown achieved.

To further knockdown the expression of the selected ALDHs, a lower seeding density of 1.5 x $10^5$cells/T25 flask was then investigated and the siRNA concentration was examined by a titration experiment of 20nM, 40nM and 80nM siRNA against ALDH1A3 and ALDH7A1. Figure 37 shows the knockdown achieved. Taken together, a selection of 40nM and a lower seeding density of 1.5 x $10^5$cells/T25 flask gave the most efficient knockdown of about 90%.

Efficiency of knockdown against ALDH1A3 was further tested in PC3 cells with either 2 x $10^5$cells/T25 flask with 20nM siRNA or 1.2 x $10^5$cells/T25 flask with 40nM siRNA. Figure 38 shows knockdown achieved with these two combinations. At protein level, 74% knockdown of ALDH1A3 was achieved following siRNA treatment (Figure 38).

Therefore, all subsequent knockdown experiments were performed using 40nM siRNA with 1.5 x $10^5$cell/T25 flask in primary cultures.

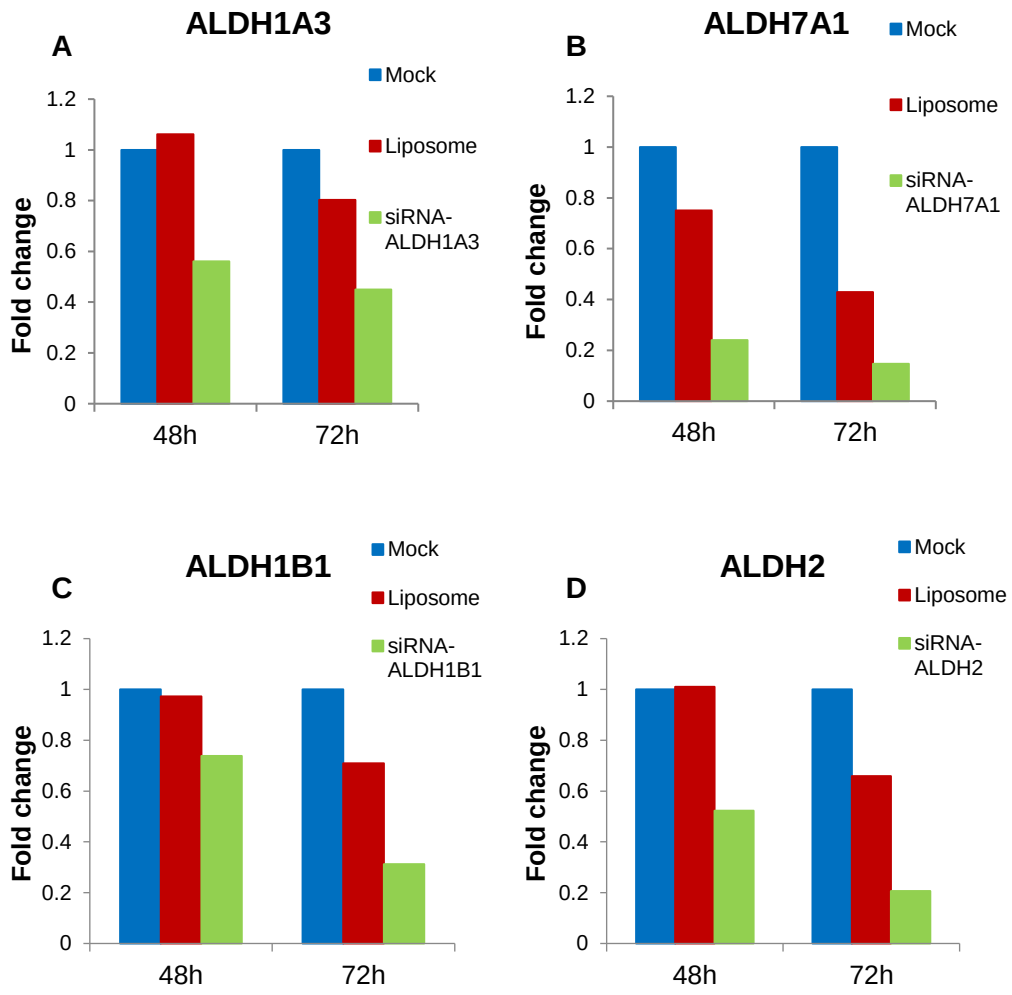


**Figure 36. Knockdown of ALDH achieved in SerBob cells at 20nM siRNA.**

qPCR analysis of ALDH expression following siRNA knockdown of (A) ALDH1A3, (B) ALDH7A1, (C) ALDH1B1 and (D) ALDH2 in SerBob cell line seeded at a cell density of 2.75 x $10^5$cells/T25 at a concentration of 20nM siRNA transfection at 48h and 72h time points. RPLP0 was used as the reference gene and fold change in expression was relative to mock control. Mock control (Cells only, no oligofectamine, no siRNA), Liposome control (oligofectamine only, no siRNA), and siRNA (oligofectamine and siRNA). Experiment carried out once for optimisation, therefore no statistical significance of the means compared.

| KD | 48h | 72h |
|---|---|---|
| **ALDH1A3** | 44% | 65% |
| **ALDH7A1** | 76% | 85% |
| **ALDH2** | 50% | 80% |
| **ALDH1B1** | 26% | 69% |

**Table 21. Percentage ALDH knockdown in SerBob cells at 20nM siRNA**
Percentage of knockdown achieved after using siRNA at 48h and 72 hour transfection in the SerBob cell line seeded at a cell seeding density of 2.75 x $10^5$cells/T25 using 20nM siRNA.

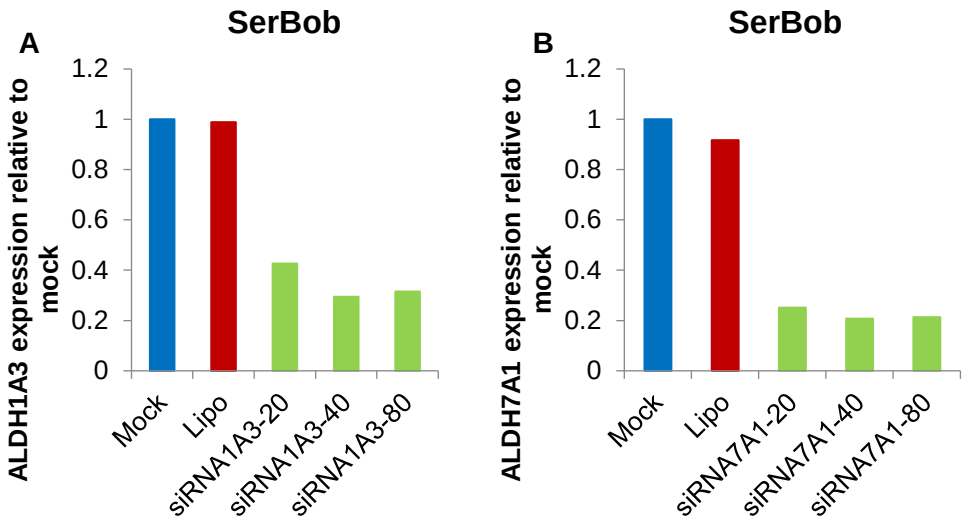


**Figure 37. Relative expression of (A) ALDH1A3 and (B) ALDH7A1 following titration of siRNA in SerBob cells at 48hr.**
qPCR analysis of ALDH expression following siRNA knockdown of (A) ALDH1A3, and (B) ALDH7A1 in SerBob cell line seeded at a cell seeding density of 1.5 x $10^5$cells/T25 at a concentration of 20nM, 40nM and 80nM siRNA at 48h time point. RPLP0 was used as the reference gene and fold change in expression was relative to mock control. Mock control (Cells only, no oligofectamine, no siRNA), Liposome control (oligofectamine only, no siRNA), and siRNA (oligofectamine and siRNA). Experiment carried out once for optimisation, therefore no statistical significance of the means compared.

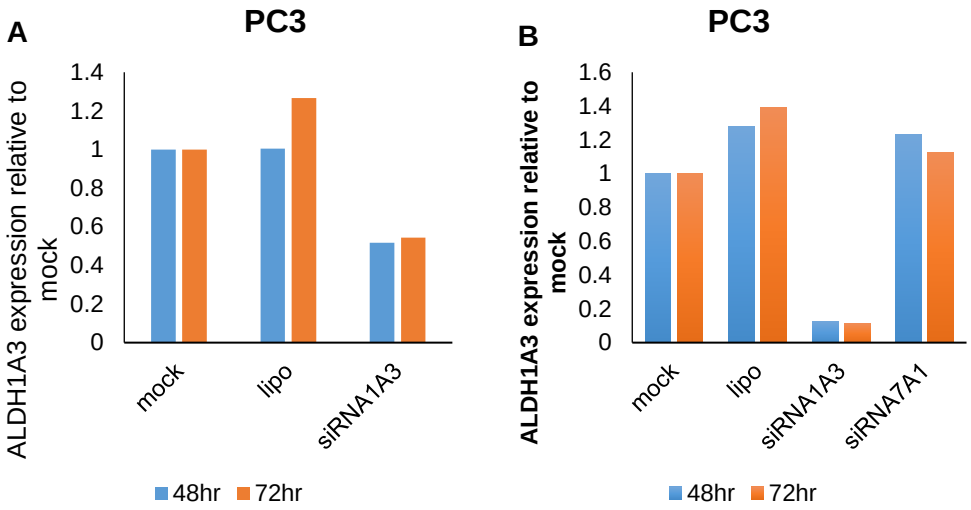
A
PC3
ALDH1A3 expression relative to mock
1.4
1.2
1
0.8
0.6
0.4
0.2
0
mock
lipo
siRNA1A3
48hr
72hr
B
PC3
ALDH1A3 expression relative to mock
1.6
1.4
1.2
1
0.8
0.6
0.4
0.2
0
mock
lipo
siRNA1A3
siRNA7A1
48hr
72hr

C

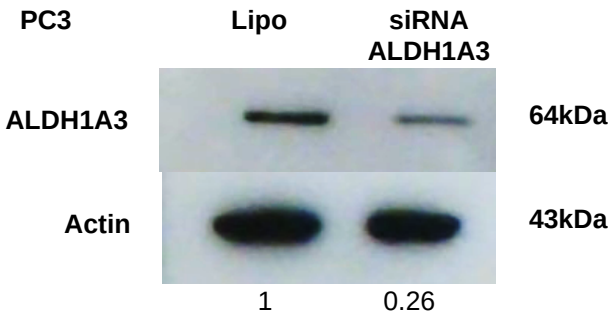
PC3
Lipo
siRNA ALDH1A3
ALDH1A3
64kDa
Actin
43kDa
1
0.26

**D**

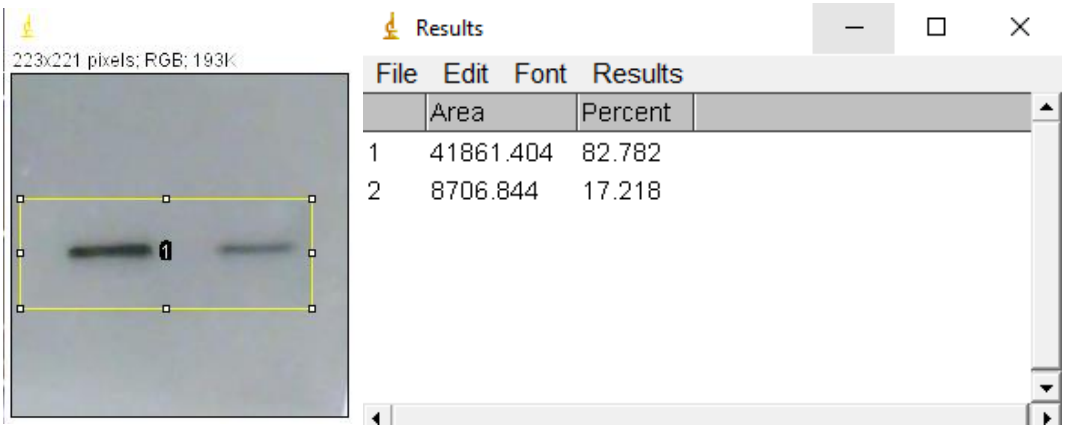
223x221 pixels; RGB; 193K
1
Results
File Edit Font Results
Area Percent
1 41861.404 82.782
2 8706.844 17.218

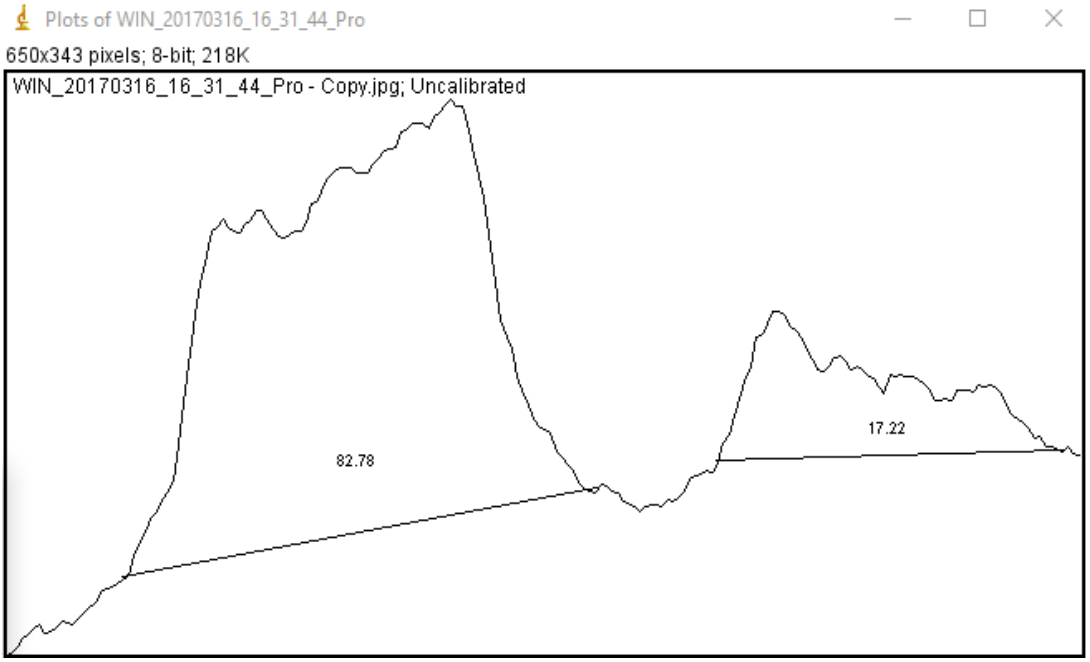
Plots of WIN_20170316_16_31_44_Pro
650x343 pixels; 8-bit; 218K
WIN_20170316_16_31_44_Pro - Copy.jpg; Uncalibrated
82.78
17.22

**E**

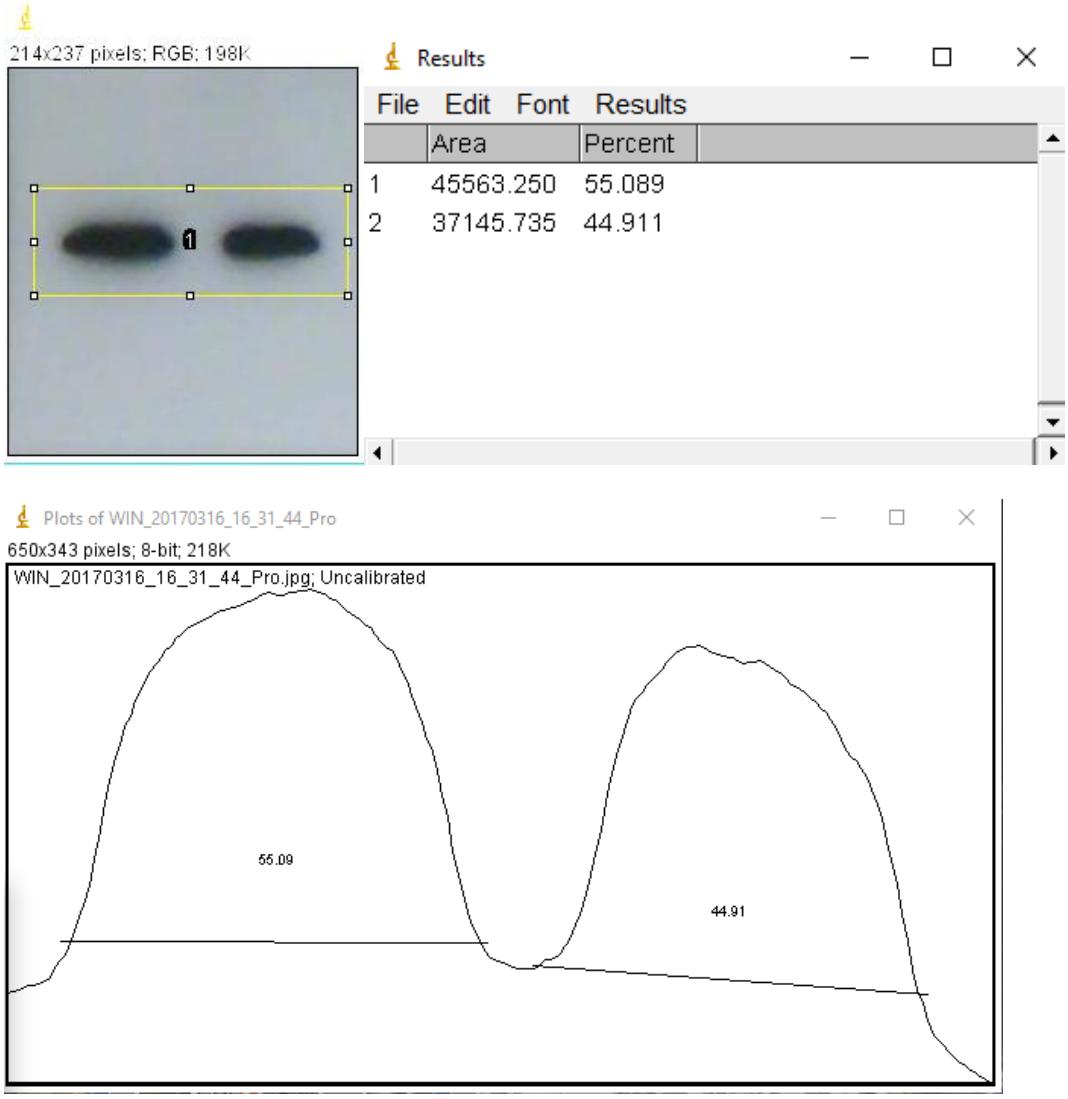


**Figure 38. ALDH1A3 expression after knockdown in PC3 cells.**
qPCR analysis of ALDH1A3 expression following siRNA knockdown at (A) 2 x $10^5$cells/T25 flask cell seeding density with 20nM siRNA or (B) 1.2 x $10^5$cells/T25 flask cell seeding density with 40nM siRNA in PC3 cell line at 48 and 72hr time points. RPLP0 was used as the reference gene and fold change in expression was relative to mock control. Mock control (Cells only, no oligofectamine, no siRNA), Liposome control (oligofectamine only, no siRNA), and siRNA (oligofectamine and siRNA). Experiment carried out once for optimisation, therefore no statistical significance of the means compared. (C) Western blot analysis of ALDH1A3 expression following siRNA knockdown at 40nM in PC3 cell line seeded at 1.2 x $10^5$cells/T25 flask density at 48h time point. Actin was used to normalise protein expression. ALDH1A3 knockdown was relative to Lipo control. Lipo control (oligofectamine only, no siRNA). Experiment carried out once for optimisation, therefore no repeated blots. (D) Densitometry plot for ALDH1A3 expression and (E) densitometry plot for actin expression.

## 4.5 Cell number changes in primary prostate epithelial cells upon ALDH knockdown

Images were taken at 48-hour and 72-hour time points to monitor any phenotypic changes of cells following transfection with ALDH siRNA in H507/14 LM and H507/14 RB primary cells derived from Gleason 7 cancer.

These preliminary results seemed to show a small reduction in cell viability upon knockdown of ALDH1A3 and ALDH7A2 only at 48-hour time point compared to liposomal control in both samples (Figure 39 A and C). At 72-hour, not much phenotype difference was observed between liposomal control and ALDH1A3 and ALDH7A1 in both samples (Figure 39 B and D). Only a small reduction was observed in the co-transfection of the two isoforms in the H507/14 LM samples (Figure 39 B). ALDH1B1 and ALDH2 knockdown were included at the 72-hour time point only to assess if they have an effect on morphological changes and no changes were observed when compared to liposomal control (Figure 39 B and D).

H405/14 and H415/15 BPH samples were also included to assess if they were phenotypically different from the cancer samples post transfection of ALDH1A3, ALDH7A1 and their combination. At 48-hour post transfection, no changes were observed in the siRNA transfected cells as compared to liposomal control in both BPH samples (Figure 39 E).

Following this observation, to assess cell number changes upon ALDH silencing, cell viability assays were performed and described later in this chapter.

**A**

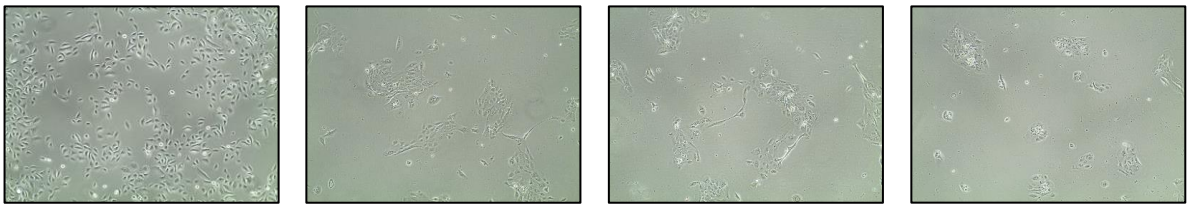

H507/14 LM Mock 48h | H507/14 LM Lipo 48h | ALDH1A3 | ALDH7A1

**B**

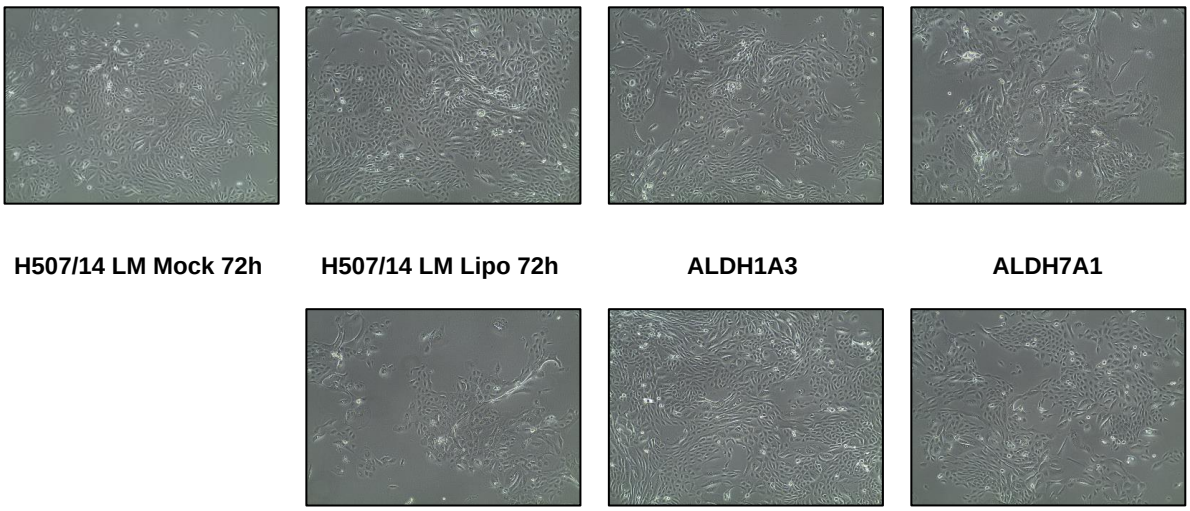

H507/14 LM Mock 72h | H507/14 LM Lipo 72h | ALDH1A3 | ALDH7A1

COMBO | ALDH1B1 | ALDH2

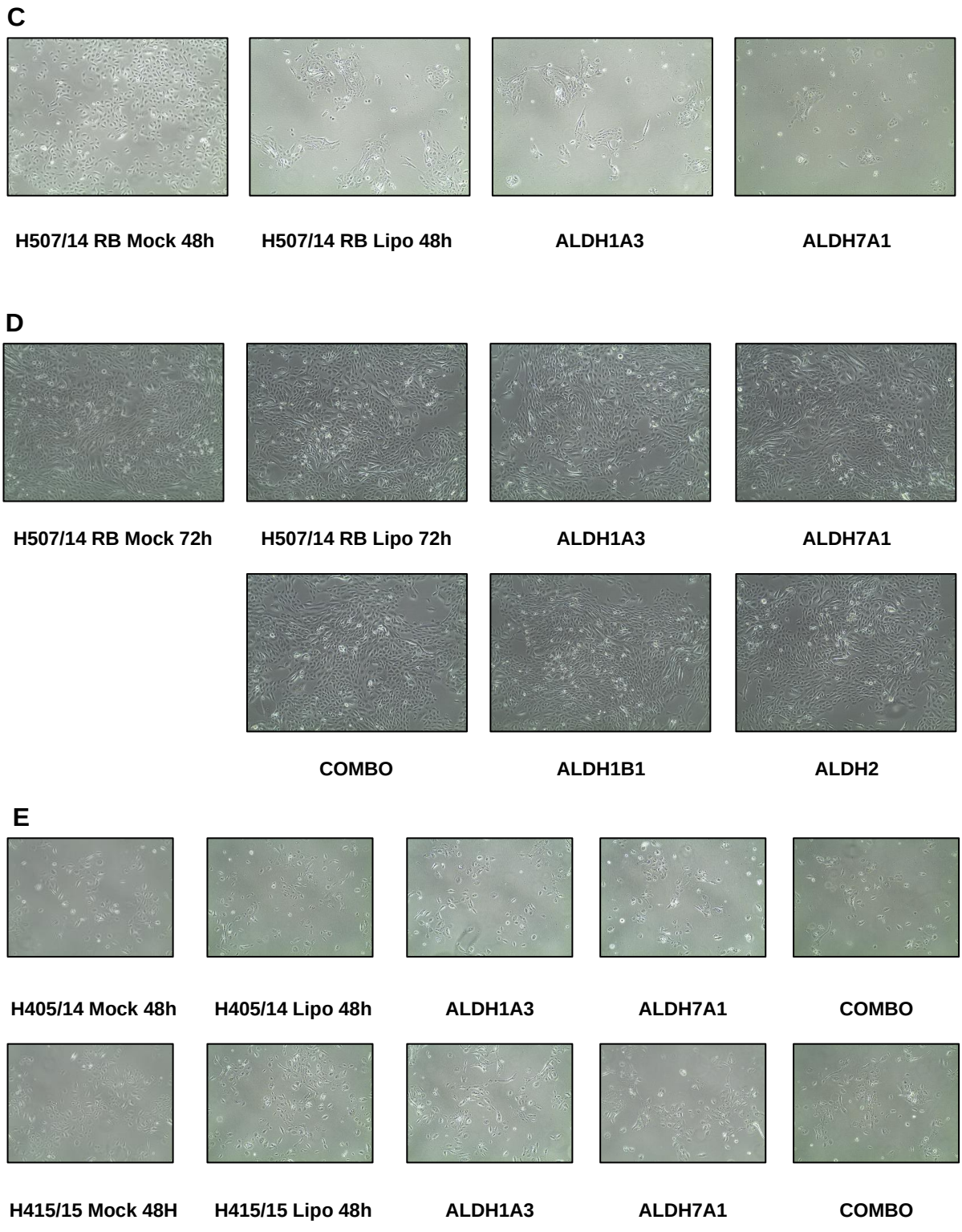


**Figure 39. Morphology of primary BPH and cancer cells following ALDH knockdown.** Cancer sample H507/14 LM at (A) 48h (B) 72h post transfection. Cancer sample H507/12 RB at (C) 48h (D) 72h post transfection. Benign samples H405/14 and H415/15 at (E) 48h post transfection. Mock control excludes oligofectamine and siRNA. Lipo control is oligofectamine only and no siRNA. ALDH1A3, ALDH7A1, COMBO, ALDH1B1 and ALDH2 illustrate cell morphology following corresponding siRNA knockdown. COMBO is ALDH1A3 and ALDH7A1 co-silencing by siRNA. Images taken at x10 magnification using a light microscope.

## 4.6 Evaluation of ALDH knockdown on RNA and protein expression in primary prostate epithelial cultures

qPCR analysis and Western blots were performed to assess percentage mRNA knockdown and protein level respectively of selected ALDHs upon transfecting cells with relevant ALDH siRNAs.

## 4.7 RNA expression

Cancer cells were harvested 48 hours, 72 hours and 120 hours after transfection to assess their ALDH silencing profile at mRNA level in H507/14 LM and H507/14 RB cancer samples. Knockdown of ALDH1A3 and ALDH7A1 was first assessed at 48 and 72 hours post transfection (Figure 40). Then another time point of 120 hours was added to the investigation and a combination knockdown of ALDH1A3 and ALDH7A1 was also assessed. ALDH1B1 and ALDH2 were also included in the investigation (Figure 41, 42).

Figure 40 show the percentage knockdown achieved at 48-hour and 72-hour post siRNA transfection in H507/14 LM and H507/14 RB cells.

It was noticed that ALDH7A1 knockdown resulted in an upregulation of ALDH1A3 expression by 3-fold at 48 hours and by 8-fold at 72 hours in both samples. The contrary however was not observed with no effect on ALDH7A1 expression upon ALDH1A3 knockdown at mRNA level (Figure 40).

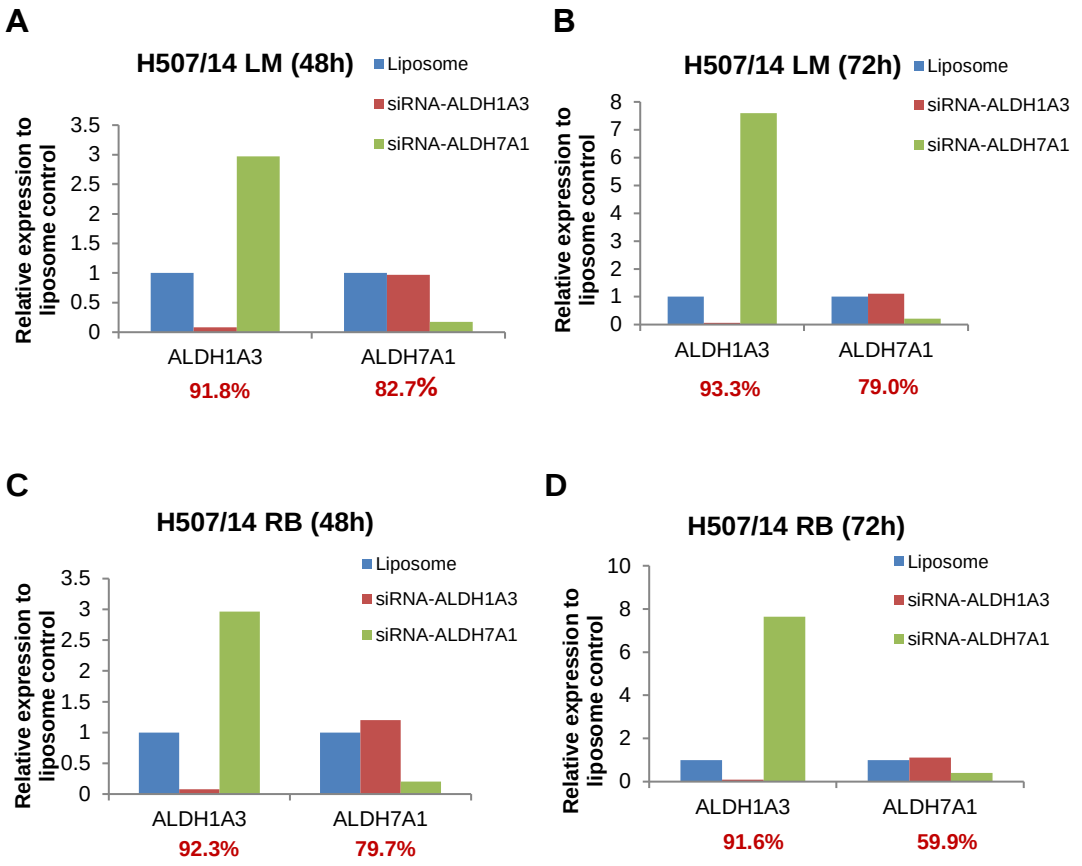


**Figure 40. Relative ALDH1A3 and ALDH7A1 RNA expression to liposomal control post siRNA transfection.**
qPCR analysis show RNA expression of ALDH1A3 and ALDH7A1 in H507/14 LM cells transfected with either ALDH1A3 or ALDH7A1 siRNA at (A) 48 hr and (B) 72 hr, or in H507/14 RB cells at (C) 48 hr and (D) 72 hr. Liposome control is cells treated with oligofectamine only. Experiment was done once and therefore a comparison of the means could not be statistically tested. Preliminary data to identify optimal transfection time.

A further time point of 120 hours post transfection was then assessed in the same samples. ALDH1A3 and ALDH7A1 co-transfection (to counteract upregulation of ALDH1A3 upon ALDH7A1 silencing), ALDH1B1 and ALDH2 were also investigated. Figure 41 and 42 show the percentage knockdown achieved at 72-hour and 120-hour post siRNA transfection in H507/14 LM and H507/14 RB cells.

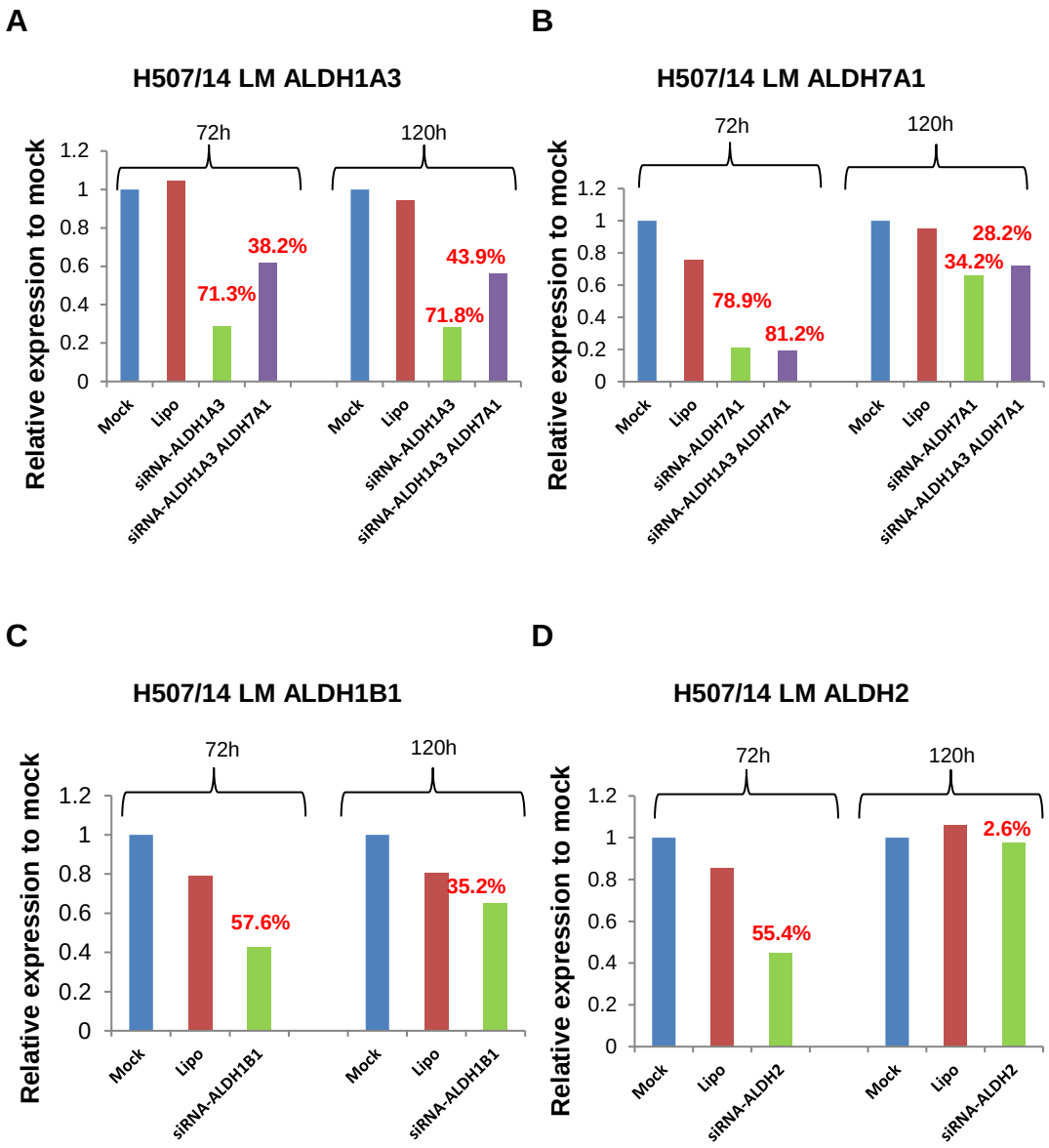


**Figure 41. Relative ALDH RNA expression to mock control post 72 and 120 hours of siRNA transfection in H507/14 LM cells.**

qPCR analysis show RNA expression of (A) ALDH1A3, (B) ALDH7A1, (C), ALDH1B1 and (D) ALDH2 in H507/14 LM cells transfected with either ALDH1A3 (A), ALDH7A1 (B), ALDH1B1 (C) and ALDH2 (D) siRNA at 72 or 120 hours. Expression was compared to mock control with no oligofectamine or siRNA. Lipo control included oligofectamine only. Experiment was done once and therefore a comparison of the means could not be statistically tested. Preliminary data to identify optimal transfection time.

It is demonstrated in Figure 41 that the knockdown of ALDH1A3 and ALDH7A1 in H507/14 LM cells achieved at 72 and 120-hour was less than the knockdown achieved at 48-hour transfection. Therefore, the 48-hour time point was selected for transfection experiments as a high efficiency of knockdown of ALDH1A3 and ALDH7A1 was achieved at this time point as shown in Figure 40. Furthermore, knockdown of ALDH1B1 and ALDH2 showed inefficient knockdown at longer time points (Figure 41) and although their efficiency was not assessed at 48-hour, this time point was selected for these two isoforms based on the findings from ALDH1A3 and ALDH7A1 knockdown at 48 hours.

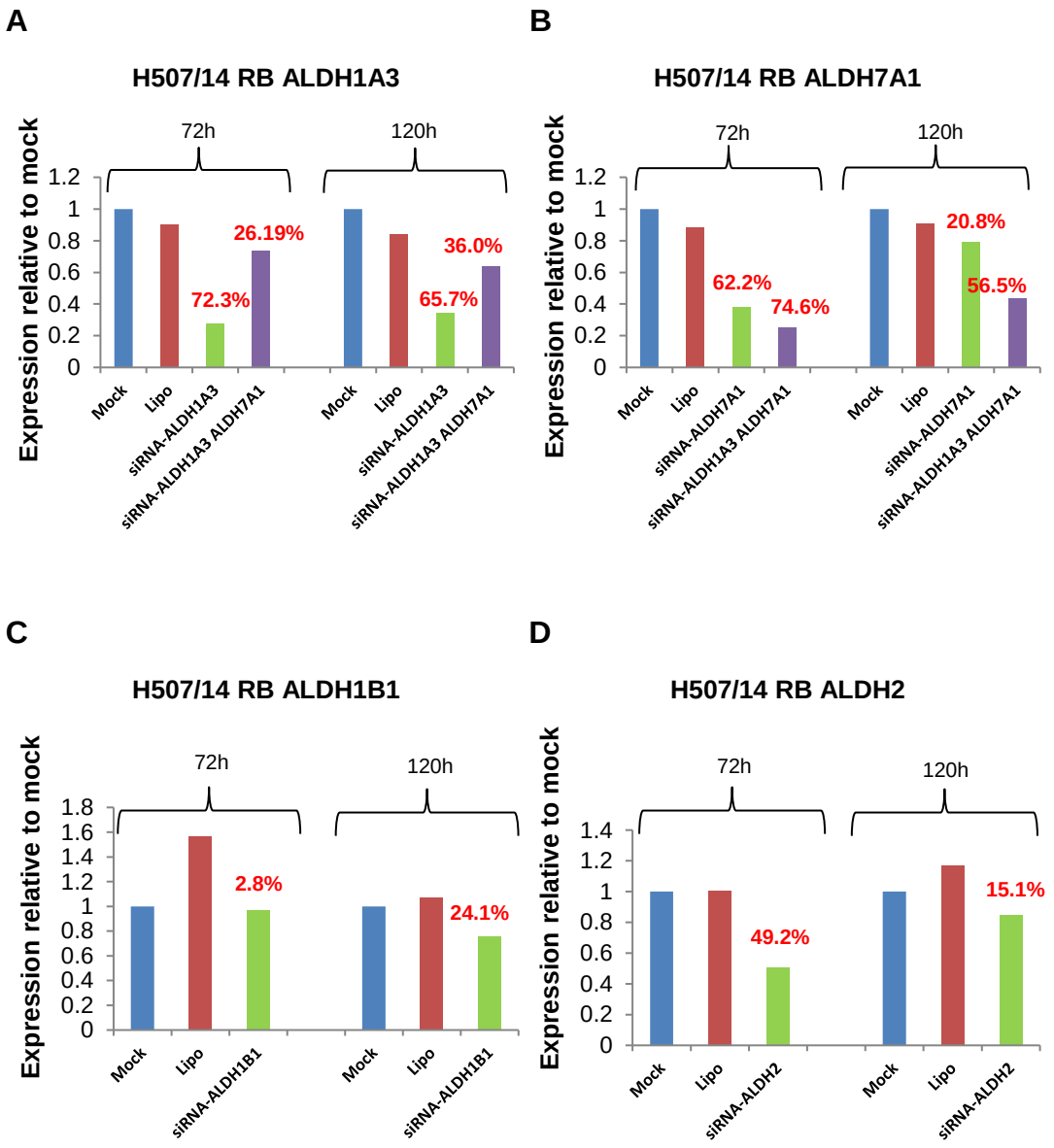


**Figure 42. Relative ALDH RNA expression to mock control post 72 and 120 hours of siRNA transfection in H507/14 RB cells.**
qPCR analysis show RNA expression of (A) ALDH1A3, (B) ALDH7A1, (C), ALDH1B1 and (D) ALDH2 in H507/14 LM cells transfected with either ALDH1A3 (A), ALDH7A1 (B), ALDH1B1 (C) and ALDH2 (D) siRNA at 72 or 120 hours. Expression was compared to mock control with no oligofectamine or siRNA. Lipo control included oligofectamine only. Experiment was done once and therefore a comparison of the means could not be statistically tested. Preliminary data to identify optimal transfection time.

The trend in knockdown efficiency appeared similar in H507/14 RB cells as compared to H507/14 LM cells. Figure 42 shows less efficient knockdown of the ALDHs at longer time points compared to a high efficiency at 48 hours (Figure 40). For all subsequent transfection experiments the 48-hour time

point for transfection was selected for downstream functional assays outlined in this chapter, unless otherwise stated.

### 4.8 Protein expression

Cell lysates were prepared from H488/14 RM cancer cells and protein expression was analysed to investigate the effect of knocking down ALDH1A3, ALDH7A1 and their combination on protein expression.

There was a complete knockdown of ALDH1A3 at protein level after transfection as shown in Figure 43. The co-transfection of ALDH1A3 and ALDH7A1 (Combo) also showed complete knockdown of ALDH1A3. Interestingly, there was a 1.59-fold increase (59%) in the protein expression of ALDH1A3 upon ALDH7A1 knockdown correlating to mRNA expression in H507/14 LM and H507/14 RB cells as shown in this chapter. Therefore, co-transfection of ALDH1A3 and ALDH7A1 was included in subsequent functional assays outlined in this chapter to ensure efficient silencing of both ALDH1A3 and ALDH7A1. This was to ensure that the knockdown of one isoform does not upregulate the expression of the other (as shown in Figure 40) and therefore, co-transfection of both were studied. For example, knockdown of ALDH1A3, reduced ALDH1A3 expression only, not ALDH7A1, and vice versa and so each siRNA was considered a negative control for the expression of the other isoform. However, the knockdown of ALDH7A1 which lead to an increase in expression of ALDH1A3 suggested a compensatory role of ALDH1A3 in the absence of ALDH7A1. Co-transfection was included to assess any differences in biological processes when compared with ALDH1A3 and ALDH7A1 knockdown alone, for subsequent studies in this chapter.

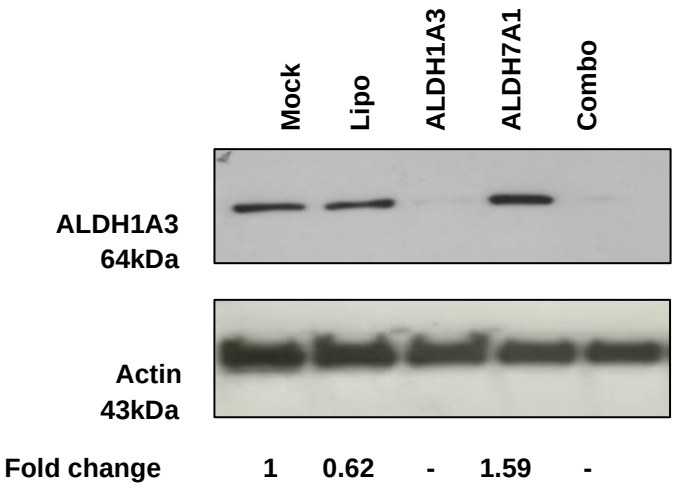


**Figure 43. ALDH1A3 protein expression in H488/14 RM cancer cells after transfection.** Expression of ALDH1A3 was normalised to Actin and fold change in expression was relative to mock control. Samples included mock (no oligofectamine, no siRNA), lipo (no siRNA), ALDH1A3 siRNA, ALDH7A1 siRNA and Combo (ALDH1A3 and ALDH7A1 siRNA).

No apparent knockdown of ALDH7A1 was observed in H488/14 RM cancer cells at the protein level for siRNA-ALDH7A1. A 30% knockdown of ALDH7A1 was achieved with the siRNA- ALDH1A3 and ALDH7A1 combo. Interestingly, there was a 4.73-fold increase in the protein expression of ALDH7A1 with siRNA-ALDH1A3 as shown in Figure 44. However, at the mRNA level, the knockdown of ALDH1A3 did not increase ALDH7A1 expression in H507/14 LM and H507/14 RB cancer cells.

As mentioned previously, all subsequent functional assay included the ALDH1A3 and ALDH7A1 combo to ensure efficient silencing of both genes.

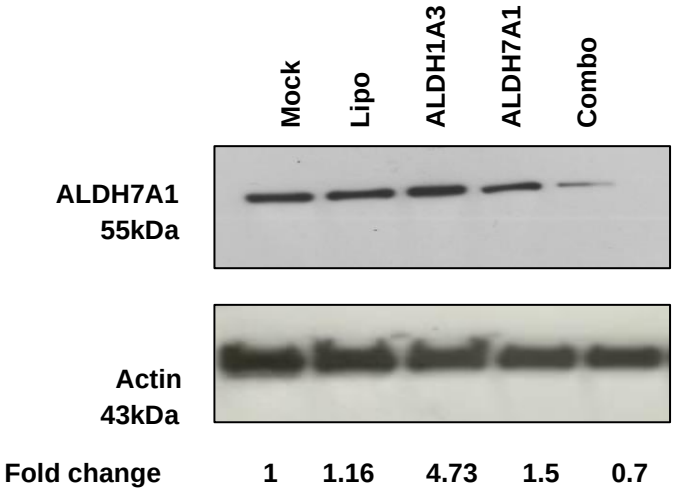


**Figure 44. ALDH7A1 protein expression in H488/14 RM cancer cells after transfection.** Expression of ALDH7A1 was normalised to Actin and fold change in expression was relative to mock control. Samples included mock (no oligofectamine, no siRNA), lipo (no siRNA), ALDH1A3 siRNA, ALDH7A1 siRNA and Combo (ALDH1A3 and ALDH7A1 siRNA).

## 4.9 Effect of silencing the expression of ALDHs on cell proliferation in primary prostate epithelial cultures

Observation of cells showed a small reduction in cell number upon transfection of ALDH1A3 and ALDH7A1 siRNAs. Accordingly, the role ALDH1A3, ALDH1B1, ALDH2 and ALDH7A1 play in cell proliferation was explored in benign and cancer patient samples using trypan blue exclusion assay upon knocking down their expression by siRNA.

Figure 45 (A-C) showed there was a reduction in cell number after transfection of ALDH1A3, ALDH7A1 and a combination of both in BPH samples in comparison to mock and liposomal control post transfection. Figure 45 (D-H) showed the same trend of reduction in cell numbers post transfection of ALDH1A3, ALDH7A1, and their combination. ALDH1B1 and ALDH2 transfection also showed reduction in cell viability in some samples.

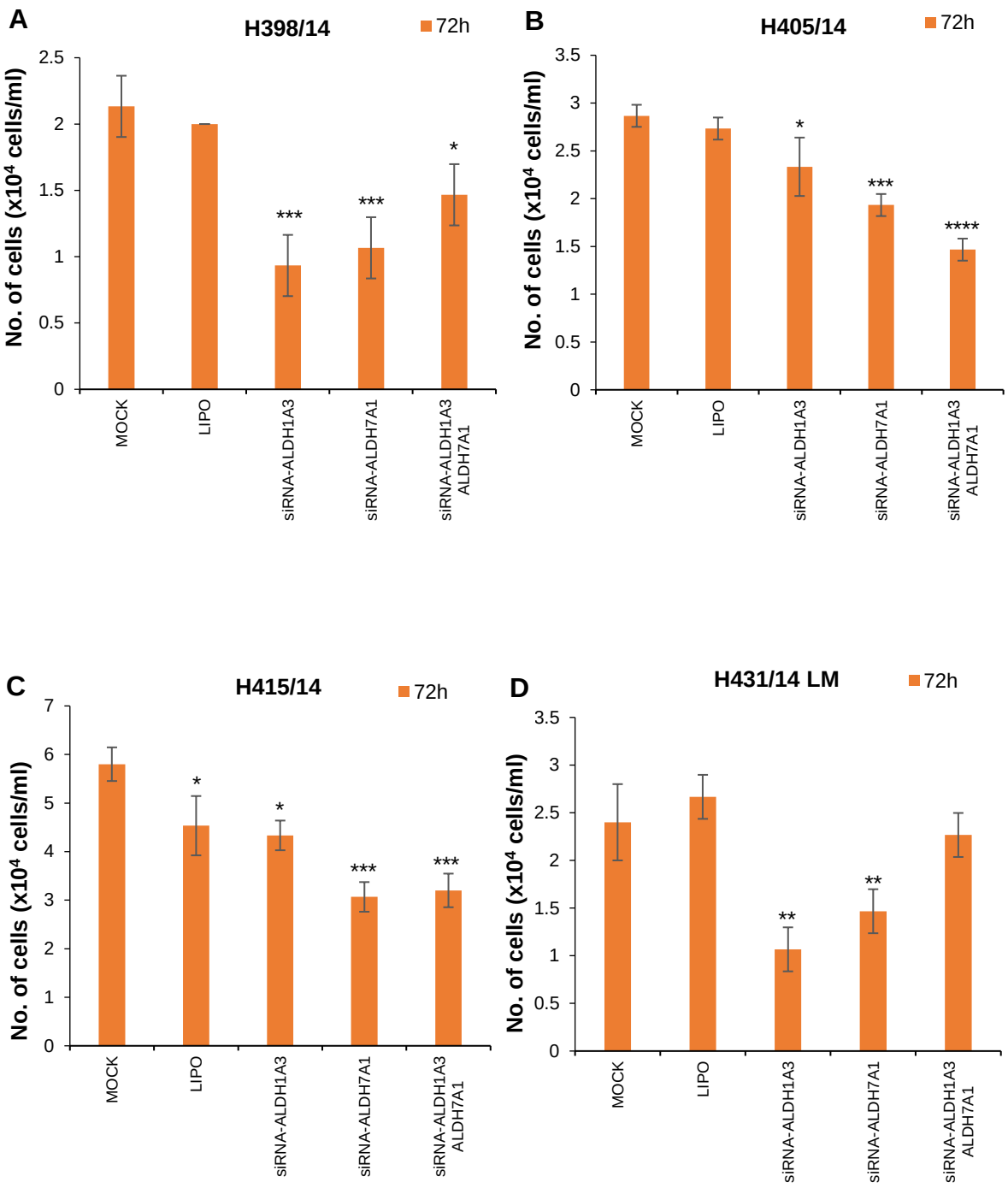
A
H398/14
72h
No. of cells (x10⁴ cells/ml)
2.5
2
1.5
1
0.5
0
***
***
*
MOCK
LIPO
siRNA-ALDH1A3
siRNA-ALDH7A1
siRNA-ALDH1A3 ALDH7A1
B
H405/14
72h
No. of cells (x10⁴ cells/ml)
3.5
3
2.5
2
1.5
1
0.5
0
*
***
****
MOCK
LIPO
siRNA-ALDH1A3
siRNA-ALDH7A1
siRNA-ALDH1A3 ALDH7A1
C
H415/14
72h
No. of cells (x10⁴ cells/ml)
7
6
5
4
3
2
1
0
*
*
***
***
MOCK
LIPO
siRNA-ALDH1A3
siRNA-ALDH7A1
siRNA-ALDH1A3 ALDH7A1
D
H431/14 LM
72h
No. of cells (x10⁴ cells/ml)
3.5
3
2.5
2
1.5
1
0.5
0
**
**
MOCK
LIPO
siRNA-ALDH1A3
siRNA-ALDH7A1
siRNA-ALDH1A3 ALDH7A1

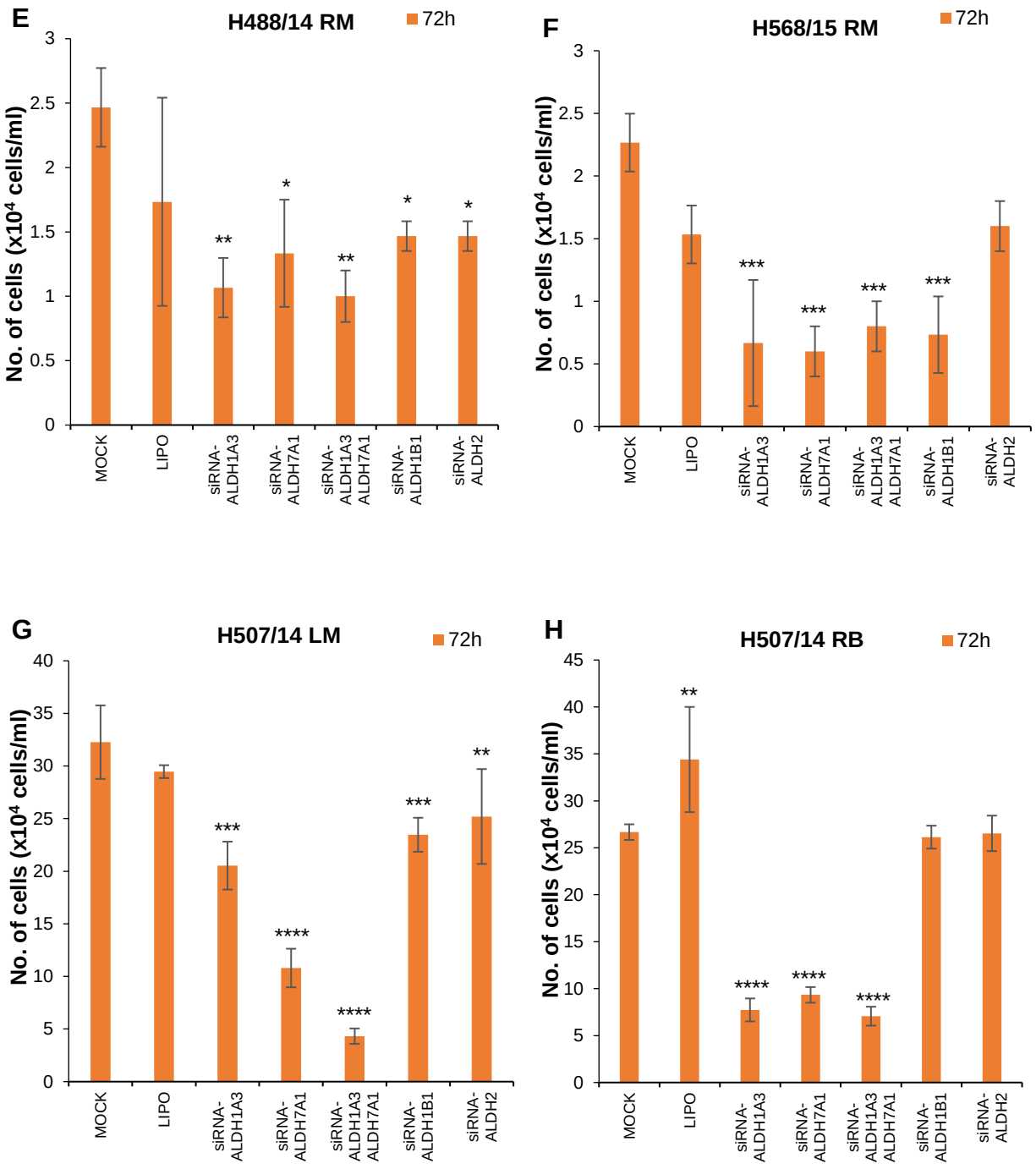


**Figure 45. Determination of cell proliferation using trypan blue exclusion assay.**
Cell proliferation was analysed in primary cells post siRNA transfection of ALDH1A3, ALDH7A1, ALDH1A3+ALDH7A1, ALDH1B1 and ALDH2 using the trypan blue exclusion assay. Cells stained blue were not counted. Values represent mean and standard deviation of 3 independent experiments. Cells were seeded at a density of 3 x $10^4$ cells/ml at t=0 and counted 48 hours post transfection and 72h post initial seeding. Statistical significance was applied using one-way ANOVA to compare the means of Mock with multiple other treatment groups. * p = 0.01 to 0.05, ** p = 0.001 to 0.01, *** p = 0.0001 to 0.001, **** p < 0.0001). *Note difference in scale.

## 4.10 Analysis of the cell cycle profile of primary prostate epithelial cells upon silencing ALDH expression

Deregulated proliferation occurs due to accumulation of mutations that result in constitutive mitogenic signalling. Cell cycle defects include unscheduled proliferation, genomic instability and chromosomal instability which are mediated by misregulation of CDKs. The activity of CDK requires binding of regulatory subunits known as cyclins, which are synthesised and destroyed at specific times during the cell cycle, thereby regulating kinase activity. Cancer cell mutations often deregulate certain CDK-cyclin complexes, leading to either continued proliferation or unscheduled re-entry into the cell cycle [516].

Progression through the cell cycle is monitored by checkpoints in which possible defects during DNA synthesis and chromosome segregation can be detected upon which these checkpoints are activated to induce cell cycle arrest by modulating CDK activity. Cell cycle arrest allows repairs of defects to prevent their transmission to the resulting daughter cells. If repair is ineffective, cells may enter senescence or undergo apoptosis. However, accumulation of DNA alterations could cause genomic instability resulting in cell transformation and oncogenesis [516].

This study investigated whether silencing of the ALDHs induced cell cycle arrest. The DNA content of the samples was measured by PI dye which binds proportionally to the amount of DNA present in the cell. The intensity of fluorescence is a measure of DNA content present in the different cell cycle phases. So the more the DNA content (such as S phase will have more DNA than cells in G1 phase), the higher the fluorescence intensity. This allows

determination of cells in either the G0/G1, S and G2/M phase of the cell cycle.

Flow cytometry analysis was carried out to investigate if ALDH1A3, ALDH1B1, ALDH2 and ALDH7A1 knockdown had an effect on the cell cycle. H507/14 LM, H507/14 RB, H488/14 RM and H568/15 RM cancer cells were used to investigate cell cycle distribution. In all samples, cells mainly resided in the G0/G1 phase (50-60%), with 10-15% in the S phase and 15-30% in the G2/M phase and no apparent differences were seen following ALDH knockdown. H507/14 LM cells showed a slight increase in G1 phase with ALDH2, ALDH7A1 and combination (ALDH1A3 and ALDH7A1) knockdowns. A reduction in G2 phase occurred with ALDH7A1 and combination knockdown (Figure 46 A). H507/14 RB cells showed slight increase in G1 with most single treatments and a reduction in G2 with ALDH7A1 and combination knockdowns (Figure 46 B). The H488/14 RM cultures showed a slight increase in the percentage of cells in the G1 phase with combination knockdown, a small increase in S phase after ALDH1B1, ALDH2 and combination knockdown, and a slight reduction in G2 phase by ALDH1B1, ALDH2, ALDH7A1 and combination knockdown (Figure 46 C). Small differences in cell cycle profile were seen in H568/15 RM culture post knockdown of ALDH1A3, ALDH1B1, ALDH2 and ALDH7A1 as compared to mock control (Figure 46 D). Taken together, cell cycle analysis indicated that ALDH1A3, ALDH1B1, ALDH2 and ALDH7A1 only exert minimal effect on the cell cycle with no obvious cell cycle arrest by these ALDH isoforms. Although some changes appeared significant, the changes were very small (less than 9% in every case with the exception of combination treatment in H488/14 RM cells which was 16%) and were not

consistent throughout all the four samples, therefore overall a change in cell cycle is not a key change following the siRNA treatment.

Therefore, the reduction in cell viability post transfection of ALDH1A3 and ALDH7A1 reported in this chapter is potentially due to a mechanism other than cell cycle arrest. It may be speculated that other mechanisms such as apoptosis, autophagy or necrosis are potentially involved in the observed reduction of cell number upon ALDH silencing. Future studies could evaluate caspase activity and DNA fragmentation for apoptosis [517], microtubule-associated protein 1 light chain 3 beta (LC3B) and p62 expression for autophagy [518] and determine plasma membrane breakdown by measuring LDH release for necrosis [519].

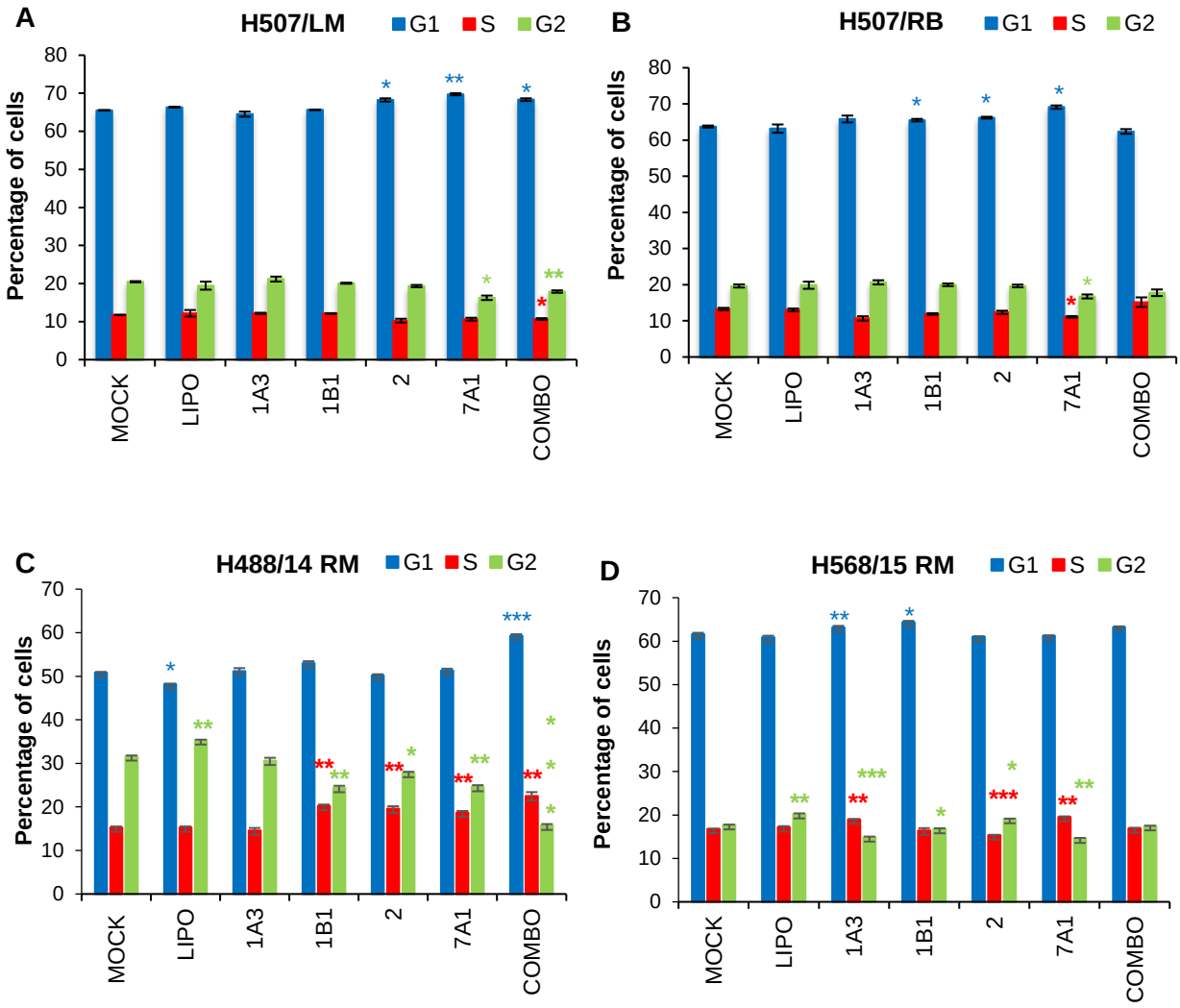
A
H507/LM
G1
S
G2
Percentage of cells
MOCK
LIPO
1A3
1B1
2
7A1
COMBO
B
H507/RB
C
H488/14 RM
D
H568/15 RM

**E**

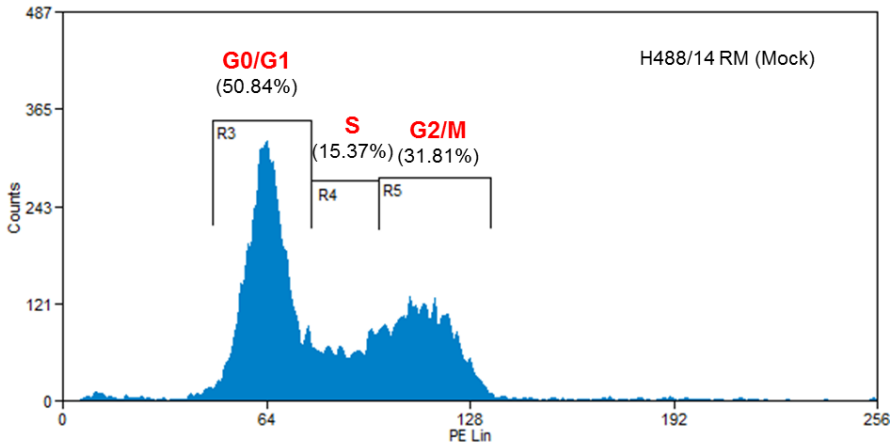


**Figure 46. Flow cytometry cell cycle analysis of primary prostate epithelial cells following siRNA transfection of ALDH1A3, ALDH1B1, ALDH2 and ALDH7A1.**
H507/14 LM (A), H507/14 RB (B), H488/14 RM (C), and H568/15 RM (D) cancer cells 48 hours post transfection. (E) Representative cell cycle profile (H488/14 RM-mock). Mock is cells only, Lipo is oligofectamine with cells only, 1A3, 1B1, 2, 7A1 are siRNA against these ALDH isoforms and COMBO is ALDH1A3 and ALDH7A1 siRNA. All measurements were taken in triplicate and graphs represent the average values. Standard deviations showed consistency between the triplicate samples. Four biological replicates were analysed (n=4). Statistical significance was applied using the one-way ANOVA for paired samples, comparing mock with siRNA treated samples for G1 (blue asterisks), S (red asterisks) and G2 (green asterisks) phase for 4 samples.

## 4.11 Regulation of cell motility in primary prostate epithelial cultures by ALDHs

Knockdown of ALDH1A3 has shown reduced cell migration in HuCCT1 cholangiocarcinoma cells (bile duct cancer) [520]. It has also been demonstrated that ALDH7A1 is involved in promoting cell migration in prostate cancer cell line PC3 cells with stable ALDH knockdown by lentiviral shRNA [490]. However, this has not yet been investigated in primary prostate cells. The present study therefore studied the migratory phenotype of primary prostate cancer cells after ALDH knockdown using the wound healing assay which mimics cell migration [521].

There was a complete closure of the wound 24 hours after initial scratching of H507/14 LM (Figure 47 A) and H507/14 RB (Figure 47 B) cancer cells that were transfected with siRNAs against ALDH1A3, ALDH7A1, combination, ALDH2 and ALDH1B1. Consequently, H488/14 RM and H568/15 RM transfected cancer cells were then assessed at various time points of 3 hours, 6 hours and 24 hours post initial scratching to assess the migratory rate of the cells.

The H488/14 RM cells transfected with siRNAs against ALDH1A3, ALDH7A1 and combo showed reduction in cell migration rate at 3 hours relative to mock control but this was not statistically significant. At the 6-hour time point, the same pattern was observed with a significant reduction of migratory rate in ALDH7A1 treatment. At the 24-hour time point, there was a significant reduction in cell migration with ALDH1A3, ALDH7A1, ALDH1B1 and ALDH2 treatments (Figure 47 C).

The H568/15 RM cells showed reduction in cell migration at the 3-hour time point with ALDH1A3 treatment. At the 6-hour time point, although there was reduction observed in ALDH1A3 knockdown, only Lipo control showed statistically significant increase in migration rate. At the 24-hour time point, ALDH1A3, Combo and ALDH2 knockdown showed significant reduction in cell migration rate (Figure 47 D).

Therefore, ALDH1A3, ALDH7A1, ALDH1B1 and ALDH2 may be involved in promoting cell migration in primary prostate epithelial cultures to various extents.

H507/14 cells showed a complete closure of the scratch after 24 hours in all the conditions. A control which includes low cell seeding density could have been included to test the change in migratory rate between different cell seeding densities, hence selecting an optimal density for the experiment. Furthermore, controls that included serum/no serum, supplements/no supplements would have allowed to test the change in migratory rate between cells with different nutritional conditions. A higher migration rate in the presence of serum may be indicative of cell proliferation.

Cell migration can also be measured by other methods such as using the Boyden Chamber Assay in which cells are seeded in an insert in serum-free media and placed in the well of a cell culture plate containing media with chemoattractant. Cells migrate through a porous membrane and are counted to determine number of migratory cells. Another similar method uses Fluorobloks which are cell culture inserts that allow measuring of the

fluorescently labelled migratory cells in a plate reader format or by a microscope.

A

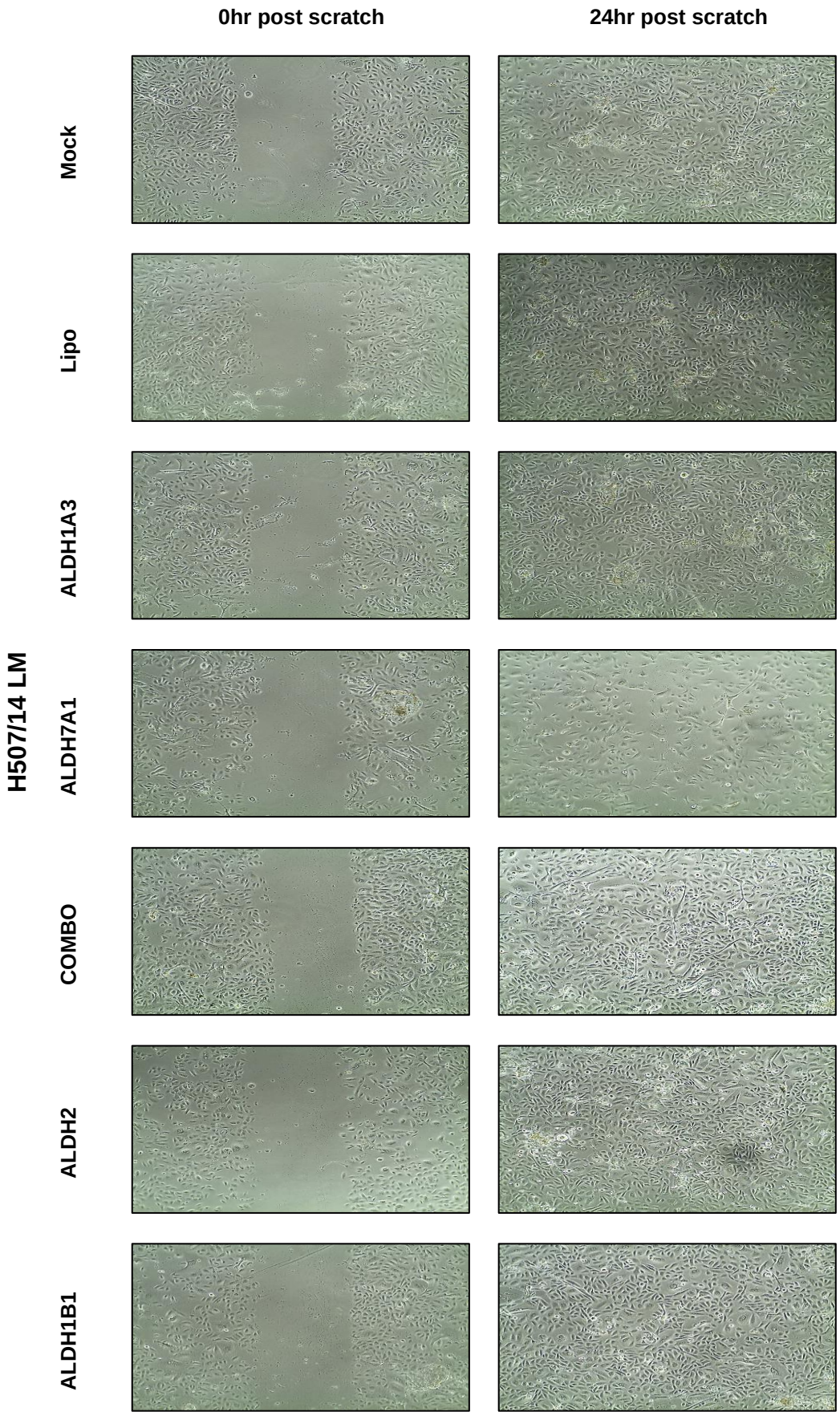
0hr post scratch
24hr post scratch
H507/14 LM
Mock
Lipo
ALDH1A3
ALDH7A1
COMBO
ALDH2
ALDH1B1

**B**

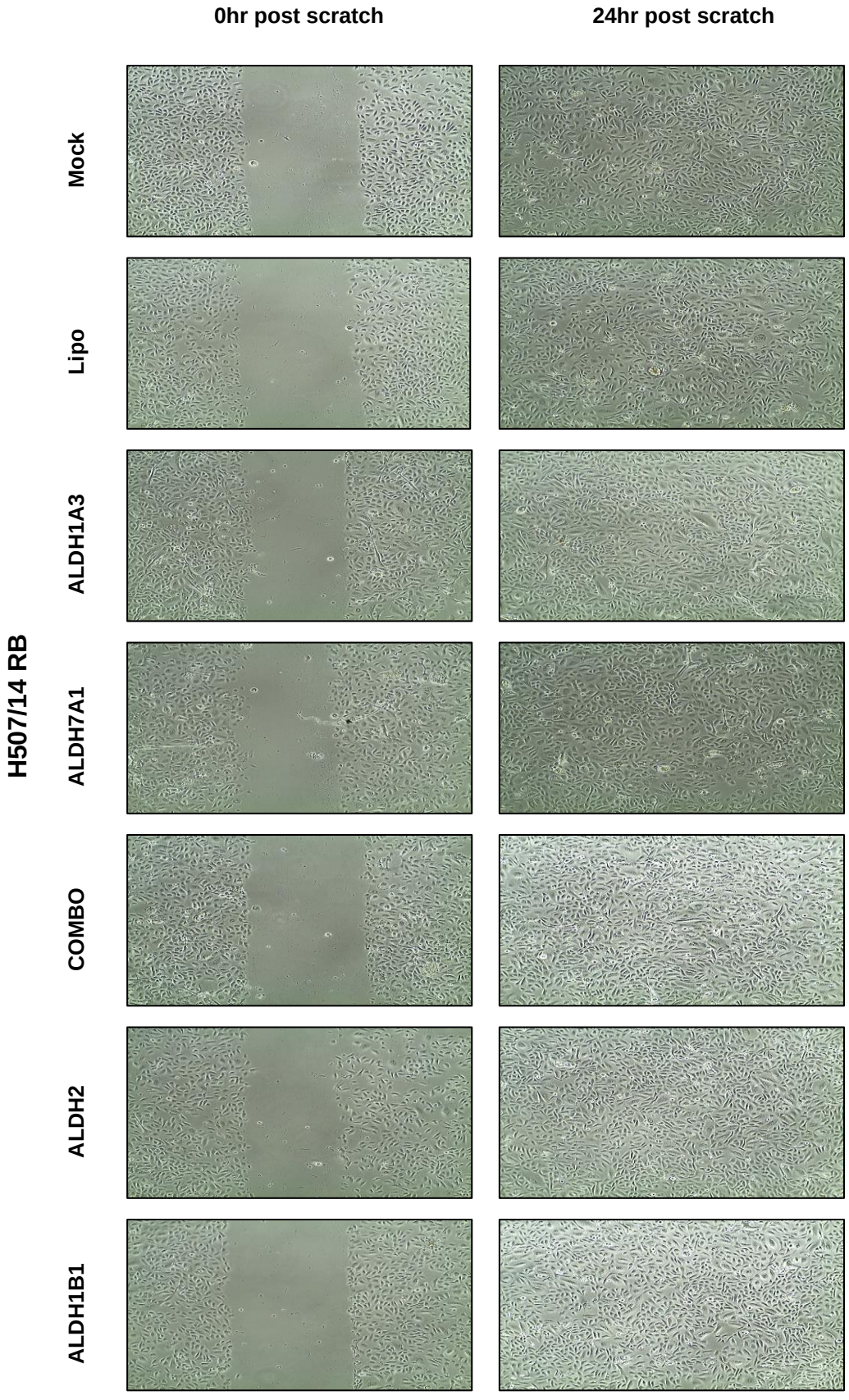
0hr post scratch
24hr post scratch
H507/14 RB
Mock
Lipo
ALDH1A3
ALDH7A1
COMBO
ALDH2
ALDH1B1

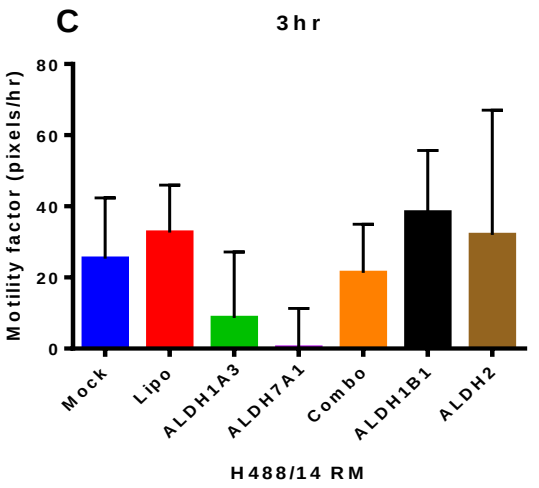
C
3hr
Motility factor (pixels/hr)
80
60
40
20
0
Mock
Lipo
ALDH1A3
ALDH7A1
Combo
ALDH1B1
ALDH2
H488/14 RM

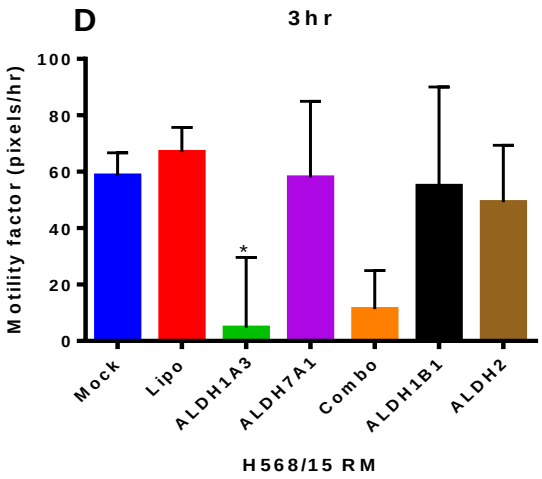
D
3hr
Motility factor (pixels/hr)
100
80
60
40
20
0
*
Mock
Lipo
ALDH1A3
ALDH7A1
Combo
ALDH1B1
ALDH2
H568/15 RM

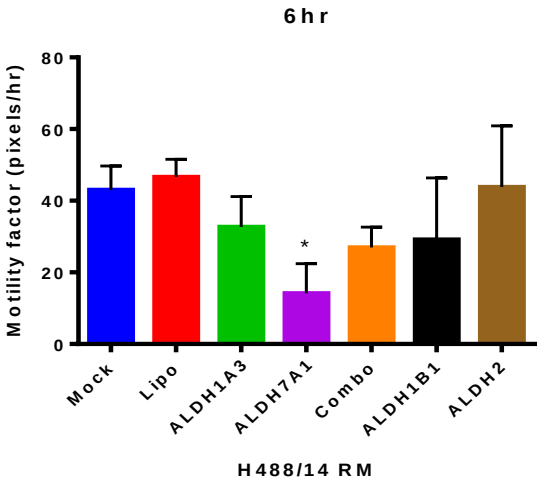
6hr
Motility factor (pixels/hr)
80
60
40
20
0
*
Mock
Lipo
ALDH1A3
ALDH7A1
Combo
ALDH1B1
ALDH2
H488/14 RM

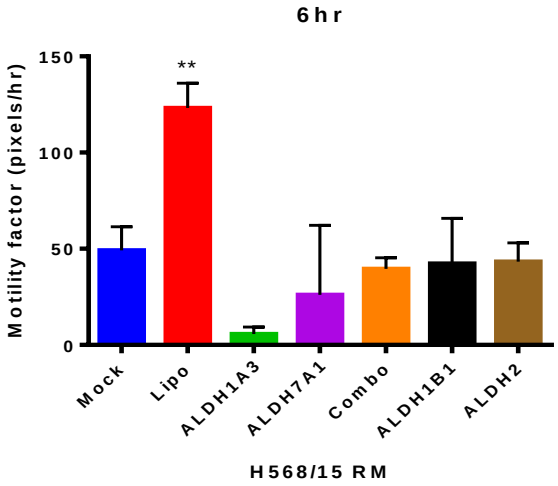
6hr
Motility factor (pixels/hr)
150
100
50
0
**
Mock
Lipo
ALDH1A3
ALDH7A1
Combo
ALDH1B1
ALDH2
H568/15 RM

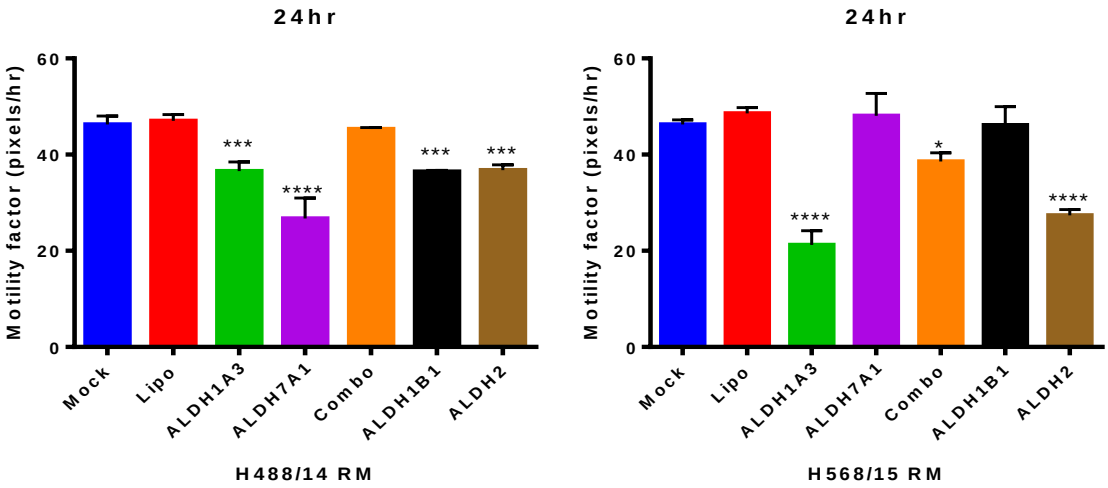


**Figure 47. Wound healing assay after modulation of ALDH expression in primary prostate epithelial cells.**

Representative images of wound healing in (A) H507/14 LM cells (B) H507/14 RB cells (C) H488/14 RM cell and (D) H568/15 RM cells. Migration rate of cells post knockdown of ALDH1A3, ALDH7A1, Combo (ALDH1A3 and ALDH7A1), ALDH1B1 and ALDH2 in (C) H488/14 RM cells (left panel) and (D) H568/15 RM cells (right panel). Values represent mean and SD of 3 repeats. Statistical significance was measured by one-way ANOVA for multiple comparisons of paired groups, mock compared to treated groups. $p<0.05$*, $p<0.01$**, $p<0.001$*** and $p<0.0001$****. *Note difference in scale.

## 4.12 Effect of ALDH silencing on the colony forming ability of primary prostate epithelial cultures

ALDH1A3 is highly upregulated in NSCLC with clonogenic and tumorigenic properties [522]. ALDH$^{high}$ cells have also shown clonogenic and metastatic capacity *in vitro* using prostate cancer cell lines LNCaP and PC3 [523]. The involvement of ALDH in clonogenicity has not yet been explored down to its specific isoforms except for ALDH7A1 which has shown reduced colony forming ability of cells upon ALDH7A1 knockdown in prostate cancer cell lines [490]. Accordingly, this study also explored whether ALDH1A3 and ALDH7A1 play a role in colony formation of primary prostate epithelial cells and whether the observed reduction in cell number following knockdown of these isoforms was correlated with colony formation.

The colony formation assay was employed followed by the knockdown of ALDH1A3, ALDH7A1 or a combination of both. siRNA ALDH1A3, ALDH7A1 and a combination knockdown resulted in a reduction in the percentage of colonies formed relative to mock control in both the BPH samples (Figure 48 A and C) and cancer samples (Figure 48 B and D). Interestingly the effect was more pronounced in BPH samples than cancer samples and patient variability was observed. A significant colony reduction was observed after ALDH1A3, ALDH7A1, and combination knockdown in BPH cells (Figure 48 C). Knockdown of the ALDH isoforms in cancer cells did not show a significant reduction in colonies, however the trend was the same as in BPH (Figure 48 D). Taken together, the results suggest that both ALDH1A3 and ALDH7A1 expression affects colony formation with ALDH7A1 silencing decreasing the colony forming ability to a greater extent than ALDH1A3 silencing.

**A**

**BPH**

**H415/15**

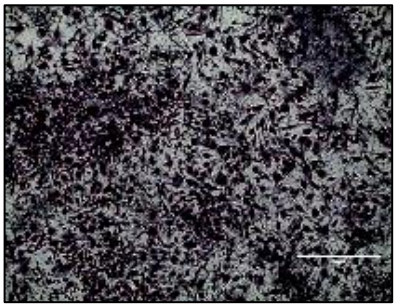

**Mock**

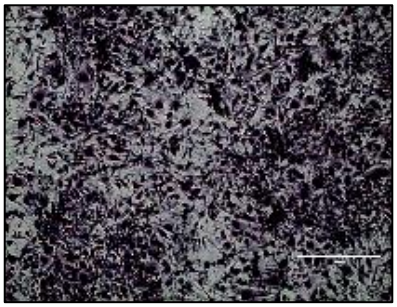

**Lipo**

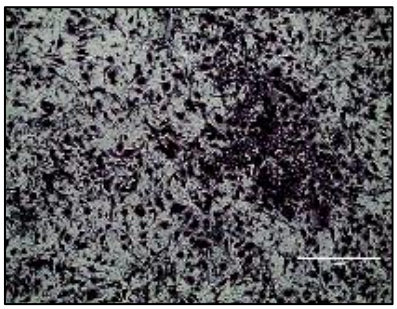

**siRNA-ALDH1A3**

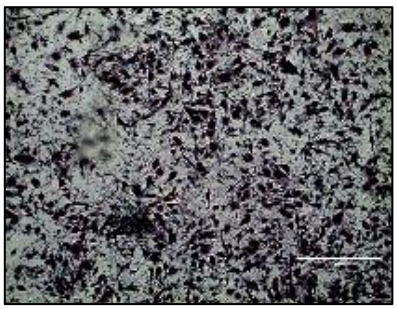

**siRNA-ALDH7A1**

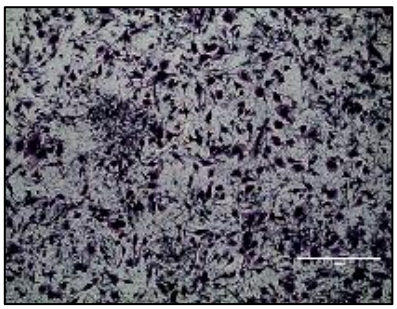

**siRNA-ALDH1A3 +ALDH7A1**

**B**

**Cancer**

**H568/15 RM**

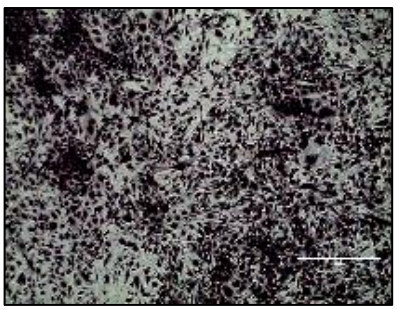

**Mock**

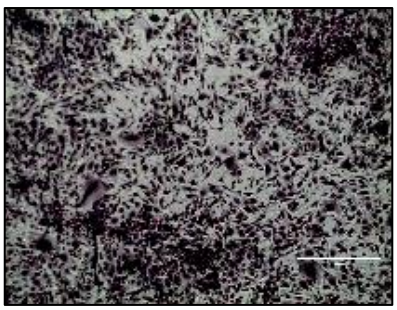

**Lipo**

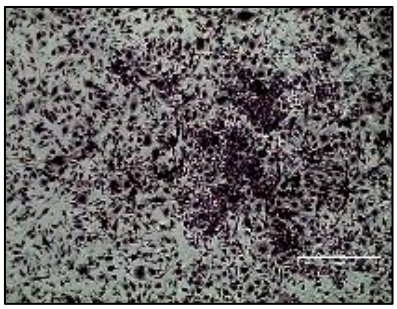

**siRNA-ALDH1A3**

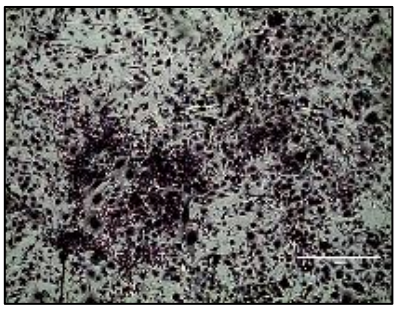

**siRNA-ALDH7A1**

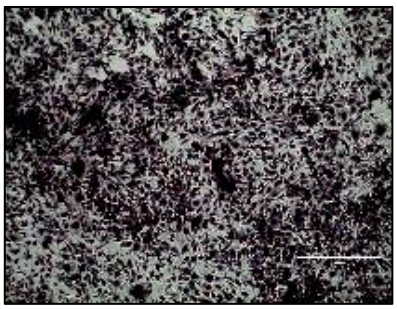

**siRNA-ALDH1A3 +ALDH7A1**

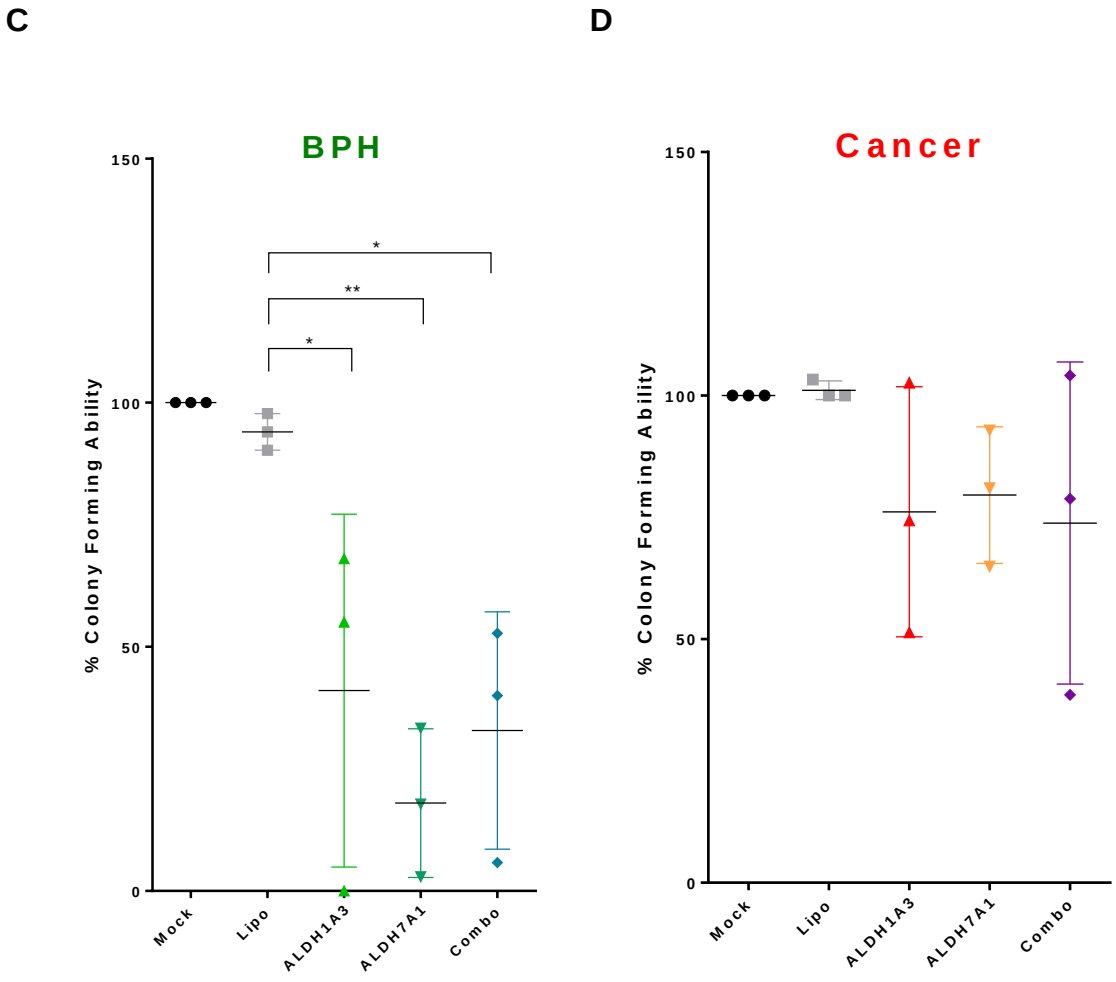


**Figure 48. Colony forming ability of primary cultures following siRNA knockdown of ALDH1A3 and ALDH7A1.**

Crystal violet staining images of (A) BPH cultures, (B) cancer cultures. % colony forming ability of (C) BPH cultures and (D) cancer cultures relative to mock control. Experiment was carried out in triplicate and values presented are the mean of 3 technical repeats. BPH n=3, cancer n=3. Statistical significance analysis performed using a one-way ANOVA test for multiple comparisons and samples compared to liposomal control, *P<0.05, **P<0.01 and ***P<0.001. Liposomal control (Lipo) was about 10% above or below the 100% mark due to cell plating error as hemocytometer estimates the cell count, therefore giving room for error. Cells were treated with siRNA for 48 hours before being seeded at 500 cells/well for colony formation, along with 200,000 – 250, 000 feeder STO cells.

## 4.13 Analysis of ALDH knockdown on primary prostate epithelial cell differentiation

Patients with acute promyelocytic leukemia undergoing RA treatment have shown improved clinical outcomes with hematopoietic stem/progenitor cell differentiation [524]. However, there are mixed clinical trial results when RA was used to treat other cancer types in an attempt to induce cancer cell differentiation [525]. In prostate cancer, the biological implication individual ALDH isoforms have on cancer cell differentiation has not yet been elucidated. As a consequent, the cell differentiation status upon knocking down ALDH1A3 and ALDH7A1 was explored to investigate if it correlates and therefore plays a role in mediating colony formation observed upon the silencing of these ALDH isoforms.

The cell surface marker CD49b expression was used as a marker for TA cells to investigate whether ALDH1A3 and ALDH7A1 play a role in cell differentiation process. A reduction of CD49b expression is indicative of cell differentiation from transit amplifying cells to committed basal cells therefore towards differentiation. CD49b antibody was used to measure $\alpha_2$integrin. TA cells are $\alpha_2\beta_1$integrin$^{high}$ cells whereas CB cells are $\alpha_2\beta_1$integrin$^{low}$ cells. CD49b is the $\alpha_2$integrin part of $\alpha_2\beta_1$integrin.

ALDH1A3 knockdown after 48 hours showed up to 28% decrease in TA cells and 11% increase in CB cells when compared to mock control in H415/15 cells (Figure 49 A). ALDH7A1 knockdown showed up to 38% decrease in TA cells and 27% increase in CB cells in H431/14 LM cells (Figure 49 F). In addition, there was a 38% reduction in TA cells and 18% increase in CB cells in the H431 sample (Figure 49 F). All other samples showed the same pattern

of differentiation of cells but to a lesser extent (Figure 49 B, C, D, E). Figure 49 G shows the CD49b FITC median expression of BPH and cancer samples. In all the samples studied there was a reduction in CD49b expression indicating cell differentiation. ALDH7A1 knockdown showed a higher level of cell differentiation in most cases. However, the trend was found to be more striking in BPH.

6 biological samples were investigated (BPH n=2, cancer n=4). If available it would have been better to include at least one more BPH sample so that patient variability could have been accounted for with a higher number of samples, and also to make more precise comparisons with cancer samples. However, since the trend was the same regardless of disease state, all six samples could be plotted together with statistics indicating a significant change in cell differentiation.

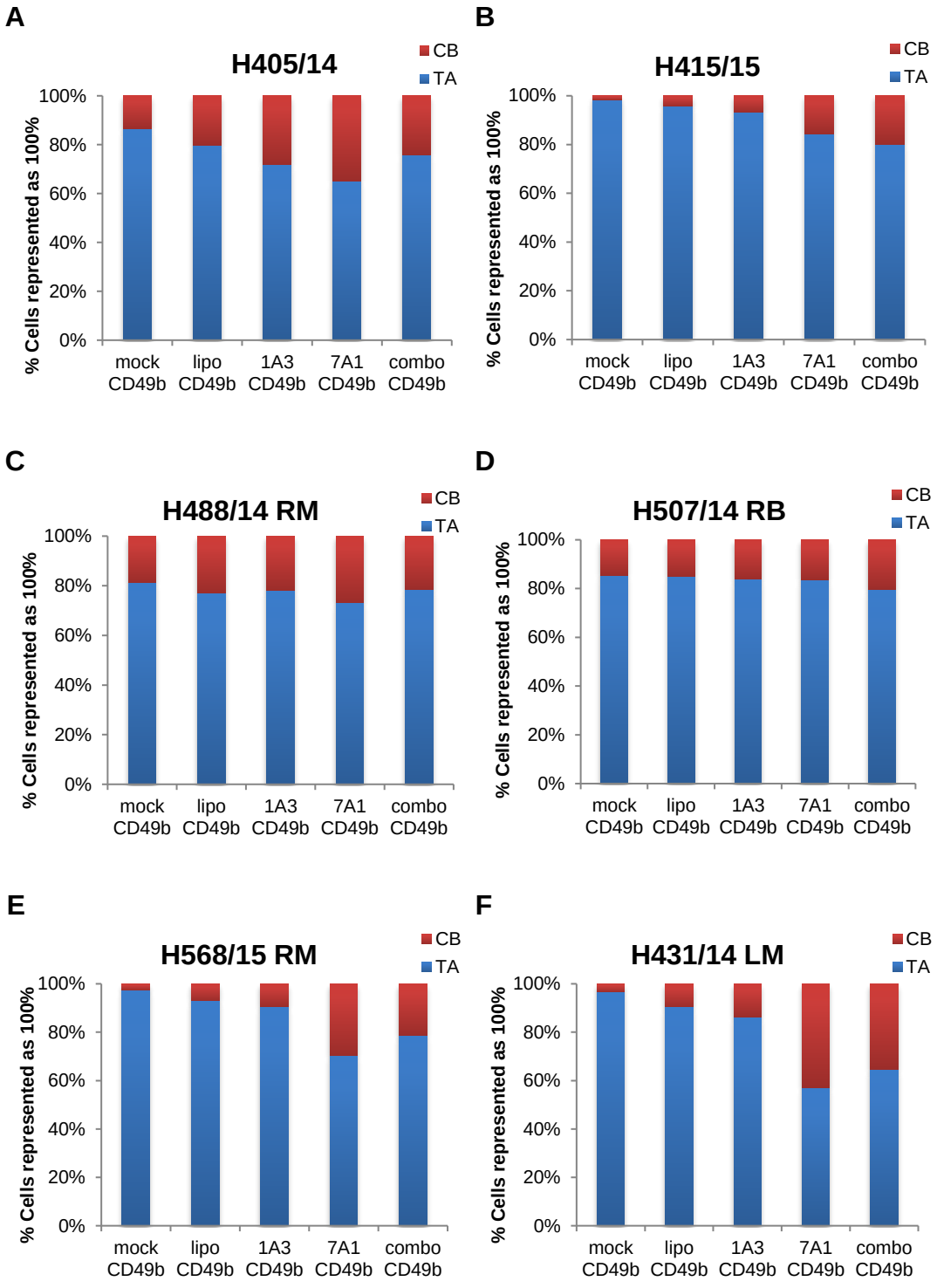
A
H405/14
CB
TA
% Cells represented as 100%
100%
80%
60%
40%
20%
0%
mock CD49b
lipo CD49b
1A3 CD49b
7A1 CD49b
combo CD49b
B
H415/15
C
H488/14 RM
D
H507/14 RB
E
H568/15 RM
F
H431/14 LM

**G**

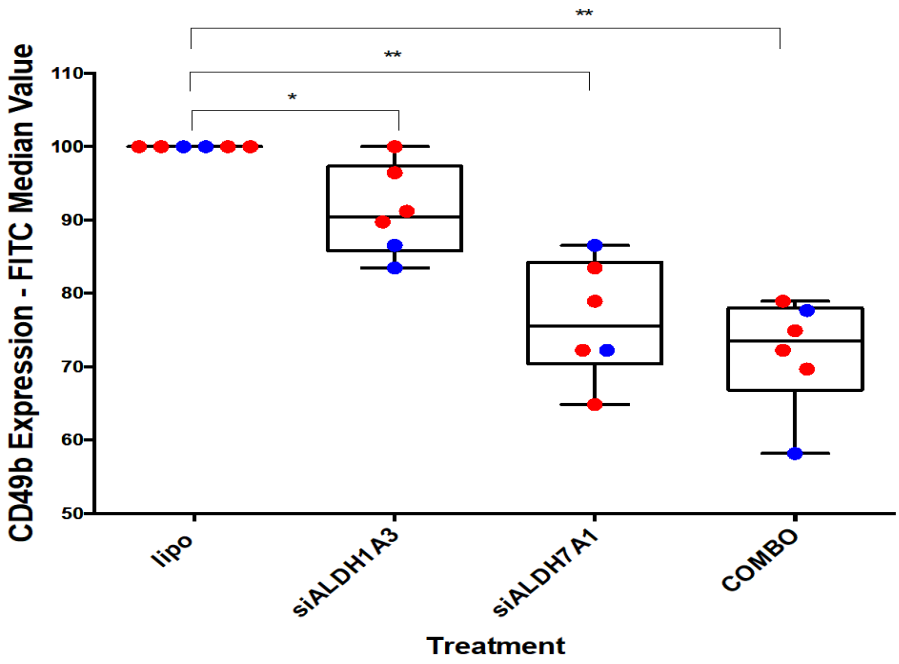


**Figure 49. FACS analysis of CD49b differentiation marker expression in primary BPH and cancer cells post transfection of ALDH1A3, ALDH7A1 and a combination of both.** Percentage of transit amplifying (TA) and committed basal (CB) cells in (A, B) BPH cells and (C-F) cancer cells. (G) FITC median relative to liposomal control measured at excitation 495nm / emission 519nm. Statistical significance was measured using the Mann Whitney U test (n=6) for unpaired groups and non-parametric distribution. Blue dots are BPH samples and red dots are cancer samples.

## 4.14 Evaluation of ALDH hit compounds on cell viability of primary prostate epithelial cultures

ALDHs play a protective role in cancer cells by inactivating cancer drugs by various mechanisms and are therefore also involved in cancer cell survival [357]. It has been found that ALDHs are co-expressed with antioxidant factors and drug efflux channels in cells with high ALDH activity [373]. Alkylating agents including CP and other oxazaphosphorines are enzymatically inactivated by ALDH1A1 and ALDH3A1 [462]. ALDHs also confer resistance to doxorubicin, cisplatin, temozolemide and taxanes [357].

Current treatments for CRPC include chemotherapeutic drugs including docetaxel, paclitaxel and vinblastine which work by microtubule stabilisation of dividing cells. However, a substantial number of patients soon develop resistance to these drugs by various resistance mechanisms such as the existence of subpopulations of cancer cells with cellular mechanisms of resistance, inefficient drug delivery to cancer cells and resistance linked to cancer cells and the microenvironment [526]. Therefore, there is a need to develop new therapies which are more selective for CSCs to target the tumour-initiating population of cancer cells. Accordingly, this chapter also focused on testing novel hit ALDH compounds on cell survival as a single treatment and as a combination treatment with docetaxel.

Pan ALDH inhibitor DEAB and three analogues of DEAB; ALII-9, ALII-14 and ALII-18 were tested against 5 patient samples (4 cancers and 1 BPH) to investigate if they had an effect on cell viability. Patient samples assessed included BPH sample H415/15, and cancer samples H568/15 RM, H431/14 LM, H488/14 RM, and H517/15 RM. All 4 compounds showed reduction in

percentage cell viability of primary prostate epithelial cultures at high concentration of 200μM (Figure 50 A-D). Interestingly, ALII-14 and ALII-18 showed a synergistic reduction as part of a combination treatment with docetaxel (Figure 50 C and D). As initial testing, a concentration of 50 and 200μM of the ALDH inhibitors was selected as these compounds had not been tested before, and are not cytotoxic agents. Therefore, a lower and a higher concentration was selected. Future studies would incorporate a larger range of concentrations. The 1nM concentration of docetaxel was selected based on its optimization previously done in Prof. Norman Maitland's group.

Taken together, such inhibitors could be further designed to push cells towards differentiation allowing current treatments such as docetaxel to work better when used in combination with specific ALDH inhibitors.

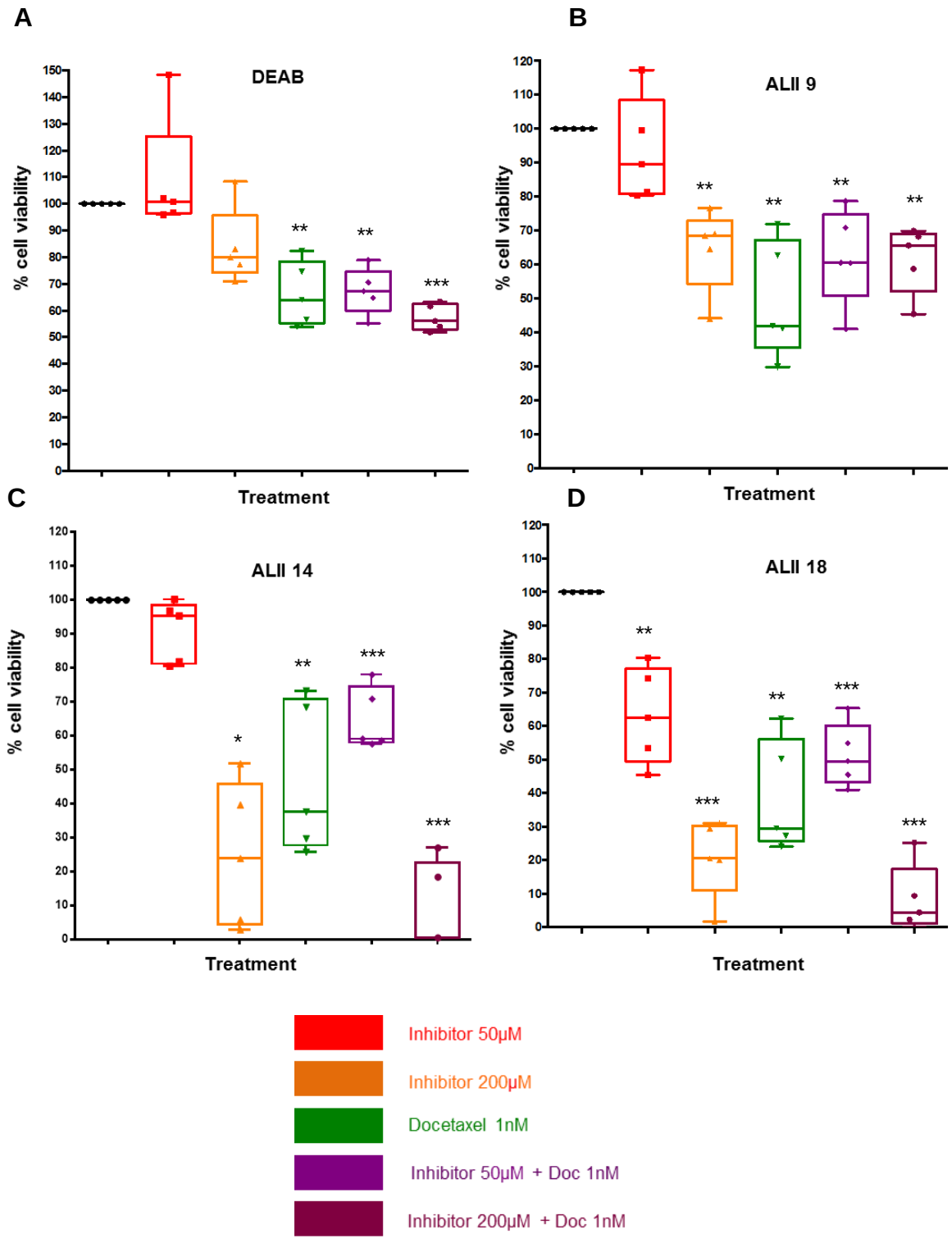


**Figure 50. Cell viability of primary cells following treatment with pan ALDH inhibitors as a single or combination treatment with docetaxel.**
Treatment with DEAB (A), treatment with ALII-9 (B), treatment with ALII-14 (C) and treatment with ALII18 (D). 5 patient samples were analysed per condition, BPH (n=1) and cancer (n=4). Experiment was carried out in triplicate and values represented as the mean. Statistical significance was calculated using a paired two-tailed student's t-test in which the mean of untreated cells was compared with the mean of treated cells, *p<0.05, **p<0.01 and ***p<0.001.

# Chapter 5

## Pharmacological implications of small molecule inhibitors in docetaxel-resistant prostate cancer and lung cancer

## 5.1 Introduction

It is becoming increasingly evident that ALDHs play a pivotal role in carcinogenesis mainly due to their role as a CSC marker, and association with therapy resistance, making them an attractive target for therapeutic intervention. Published studies and the work described in chapter 2 and 3 suggest ALDH1A3 and ALDH7A1 as isoforms that may be exploited as cancer markers and/or for therapeutic intervention.

A library of ALDH-affinic compounds based on the DEAB pharmacophore were designed and developed by Mr. Ali Ibrahim (Dr. Klaus Pors' group, University of Bradford) and used in the present study. These compounds contain structural differences to the pan-ALDH inhibitor DEAB, which were incorporated in an attempt to achieve improved ALDH isoform selectivity.

In addition, HAN00316 (HAN) compound was purchased from Maybridge company based on its high binding affinity to ALDH7A1 and was used in this study to determine its effects on the viability of docetaxel-sensitive and -resistant PC3 cells. HAN was discovered from a virtual screen study using computational modelling of a library of thousands of compounds against the ALDH7A1 crystal structure (unpublished observations; the virtual screen was carried out by Dr Zoe Cournia, Biomedical Research Foundation Academy of Athens).

Only very recently has the first crystal structure of ALDH1A3 been revealed by Moretti et.al's group [527] and is now available for structure-based design of selective inhibitors and substrates. Unfortunately, this was not available during the time of the present study for detailed investigation. ALDH1A3 has emerged

as a key ALDH isoform in prostate cancer progression from this study. Therefore, future work could focus on designing and developing selective ALDH1A3 inhibitors based on the available crystal structure and investigate their potential in targeting ALDH1A3 in prostate cancer.

In an attempt to unravel the ALDH expression in aggressive drug resistant prostate cancer, the androgen independent PC3 cell line pair sensitive and resistant to docetaxel (PC3 Ag and PC3 D8 respectively) was acquired from Dr. Amanda J O'Neill (University College Dublin, Ireland).

To further investigate the potential of a library of ALDH inhibitors generated by Dr. Klaus Pors' group, the NSCLC cell lines H1299/mock and H1299/7A1 were obtained from Prof. Jan Moreb (University of Florida). This parental cell line has low endogenous ALDH expression [484] and was therefore a good model for stable transfection with ALDH7A1 allowing the development of an isogenic cell line pair. Although not a prostate cancer cell line, this was a good initial model for screening ALDH compounds.

The present study included another lung cancer cell line A549 to screen the ALDH compounds that naturally expresses ALDH1A1 and 3A1 [528], hence a useful comparative cell line to the ALDH7A1/mock isogenic cell line pair.

Future work is required to fully show ALDH isoform expression in prostate cancer cell models with higher sample number and further target validation. However, ALDH-affinic compounds were already designed and developed to test against cell lines for other cancers (another project under Dr. Klaus Pors group), and therefore due to their availability this study carried out initial screening in prostate and lung cancer cell lines.

## 5.2 Aims and Objectives

The aim of this chapter was to first investigate the expression of ALDHs in drug-resistant prostate cancer and the effect of ALDH-affinic compounds on cell viability. Specific objectives were:

- Evaluate selected ALDH compounds for activity against H1299/mock, H1299/7A1 and A549 cells at various concentrations

- Evaluate gene expression of selected ALDHs in PC3 Ag and PC3 D8 cells

- Explore the effect of selected ALDH-affinic compounds on the cell viability of PC3 Ag and PC3 D8 cells

## 5.3 Results

## 5.4 Effect of a library of ALDH inhibitors on cell viability in H1299/mock, H1299/7A1 cells and A549 cells

This study used an isogenic cell line pair of H1299 NSCLC cells to assess a library of novel lead ALDH-affinic compounds for their activity. The H1299 cell line was used as it has low endogenous ALDH expression [484] and is an ideal model for stable transfection of ALDH7A1 allowing interrogation of lead ALDH inhibitors against the isogenic cell line pair (H1299/mock and H1299/7A1). Furthermore, the NSCLC cell line A549 was used as a comparative model. The preliminary screen using the MTT assay and two dose points in all three cell lines (50 and 200μM) revealed several compounds of the 39 compounds evaluated as potential agonists and antagonists.

Preliminary data from this study displayed several compounds including ALII-9, -14 and -18 as agonists and antagonists against the isogenic pair of H1299 NSCLC cells (Figure 51 A and B). These 3 inhibitors were tested in this chapter first, and were later selected for evaluation in primary prostate epithelial cells as described in experimental chapter 4. Further exploitation of these compounds may identify small molecules with potential to selectively target certain ALDH isoforms in NSCLC at the first instance, however they may also potentially be active against prostate cancer.

In A549 cells, compounds ALII-7, ALII-37 and ALII-38 resulted in decreased % cell survival when used at a concentration of 200μM compared to other compounds screened. In contrast to the isogenic H1299 cell line pair, compounds Ali 9, Ali 14 and Ali 18 did not show any activity against A549 cells

at both concentrations. Furthermore, compounds such as ALII-8, ALII-17, ALII-34 and ALII-35 showed no activity against the cells (Figure 51 C).

A

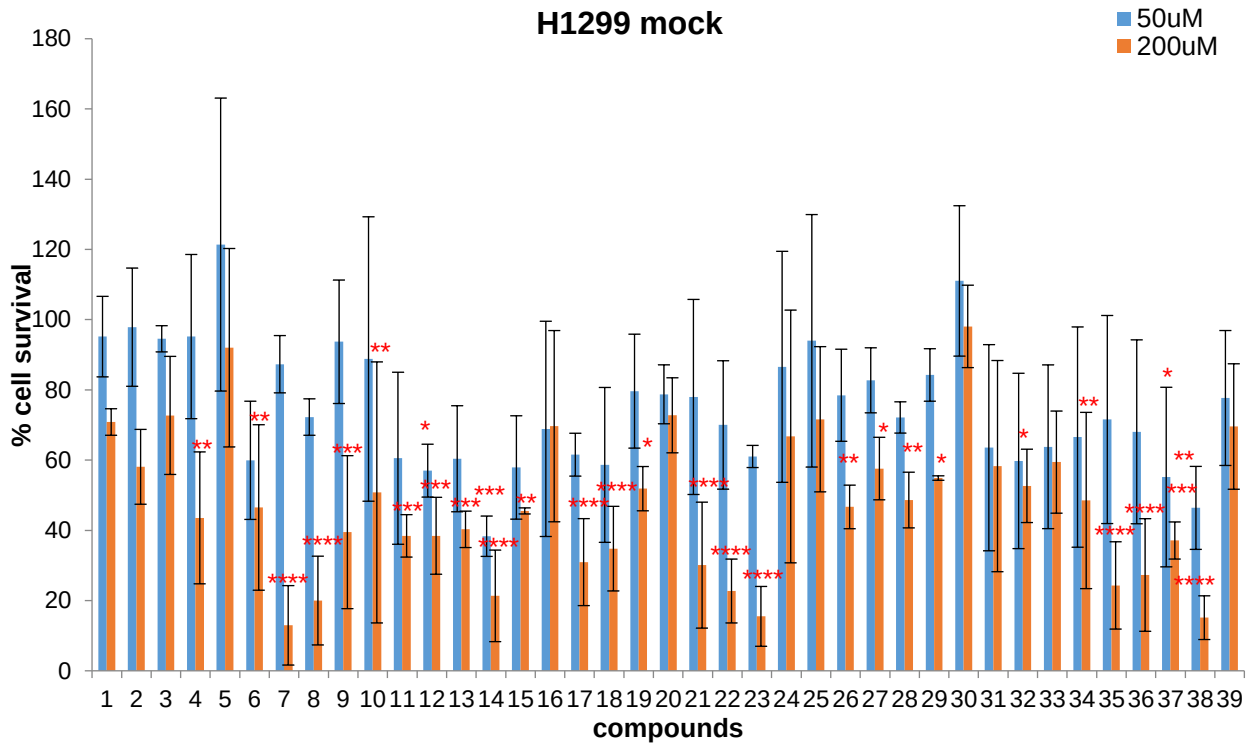
H1299 mock
50uM
200uM
% cell survival
compounds

B

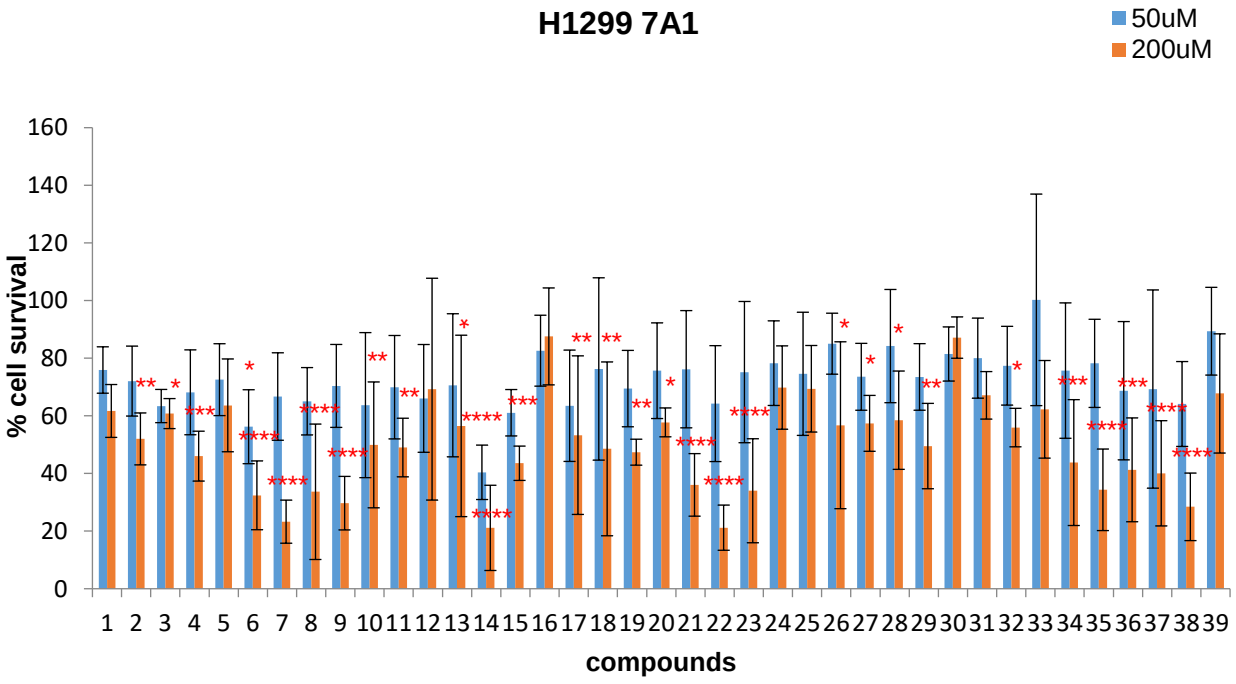
H1299 7A1
50uM
200uM
% cell survival
compounds

C

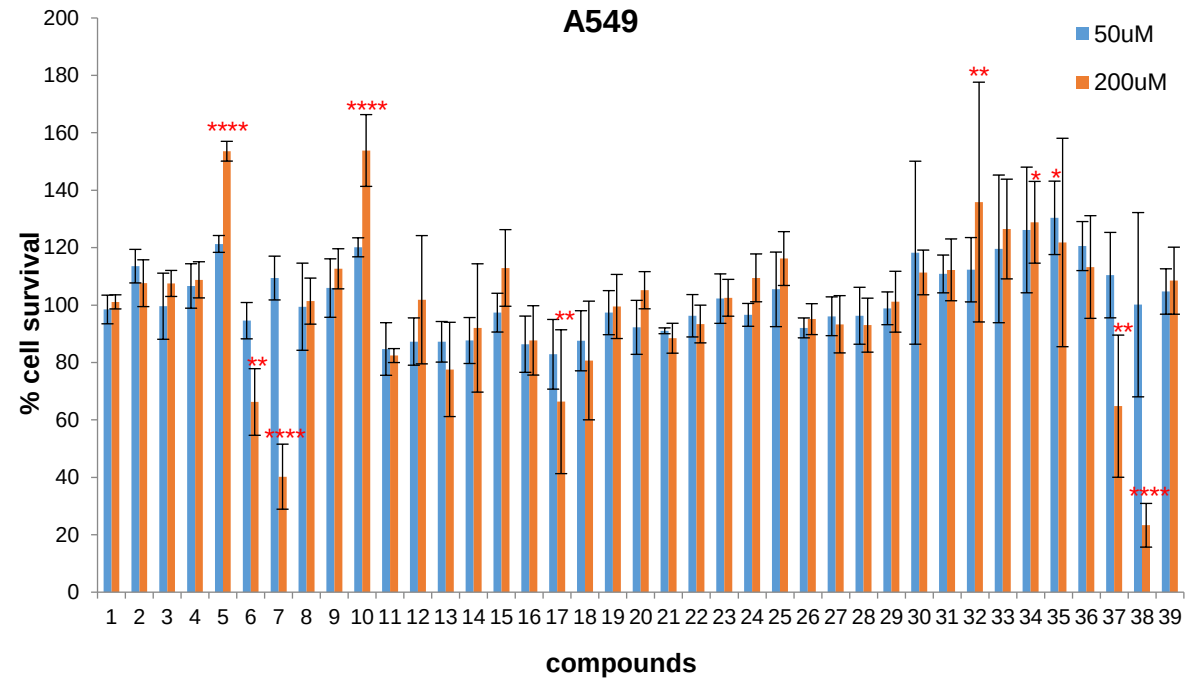


**Figure 51. Percentage cell survival after ALDH-affinic compound treatment in NSCLC cell lines.**

A library of ALDH-affinic compounds screened for chemosensitivity at 50µM and 200µM, (A) in H1299/mock cells, (B) in H1299/7A1 cells and (C) in A549 cells. The values represent a mean and SD of 3 independent experiments. Compound ALII-39 represents DEAB. Statistical significance was applied using the one-way ANOVA test for paired groups in which the means of % cell survival from multiple compounds at both concentrations were compared with control untreated cells which were at 100% cell survival. $p<0.05$*, $p<0.01$**, $p<0.001$*** and $p<0.0001$****.

### 5.5 Chemosensitivity analysis of selected ALDH-affinic compounds

Based on the outcome from the study of three cell lines, selected compounds were assessed for effect on cell viability using a larger concentration range. The compounds selected were ALII-7, ALII-8, ALII-9, ALII-14, ALII-17, ALII-18, ALII-34, ALII-35, ALII-37 and ALII-38. Cell lines used for the first screen were used again and all compounds were tested at 12.5µM, 25µM, 50µM, 100µM and 200µM. Docetaxel and DEAB were included as controls.

In H1299/mock and H1299/7A1 cells there was a dose dependent decrease in cell survival with treatment of docetaxel (Figure 52 A), ALII-7 (Figure 52 C), ALII-14 (Figure 52 F), ALII-17 (Figure 52 G), ALII-35 (Figure 52 J), ALII-37 (Figure 52 K) and ALII-38 (Figure 52 L). Whereas this effect was reduced across the range of concentrations by ALII-8 (Figure 52 D), and ALII-34 (Figure 52 I). ALII-9 (Figure 52 E) and ALII-18 (Figure 52 H), and these compounds only showed a decrease in cell survival at 200µM.

The trend in cell survival following treatment of ALDH compounds was found similar in both H1299 cell lines. A direct comparison cannot be made as the experiments were carried out at different times. However, compounds ALII 9, 14 and 18 which were also tested in primary prostate epithelial cells as described in experimental chapter 4, showed similar reduction in cell survival to H1299 cells when used at 200µM. The ALDH-affinic inhibitors are generally not cytotoxic compounds, they are analogues of DEAB designed to target the ALDHs. Only when used at much higher concentrations they exhibited some cytotoxicity. None of the compounds showed full toxicity, which would equate to 0% cell survival, however, ALII-35 showed about 20% cell survival only in

both H1299 cell lines, making this compound the most potent amongst others tested.

In A549 cells, most compounds had no effect on cell survival across the different range of concentrations except for ALII-37 (Figure 53 K) and ALII38 (Figure 53 L). ALII-37 showed reduction in cell survival only at 200µM concentration (Figure 53 C and K), whereas ALII-38 showed a dose dependent decrease in cell survival with only about 20% cell survival at 200µM concentration (Figure 53 L). The results are summarised as outlined in Table 22.

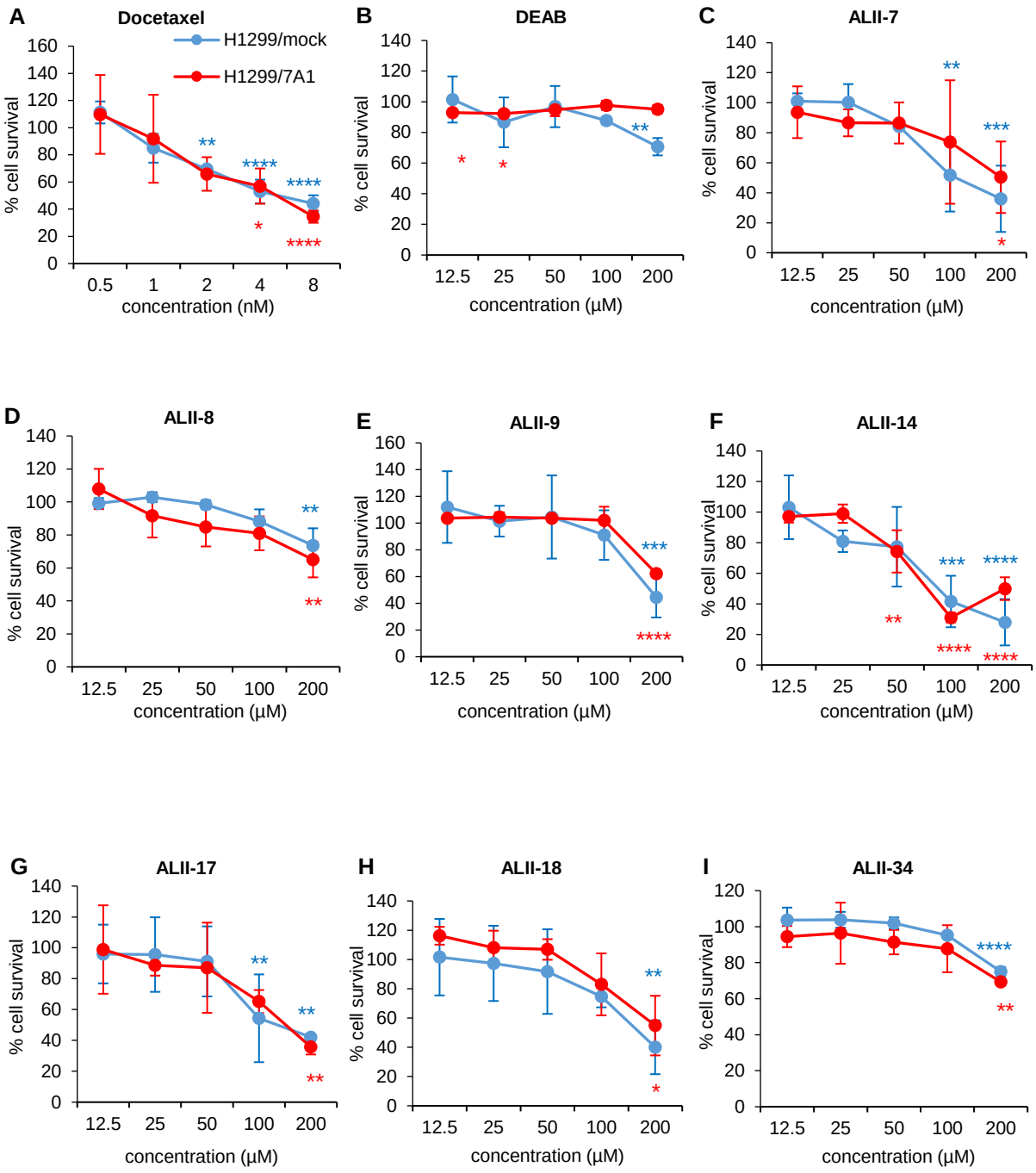
A
Docetaxel
H1299/mock
H1299/7A1
% cell survival
concentration (nM)
0.5
1
2
4
8
B
DEAB
% cell survival
concentration (μM)
12.5
25
50
100
200
C
ALII-7
% cell survival
concentration (μM)
D
ALII-8
% cell survival
concentration (μM)
E
ALII-9
% cell survival
concentration (μM)
F
ALII-14
% cell survival
concentration (μM)
G
ALII-17
% cell survival
concentration (μM)
H
ALII-18
% cell survival
concentration (μM)
I
ALII-34
% cell survival
concentration (μM)

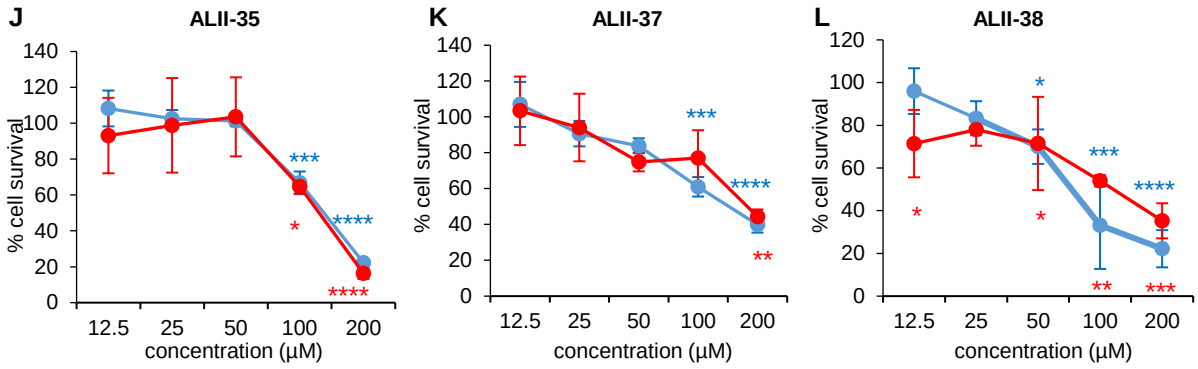


**Figure 52. Chemosensitivity testing of selected ALDH-affinic compounds in H1299/mock and H1299/7A1 cells.**

Percentage cell survival after treatment with (A) docetaxel, (B) DEAB, (C) ALII-7, (D) ALII-8, (E) ALII-9, (F) ALII-14, (G) ALII-17, (H) ALII-18, (I) ALII-34, (J) ALII-35, (K) ALII-37 and (L) ALII-38. Values represent the mean and SD of 3 independent experiments. Blue line represents H1299/mock and red line represents H1299/7A1. Statistical significance carried out using the one-way ANOVA for paired groups comparing the mean of treated cells with untreated control cells at 100% cell survival. $p<0.05$*, $p<0.01$**, $p<0.001$*** and $p<0.0001$****. Blue asterisks represent significance in H1299/mock cells and red asterisks represent significance in H1299/7A1 cells.

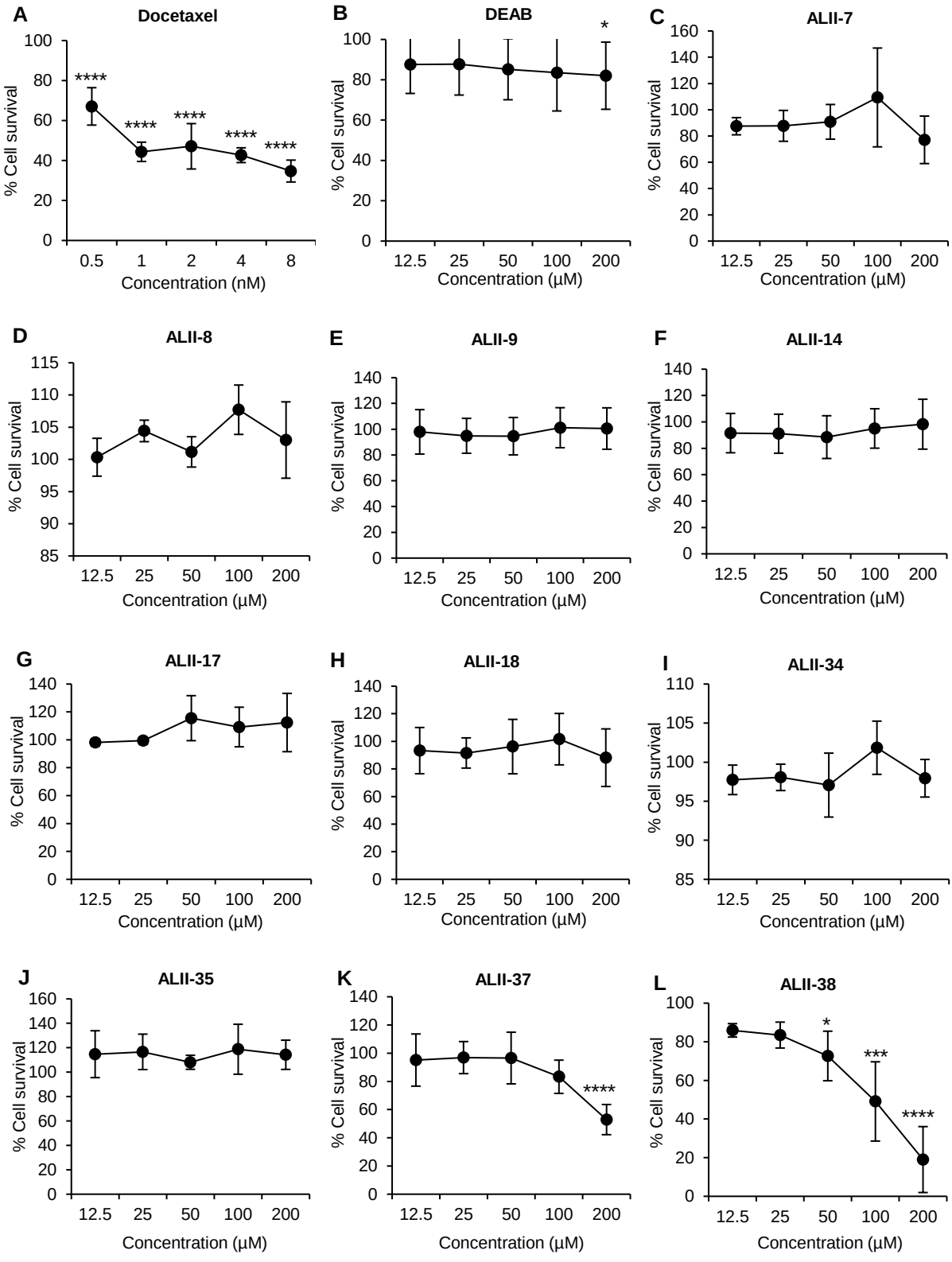


**Figure 53. Chemosensitivity testing of ALDH-affinic compounds in A549 cells.**
Percentage cell survival after treatment with (A) docetaxel, (B) DEAB, (C) ALII-7, (D) ALII-8, (E) ALII-9, (F) ALII-14, (G) ALII-17, (H) ALII-18, (I) ALII-34, (J) ALII-35, (K) ALII-37 and (L) ALII-38. Values represent the mean and SD of 3 independent experiments. Statistical significance carried out using the one-way ANOVA for paired groups comparing the mean of treated cells with untreated control cells at 100% cell survival. $p<0.05$*, $p<0.01$**, $p<0.001$*** and $p<0.0001$****.

| | **Indication of effect**<br>- = compound had no effect on cell survival<br>+/- = compound had minimal to no effect on cell survival<br>+ = compound reduced cell survival<br>++ = compound further reduced cell survival<br>+++ = compound greatly reduced cell survival | | |
|---|---|---|---|
| **Compound** | **NSCLC cell line** | | |
| | **H1299/mock** | **H1299/7A1** | **A549** |
| Docetaxel | +++ | +++ | +++ |
| DEAB | +/- | - | +/- |
| ALII-7 | +++ | ++ | + |
| ALII-8 | + | + | - |
| ALII-9 | ++ | ++ | - |
| ALII-14 | +++ | +++ | - |
| ALII-17 | ++ | ++ | - |
| ALII-18 | ++ | ++ | - |
| ALII-34 | + | + | - |
| ALII-35 | +++ | +++ | - |
| ALII-37 | ++ | ++ | ++ |
| ALII-38 | +++ | ++ | +++ |

**Table 22. Summary of the effect of selected ALDH-affinic compounds on NSCLC cell lines.**

## 5.6 ALDH expression pattern in docetaxel-sensitive and –resistant cells

In order to understand the role of ALDHs in cancer cell resistance to therapy, the ALDH gene expression was investigated in a pair of docetaxel-sensitive and docetaxel resistant PC3 cells by qPCR. It was shown that amongst the seven different ALDH isoforms analysed, ALDH1A3 was found to be highly expressed in the PC3 cell line. Furthermore, the expression was higher in the docetaxel-sensitive (Ag) PC3 cells compared to the docetaxel-resistant (D8) PC3 cells (Figure 54 B). However, the higher expression of ALDH1A3 observed in PC3 Ag cells was not statistically significant as compared to PC D8 cells. Consistent and in correlation with the data represented in chapter 3 of this thesis and shown again in Figure 54 (A), ALDH1A3 was the highest expressing isoform in PC3 cells, with observed expression of ALDH1B1, ALDH3A1 and ALDH7A1. However, the expression of ALDH1A3 found in this PC3 cell line pair is much higher (with relative expression of ~175 in PC3 Ag and ~140 in PC3 D8) than the previously analysed PC3 cells (with relative expression of ~ 50) (Figure 54). This may be potentially due to a higher passage number of this cell line pair due to repeated passages to maintain a resistant phenotype and its control sensitive cells (Figure 54 B). The expression of ALDH3A1 was significantly higher in PC3 D8 cells as compared to PC3 Ag cells. Taken together, this data confirms ALDH1A3 to be the highest expressing ALDH isoform in the malignant PC3 cell line and its expression is also high in docetaxel-resistant cells.

**A**

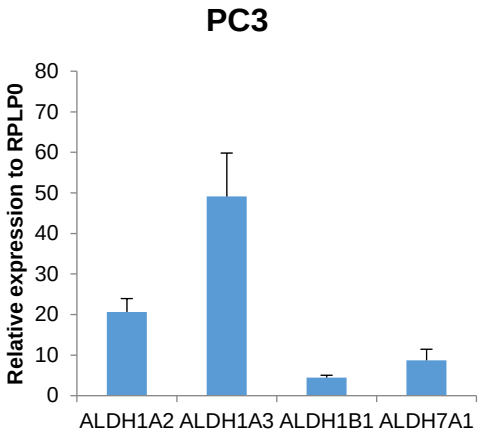


**B**

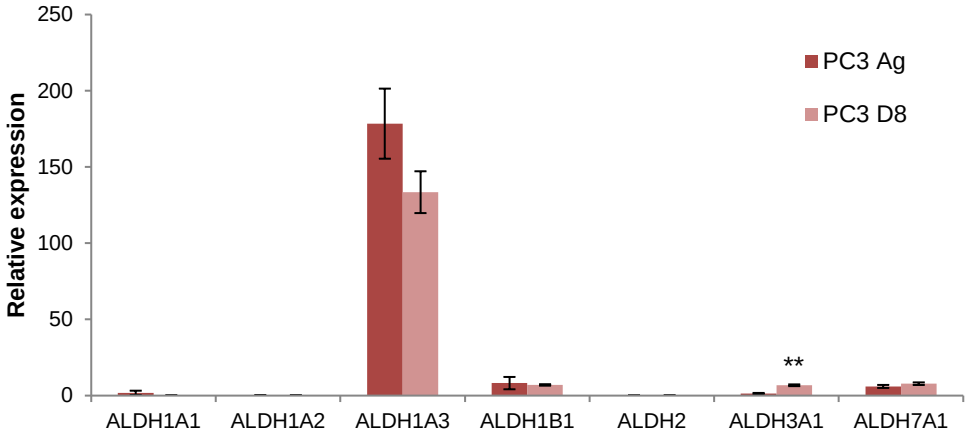


**Figure 54. ALDH gene expression in PC3 cells.**
qPCR analysis of ALDH gene expression in (A) PC3 cell line used in chapter 3 and (B) docetaxel-sensitive (Ag) and docetaxel-resistant (D8) PC3 cell line pair. $2^{-dCT}$ was used to calculate relative expression to housekeeping gene RPLP0. Values represent the mean and SD of 3 independent experiments. No statistical significance test was applied to (A) as the graph only shows endogenous expression of ALDHs in PC3 cells and is not compared to a normal control. Statistical significance was applied to (B) using student's t-test for paired groups using parametric distribution, Ag was compared to D8 for the expression of each ALDH isoform. $p<0.05$*, $p<0.01$**, and $p<0.001$***. PC3 Ag (docetaxel-sensitive cells) and D8 (docetaxel-resistant cells).

## 5.7 Effect of ALDH-affinic compounds and docetaxel on cell viability

Given the importance of targeting the CSC population in prostate cancer for a more effective treatment outcome, it was hypothesised that an ALDH inhibitor could be used to sensitise cells to docetaxel. Accordingly, evaluation of ALDH-affinic compounds as single agents and in combination with docetaxel was carried out to understand if an additive/synergistic effect could be achieved. The MTT assay was employed to explore viability of the cells after treatment with a range of drug concentrations with or without 1nM of docetaxel.

As expected, there was a significant reduction in cell viability of PC3 Ag cells after docetaxel treatment with increasing concentrations compared to the resistant PC3 D8 cells (Figure 55 A). The ALDH pan inhibitor DEAB showed no effect on cell viability in PC3 Ag and PC3 D8 cells, however, there was reduction in cell survival in both cell lines when used with 1nM docetaxel. PC3 Ag showed the most reduction in cell survival (Figure 55 B). Compound ALII-9 had no effect on cell viability in the PC3 Ag cells but there was a reduction in cell viability at the highest concentration of 200µM in the PC3 D8 cells. Treatment with 1nM docetaxel showed a high reduction in cell viability in combination with ALII-9 at 12.5µM in PC3 Ag cells whereas this combination only showed reduction in viability at 100µM and 200µM concentration in PC3 D8 cells (Figure 55 C). Compound Ali 14 showed a dose dependent decrease in cell viability of PC3 Ag cells with a more pronounced effect in the PC3 D8 cells. The same trend was observed when cells were treated in combination with 1nM of docetaxel, however the reduction in cell viability was greater with the most reduction in PC3 Ag cell even at 12.5µM concentration (Figure 55 D). Compound ALII-18 showed a similar pattern of effect on cell viability as ALII-

14, however the reduction in cell survival was less in the single treatments even at 200µM in the PC3 Ag and D8 cells (Figure 55 E). The ALDH7A1 inhibitor (HAN) showed reduction in cell survival only at high concentrations of 100µM and 200µM except for PC3 Ag cells also treated with 1nM docetaxel where, a great reduction was observed even at a low concentration of 12.5µM (Figure 55 F).

Due to the difference in range of concentrations used for docetaxel (nM) as compared to other compounds (µM), it was not feasible to plot them on the same graph and perform statistical analysis on them. Therefore, the concentration 200µM was selected as it showed the highest cell kill to illustrate the data in a different format as shown in Figure 56. Only one most effective concentration was selected for illustration as including all the concentrations would have generated too many graphs. A representative illustration of the drug treatments at 200µM, with and without 1nM docetaxel treatment are shown in Figure 56. The negative number of cells observed in Figure 56 E may be due to variation or inconsistency in cell numbers plated during experimental repeats.

Taken together, ALDH-affinic compounds have demonstrated the potential to reduce viability of docetaxel sensitive and resistant prostate cancer cell line PC3. This underpins the potential of such compounds to reverse resistance to docetaxel by inhibiting ALDH functional activity.

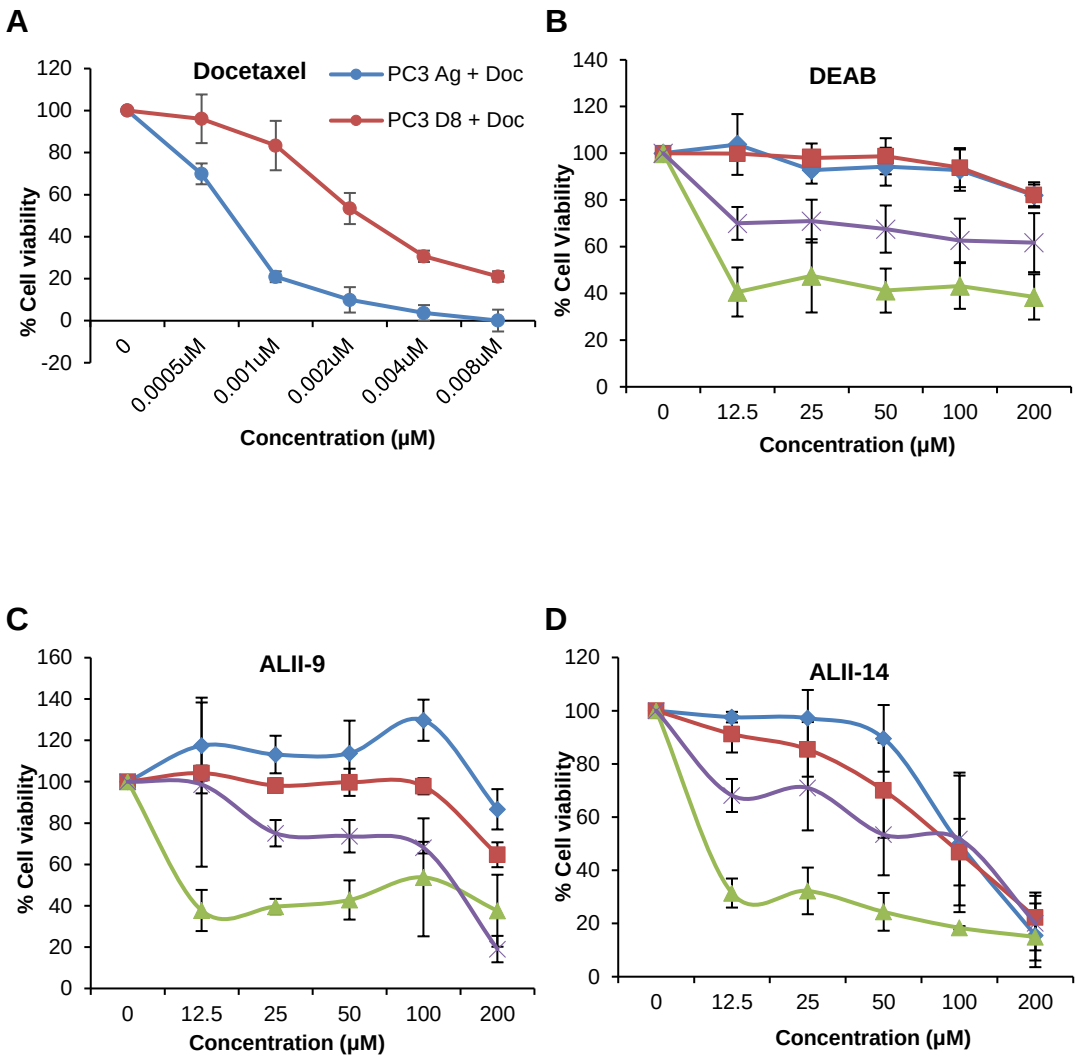
A
Docetaxel
PC3 Ag + Doc
PC3 D8 + Doc
% Cell viability
120
100
80
60
40
20
0
-20
0
0.0005uM
0.001uM
0.002uM
0.004uM
0.008uM
Concentration (μM)
B
DEAB
% Cell Viability
140
120
100
80
60
40
20
0
0
12.5
25
50
100
200
Concentration (μM)
C
ALII-9
% Cell viability
160
140
120
100
80
60
40
20
0
0
12.5
25
50
100
200
Concentration (μM)
D
ALII-14
% Cell viability
120
100
80
60
40
20
0
0
12.5
25
50
100
200
Concentration (μM)

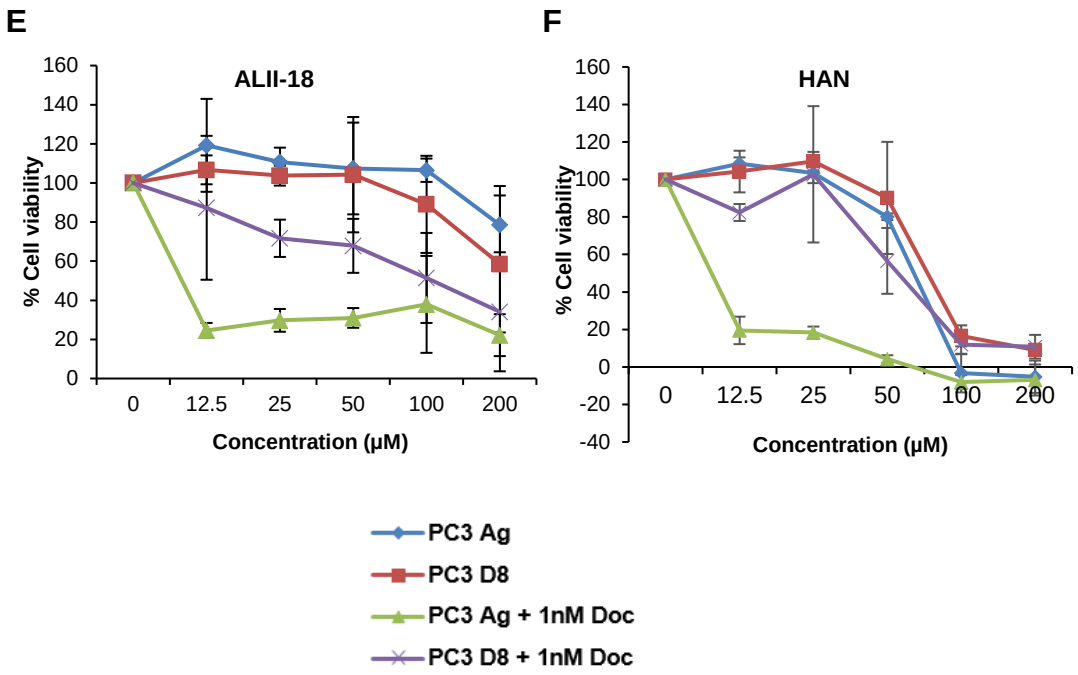


**Figure 55. Cell viability upon docetaxel and ALDH inhibitors treatment in PC3 docetaxel-sensitive and resistant cells.**

Graphs shows an overview of cell viability upon treatment with different compounds using a range of concentrations. PC3 Ag and PC3 D8 cells treated with (A) Docetaxel, (B) DEAB, (C) ALII-9, (D) ALII-14, (E) ALII-18 and (F) HAN with or without 1nM docetaxel. Values represent a mean and SD of 3 independent experiments. Statistical significance selected for the 200µM concentration as illustrated in Figure 56 Ag (docetaxel-sensitive) and D8 (docetaxel-resistant).

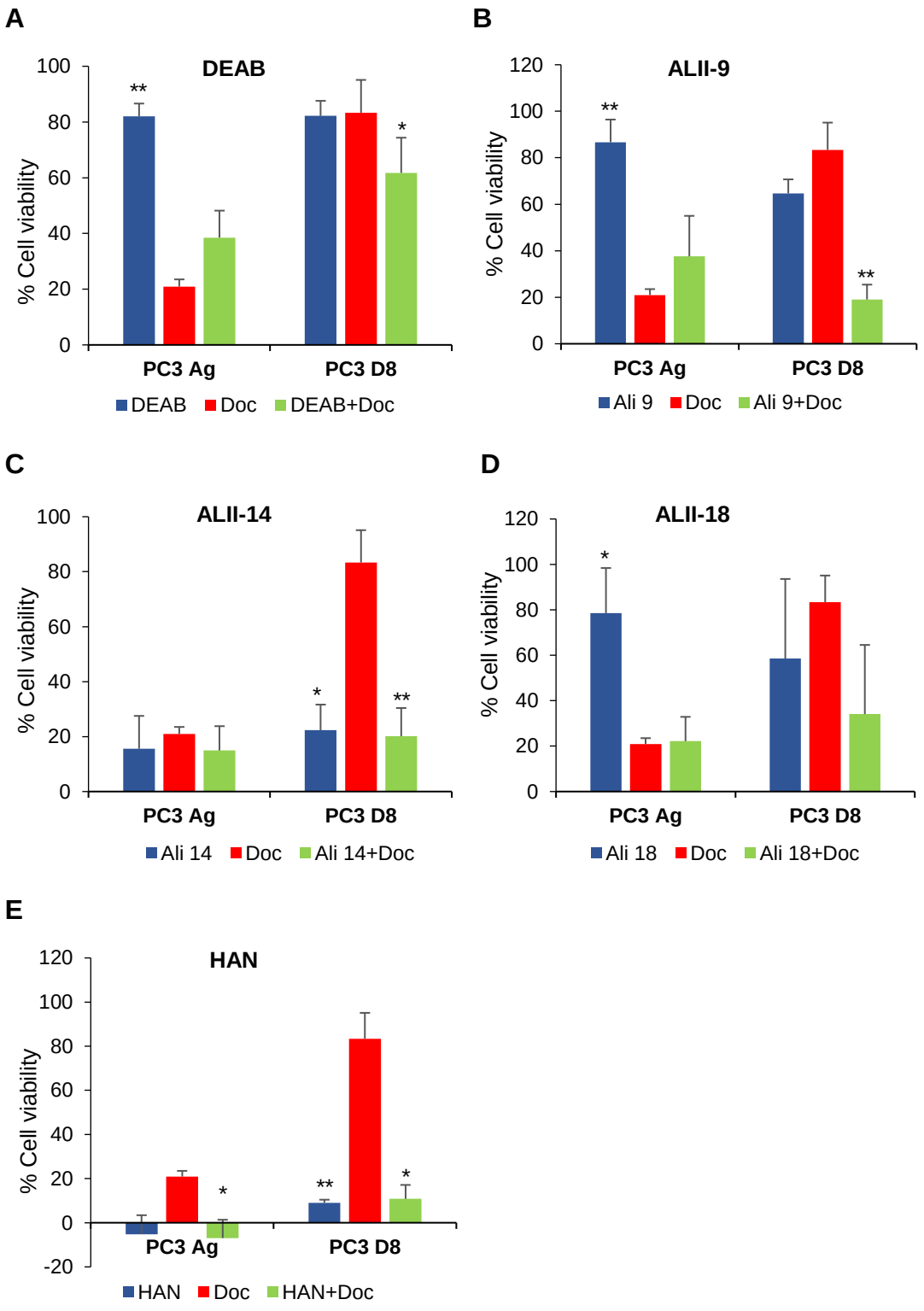


**Figure 56. A representative illustration of drug treatments at 200μM with or without combination treatment with 1nM docetaxel in PC3 Ag and PC3 D8 cells.**

(A) DEAB, (B) ALII-9, (C) ALII-14, (D) ALII-18 and (E) HAN. Percentage cell viability following drug treatments. Statistical significance was carried out using Student's t-test for comparisons of paired groups, parametric distribution, comparing the mean of docetaxel with the mean of ALDH-affinic inhibitors. $p<0.05$*, $p<0.01$**, and $p<0.001$***. Ag (docetaxel-sensitive) and D8 (docetaxel-resistant).

# Chapter 6

## Discussion

## 6.1 Discussion

## 6.2 ALDH isoforms in prostate cancer

To date, most studies have used ALDH high activity to isolate putative stem-like cells, which exhibit tumour-initiating and propagating properties, however, only few studies have explored the different ALDH isoforms in cancer. ALDH1A1 is commonly known to be responsible for the ALDH activity of SCs and CSCs, however recent evidence suggests that other isoforms such as ALDH1A3 contribute significantly to aldefluor activity [392]. Other isoforms such as ALDH3A1 have been reported to be upregulated in prostate cancer cell lines, xenograft models and primary tumours [501]. The purpose of the present study was to understand if ALDH expression in benign and malignant disease was different. Potential mechanisms impacting on ALDH expression such as epigenetic regulation, hypoxia regulation and RA induced expression of ALDHs were explored.

## 6.3 ALDH expression pattern analysis

Differential expression of the ALDHs was observed in the normal and cancer cell lines and primary cultures. This indicates that specific ALDH isoform expression is cell line/primary culture dependent. Our data showed that other ALDH isoforms including ALDH1A3, -1B1 -2 and -7A1, as opposed to the most reported ALDH1A1 in most cancers, were highly expressed in prostate cancer cell lines and primary cultures (except ALDH7A1 in primary cancer cultures).

*ALDH1A2*

ALDH1A2 is downregulated in bladder cancer due to aberrant methylation [489]. It has also been reported as a TSG in prostate cancer due to its down regulation by dense hypermethylation of the promoter region [474]. The epigenetic silencing of ALDH1A2 in the aforementioned studies may explain the absence of its expression in most cell lines and primary cultures in the present study. Aberrant methylation of ALDH1A2 may be the reason for gene transcriptional inactivation. Future studies could investigate the methylation status of *ALDH1A2* in prostate cancer cells by bisulfite pyrosequencing to explore if silencing is due to methylated CpG islands of the promoter region of *ALDH1A2*.

*ALDH1A3*

It has been reported that the RA producing ALDH isoform ALDH1A3 is associated with haematopoietic and solid tumours. ALDH1A3 is functionally involved in lung and breast cancer cell invasion and migration, but the underlying mechanisms are not yet established [529, 530]. Furthermore, ALDH1A3 expression has been correlated with expression of RA inducible genes with RAREs and poorer patient survival in breast cancer patients [529]. In neuroblastoma (NB), ALDH1A3 is widely expressed in NB cell lines and moreover, it has been reported to be associated with poor survival. ALDH1A3 activity contributes to clonogenicity and CP resistance [531]. In non-small cell lung cancer (NSCLC), ALDH1A3 is the predominant isoform responsible for ALDH activity and tumourigenicity [522]. In regard to prostate cancer, a recent study revealed the correlation of ALDH1A3 with luminal phenotype in prostate

cancer [532], while the study also reported on its association with proliferation, invasion and cell cycle [532]. Another recent paper highlighted increased expression of ALDH1A3 in prostate cancer samples and its inverse correlation to miR-187 using a proteomics approach suggesting ALDH1A3 may be a candidate tumour biomarker [533]. The data presented in this chapter demonstrated ALDH1A3 to be the highest expressing isoform amongst all ALDH isoforms studied and supports the two aforementioned studies as an isoform that is worthy of further studies in prostate cancer.

*ALDH7A1*

ALDH7A1 expression has already been reported in prostate cancer [273, 490], however, gene and protein data from cell lines and primary cultures from this chapter showed lower expression of ALDH7A1 than expected given the results by Hoogen et al. The difference in expression may be due to patient variability for primary cultures and prolonged culturing of cell lines. In addition, experiments carried out on different days and in different laboratories may also affect reproducibility.

*ALDH gene expression in sub-population of cells*

The present study demonstrated that ALDH expression was similar in the different cell populations of a heterogeneous tumour. ALDH1A3 and ALDH7A1 were highly expressed in all samples. Expression of ALDH1A3 was high in the SC component in contrast to ALDH1A1. Accumulating evidence suggests increased ALDH1A3 expression selects for tumour cell sub-populations that exhibit a stem-like/aggressive tumour cell phenotype, indicating that the tumourigenic “branch” of the RA pathway may be selected in some tumours

and/or that other non-RA-dependent functional roles of ALDH1A3 might be involved in tumourigenesis [357]. Further studies are needed to determine if high ALDH1A3 expression in SCs is associated with tumourigenic processes. As such, a study has described the aggressive phenotypes of mesenchymal glioma SCs as compared to proneural glioma SCs by higher *in vitro* cell growth and faster *in vivo* generation of tumours. In addition, this study showed that mesenchymal SCs have a higher ALDH1A3 activity with resistance to radiation treatment as compared to the proneural SCs [534]. Future studies will also need more samples to further separate the populations into BPH and cancer to enable a better understanding of the biology of the disease.

### 6.4 Epigenetic regulation of ALDHs

To date, very little is known about the epigenetic regulation of ALDHs. Only two studies have reported silencing by hypermethylation of the gene promoter of ALDH1A2 in prostate cancer [474] and bladder cancer [489], reporting it as a candidate TSG. Consequently, the present study explored the effect of demethylating agent DAC and the HDAC inhibitors TSA, MS275 and SAHA have on the expression of selected ALDHs.

In line with the aforementioned studies, data from this chapter showed increased ALDH1A2 expression at mRNA level following epigenetic treatment in most cell lines, further supporting its potential epigenetic silencing and perhaps a role as a TSG in prostate cancer. Future studies could confirm the methylation status of the promoter of ALDH1A2 and assess the biological responses upon the knockdown and over-expression of ALDH1A2 using transfected cells to support the data in this chapter. The expression of ALDH3A1 and ALDH7A1 was significantly increased following DAC/HDAC

inhibitor treatment at mRNA (qPCR) and protein (western blot) level in Bob and LNCaP cells respectively. Bob cells represent a more basal phenotype than the more differentiated SerBob cells, it may be that the expression of ALDH3A1 is epigenetically silenced in the progenitor cells as compared to the more differentiated cells. In contrast to the previous study by Hoogen et al. [273] data is this chapter showed low expression of ALDH7A1. Upon epigenetic treatment there was a robust increase at mRNA and protein level of ALDH7A1 in LNCaP cells only as compared to other cell lines. Other metastatic prostate cancer cell lines such as DU145 and PC3 did not show this observation. LNCaP cells are derived from lymph node metastasis, and its epigenetic status has not previously been assessed. Future studies could investigate methylation status of ALDH7A1 promoter in cell lines and primary cultures to provide information on the low expression observed in the present study. It has been previously reported by Pellacani et al that methylation of cell lines is very different to primary cells, therefore cell lines may not be indicative of gene regulation in the patient [62]. As a starting point, this study investigated epigenetic treatment using TSA on ALDH expression in primary cultures (BPH and cancer). TSA treatment caused increased expression of the ALDHs when compared to DMSO control (set at 1), however BPH compared to cancer samples showed no difference.

It may be speculated that there is possible epigenetic silencing due to CpG island hypermethylation of ALDH3A1 and ALDH7A1 gene promoters, in addition to histone modification of ALDH3A1. To confirm this, future studies need to determine the DNA methylation status of these isoforms by using pyrosequencing technique and analysis of the acetylation/methylation of

amino acid residues on the histones (chromatin structure) should also be explored using chromatin immunoprecipitation (ChIP) for defined isoforms. The epigenetic treatment findings from the present study only used drugs to interrogate possible links, therefore, this should then be correlated with methylation/acetylation status in follow-up studies to validate potential epigenetic silencing.

A previous study showed DAC treatment of prostate cancer cells was followed by direct DNA methylation measurement to verify correlation of drug treatment with epigenetic silencing of ALDH1A2 [474]. Another study reported epigenetic silencing of the prostate SC marker CD133 by histone modification by treating with HDAC inhibitors and performing ChIP analysis [62].

Current methods for quantifying DNA methylation mostly use bisulfite conversion of DNA to mediate the deamination of un-methylated cytosine into uracil, thereby distinguishing between methylcytosine and cytosine. A comparison of the bisulfite converted sequence to an untreated DNA sample enables the detection of the methylated cytosines. However, this technique comes with it limitations. Bisulfite conversion reduces genome complexity to 3 nucleotides, and therefore post-next generation sequence alignment becomes a more difficult task. Furthermore, bisulfite treatment results in DNA fragmentation, making amplification of long fragments difficult and may potentially result in the generation of chimeric products [535]. Subsequent pyrosequencing requires specialised equipment which is expensive.

Another method of assessing DNA methylation is PCR with high resolution melting. Herein, the amplified PCR product is analysed using high resolution

melting with the use of intercalating dye such as Eva green which binds double stranded DNA and is highly fluorescent. As the temperature increases, the DNA is dissociated resulting in reduced fluorescence. Methylated DNA retains the cytosines and has a higher melting point compared to un-methylated cytosines. The level of methylation is correlated with the melting profile of the product. The advantage of this method is if a pure PCR product is obtained, then even small differences (5%-10%) in DNA methylation could be detected [536].

A commonly used method for studying protein-DNA interaction includes ChIP analysis in which acetylation can be studied. Briefly, the technique involves chromatin bound protein fixation by formaldehyde (induces cross-linking), sonication or nuclease treatment to fragment the DNA, immunoprecipitation using specific antibodies, and analysis of the immunoprecipitated DNA. The drawback of this method is that is requires a high number of cells (about 10 million) and it is a more qualitative approach than a quantitative one. It is difficult to determine if the association of a specific protein with DNA is the same for every cell in the cell lysate. There can be variability in cross-linking between DNA and target protein. The antibodies may not efficiently immunoprecipitate all of the antigen [537].

Another assay which can be used instead of ChIP is DNaseI hypersensitivity assay. This assay provides a more general determination of the changes chromatin has undergone. DNaseI hypersensitivity sites are mainly harboured in or around promoter regions thus, allowing for mapping of transcriptionally active versus inactive chromatin [538]. Furthermore, TSA at

low concentrations inhibit HDACs allowing the determination of the role acetylation/deacetylation plays in the regulation of a specific gene [539].

### 6.5 ALDH expression regulation by RA

The RA signalling pathway was also explored as very little is known about the involvement of ALDH with RA signalling in prostate cancer. Higher expression of ALDH1A3 and ALDH3A1 after atRA treatment was detected in primary cancer cells compared to BPH and BPH-PIN cells. Thus RA induced these two ALDH isoforms in prostate cancer. Interestingly, a previous study showed atRA down-regulated ALDH1A1 and -3A1 activity and protein levels but not mRNA levels in lung cancer cell lines which resulted in a significant increase in the cytotoxicity of 4-HCPA and acetaldehyde suggesting a post-translational mechanism through which RA decreases ALDH expression [540]. Future studies could analyse the protein expression and activity of ALDH1A3 and ALDH3A1 upon atRA treatment and investigate whether a post-translational mechanism exists in prostate cancer cells.

As RA promotes cellular differentiation, the upregulated expression of ALDH1A3 and ALDH3A1 may be harboured in the more differentiated luminal cells as compared to the more stem-like cells. However, our data showed ALDH1A3 expression to be high in the SC subpopulation as well, although a higher number of samples is needed for validation. The expression of ALDH1A3 may depend on the presence and quantity of RA, whereby in higher concentrations it leads to higher expression of ALDH1A3 in the more differentiated cells, and under low concentrations, the expression of ALDH1A3 is higher in the SCs. Future studies are needed to investigate this link between ALDH1A3/RA and subcellular expression. Therefore, it would be of interest to

investigate ALDH1A3 and ALDH3A1 expression status in the sub-population of cells upon atRA treatment in benign and cancer cells.

### 6.6 Impact of hypoxia on ALDH expression

The impact of hypoxia on the regulation of ALDHs was explored since a previous study suggested that the observed upregulation of ALDH7A1 is linked to the tumour microenvironment in prostate cancer [541]. Hypoxia is a key feature of solid tumours and results in altered gene regulation. It has been reported that prostate tumours are very hypoxic and new biomarkers and drug targets are required [542]. Untreated prostate tumours are known to be very hypoxic (~0.3% oxygen), which is more than 12 times lower than oxygen levels found in the normal prostate [542]. No studies have reported the relationship between hypoxia and ALDH expression in prostate cancer, and so the effects of hypoxia on ALDH expression was investigated here. There were small but significant changes in ALDH expression upon exposure of cells to hypoxia at both gene and protein level confirming that at least in mono-layered prostate cancer cells, ALDH expression is altered by hypoxia. In an attempt to explore ALDH expression in 3D, prostate cancer spheroids were generated using the hanging-drop method. This technique can be used to grow spheroids and explore the ALDH expression in the different layers of the MCS including SL, HR and NC. Although it remains to be elucidated whether this model can be used for co-culturing with fibroblasts to account for the interplay between cancer cells and the stroma. The current study investigated the impact of hypoxia on ALDH expression in mono-layered cells as a starting point to understand ALDH regulation in a stressful environment before undertaking the work in xenograft models. Due to limitations in time, budget, and expertise in

mouse models, expression of ALDHs in xenograft models generated from cancer cell lines was not obtainable.

### 6.7 Investigating ALDH isoforms in primary prostate cells

Although established immortalised cell lines present a good model for optimising methods and providing preliminary data, prolonged culturing in media containing serum can result in chromosomal changes and hypermethylation of DNA [543-545]. Due to such limitations of using cell lines, it is essential to include primary cells as a model for investigation as they resemble the patient more closely and therefore provide more accurate data. However, primary cultures present their own limitations such as short life-span limiting the number of sub-culturing and difficulty in obtaining patient tissue biopsy from which the primary prostate epithelial cultures are derived. Biopsies are obtained from patients undergoing TURP, RP or cystectomy with their consent and ethical approval. The use of primary cells as a model is even more challenging because it requires investment and expertise in using primary cells and it is more expensive as it involves clinical contact [546].

Following the elevated expression of ALDH1A3, ALDH1B1 and ALDH2 in primary prostate epithelial cancer cells observed at both mRNA and protein level, the functional and therapeutic significance of these isoforms was investigated. Although seemingly not particular significant in this study, the importance of ALDH7A1 in prostate cancer has been demonstrated [490], therefore it was also investigated here. To date most studies have used ALDH high or low expression to study their role in cancer progression, consequently the present study explored various cancer phenotypes using specific ALDH isoforms.

## 6.8 siRNA knockdown of ALDH isoforms in primary prostate cells

There are advantages and disadvantages of using both siRNA and shRNA for gene knockdown. shRNA exhibits the advantage of using viral vectors for ease of delivery to transfect different cell types having varying sensitivities to the introduction of nucleic acids [547]. Whilst certain viral delivery protocols are transient, lentiviral or retroviral transduction stably integrates the shRNA into the cell's genome, allowing for persistent expression. A disadvantage of using shRNA lies in the difficulty of delivery of it into the nucleus of cells to work [547].

siRNAs are easily delivered in most cell types, however it may exhibit off target effects due to its short nucleotide sequence. siRNAs can be chemically altered for optimal activity to reduce such off target effects. Furthermore, siRNAs provide transient silencing of target genes suited for certain experiments [508].

In order to study biological functions of selected ALDHs in prostate cancer, siRNA transfection was employed to knock down the expression of ALDHs to investigate the effect of ALDH silencing on biological processes involved in prostate cancer progression.

Knockdown of ALDH1A3 and ALDH7A1 was achieved at mRNA level with a 60-93% knockdown in prostatic cancer cells. Interestingly, the knockdown of ALDH7A1 upregulated the expression of ALDH1A3 at both mRNA and protein level suggesting ALDH1A3 may be compensating for the absence of ALDH7A1. This study is the first to report such a compensatory relationship between these two ALDH isoforms, suggesting a possible acquired functional

advantage of the cancer cells for persistent growth. Further study is needed to explore this novel finding and address its biological significance in prostate cancer. Herein, specific ALDH inhibitors against ALDH1A3 and ALDH7A1 and their use in combination could be used to investigate effects on biological processes and SC markers in cancer. However, there is time limitation for the development of such specific inhibitors.

Preliminary experiments were carried out to limit any toxicity or off target effects from the carrier. In addition, an optimal siRNA concentration was chosen through siRNA titration experiments ensuring selection of the lowest, most effective concentration to give efficient knockdown. Off target effects are concentration dependent and hence a reduced siRNA concentration may help minimise these effects [548].

The liposomal control in comparison to mock transfected cells acted as a control to assess for any toxic or non-specific effects due to liposome formation/the transfection reagent.

The decision to use multiple siRNAs as controls was made for initial investigations to compare the effects of knockdown of different ALDH isoforms and different biological effects of them. And to determine the specificity of knockdown for the particular isoform against which the siRNA was designed. By doing so, each served as a comparative control for the other where there is an actual mRNA target present in the cell and an active RNAi process. A scrambled siRNA could have been used as a control as well as multiple independent siRNAs against the different ALDH isoforms (and also rescue experiments).

### 6.9 Observation of cell number upon ALDH knockdown

Initial observation of cells using a light microscope revealed a small reduction in cell number in cancer cells after ALDH1A3 and ALDH7A1 knockdown. These initial observations suggest that ALDH1A3 and ALDH7A1 could potentially be involved in cancer cell survival, possibly by playing a protective role in prostate cancer. It has been suggested that ALDHs are involved in promoting the tumour cell survival phenotype through direct inactivation, indirect expulsion of xenobiotics, and enhancement of the oxidative stress resistance response [357]. Based on this initial observation, ALDH isoforms ALDH1A3 and ALDH7A1 were selected as the main two isoforms for further biological investigation.

### 6.10 Cell proliferation

A study has shown the proliferative potential of ALDH3A1 by modulating its expression directly by either inhibiting its expression using inhibitors, antisense oligonucleotides, or siRNA, or indirectly by inducing the TF peroxisome proliferator-activated receptor γ (PPARγ) with polyunsaturated fatty acids or PPARγ transfection. It was indicated that the expression of ALDH3A1 was indirectly regulated by PPARγ via the inhibition of NF-κB and the TF activator protein-1 binding activity [549]. Another study demonstrated ALDH7A1 involved in the mediation of cell growth in a prostate cancer cell line [490]. Accordingly, the proliferative potential of specific ALDH isoforms was explored in primary prostate epithelial BPH and cancer cells in this study. Knockdown of ALDH1A3, ALDH7A1, ALDH1B1 and ALDH2 expression reduced the growth or proliferation significantly. Future studies need to confirm the role of these isoforms in cell proliferation by measuring

the Ki67 expression. As the reduction in cell proliferation was not associated with cell cycle arrest, it may be speculated that other mechanisms such as induction of PPARγ may have resulted in the reduction of cell proliferation. Furthermore, investigation of the death mechanisms including apoptosis, autophagy and necrosis may unravel potential pathways involved in the observed reduction in cell number. To confirm if the ALDHs are involved in promoting cell proliferation, experiments will ideally need to be carried out using cell line pairs that include over expression or no expression of the ALDHs to observe a direct effect on cell proliferation.

### 6.11 Migration

An integral part of cancer progression includes tumour invasion and metastasis forming one of the major hallmarks of cancer amongst other multistep processes [550]. Cancer cells exhibit enhanced migratory capacity and subsequently acquire invasive properties thereby invading surrounding tissues causing metastasis.

Although published studies have shown involvement of $ALDH^{high}$ cells in migratory phenotype [551], only relatively few studies describe individual ALDH isoforms responsible for the observed effects. In line with Hoogen et al's findings, this study showed ALDH7A1 knockdown leads to significant reduction in cell migration in primary cancer cells. For the first time our data showed that knockdown of ALDH1A3, ALDH1B1 and ALDH2 significantly reduced cell migration in prostate primary cells suggesting their indirect or direct role in migration. It would be of interest for future studies to investigate a role of these isoforms in bone metastasis using *in vivo* models as bone is a common site for metastasis in prostate cancer. Future studies should also determine the

invasive properties of these reported ALDH isoforms by exploring their involvement in the EMT such as E-cadherin loss, and gain of N-cadherin and vimentin expression [552].

### 6.12 Colony Formation and Cell Differentiation

Most studies to date have focused on cells sorted based on high and low ALDH activity for studying biological functions in cancer [523] with only few studies studying specific ALDH isoforms. One such study has shown that ALDH1A3 is responsible for clonogenicity in NSCLC [522]. To assess the role ALDH1A3 and ALDH7A1 play on colony formation, the colony forming assay was performed following knockdown of these isoforms. This assay measures the self-renewing, proliferating capacity and potential of the cells to initiate colony growth. Our data showed for the first time that the absence of both isoforms inhibited colony growth in primary prostate BPH and cancer cells. Therefore, this suggests that when upregulated, these isoforms may enhance self-renewal and proliferative potential of prostate SCs. This finding is in concordance with published data by Van den Hoogen et al that showed ALDH7A1 increases colony formation efficiency in a prostate cancer cell line [490]. The present study therefore indicates that at least ALDH1A3 and ALDH7A1 are essential for the acquisition of a metastatic stem/progenitor cell phenotype in prostate cancer.

Our data for the first time revealed that silencing of both isoforms ALDH1A3 and ALDH7A1 caused reduction in CD49b levels indicating cell differentiation and expansion of the differentiated pool of cells. This data suggests a role for ALDH1A3 and ALDH7A1 in maintaining a more stem-like/progenitor cell phenotype in prostate cancer and supports our speculation of their association

with promoting colony formation reinforcing that their high activity found in CSCs/progenitor cells may contribute to tumorigenicity.

Taken together, these results indicate that ALDH1A3 and to a greater extent ALDH7A1 may be involved in driving expansion of undifferentiated SC and TA cells which exert more clonogenic potential as compared to differentiated primary prostate epithelial cells.

### 6.13 Inhibitors

With growing evidence of the importance of targeting CSCs as a therapeutic strategy to overcome drug resistance and relapse in the clinic it is crucial to design compounds that would selectively target the CSC population [504]. Based on the high activity of ALDHs found in CSCs and our findings that support high ALDH expression with cancer progression, compounds designed against the ALDHs may potentially result in a better clinical outcome. Accordingly, ALDH chemical probes that are in their early stages of development were tested against primary prostate epithelial cultures in this study. All compounds showed reduced cell survival when used at high concentrations with inhibitors ALII-14 and -18 showing a synergistic reduction in cell viability when used in combination with docetaxel. Therefore, it may be speculated that targeting both the undifferentiated progenitor cell population by use of ALDH inhibitors as well as the differentiated dividing cell population by using current therapeutics may potentially lead to tumour remission and subsequently a better patient prognosis. Data from this study suggests that targeting ALDHs sensitises the resistant cell population to docetaxel and hence may have clinical potential in prostate cancer. Results from this study also highlight the necessity to design and develop specific inhibitors against

both ALDH1A3 and ALDH7A1 to overcome the compensatory mechanism that these two isoforms exhibit in prostate cancer. Further studies are needed to design such isoform specific inhibitors and investigate their potential in overcoming tumourigenesis in prostate cancer.

The limitations of current treatments for prostate cancer reflects the heterogeneity of this cancer type indicating the importance of the CSC hypothesis in which targeting the CSC population is crucial for successful treatment [553]. Although this presents the challenge of targeting the rare population of SCs which reside in a protected niche, ALDH specific inhibitors may potentially eradicate CSCs based on the $ALDH^{high}$ phenotype by various mechanisms including overcoming CSC resistance [554] and promoting CSC differentiation. Together with current treatments that function by eradicating the tumour bulk, combination with ALDH specific inhibitors may provide an effective therapeutic strategy.

### 6.14 ALDH and drug resistance

To date, studies have reported the association of ALDHs with drug resistance in a number of cancer types. However, no studies have explored the role of ALDH1A3 in mediating drug resistance in prostate cancer. Only recently, a study revealed high expression of ALDH7A1 in a zoledronic acid resistant DU145 prostate cancer cell line through proteomics analysis [502]. ALDH1A3 and ALDH7A1 expression in prostate cancer appears to contribute to the aggressiveness of this disease, in ways that are poorly understood.

Through initial screening of 39 ALDH-affinic compounds in NSCLC cell lines, several compounds have emerged as potential agonists for cell viability

highlighting that future studies should focus on these compounds in prostate cancer cell lines to validate their usefulness in prostate cancer as potential therapeutics.

The use of the isogenic cell line pair, H1299/mock and H1299/7A1 showed minimal difference of cell survival in response to these compounds suggesting ALDH7A1 expression status made no significant difference in cell viability. Compounds designed more selectively for ALDH7A1 are required to further understand the role of ALDH7A1 in cell viability.

Although ALDH1A3 expression was high in the PC3 sensitive and resistant cells, and in experimental chapter 3, a direct comparison cannot be made as it is very difficult to compare results run on different plates and different days due to experimental variability in conduction of the experiments.

The use of a highly specific ALDH1A3 inhibitor may be useful in identifying changes at both molecular and cellular level. The crystal structure of ALDH1A3 has only very recently been revealed [527] and therefore biomarker and drug discovery against this isoform is only in its infancy. Selective chemical probes and inhibitors designed against ALDH1A3 can act as tools to probe the enzyme's role in prostate cancer and potentially be used to progress new types of therapies [370].

Docetaxel is used in the treatment of CRPC patients and its therapeutic effect could potentially be enhanced when used in combination with an ALDH inhibitor as indicated with early-staged compounds in this study. These ALDH-affinic inhibitors may reverse resistance to docetaxel but further studies are needed to investigate this notion. Herein, cells resistant and sensitive to

docetaxel could be investigated using ALDH-affinic inhibitors as single agents and in combination with docetaxel. Another possible suggestion is that the presence of ALDH inhibitor may push cells towards differentiation thereby increasing their susceptibility to current treatments by reducing the therapy resistant fraction allowing current treatments such as docetaxel to work better when used in combination with specific ALDH inhibitors. However, these compounds need further developing to prove ALDH specificity.

Future studies will need to include virtual screening of more ALDH isoforms and isogenic cell line pairs deficient/proficient in target ALDHs. Importantly, biochemical assays using purified recombinant ALDHs could be employed to understand how effective the ALDH-affinic compounds are in inhibiting the functional activity of the ALDHs, enabling a better understanding of the selectivity profile [484].

### 6.15 Overall Conclusions

Prostate cancer is the second most common form of cancer and accounts for a fifth of all cancer-related deaths to affect men worldwide (cancer research UK 2014). Despite improvement in overall survival rates, many patients relapse with a disease that is more aggressive, drug-resistant and metastatic. Emerging information suggests that ALDHs are enzymes that contribute to drug-resistance, cellular proliferation and aggressiveness of several cancer types including prostate cancer. The elevated expression of ALDHs in CSCs helps to protect the SC niche, suggesting their contribution to MDR and enhanced tumourigenicity of CSCs [555]. Furthermore, the lower oxygen tension increases resistance to radiotherapy and also enriches the CSC niche. A recent study revealed that primary human prostate cancer samples express

both elevated levels of ALDH1A1 and HIF-1α, which have been linked to radio-resistance [556]. Another recent study [557] demonstrated that irradiation enriched the CSC population of DU145 and PC3 cells. ALDH$^{high}$ sub-populations were shown to possess enhanced DNA damage response activity and *in vivo* the irradiated cells were shown to exert tumorigenic properties, suggesting these might be radio-resistant *in vivo*. In the context of these and other ALDH investigations, this study set out to explore the regulation and function of this class of enzymes in prostate cancer with the principal aim of gathering information for discovering novel biomarker and/or drug opportunities.

Traditionally, ALDH1A1 or just ALDH1 functional activity has been associated with sub-population of cells with stem-like cell features while more recent studies indicate ALDH1A3 also play vital roles in these rare cell types [558]. However, it is likely other members from the ALDH1 family could be expressed in prostate cancer cells and hence ALDH1A1, 1A2, 1A3 and 1B1 were investigated. Additionally, a member from the 2, 3 and 7 family were included to broaden the scope of the study to include an isoform involved in acetaldehyde metabolism (ALDH2: important in detoxification and osteoporosis), drug resistance (ALDH3A1: e.g. nitrogen mustard prodrugs) and metastasis (ALDH7A1: link with stemness features and migration).

In the present study, ALDH1A3 was shown to be highly expressed in prostate cancer cell lines, primary prostate cancer cells compared with benign cells and docetaxel-resistant PC3 cells compared to other isoforms, suggesting a potential link to malignancy and drug resistance.

miRNAs regulate gene expression [559] and can function as either a tumour suppressor or oncogene, depending on the target gene [560] in which they contribute to the initiation and development of prostate cancer [561]. Interestingly, a study identified the potential use of ALDH1A3 as a tumour biomarker in prostate cancer [529]. It was found that ALDH1A3 expression was significantly downregulated in prostate cancer cell lines after the reintroduction of the tumour suppressor miRNA miR-187 [562]. A follow up study from the same group measured ALDH1A3 expression in patient urine samples to evaluate its predictive capability as a biomarker for prostate cancer using an ELISA assay [533]. Urine samples were centrifuged and supernatant was used to estimate the ALDH1A3 protein level. It was shown that both PSA and ALDH1A3 were significantly associated with a positive biopsy of prostate cancer. This study provided insight into the utility of ALDH1A3 as a new biomarker for prostate cancer in a diagnostic setting [533]. An ELISA (enzyme-linked immunosorbent assay) assay works by having an immobile antigen or capture antibody on a plate (e.g. a 96-well plate). The urine or plasma from the patient would then be added to the plate and any antigen of interest (in this case ALDH1A3) would bind to the capture antibody. A further primary (direct detection) or primary and secondary antibody (indirect detection) would then be used to detect how much antigen of interest is present. This is detected through a conjugated substrate on the antibody such as alkaline phosphatase (AP) or horseradish peroxidase (HRP).

It would be interesting in future experiments to investigate if a secreted form, such as a peptide or the protein of ALDH1A3 and ALDH7A1 is present in conditioned media from benign and cancer cells using ELISA assay.

Furthermore, the ALDH expression of these isoforms from urine samples (from patients with BPH or cancer) can also be evaluated using ELISA assay for a more clinically relevant experiment. Urine is an excellent source of material for new biomarker identification because it provides an ease of sample collection for diagnosis.

Several investigations have linked ALDH expression with RA synthesis and cell differentiation [529]. In the present investigation, results indicated that both ALDH1A3 and ALDH3A1 were induced in primary prostate cancer cells following treatment with atRA. However, no induction of ALDH1A1 and ALDH1A2 was observed, which has previously been reported to be involved in the RA signalling pathway [563]. As previously reported by other groups, high ALDH1A3 has been associated with more aggressive forms of breast, glioblastoma, gall bladder cancer and pancreatic cancer [529]. In breast cancer, it has been reported that ALDH1A3 expression in patient samples correlates with expression of RA-inducible genes RARβ and RARRES1, poorer patient survival and triple-negative breast cancers, strengthening the link between ALDH1A3 expression and RA signalling in aggressive cancer [529]. To unravel these observations and understand the importance of the ALDH-RA link in prostate cancer, future directions should be focused on exploring the downstream RA signalling pathway to identify modulators involved in the upregulation of ALDHs, thereby providing mechanistic insight to their regulation.

The literature is sparse on epigenetic regulation of ALDHs, however one key study revealed ALDH1A2 as a TSG that become silenced in prostate cancer [474]. Treatment of PNT2C2, Bob, SerBob, and DU145 cell lines supported

the previous study by Kim et al, demonstrating higher expression of ALDH1A2 after DAC/HDAC inhibitors treatment. Although DNA methylation of the ALDH1A2 gene promoter was not analysed, the results supports this gene is under epigenetic control. In some cell lines there was indication that DAC and the HDAC inhibitors modulated gene expression, but analysis at the protein level did not confirm a constant pattern and suggest expression may be cell line specific and unlikely to be clinically relevant apart from ALDH1A2 results. Treatment of prostate cancer cell lines with DAC indicated ALDH1A2 is likely to be under epigenetic control via methylation of the gene promoter region. DNA methylation analysis (e.g. via classical bisulphite sequencing or Combined Bisulphite Restriction Analysis (COBRA) [564] of treated samples is required to validate this finding.

A larger study (>200 samples) is required to understand if the epigenetic regulation of ALDH1A2 can be used to distinguish benign from malignant cancer and if this isoform can be used to identify patients at risk of progressing to advanced stages of prostate cancer.

Another research objective was to explore the influence of hypoxia on ALDH expression as alluded to earlier in this chapter. Although the data presented here only showed minimal changes in ALDH expression following exposure of cells to hypoxia, the role of the tumour microenvironment cannot be underestimated in the modulation of ALDH expression. Hypoxia is known to accelerate the Warburg effect and interaction in the tumour microenvironment [565] and interaction with e.g. fibroblast and stroma tissue. The cell lines used in this study therefore does not serve as a great model in regard to clinical relevance and it is possible hypoxia will have a larger impact in an *in vivo*

environment with functional vascular network [566]. In future studies, it is suggested that prostate tumours could be grown *in vivo* followed by ALDH and hypoxia marker (e.g. LDA, GLUT1 or CAIX) co-expression analysis to evaluate the impact of hypoxia on ALDH expression [566].

Knockdown studies of ALDH1A3 and ALDH7A1 were performed to unravel mechanisms of regulation. Interestingly, knockdown by siRNA of either isoform in primary prostate epithelial cells was compensated by the upregulation of the other isoform and may have implications for biomarker and/or drug discovery. Specifically, siRNA reduced the viable cell number in primary prostate cells suggesting an induction of cell death or reduction in cell proliferation while cell cycle analysis indicated suppression of these isoforms leads to reduced proliferative potential, perhaps due to increased doubling time rather than initiating cell cycle arrest or cell death [567]. It has been reported that ALDH7A1 knockdown decreases the stem/progenitor cell subpopulation in prostate cancer cell line PC-3M-Pro4 [490], supporting the reduced viable cell number observed in our study upon ALDH7A1 knockdown.

The migratory role of ALDH1A3, 1B1 and 2 in prostate cancer progression was a novel finding. Furthermore, ALDH7A1 exhibited similar migratory capacity to these aforementioned isoforms which is in agreement with Van den Hoogen's finding [490]. The contribution of ALDHs to migration and potentially metastasis is poorly explored but could be linked with cells harbouring stemness features. The investigation also revealed for the first time that ALDH1A3 and ALDH7A1 knockdown reduced colony formation. This could mean that they have a role in stimulating colony forming ability causing proliferation and self-renewal of the SCs. This suggests that these isoforms

may contribute to a metastatic stem/progenitor phenotype in prostate cancer, although this would have to be further investigated. In line with this, the present study revealed that knockdown of these isoforms induced cell differentiation, causing cells to differentiate from a TA state to a CB state. This reinforces the hypothesis that the role of these ALDH isoforms is to maintain a more CSC-like/progenitor phenotype in prostate cancer.

The final research objective of this study was to explore ALDH expression in docetaxel-resistant cells and examine a library of small molecules to identify potential hit compounds, which could serve as starting points for discovery of more drug-like potent and selective ALDH inhibitors. The importance of therapeutic targeting of the rare population of CSCs for improved clinical outcomes requires the development of new therapies. ALDH expression is high in CSCs and as such, suitable target for biomarker and drug discovery.

DEAB is a poorly characterised commercial ALDH inhibitor with studies describing it as a reversible competitive inhibitor of ALDH1 [568]. It is also commonly used as an ALDH1A1-specific inhibitor in the Aldefluor assay [569] while it has also been shown to irreversibly inactivate ALDH7A1 via a stable covalent acyl-enzyme species [570]. To improve on DEAB as a chemical probe, several analogues were evaluated in this study and were shown to be anti-proliferative at high doses (200 µM) as single agents and in combination with docetaxel in primary prostate cancer cells and in docetaxel-resistant PC3 cells. The data indicated that synergy with docetaxel is possible and supports further optimisation of such chemical probes to target ALDH1A3 and other ALDHs; modulation of ALDH levels could increase susceptibility of prostate cancer to other treatments by reducing the therapy resistant fraction. It will be

important for future studies to design and biologically evaluate chemical probes highly selective for ALDH1A3 and ALDH7A1 to firstly, circumvent the compensatory effects of these two isoforms when used together in prostate cancer and secondly, deplete the SC pool of cells that are tumourigenic. ALDH-targeted drugs could be used to circumvent drug resistance to docetaxel in patients with aggressive forms of prostate cancer and extend overall survival rates. Accordingly, this investigation supports further the important roles that some ALDHs such as ALDH1A3 and ALDH7A1 play in prostate cancer [273, 490]. The crystal structures of ALDH1A3 and ALDH7A1 are now both available and hence drug design using *in silico* can speed up the drug discovery process of developing more selective and potent inhibitors. Future studies could also include liquid chromatography mass spectrometry metabolism studies using recombinant ALDH isoforms and docetaxel to identify key isoforms that confer docetaxel resistance.

A recent study examined > 11,000 individuals from Chinese and Caucasian populations and discovered a SNP ALDH7A1 susceptibility gene associated with hip osteoporotic fracture and low bone mineral density. The authors of the study postulated that ALDH7A1 might be involved in inhibiting osteoblast proliferation and decrease bone formation via detoxification of acetaldehyde. Given the involvement of ALDH7A1 in metastatic prostate cancer [490] and acetaldehyde detoxification it is tempting to speculate that ALDH7A1 is highly expressed in the bone microenvironment. In this regard, ALDH7A1 or a SNP variant lends itself as a potential novel biomarker and drug target for treatment of prostate cancer that has metastasised to the bone, which currently is an unmet clinical disease. Further studies are required to validate this rationale.

### 6.16 Potential for route to clinic

To date, most prostate cancer research has focused on androgen signalling, however with the knowledge that basal cells, including SCs are largely independent of androgen signalling, future work ought to focus on (i) the CSC population and (ii) prostate cancer cell heterogeneity. Work could be focused on combination therapies, including differentiation therapy, e.g. with RA or other differentiating agents, to diminish the SC pool and/or novel ALDH inhibitors targeting the SC niche to deliver a treatment option aimed at removing the roots that may be responsible for treatment relapse. Specifically, inhibitors designed and optimised against ALDH1A3 and ALDH7A1 may provide an effective treatment strategy of aggressive prostate cancer disease. This study supports ALDH1A2, 1A3 and/or ALDH7A1 as potential biomarkers and therapeutic targets for prostate cancer.

Many studies, including the data presented here, support the potential for ALDH inhibitors to be anti-cancer therapeutics. Many ALDH inhibitors have been generated and the focus for successful therapeutic relevance is selectivity. The large number of ALDH isoforms means that cross-selectivity can be a problem with novel compounds [368]. In terms of using ALDH isoforms as a biomarker, there is again potential with high expression of ALDH isoforms correlating with metastasis. However, the path to generate a meaningful biomarker that could be used for diagnosis and prognosis is a rigorous one. In particular, the need for a consistent and sensitive detection method combined with a clear range of informative measurements is required. Much validation would be required before a new biomarker such as this could be implemented in clinical practice [357]. The next steps to take this work

forward would be to (i) significantly increase the number of samples used to further stratify ALDH expression in SC, TA and CB cell populations in samples obtained from benign and cancer tissues to validate a diagnostic role of ALDHs within a complex heterogeneity, (ii) include tissue samples of different Gleason grades to explore a prognostic role of ALDHs and (iii) further design highly selective compounds against ALDH1A3 and ALDH7A1 to enable a better understanding of the importance of ALDH biological functions, use in detection of ALDH activity and their therapeutic significance.

# Chapter 7

## References

# References


https://www.cancerresearchuk.org/ Cancer Research UK (2014)

https://prostatecanceruk.org/ Prostate Cancer UK (2016)

1. Raychaudhuri, B. and D. Cahill, *Pelvic fasciae in urology.* The Annals of The Royal College of Surgeons of England, 2008. **90**(8): p. 633-637.
2. McNeal, J.E., *The zonal anatomy of the prostate.* The prostate, 1981. **2**(1): p. 35-49.
3. Zhu, Y., S. Williams, and R. Zwiggelaar, *Computer technology in detection and staging of prostate carcinoma: a review.* Medical Image Analysis, 2006. **10**(2): p. 178-199.
4. Cohen, R.J., et al., *Central zone carcinoma of the prostate gland: a distinct tumor type with poor prognostic features.* The Journal of urology, 2008. **179**(5): p. 1762-1767.
5. Bibel, B.M., *The Whole Life Prostate Book: Everything that Every Man-at Every Age-Needs To Know About Maintaining Optimal Prostate Health*. 2012, REED BUSINESS INFORMATION 360 PARK AVENUE SOUTH, NEW YORK, NY 10010 USA.
6. Xu, X., et al., *Current opinion on the role of testosterone in the development of prostate cancer: a dynamic model.* 2015. **15**(1): p. 806.
7. Jiang, M., et al., *Androgen-responsive gene database: integrated knowledge on androgen-responsive genes.* 2009. **23**(11): p. 1927-1933.
8. Wen, S., et al., *Stromal androgen receptor roles in the development of normal prostate, benign prostate hyperplasia, and prostate cancer.* The American journal of pathology, 2015. **185**(2): p. 293-301.
9. Winter, J., C. Faiman, and F. Reyes, *Sexual endocrinology of fetal and perinatal life*. 1981, Academic Press, New York.
10. Cunha, G.R., *Epithelio-mesenchymal interactions in primordial gland structures which become responsive to androgenic stimulation.* The Anatomical Record, 1972. **172**(2): p. 179-195.
11. Pereira de Jésus-Tran, K., et al., *Comparison of crystal structures of human androgen receptor ligand-binding domain complexed with various agonists reveals molecular determinants responsible for binding affinity.* Protein Science, 2006. **15**(5): p. 987-999.
12. Lee, C., J.M. Kozlowski, and J.T. Grayhack, *Etiology of benign prostatic hyperplasia.* The Urologic clinics of North America, 1995. **22**(2): p. 237-246.
13. Marker, P.C., et al., *Hormonal, cellular, and molecular control of prostatic development.* Developmental biology, 2003. **253**(2): p. 165-174.
14. Visakorpi, T., et al., *In vivo amplification of the androgen receptor gene and progression of human prostate cancer.* 1995. **9**(4): p. 401.
15. Dai, C., H. Heemers, and N. Sharifi, *Androgen signaling in prostate cancer.* Cold Spring Harbor perspectives in medicine, 2017. **7**(9): p. a030452.
16. Traish, A. and A. Morgentaler, *Epidermal growth factor receptor expression escapes androgen regulation in prostate cancer: a potential molecular switch for tumour growth.* British journal of cancer, 2009. **101**(12): p. 1949.
17. Isaacs, J.T., *The biology of hormone refractory prostate cancer: why does it develop?* Urologic Clinics of North America, 1999. **26**(2): p. 263-273.
18. Taylor, R.A., et al., *Human epithelial basal cells are cells of origin of prostate cancer, independent of CD133 status.* Stem Cells, 2012. **30**(6): p. 1087-1096.
19. Schmelz, M., et al., *Identification of a stem cell candidate in the normal human prostate gland.* European journal of cell biology, 2005. **84**(2): p. 341-354.
20. Van Leenders, G. and J. Schalken, *Stem cell differentiation within the human prostate epithelium: implications for prostate carcinogenesis.* BJU international, 2001. **88**(s2): p. 35-42.
21. Schalken, J.J.B.i., *Molecular and cellular prostate biology: origin of prostate-specific antigen expression and implications for benign prostatic hyperplasia.* 2004. **93**: p. 5-9.
22. Bonkhoff, H. and K. Remberger, *Widespread distribution of nuclear androgen receptors in the basal cell layer of the normal and hyperplastic human prostate.* Virchows Archiv, 1993. **422**(1): p. 35-38.
23. Hudson, D.L., et al., *Epithelial cell differentiation pathways in the human prostate: identification of intermediate phenotypes by keratin expression.* Journal of Histochemistry & Cytochemistry, 2001. **49**(2): p. 271-278.

24. van Leenders, G.J., et al., *Expression of basal cell keratins in human prostate cancer metastases and cell lines.* The Journal of pathology, 2001. **195**(5): p. 563-570.
25. Murant, S., et al., *Co-ordinated changes in expression of cell adhesion molecules in prostate cancer.* European journal of cancer, 1997. **33**(2): p. 263-271.
26. Maitland, N.J. and A.T. Collins, *Prostate cancer stem cells: a new target for therapy.* Journal of clinical oncology, 2008. **26**(17): p. 2862-2870.
27. Verhagen, A.P., et al., *Colocalization of basal and luminal cell-type cytokeratins in human prostate cancer.* Cancer research, 1992. **52**(22): p. 6182-6187.
28. Okada, H., et al., *Keratin profiles in normal/hyperplastic prostates and prostate carcinoma.* Virchows Archiv, 1992. **421**(2): p. 157-161.
29. Sherwood, E.R., et al., *Differential cytokeratin expression in normal, hyperplastic and malignant epithelial cells from human prostate.* The Journal of urology, 1990. **143**(1): p. 167-171.
30. Sherwood, E.R., et al., *Differential expression of specific cytokeratin polypeptides in the basal and luminal epithelia of the human prostate.* The Prostate, 1991. **18**(4): p. 303-314.
31. Schalken, J.A. and G. van Leenders, *Cellular and molecular biology of the prostate: stem cell biology.* Urology, 2003. **62**(5): p. 11-20.
32. Denmeade, S.R., X.S. Lin, and J.T. Isaacs, *Role of programmed (apoptotic) cell death during the progression and therapy for prostate cancer.* The Prostate, 1996. **28**(4): p. 251-265.
33. Liu, A.Y., et al., *Cell–cell interaction in prostate gene regulation and cytodifferentiation.* Proceedings of the National Academy of Sciences, 1997. **94**(20): p. 10705-10710.
34. Isaacs, J., *Growth regulation of normal and malignant prostatic cells.* First international consulation on prostate cancer., 1996: p. 31-81.
35. Bonkhoff, H., U. Stein, and K. Remberger, *The proliferative function of basal cells in the normal and hyperplastic human prostate.* The Prostate, 1994. **24**(3): p. 114-118.
36. Nagle, R.B., et al., *Phenotypic relationships of prostatic intraepithelial neoplasia to invasive prostatic carcinoma.* The American journal of pathology, 1991. **138**(1): p. 119.
37. Yang, Y., et al., *Differential expression of cytokeratin mRNA and protein in normal prostate, prostatic intraepithelial neoplasia, and invasive carcinoma.* The American journal of pathology, 1997. **150**(2): p. 693.
38. Van Leenders, G., et al., *Demonstration of intermediate cells during human prostate epithelial differentiation in situ and in vitro using triple-staining confocal scanning microscopy.* Laboratory investigation, 2000. **80**(8): p. 1251.
39. Richardson, G.D., et al., *CD133, a novel marker for human prostatic epithelial stem cells.* Journal of cell science, 2004. **117**(16): p. 3539-3545.
40. Signoretti, S., et al., *p63 is a prostate basal cell marker and is required for prostate development.* The American journal of pathology, 2000. **157**(6): p. 1769-1775.
41. van Leenders, G.J., et al., *Intermediate cells in human prostate epithelium are enriched in proliferative inflammatory atrophy.* The American journal of pathology, 2003. **162**(5): p. 1529-1537.
42. Nakada, S.Y., et al., *The androgen receptor status of neuroendocrine cells in human benign and malignant prostatic tissue.* Cancer research, 1993. **53**(9): p. 1967-1970.
43. Schalken, J., *Androgen receptor mediated growth of prostate (cancer).* European Urology Supplements, 2005. **4**(8): p. 4-11.
44. Bonkhoff, H., et al., *Relation of endocrine-paracrine cells to cell proliferation in normal, hyperplastic, and neoplastic human prostate.* The Prostate, 1991. **19**(2): p. 91-98.
45. Blaschko, H., et al., *Secretion of a chromaffin granule protein, chromogranin, from the adrenal gland after splanchnic stimulation.* 1967. **215**(5096): p. 58.
46. Parimi, V., et al., *Neuroendocrine differentiation of prostate cancer: a review.* 2014. **2**(4): p. 273.
47. Schmechel, D., P.J. MARANGOS, and M.J.N. BRIGHTMAN, *Neurone-specific enolase is a molecular marker for peripheral and central neuroendocrine cells.* 1978. **276**(5690): p. 834.
48. Magi-Galluzzi, C. and M. Loda, *Molecular events in the early phases of prostate carcinogenesis.* European urology, 1996. **30**: p. 167-176.
49. Oldridge, E.E., et al., *Prostate cancer stem cells: are they androgen-responsive?* Molecular and cellular endocrinology, 2012. **360**(1): p. 14-24.
50. Potten, C.S., *The epidermal proliferative unit: the possible role of the central basal cell.* Cell Proliferation, 1974. **7**(1): p. 77-88.

51. Miller, S.J., R.M. Lavker, and T.-T. Sun, *Interpreting epithelial cancer biology in the context of stem cells: tumor properties and therapeutic implications.* Biochimica et Biophysica Acta (BBA)-Reviews on Cancer, 2005. **1756**(1): p. 25-52.
52. Baum, C.M., et al., *Isolation of a candidate human hematopoietic stem-cell population.* Proceedings of the National Academy of Sciences, 1992. **89**(7): p. 2804-2808.
53. Hudson, D.L., et al., *Proliferative heterogeneity in the human prostate: evidence for epithelial stem cells.* Laboratory investigation, 2000. **80**(8): p. 1243.
54. Collins, A.T., et al., *Identification and isolation of human prostate epithelial stem cells based on α2β1-integrin expression.* Journal of cell science, 2001. **114**(21): p. 3865-3872.
55. English, H.F., R.J. Santen, and J.T. Lsaacs, *Response of glandular versus basal rat ventral prostatic epithelial cells to androgen withdrawal and replacement.* The Prostate, 1987. **11**(3): p. 229-242.
56. Evans, G. and J. Chandler, *Cell proliferation studies in the rat prostate: II. The effects of castration and androgen-induced regeneration upon basal and secretory cell proliferation.* The Prostate, 1987. **11**(4): p. 339-351.
57. Kelly, K. and J.J. Yin, *Prostate cancer and metastasis initiating stem cells.* Cell research, 2008. **18**(5): p. 528.
58. Isaacs, J.T., H. Schulze, and D.S. Coffey, *Development of androgen resistance in prostatic cancer.* Progress in clinical and biological research, 1987. **243**: p. 21-31.
59. Isaacs, J.T. and D.S. Coffey, *Etiology and disease process of benign prostatic hyperplasia.* The Prostate, 1989. **15**(S2): p. 33-50.
60. Collins, A.T. and N.J. Maitland, *Prostate cancer stem cells.* European Journal of Cancer, 2006. **42**(9): p. 1213-1218.
61. Yin, A.H., et al., *AC133, a novel marker for human hematopoietic stem and progenitor cells.* Blood, 1997. **90**(12): p. 5002-5012.
62. Pellacani, D., et al., *Regulation of the stem cell marker CD133 is independent of promoter hypermethylation in human epithelial differentiation and cancer.* Molecular cancer, 2011. **10**(1): p. 94.
63. Lathia, J.D. and H.J.T.o. Liu, *Overview of cancer stem cells and stemness for community oncologists.* 2017. **12**(4): p. 387-399.
64. Maitland, N.J., et al., *Prostate cancer stem cells: do they have a basal or luminal phenotype?* Hormones and Cancer, 2011. **2**(1): p. 47-61.
65. Miller, S.J., R.M. Lavker, and T.-T.J.B.e.B.A.-R.o.C. Sun, *Interpreting epithelial cancer biology in the context of stem cells: tumor properties and therapeutic implications.* 2005. **1756**(1): p. 25-52.
66. Lang, S.H., et al., *Modeling the prostate stem cell niche: an evaluation of stem cell survival and expansion in vitro.* Stem cells and development, 2010. **19**(4): p. 537-546.
67. Morrison, S.J. and J. Kimble, *Asymmetric and symmetric stem-cell divisions in development and cancer.* nature, 2006. **441**(7097): p. 1068.
68. Blackwood, J.K., et al., *In situ lineage tracking of human prostatic epithelial stem cell fate reveals a common clonal origin for basal and luminal cells.* The Journal of pathology, 2011. **225**(2): p. 181-188.
69. Frame, F.M., et al., *Development and limitations of lentivirus vectors as tools for tracking differentiation in prostate epithelial cells.* Experimental cell research, 2010. **316**(19): p. 3161-3171.
70. Gaisa, N.T., et al., *Clonal architecture of human prostatic epithelium in benign and malignant conditions.* The Journal of pathology, 2011. **225**(2): p. 172-180.
71. Verhagen, A.P., et al., *Differential expression of keratins in the basal and luminal compartments of rat prostatic epithelium during degeneration and regeneration.* The Prostate, 1988. **13**(1): p. 25-38.
72. Maitland, N.J. and A.T. Collins, *Cancer stem cells-A therapeutic target?* Current opinion in molecular therapeutics, 2010. **12**(6): p. 662-673.
73. Watt, F.M. and B.L. Hogan, *Out of Eden: stem cells and their niches.* Science, 2000. **287**(5457): p. 1427-1430.
74. Krieger, J., *Classification, epidemiology and implications of chronic prostatitis in North America, Europe and Asia.* Minerva urologica e nefrologica= The Italian journal of urology and nephrology, 2004. **56**(2): p. 99-107.
75. Keltikangas-Järvinen, L., H. Järvinen, and T.J.A.o.c.r. Lehtonen, *Psychic disturbances in patients with chronic prostatis.* 1981. **13**(1): p. 45-49.

76. Krieger, J.N., et al., *Chronic pelvic pains represent the most prominent urogenital symptoms of "chronic prostatitis".* 1996. **48**(5): p. 715-722.
77. Miller, H.C.J.U., *Stress prostatitis.* 1988. **32**(6): p. 507-510.
78. Kohnen, P.W. and G.W. Drach, *Patterns of inflammation in prostatic hyperplasia: a histologic and bacteriologic study.* The Journal of urology, 1979. **121**(6): p. 755-760.
79. Nickel, J., *Prostatic inflammation in benign prostatic hyperplasia-the third component?* The Canadian journal of urology, 1994. **1**(1): p. 1-4.
80. Odunjo, E. and E. Elebute, *Chronic prostatitis in benign prostatic hyperplasia.* BJU International, 1971. **43**(3): p. 333-337.
81. Nickel, J., et al., *Asymptomatic inflammation and/or infection in benign prostatic hyperplasia.* BJU international, 1999. **84**: p. 976-981.
82. Der Heul-Nieuwenhuijsen, V., et al., *Gene expression profiling of the human prostate zones.* BJU international, 2006. **98**(4): p. 886-897.
83. Patel, N.D. and J.K.J.I.j.o.u.I.j.o.t.U.S.o.I. Parsons, *Epidemiology and etiology of benign prostatic hyperplasia and bladder outlet obstruction.* 2014. **30**(2): p. 170.
84. Schauer, I.G. and D.R.J.D. Rowley, *The functional role of reactive stroma in benign prostatic hyperplasia.* 2011. **82**(4-5): p. 200-210.
85. Claus, S., et al., *Immunohistochemical determination of age related proliferation rates in normal and benign hyperplastic human prostates.* 1993. **21**(5): p. 305-308.
86. Morrison, C., J. Thornhill, and E.J.U.r. Gaffney, *The connective tissue framework in the normal prostate, BPH and prostate cancer: analysis by scanning electron microscopy after cellular digestion.* 2000. **28**(5): p. 304-307.
87. Persu, C., et al., *TURP for BPH. How large is too large?* Journal of medicine and life, 2010. **3**(4): p. 376.
88. Tacklind, J., et al., *Finasteride for benign prostatic hyperplasia.* Cochrane Database Syst Rev. CD0060152010. PubMed/NCBI, 2009.
89. Lee, F., et al., *Use of transrectal ultrasound and prostate-specific antigen in diagnosis of prostatic intraepithelial neoplasia.* Urology, 1989. **34**(6 Suppl): p. 4-8.
90. Sakr, W., et al., *The frequency of carcinoma and intraepithelial neoplasia of the prostate in young male patients.* The Journal of urology, 1993. **150**(2): p. 379-385.
91. Bostwick, D.G., et al., *High-grade prostatic intraepithelial neoplasia.* Reviews in urology, 2004. **6**(4): p. 171.
92. McNeal, J.E. and C.E. Yemoto, *Spread of adenocarcinoma within prostatic ducts and acini: morphologic and clinical correlations.* The American journal of surgical pathology, 1996. **20**(7): p. 802-814.
93. McNeal, J.E. and D.G. Bostwick, *Intraductal dysplasia: a premalignant lesion of the prostate.* Human pathology, 1986. **17**(1): p. 64-71.
94. Bostwick, D.G. and M.K. Brawer, *Prostatic intra-epithelial neoplasia and early invasion in prostate cancer.* Cancer, 1987. **59**(4): p. 788-794.
95. Montironi, R., et al., *Prostatic intraepithelial neoplasia: its morphological and molecular diagnosis and clinical significance.* BJU international, 2011. **108**(9): p. 1394-1401.
96. McNeal, J.E., et al., *Zonal distribution of prostatic adenocarcinoma. Correlation with histologic pattern and direction of spread.* 1988. **12**(12): p. 897-906.
97. Abdalla, I., et al., *Comparison of serum prostate-specific antigen levels and PSA density in African-American, white, and Hispanic men without prostate cancer.* 1998. **51**(2): p. 300-305.
98. Van den Broeck, T., et al., *The role of single nucleotide polymorphisms in predicting prostate cancer risk and therapeutic decision making.* BioMed research international, 2014. **2014**.
99. Xu, J., et al., *Prostate cancer risk associated loci in African Americans.* 2009. **18**(7): p. 2145-2149.
100. Freedman, M.L., et al., *Admixture mapping identifies 8q24 as a prostate cancer risk locus in African-American men.* 2006. **103**(38): p. 14068-14073.
101. Stanford, J.L. and E.A. Ostrander, *Familial prostate cancer.* Epidemiologic reviews, 2001. **23**(1): p. 19-23.
102. Lojanapiwat, B., et al., *Correlation and diagnostic performance of the prostate-specific antigen level with the diagnosis, aggressiveness, and bone metastasis of prostate cancer in clinical practice.* Prostate international, 2014. **2**(3): p. 133-139.
103. Jewett, H.J., *Significance of the palpable prostatic nodule.* Journal of the American Medical Association, 1956. **160**(10): p. 838-839.

104. Stone, N.N., E.P. DeAntoni, and E.D. Crawford, *Screening for prostate cancer by digital rectal examination and prostate-specific antigen: results of prostate cancer awareness week, 1989–1992.* Urology, 1994. **44**(6): p. 18-25.
105. Smith, D.S. and W.J. Catalona, *Interexaminer variability of digital rectal examination in detecting prostate cancer.* Urology, 1995. **45**(1): p. 70-74.
106. Palmerola, R., et al., *The digital rectal examination (DRE) remains important-outcomes from a contemporary cohort of men undergoing an initial 12-18 core prostate needle biopsy.* The Canadian journal of urology, 2012. **19**(6): p. 6542-6547.
107. Bosch, J., A. Bohnen, and F.J.E.u. Groeneveld, *Validity of digital rectal examination and serum prostate specific antigen in the estimation of prostate volume in community-based men aged 50 to 78 years: the Krimpen Study.* 2004. **46**(6): p. 753-759.
108. Gann, P.H., C.H. Hennekens, and M.J. Stampfer, *A prospective evaluation of plasma prostate-specific antigen for detection of prostatic cancer.* Jama, 1995. **273**(4): p. 289-294.
109. Wang, M., et al., *Purification of a human prostate specific antigen.* Investigative urology, 1979. **17**(2): p. 159-163.
110. Andriole, G., et al., *The case for prostate cancer screening with prostate-specific antigen.* european urology supplements, 2006. **5**(12): p. 737-745.
111. Smith, M.R., S. Biggar, and M. Hussain, *Prostate-specific antigen messenger RNA is expressed in non-prostate cells: implications for detection of micrometastases.* Cancer research, 1995. **55**(12): p. 2640-2644.
112. Placer, J. and J. Morote, *Usefulness of prostatic specific antigen (PSA) for diagnosis and staging of patients with prostate cancer.* Archivos espanoles de urologia, 2011. **64**(8): p. 659-680.
113. M'liss, A.H., R.R. Bahnson, and W.J. Catalona, *Clinical use of prostate specific antigen in patients with prostate cancer.* The Journal of urology, 1989. **142**(4): p. 1011-1017.
114. Borley, N. and M.R. Feneley, *Prostate cancer: diagnosis and staging.* Asian journal of andrology, 2009. **11**(1): p. 74.
115. Thompson, I.M., et al., *Prevalence of prostate cancer among men with a prostate-specific antigen level≤ 4.0 ng per milliliter.* 2004. **350**(22): p. 2239-2246.
116. Parekh, D.J., et al., *Biomarkers for prostate cancer detection.* 2007. **178**(6): p. 2252-2259.
117. Thompson, I.M., et al., *Operating characteristics of prostate-specific antigen in men with an initial PSA level of 3.0 ng/ml or lower.* 2005. **294**(1): p. 66-70.
118. Ross, K.S., et al., *Comparative efficiency of prostate-specific antigen screening strategies for prostate cancer detection.* 2000. **284**(11): p. 1399-1405.
119. Crawford, D., P. Pinsky, and D. Chia. *PSA changes as related to the initial PSA: Data from the prostate, lung, colorectal, and ovarian (PLCO) cancer screening trial*. in *Am Soc Clin Oncol*. 2002.
120. Schröder, F.H., et al., *4-year prostate specific antigen progression and diagnosis of prostate cancer in the European Randomized Study of Screening for Prostate Cancer, section Rotterdam.* 2005. **174**(2): p. 489-494.
121. Arnsrud, R.G., et al., *Opportunistic testing versus organized prostate-specific antigen screening: outcome after 18 years in the Göteborg randomized population-based prostate cancer screening trial.* European urology, 2015. **68**(3): p. 354-360.
122. Gleason, D.F., et al., *Prediction of prognosis for prostatic adenocarcinoma by combined histological grading and clinical staging.* The Journal of urology, 1974. **111**(1): p. 58-64.
123. Gleason, D.F., *Classification of prostatic carcinomas.* Cancer chemotherapy reports, 1966. **50**(3): p. 125-128.
124. Gleason, D.F., *Histologic grading of prostate cancer: a perspective.* Human pathology, 1992. **23**(3): p. 273-279.
125. Chen, N. and Q.J.C.J.o.C.R. Zhou, *The evolving Gleason grading system.* 2016. **28**(1): p. 58.
126. Epstein, J.I., *Gleason score 2–4 adenocarcinoma of the prostate on needle biopsy: a diagnosis that should not be made*. 2000, LWW.
127. Epstein, J.I., *An update of the Gleason grading system.* The Journal of urology, 2010. **183**(2): p. 433-440.
128. Pierorazio, P.M., et al., *Prognostic G leason grade grouping: data based on the modified G leason scoring system.* 2013. **111**(5): p. 753-760.
129. Epstein, J.I., et al., *A contemporary prostate cancer grading system: a validated alternative to the Gleason score.* 2016. **69**(3): p. 428-435.
130. Berney, D.M., et al., *Validation of a contemporary prostate cancer grading system using prostate cancer death as outcome.* 2016. **114**(10): p. 1078.

131. Epstein, J.I., *New prostate cancer grade group system correlates with prostate cancer death in addition to biochemical recurrence*. 2016, Nature Publishing Group.
132. Epstein, J.I., et al., *The 2014 International Society of Urological Pathology (ISUP) consensus conference on Gleason grading of prostatic carcinoma.* 2016. **40**(2): p. 244-252.
133. Van Der Kwast, T.H., et al., *International Society of Urological Pathology (ISUP) consensus conference on handling and staging of radical prostatectomy specimens. Working group 2: T2 substaging and prostate cancer volume.* 2011. **24**(1): p. 16.
134. Beahrs, O., et al., *American Joint Committee on Cancer Staging: Manual for Staging of Cancer*. 1992, Philadelphia, PA: Lippincott.
135. Buyyounouski, M.K., et al., *Prostate cancer–major changes in the American Joint Committee on Cancer eighth edition cancer staging manual.* 2017. **67**(3): p. 245-253.
136. Cheng, L., et al., *Evidence of independent origin of multiple tumors from patients with prostate cancer.* 1998. **90**(3): p. 233-237.
137. Ilyin, S.E., S.M. Belkowski, and C.R.J.T.i.b. Plata-Salamán, *Biomarker discovery and validation: technologies and integrative approaches.* 2004. **22**(8): p. 411-416.
138. Bensalah, K., F. Montorsi, and S.F.J.E.u. Shariat, *Challenges of cancer biomarker profiling.* 2007. **52**(6): p. 1601-1609.
139. Prensner, J.R., et al., *Beyond PSA: the next generation of prostate cancer biomarkers.* 2012. **4**(127): p. 127rv3-127rv3.
140. Amin Al Olama, A., et al., *Multiple novel prostate cancer susceptibility signals identified by fine-mapping of known risk loci among Europeans.* 2015. **24**(19): p. 5589-5602.
141. Saunders, E.J., et al., *Fine-mapping the HOXB region detects common variants tagging a rare coding allele: evidence for synthetic association in prostate cancer.* 2014. **10**(2): p. e1004129.
142. Ewing, C.M., et al., *Germline mutations in HOXB13 and prostate-cancer risk.* 2012. **366**(2): p. 141-149.
143. Schnitt, S.J.J.J.M., *Traditional and newer pathologic factors.* 2001. **2001**(30): p. 22-26.
144. Balk, S.P., Y.-J. Ko, and G.J.J.J.o.C.O. Bubley, *Biology of prostate-specific antigen.* 2003. **21**(2): p. 383-391.
145. Hedenfalk, I., et al., *Gene-expression profiles in hereditary breast cancer.* 2001. **344**(8): p. 539-548.
146. Brawer, M.K.J.C.a.c.j.f.c., *Prostate-specific antigen: Current status.* 1999. **49**(5): p. 264-281.
147. Lilja, H., D. Ulmert, and A.J.J.N.R.C. Vickers, *Prostate-specific antigen and prostate cancer: prediction, detection and monitoring.* 2008. **8**(4): p. 268.
148. Wolf, A.M., et al., *American Cancer Society guideline for the early detection of prostate cancer: update 2010.* 2010. **60**(2): p. 70-98.
149. Schröder, F.H., et al., *Early detection of prostate cancer in 2007: part 1: PSA and PSA kinetics.* 2008. **53**(3): p. 468-477.
150. Lucia, M.S., et al., *Pathologic characteristics of cancers detected in the Prostate Cancer Prevention Trial: implications for prostate cancer detection and chemoprevention.* 2008. **1**(3): p. 167-173.
151. Stamey, T.A., et al., *Prostate-specific antigen as a serum marker for adenocarcinoma of the prostate.* 1987. **317**(15): p. 909-916.
152. Carter, H.B., et al., *Detection of life-threatening prostate cancer with prostate-specific antigen velocity during a window of curability.* 2006. **98**(21): p. 1521-1527.
153. Ulmert, D., et al., *Long-term prediction of prostate cancer: prostate-specific antigen (PSA) velocity is predictive but does not improve the predictive accuracy of a single PSA measurement 15 years or more before cancer diagnosis in a large, representative, unscreened population.* 2008. **26**(6): p. 835-841.
154. Lilja, H., et al., *Prostate-specific antigen in serum occurs predominantly in complex with alpha 1-antichymotrypsin.* 1991. **37**(9): p. 1618-1625.
155. Catalona, W.J., et al., *Use of the percentage of free prostate-specific antigen to enhance differentiation of prostate cancer from benign prostatic disease: a prospective multicenter clinical trial.* 1998. **279**(19): p. 1542-1547.
156. Prestigiacomo, A.F., et al., *A comparison of the free fraction of serum prostate specific antigen in men with benign and cancerous prostates: the best case scenario.* 1996. **156**(2): p. 350-354.
157. Catalona, W.J., et al., *Serum pro-prostate specific antigen preferentially detects aggressive prostate cancers in men with 2 to 4 ng/ml prostate specific antigen.* 2004. **171**(6): p. 2239-2244.

158. Piironen, T., et al., *In vitro stability of free prostate-specific antigen (PSA) and prostate-specific antigen (PSA) complexed to α1-antichymotrypsin in blood samples.* 1996. **48**(6): p. 81-87.
159. Ornstein, D.K., et al., *Effect of digital rectal examination and needle biopsy on serum total and percentage of free prostate specific antigen levels.* 1997. **157**(1): p. 195-198.
160. Heidenreich, A., et al., *EAU guidelines on prostate cancer.* 2008. **53**(1): p. 68-80.
161. Carter, H.B., et al., *Estimation of prostatic growth using serial prostate-specific antigen measurements in men with and without prostate disease.* 1992. **52**(12): p. 3323-3328.
162. Makarov, D.V., et al., *The natural history of men treated with deferred androgen deprivation therapy in whom metastatic prostate cancer developed following radical prostatectomy.* 2008. **179**(1): p. 156-162.
163. Pound, C.R., et al., *Natural history of progression after PSA elevation following radical prostatectomy.* 1999. **281**(17): p. 1591-1597.
164. Leibovici, D., et al., *Prostate cancer progression in the presence of undetectable or low serum prostate-specific antigen level.* 2007. **109**(2): p. 198-204.
165. Bussemakers, M.J., et al., *DD3:: A new prostate-specific gene, highly overexpressed in prostate cancer.* 1999. **59**(23): p. 5975-5979.
166. Hessels, D. and J.A.J.N.R.U. Schalken, *The use of PCA3 in the diagnosis of prostate cancer.* 2009. **6**(5): p. 255.
167. Roobol, M.J., et al., *Performance of the prostate cancer antigen 3 (PCA3) gene and prostate-specific antigen in prescreened men: exploring the value of PCA3 for a first-line diagnostic test.* 2010. **58**(4): p. 475-481.
168. Haese, A., et al., *Clinical utility of the PCA3 urine assay in European men scheduled for repeat biopsy.* 2008. **54**(5): p. 1081-1088.
169. Ashley, V.A., et al., *The Use of Biomarkers in Prostate Cancer Screening and Treatment.* 2017. **19**(4): p. 221.
170. Aubin, S.M., et al., *Prostate cancer gene 3 score predicts prostate biopsy outcome in men receiving dutasteride for prevention of prostate cancer: results from the REDUCE trial.* 2011. **78**(2): p. 380-385.
171. Nakanishi, H., et al., *PCA3 molecular urine assay correlates with prostate cancer tumor volume: implication in selecting candidates for active surveillance.* 2008. **179**(5): p. 1804-1810.
172. Marks, L.S., et al., *PCA3 molecular urine assay for prostate cancer in men undergoing repeat biopsy.* 2007. **69**(3): p. 532-535.
173. Schröder, F.H., et al., *Prostate cancer antigen 3: diagnostic outcomes in men presenting with urinary prostate cancer antigen 3 scores≥ 100.* 2014. **83**(3): p. 613-616.
174. Wang, R., et al., *Rational approach to implementation of prostate cancer antigen 3 into clinical care.* 2009. **115**(17): p. 3879-3886.
175. Merola, R., et al., *PCA3 in prostate cancer and tumor aggressiveness detection on 407 high-risk patients: a National Cancer Institute experience.* Journal of Experimental & Clinical Cancer Research, 2015. **34**(1): p. 15.
176. Hessels, D., et al., *Detection of TMPRSS2-ERG fusion transcripts and prostate cancer antigen 3 in urinary sediments may improve diagnosis of prostate cancer.* 2007. **13**(17): p. 5103-5108.
177. Tomlins, S.A., et al., *Urine TMPRSS2: ERG fusion transcript stratifies prostate cancer risk in men with elevated serum PSA.* 2011. **3**(94): p. 94ra72-94ra72.
178. Steurer, S., et al., *TMPRSS2-ERG fusions are strongly linked to young patient age in low-grade prostate cancer.* 2014. **66**(6): p. 978-981.
179. Schaefer, G., et al., *Distinct ERG rearrangement prevalence in prostate cancer: higher frequency in young age and in low PSA prostate cancer.* 2013. **16**(2): p. 132.
180. Leyten, G.H., et al., *Prospective multicentre evaluation of PCA3 and TMPRSS2-ERG gene fusions as diagnostic and prognostic urinary biomarkers for prostate cancer.* 2014. **65**(3): p. 534-542.
181. Salami, S.S., et al. *Combining urinary detection of TMPRSS2: ERG and PCA3 with serum PSA to predict diagnosis of prostate cancer*. in *Urologic Oncology: Seminars and Original Investigations*. 2013. Elsevier.
182. Tomlins, S.A., et al., *Urine TMPRSS2: ERG plus PCA3 for individualized prostate cancer risk assessment.* 2016. **70**(1): p. 45-53.
183. Grönberg, H., et al., *Prostate cancer screening in men aged 50–69 years (STHLM3): a prospective population-based diagnostic study.* 2015. **16**(16): p. 1667-1676.

184. Cucchiara, V., et al., *Genomic markers in prostate cancer decision making.* 2017.
185. Cuzick, J., et al., *Prognostic value of an RNA expression signature derived from cell cycle proliferation genes in patients with prostate cancer: a retrospective study.* 2011. **12**(3): p. 245-255.
186. Mohler, J.L., et al., *Prostate cancer, version 1.2016.* 2016. **14**(1): p. 19-30.
187. Cuzick, J., et al., *Prognostic value of a cell cycle progression signature for prostate cancer death in a conservatively managed needle biopsy cohort.* 2012. **106**(6): p. 1095.
188. Cooperberg, M.R., et al., *Validation of a cell-cycle progression gene panel to improve risk stratification in a contemporary prostatectomy cohort.* 2013.
189. Erho, N., et al., *Discovery and validation of a prostate cancer genomic classifier that predicts early metastasis following radical prostatectomy.* 2013. **8**(6): p. e66855.
190. Boström, P.J., et al., *Genomic predictors of outcome in prostate cancer.* 2015. **68**(6): p. 1033-1044.
191. Gaudreau, P.-O., et al., *The Present and Future of Biomarkers in Prostate Cancer: Proteomics, Genomics, and Immunology Advancements: Supplementary Issue: Biomarkers and their Essential Role in the Development of Personalised Therapies (A).* 2016. **8**: p. BIC. S31802.
192. Klein, E.A., et al., *A 17-gene assay to predict prostate cancer aggressiveness in the context of Gleason grade heterogeneity, tumor multifocality, and biopsy undersampling.* 2014. **66**(3): p. 550-560.
193. Cullen, J., et al., *A biopsy-based 17-gene genomic prostate score predicts recurrence after radical prostatectomy and adverse surgical pathology in a racially diverse population of men with clinically low-and intermediate-risk prostate cancer.* 2015. **68**(1): p. 123-131.
194. Sharma, P., K. Zargar-Shoshtari, and J.M.J.F.s.O. Pow-Sang, *Biomarkers for prostate cancer: present challenges and future opportunities.* 2016. **2**(1).
195. Helfand, B.T., et al., *Clinical validity and utility of genetic risk scores in prostate cancer.* 2016. **18**(4): p. 509.
196. Johns, L. and R.J.B.i. Houlston, *A systematic review and meta-analysis of familial prostate cancer risk.* 2003. **91**(9): p. 789-794.
197. Helfand, B.T. and W.J.J.T.U.c.o.N.A. Catalona, *The epidemiology and clinical implications of genetic variation in prostate cancer.* 2014. **41**(2): p. 277-297.
198. Al Olama, A.A., et al., *A meta-analysis of 87,040 individuals identifies 23 new susceptibility loci for prostate cancer.* 2014. **46**(10): p. 1103.
199. Agalliu, I., et al., *Characterization of SNPs associated with prostate cancer in men of Ashkenazic descent from the set of GWAS identified SNPs: impact of cancer family history and cumulative SNP risk prediction.* 2013. **8**(4): p. e60083.
200. Hsu, F.-C., et al., *A novel prostate cancer susceptibility locus at 19q13.* 2009. **69**(7): p. 2720-2723.
201. Ghagane, S., et al., *Single Nucleotide Polymorphisms: A New Paradigm in Predicting the Risk of Prostate Cancer.* 2016. **5**(168): p. 2.
202. Hernandez, D.J., et al., *Contemporary evaluation of the D'amico risk classification of prostate cancer.* 2007. **70**(5): p. 931-935.
203. Boorjian, S.A., et al., *Mayo Clinic validation of the D'amico risk group classification for predicting survival following radical prostatectomy.* 2008. **179**(4): p. 1354-1361.
204. D'amico, A.V., et al., *Biochemical outcome after radical prostatectomy, external beam radiation therapy, or interstitial radiation therapy for clinically localized prostate cancer.* 1998. **280**(11): p. 969-974.
205. Schiffmann, J., et al. *Heterogeneity in D' Amico classification–based low-risk prostate cancer: Differences in upgrading and upstaging according to active surveillance eligibility*. in *Urologic Oncology: Seminars and Original Investigations*. 2015. Elsevier.
206. Ahmed, H.U., et al., *Diagnostic accuracy of multi-parametric MRI and TRUS biopsy in prostate cancer (PROMIS): a paired validating confirmatory study.* 2017. **389**(10071): p. 815-822.
207. Loeb, S., et al., *Systematic review of complications of prostate biopsy.* 2013. **64**(6): p. 876-892.
208. Nagle, R.B., et al., *Cytokeratin characterization of human prostatic carcinoma and its derived cell lines.* Cancer research, 1987. **47**(1): p. 281-286.
209. Grisanzio, C. and S. Signoretti, *p63 in prostate biology and pathology.* Journal of cellular biochemistry, 2008. **103**(5): p. 1354-1368.

210. De Marzo, A.M., et al., *Prostate stem cell compartments: expression of the cell cycle inhibitor p27Kip1 in normal, hyperplastic, and neoplastic cells.* The American journal of pathology, 1998. **153**(3): p. 911-919.
211. Choucair, K., et al., *PTEN genomic deletion predicts prostate cancer recurrence and is associated with low AR expression and transcriptional activity.* 2012. **12**(1): p. 543.
212. Stambolic, V., et al., *Negative regulation of PKB/Akt-dependent cell survival by the tumor suppressor PTEN.* 1998. **95**(1): p. 29-39.
213. Li, L., et al., *The emerging role of the PI3-K-Akt pathway in prostate cancer progression.* 2005. **8**(2): p. 108.
214. Prensner, J.R., A.M.J.C.o.i.g. Chinnaiyan, and development, *Oncogenic gene fusions in epithelial carcinomas.* 2009. **19**(1): p. 82-91.
215. Han, B., et al., *Fluorescence in situ hybridization study shows association of PTEN deletion with ERG rearrangement during prostate cancer progression.* 2009. **22**(8): p. 1083.
216. Abeshouse, A., et al., *The molecular taxonomy of primary prostate cancer.* 2015. **163**(4): p. 1011-1025.
217. Boutros, P.C., et al., *Spatial genomic heterogeneity within localized, multifocal prostate cancer.* 2015. **47**(7): p. 736.
218. Cooper, C.S., et al., *Analysis of the genetic phylogeny of multifocal prostate cancer identifies multiple independent clonal expansions in neoplastic and morphologically normal prostate tissue.* 2015. **47**(4): p. 367.
219. Van Etten, J.L. and S.M.J.E.-r.c. Dehm, *Clonal origin and spread of metastatic prostate cancer.* 2016: p. ERC-16-0049.
220. Baca, S.C., et al., *Punctuated evolution of prostate cancer genomes.* 2013. **153**(3): p. 666-677.
221. Stephens, P.J., et al., *Massive genomic rearrangement acquired in a single catastrophic event during cancer development.* 2011. **144**(1): p. 27-40.
222. Abate-Shen, C., M.M.J.G. Shen, and development, *Molecular genetics of prostate cancer.* 2000. **14**(19): p. 2410-2434.
223. Ramalingam, S., V.P. Ramamurthy, and V.C. Njar, *Dissecting major signaling pathways in prostate cancer development and progression: Mechanisms and novel therapeutic targets.* The Journal of steroid biochemistry and molecular biology, 2017. **166**: p. 16-27.
224. Loblaw, D.A., et al., *Initial hormonal management of androgen-sensitive metastatic, recurrent, or progressive prostate cancer: 2007 update of an American Society of Clinical Oncology practice guideline.* Journal of Clinical Oncology, 2007. **25**(12): p. 1596-1605.
225. Pienta, K.J. and D. Bradley, *Mechanisms underlying the development of androgen-independent prostate cancer.* Clinical Cancer Research, 2006. **12**(6): p. 1665-1671.
226. Shen, M.M., C.J.G. Abate-Shen, and development, *Molecular genetics of prostate cancer: new prospects for old challenges.* 2010. **24**(18): p. 1967-2000.
227. Gregory, C.W., et al., *Androgen receptor expression in androgen-independent prostate cancer is associated with increased expression of androgen-regulated genes.* Cancer research, 1998. **58**(24): p. 5718-5724.
228. Taylor, B.S., et al., *Integrative genomic profiling of human prostate cancer.* 2010. **18**(1): p. 11-22.
229. Sharma, A., et al., *The retinoblastoma tumor suppressor controls androgen signaling and human prostate cancer progression.* 2010. **120**(12): p. 4478-4492.
230. Scher, H.I. and C.L. Sawyers, *Biology of progressive, castration-resistant prostate cancer: directed therapies targeting the androgen-receptor signaling axis.* Journal of Clinical Oncology, 2005. **23**(32): p. 8253-8261.
231. Obinata, D., et al., *Oct1 regulates cell growth of LNCaP cells and is a prognostic factor for prostate cancer.* 2012. **130**(5): p. 1021-1028.
232. Steinkamp, M.P., et al., *Treatment-dependent androgen receptor mutations in prostate cancer exploit multiple mechanisms to evade therapy.* Cancer research, 2009. **69**(10): p. 4434-4442.
233. Dehm, S.M., et al., *Selective Role of an NH2-Terminal WxxLF Motif for Aberrant Androgen Receptor Activation in Androgen Depletion–Independent Prostate Cancer Cells.* Cancer research, 2007. **67**(20): p. 10067-10077.
234. Dehm, S.M. and D.J. Tindall, *Alternatively spliced androgen receptor variants.* Endocrine-related cancer, 2011. **18**(5): p. R183-R196.
235. Gao, H., et al., *Combinatorial activities of Akt and B-Raf/Erk signaling in a mouse model of androgen-independent prostate cancer.* Proceedings of the National Academy of Sciences, 2006. **103**(39): p. 14477-14482.

236. Gao, H., et al., *Emergence of androgen independence at early stages of prostate cancer progression in Nkx3. 1; Pten mice.* Cancer research, 2006. **66**(16): p. 7929-7933.
237. Xiao-Yan, Z., et al., *Glucocorticoids can promote androgen-independent growth of prostate cancer cells through a mutated androgen receptor.* Nature medicine, 2000. **6**(6): p. 703.
238. Culig, Z., et al., *Mutant androgen receptor detected in an advanced-stage prostatic carcinoma is activated by adrenal androgens and progesterone.* Molecular endocrinology, 1993. **7**(12): p. 1541-1550.
239. Daniels, G., et al., *Mini-review: androgen receptor phosphorylation in prostate cancer.* 2013. **1**(1): p. 25.
240. Reya, T., et al., *Stem cells, cancer, and CSCs.* Nature, 2001. **414**(6859): p. 105-111.
241. Ma, I. and A.L. Allan, *The role of human aldehyde dehydrogenase in normal and cancer stem cells.* Stem cell reviews and reports, 2011. **7**(2): p. 292-306.
242. Koren, E. and Y. Fuchs, *The bad seed: Cancer stem cells in tumor development and resistance.* Drug Resistance Updates, 2016. **28**: p. 1-12.
243. Hamburger, A.W. and S.E. Salmon, *Primary bioassay of human tumor stem cells.* Science, 1977. **197**(4302): p. 461-463.
244. Sabbath, K.D., et al., *Heterogeneity of clonogenic cells in acute myeloblastic leukemia.* Journal of Clinical Investigation, 1985. **75**(2): p. 746.
245. Bonnet, D. and J.E. Dick, *Human acute myeloid leukemia is organized as a hierarchy that originates from a primitive hematopoietic cell.* Nature medicine, 1997. **3**(7): p. 730-737.
246. Al-Hajj, M., et al., *Prospective identification of tumorigenic breast cancer cells.* Proceedings of the National Academy of Sciences, 2003. **100**(7): p. 3983-3988.
247. Collins, A.T., et al., *Prospective identification of tumorigenic prostate cancer stem cells.* Cancer research, 2005. **65**(23): p. 10946-10951.
248. Heer, R., et al., *The role of androgen in determining differentiation and regulation of androgen receptor expression in the human prostatic epithelium transient amplifying population.* 2007. **212**(3): p. 572-578.
249. Williamson, S.C., et al., *Human α2β1HI CD133+ VE epithelial prostate stem cells express low levels of active androgen receptor.* 2012. **7**(11): p. e48944.
250. Eramo, A., et al., *Identification and expansion of the tumorigenic lung cancer stem cell population.* Cell death and differentiation, 2008. **15**(3): p. 504.
251. Reynolds, B.A. and S. Weiss, *Clonal and population analyses demonstrate that an EGF-responsive mammalian embryonic CNS precursor is a stem cell.* Developmental biology, 1996. **175**(1): p. 1-13.
252. Dalerba, P., et al., *Phenotypic characterization of human colorectal cancer stem cells.* Proceedings of the National Academy of Sciences, 2007. **104**(24): p. 10158-10163.
253. Li, C., et al., *Identification of pancreatic cancer stem cells.* Cancer research, 2007. **67**(3): p. 1030-1037.
254. He, X., et al., *Differentiation of a highly tumorigenic basal cell compartment in urothelial carcinoma.* Stem cells, 2009. **27**(7): p. 1487-1495.
255. Aponte, P.M. and A.J.S.c.i. Caicedo, *Stemness in cancer: stem cells, cancer stem cells, and their microenvironment.* 2017. **2017**.
256. Ma, X., et al., *Targeted biallelic inactivation of Pten in the mouse prostate leads to prostate cancer accompanied by increased epithelial cell proliferation but not by reduced apoptosis.* Cancer Research, 2005. **65**(13): p. 5730-5739.
257. Korsten, H., et al., *Accumulating progenitor cells in the luminal epithelial cell layer are candidate tumor initiating cells in a Pten knockout mouse prostate cancer model.* PLoS One, 2009. **4**(5): p. e5662.
258. Brown, M.D., et al., *Characterization of benign and malignant prostate epithelial Hoechst 33342 side populations.* The Prostate, 2007. **67**(13): p. 1384-1396.
259. Hurt, E.M., et al., *CD44+ CD24− prostate cells are early cancer progenitor/stem cells that provide a model for patients with poor prognosis.* British journal of cancer, 2008. **98**(4): p. 756.
260. Goldstein, A.S., et al., *Identification of a cell of origin for human prostate cancer.* Science, 2010. **329**(5991): p. 568-571.
261. Rajasekhar, V.K., et al., *Tumour-initiating stem-like cells in human prostate cancer exhibit increased NF-κB signalling.* 2011. **2**: p. 162.
262. Nanta, R., et al., *NVP-LDE-225 (Erismodegib) inhibits epithelial–mesenchymal transition and human prostate cancer stem cell growth in NOD/SCID IL2Rγ null mice by regulating Bmi-1 and microRNA-128.* 2013. **2**(4): p. e42.

263. Yun, E., et al., *DAB2IP regulates cancer stem cell phenotypes through modulating stem cell factor receptor and ZEB1.* 2015. **34**(21): p. 2741.
264. Yun, E.-J., et al., *Targeting cancer stem cells in castration-resistant prostate cancer.* 2016. **22**(3): p. 670-679.
265. Maitland, N.J. and A.T. Collins, *Cancer stem cells - A therapeutic target?* Curr Opin Mol Ther. **12**(6): p. 662-73.
266. Szotek, P.P., et al., *Ovarian cancer side population defines cells with stem cell-like characteristics and Mullerian Inhibiting Substance responsiveness.* Proc Natl Acad Sci U S A, 2006. **103**(30): p. 11154-9.
267. Ma, I. and A.L. Allan, *The role of human aldehyde dehydrogenase in normal and cancer stem cells.* Stem Cell Rev. **7**(2): p. 292-306.
268. Huang, E.H., et al., *Aldehyde dehydrogenase 1 is a marker for normal and malignant human colonic stem cells (SC) and tracks SC overpopulation during colon tumorigenesis.* Cancer Res, 2009. **69**(8): p. 3382-9.
269. Ginestier, C., et al., *ALDH1 is a marker of normal and malignant human mammary stem cells and a predictor of poor clinical outcome.* Cell Stem Cell, 2007. **1**(5): p. 555-67.
270. Deng, S., et al., *Distinct expression levels and patterns of stem cell marker, aldehyde dehydrogenase isoform 1 (ALDH1), in human epithelial cancers.* PLoS One. **5**(4): p. e10277.
271. Ran, D., et al., *Aldehyde dehydrogenase activity among primary leukemia cells is associated with stem cell features and correlates with adverse clinical outcomes.* Exp Hematol, 2009. **37**(12): p. 1423-34.
272. Ucar, D., et al., *Aldehyde dehydrogenase activity as a functional marker for lung cancer.* Chem Biol Interact, 2009. **178**(1-3): p. 48-55.
273. van den Hoogen, C., et al., *High aldehyde dehydrogenase activity identifies tumor-initiating and metastasis-initiating cells in human prostate cancer.* Cancer research, 2010. **70**(12): p. 5163-5173.
274. Dembinski, J.L. and S. Krauss, *Characterization and functional analysis of a slow cycling stem cell-like subpopulation in pancreas adenocarcinoma.* Clin Exp Metastasis, 2009. **26**(7): p. 611-23.
275. Franco, S.S., et al., *In vitro models of cancer stem cells and clinical applications.* BMC cancer, 2016. **16**(2): p. 738.
276. Carroll, P.R., et al., *NCCN guidelines insights: prostate cancer early detection, version 2.2016.* 2016. **14**(5): p. 509-519.
277. Moschini, M., et al., *Low-risk prostate cancer: identification, management, and outcomes.* 2017. **72**(2): p. 238-249.
278. Klotz, L., *Active surveillance for low-risk prostate cancer.* F1000 medicine reports, 2012. **4**.
279. Fascelli, M., et al., *The role of MRI in active surveillance for prostate cancer.* Current urology reports, 2015. **16**(6): p. 42.
280. Hamdy, F.C., et al., *10-year outcomes after monitoring, surgery, or radiotherapy for localized prostate cancer.* 2016. **375**(15): p. 1415-1424.
281. Crook, J.J.C.R., *The role of brachytherapy in the definitive management of prostate cancer.* 2011. **15**(3): p. 230-237.
282. Duchesne, G., *Localised prostate cancer: current treatment options.* Australian family physician, 2011. **40**(10): p. 768.
283. Koh, D.-H., et al., *Clinical outcomes of CyberKnife radiotherapy in prostate cancer patients: short-term, single-center experience.* Korean journal of urology, 2014. **55**(3): p. 172-177.
284. Ohori, M., T.M. Wheeler, and P.T.J.C. Scardino, *The new American joint committee on cancer and international union against cancer TNM classification of prostate cancer.* 1994. **74**(1): p. 104-114.
285. Trachtenberg, J., *Hormonal management of stage D carcinoma of the prostate.* Problems in urology, 1993. **7**: p. 215-215.
286. Rittmaster, R.S., *Finasteride.* New England Journal of Medicine, 1994. **330**(2): p. 120-125.
287. Peeling, W.B., *Phase III studies to compare goserelin (Zoladex) with orchiectomy and with diethylstilbestrol in treatment of prostatic carcinoma.* Urology, 1989. **33**(5): p. 45-52.
288. Mason, M.J.E.U.S., *How should we treat patients with locally advanced prostate cancer?* 2003. **2**(9): p. 14-22.
289. Labrie, F., et al., *Combination therapy with flutamide and medical (LHRH agonist) or surgical castration in advanced prostate cancer: 7-year clinical experience.* The Journal of steroid biochemistry and molecular biology, 1990. **37**(6): p. 943-950.

290. Crawford, E.D., et al., *A controlled trial of leuprolide with and without flutamide in prostatic carcinoma.* 1989. **321**(7): p. 419-424.
291. Iversen, P., et al., *Bicalutamide monotherapy compared with castration in patients with nonmetastatic locally advanced prostate cancer: 6.3 years of followup.* The Journal of urology, 2000. **164**(5): p. 1579-1582.
292. Iversen, P., et al., *Bicalutamide monotherapy compared with castration in patients with nonmetastatic locally advanced prostate cancer: 6.3 years of followup.* 2000. **164**(5): p. 1579-1582.
293. Bailar, J.C., D.P. Byar, and V.A.C.U.R. Group, *Estrogen treatment for cancer of the prostate. Early results with 3 doses of diethylstilbestrol and placebo.* Cancer, 1970. **26**(2): p. 257-261.
294. Huggins, C. and C.V.J.T.J.o.u. Hodges, *Studies on prostatic cancer: I. The effect of castration, of estrogen and of androgen injection on serum phosphatases in metastatic carcinoma of the prostate.* 2002. **168**(1): p. 9-12.
295. Nesbit, R.M. and R.T.J.S. Plumb, *Prostatic carcinoma: a follow-up on 795 patients treated prior to the endocrine era and a comparison of survival rates between these and patients treated by endocrine therapy.* 1946. **20**(2): p. 263-272.
296. Nesbit, R.M. and R.T.J.U.H.b. Plumb, *Treatment of prostatic carcinoma by castration and by administration of estrogenic hormone; a second report on comparison.* 1946. **12**: p. 14-14.
297. Blackard, C., et al., *Incidence of cardiovascular disease and death in patients receiving diethylstilbestrol for carcinoma of the prostate.* 1970. **26**(2): p. 249-256.
298. Grenader, T., et al., *Diethylstilbestrol for the treatment of patients with castration-resistant prostate cancer: retrospective analysis of a single institution experience.* 2014. **31**(1): p. 428-434.
299. Wilkins, A., et al., *Diethylstilbestrol in castration-resistant prostate cancer.* 2012. **110**(11b): p. E727-E735.
300. Rehman, Y. and J.E. Rosenberg, *Abiraterone acetate: oral androgen biosynthesis inhibitor for treatment of castration-resistant prostate cancer.* Drug design, development and therapy, 2012. **6**: p. 13.
301. Fizazi, K., et al., *Abiraterone plus prednisone in metastatic, castration-sensitive prostate cancer.* 2017. **377**(4): p. 352-360.
302. Park, J.C. and M.A. Eisenberger. *Advances in the treatment of metastatic prostate cancer*. in *Mayo Clinic Proceedings*. 2015. Elsevier.
303. Tran, C., et al., *Development of a second-generation antiandrogen for treatment of advanced prostate cancer.* 2009. **324**(5928): p. 787-790.
304. Crawford, E.D., et al., *Androgen Receptor–Targeted Treatments for Prostate Cancer: 35 Years' Progress with Antiandrogens.* 2018.
305. Hussain, M., et al., *Enzalutamide in men with nonmetastatic, castration-resistant prostate cancer.* 2018. **378**(26): p. 2465-2474.
306. Shore, N.D., et al., *Efficacy and safety of enzalutamide versus bicalutamide for patients with metastatic prostate cancer (TERRAIN): a randomised, double-blind, phase 2 study.* 2016. **17**(2): p. 153-163.
307. Yvon, A.-M.C., P. Wadsworth, and M.A. Jordan, *Taxol suppresses dynamics of individual microtubules in living human tumor cells.* Molecular biology of the cell, 1999. **10**(4): p. 947-959.
308. Graff, J.N. and E.D.J.C.e. Chamberlain, *Sipuleucel-T in the treatment of prostate cancer: an evidence-based review of its place in therapy.* 2015. **10**: p. 1.
309. Sheikh, N.A., et al., *Sipuleucel-T immune parameters correlate with survival: an analysis of the randomized phase 3 clinical trials in men with castration-resistant prostate cancer.* 2013. **62**(1): p. 137-147.
310. Higano, C.S., et al., *Integrated data from 2 randomized, double-blind, placebo-controlled, phase 3 trials of active cellular immunotherapy with sipuleucel-T in advanced prostate cancer.* 2009. **115**(16): p. 3670-3679.
311. Kantoff, P.W., et al., *Sipuleucel-T immunotherapy for castration-resistant prostate cancer.* 2010. **363**(5): p. 411-422.
312. Rane, J.K., D. Pellacani, and N.J. Maitland, *Advanced prostate cancer—a case for adjuvant differentiation therapy.* Nature reviews Urology, 2012. **9**(10): p. 595-602.
313. Brown, G. and P. Hughes, *Retinoid differentiation therapy for common types of acute myeloid leukemia.* Leukemia research and treatment, 2012. **2012**.
314. Harrison, D.E. and C.P. Lerner, *Most primitive hematopoietic stem cells are stimulated to cycle rapidly after treatment with 5-fluorouracil.* Blood, 1991. **78**(5): p. 1237-1240.

315. Bao, S., et al., *Glioma stem cells promote radioresistance by preferential activation of the DNA damage response.* Nature, 2006. **444**(7120): p. 756.
316. Liu, G., et al., *Analysis of gene expression and chemoresistance of CD133+ cancer stem cells in glioblastoma.* Molecular cancer, 2006. **5**(1): p. 67.
317. Chiou, S.-H., et al., *Identification of CD133-positive radioresistant cells in atypical teratoid/rhabdoid tumor.* PloS one, 2008. **3**(5): p. e2090.
318. Nowell, P.C.J.S., *The clonal evolution of tumor cell populations.* 1976. **194**(4260): p. 23-28.
319. Robinson, D., et al., *Integrative clinical genomics of advanced prostate cancer.* 2015. **161**(5): p. 1215-1228.
320. Grasso, C.S., et al., *The mutational landscape of lethal castration-resistant prostate cancer.* 2012. **487**(7406): p. 239.
321. Hong, M.K., et al., *Tracking the origins and drivers of subclonal metastatic expansion in prostate cancer.* 2015. **6**: p. 6605.
322. Kim, J.H., et al., *Integrative analysis of genomic aberrations associated with prostate cancer progression.* 2007. **67**(17): p. 8229-8239.
323. Lohr, J.G., et al., *Whole-exome sequencing of circulating tumor cells provides a window into metastatic prostate cancer.* 2014. **32**(5): p. 479.
324. Carreira, S., et al., *Tumor clone dynamics in lethal prostate cancer.* 2014. **6**(254): p. 254ra125-254ra125.
325. Gundem, G., et al., *The evolutionary history of lethal metastatic prostate cancer.* 2015. **520**(7547): p. 353.
326. Romanel, A., et al., *Plasma AR and abiraterone-resistant prostate cancer.* 2015. **7**(312): p. 312re10-312re10.
327. Roudier, M.P., et al., *Phenotypic heterogeneity of end-stage prostate carcinoma metastatic to bone.* 2003. **34**(7): p. 646-653.
328. Shah, R.B., et al., *Androgen-independent prostate cancer is a heterogeneous group of diseases: lessons from a rapid autopsy program.* 2004. **64**(24): p. 9209-9216.
329. Liu, W., et al., *Copy number analysis indicates monoclonal origin of lethal metastatic prostate cancer.* 2009. **15**(5): p. 559.
330. Robbins, C.M., et al., *Copy number and targeted mutational analysis reveals novel somatic events in metastatic prostate tumors.* 2011. **21**(1): p. 47-55.
331. Wan, L., K. Pantel, and Y.J.N.m. Kang, *Tumor metastasis: moving new biological insights into the clinic.* 2013. **19**(11): p. 1450.
332. Greaves, M. and C.C.J.N. Maley, *Clonal evolution in cancer.* 2012. **481**(7381): p. 306.
333. Haffner, M.C., et al., *Tracking the clonal origin of lethal prostate cancer.* 2013. **123**(11): p. 4918-4922.
334. Watson, P.A., V.K. Arora, and C.L.J.N.R.C. Sawyers, *Emerging mechanisms of resistance to androgen receptor inhibitors in prostate cancer.* 2015. **15**(12): p. 701.
335. Beltran, H., et al., *Divergent clonal evolution of castration-resistant neuroendocrine prostate cancer.* 2016. **22**(3): p. 298.
336. Hieronymus, H., et al., *Gene expression signature-based chemical genomic prediction identifies a novel class of HSP90 pathway modulators.* 2006. **10**(4): p. 321-330.
337. Chen, H., et al., *Pathogenesis of prostatic small cell carcinoma involves the inactivation of the P53 pathway.* 2012. **19**(3): p. 321-331.
338. Cunha, G. and L. Chung, *Stromal-epithelial interactions—I. Induction of prostatic phenotype in urothelium of testicular feminized (Tfm/y) mice.* Journal of steroid biochemistry, 1981. **14**(12): p. 1317-1324.
339. Tuxhorn, J.A., et al., *Reactive stroma in human prostate cancer.* Clinical Cancer Research, 2002. **8**(9): p. 2912-2923.
340. Olumi, A.F., et al., *Carcinoma-associated fibroblasts direct tumor progression of initiated human prostatic epithelium.* Cancer research, 1999. **59**(19): p. 5002-5011.
341. Polyak, K. and R.A. Weinberg, *Transitions between epithelial and mesenchymal states: acquisition of malignant and stem cell traits.* Nature reviews. Cancer, 2009. **9**(4): p. 265.
342. Mol, A., et al., *New experimental markers for early detection of high-risk prostate cancer: role of cell–cell adhesion and cell migration.* Journal of cancer research and clinical oncology, 2007. **133**(10): p. 687-695.
343. Jin, J.K., F. Dayyani, and G.E. Gallick, *Steps in prostate cancer progression that lead to bone metastasis.* International journal of cancer, 2011. **128**(11): p. 2545-2561.

344. Gravdal, K., et al., *A switch from E-cadherin to N-cadherin expression indicates epithelial to mesenchymal transition and is of strong and independent importance for the progress of prostate cancer.* Clinical Cancer Research, 2007. **13**(23): p. 7003-7011.
345. Umbas, R., et al., *Decreased E-cadherin expression is associated with poor prognosis in patients with prostate cancer.* Cancer research, 1994. **54**(14): p. 3929-3933.
346. Saha, B., et al., *Overexpression of E-cadherin and β-Catenin proteins in metastatic prostate cancer cells in bone.* The Prostate, 2008. **68**(1): p. 78-84.
347. Yilmaz, Ö.H., et al., *Pten dependence distinguishes haematopoietic stem cells from leukaemia-initiating cells.* Nature, 2006. **441**(7092): p. 475.
348. Hill, R. and H. Wu, *PTEN, stem cells, and cancer stem cells.* Journal of Biological Chemistry, 2009. **284**(18): p. 11755-11759.
349. Khemlina, G., S. Ikeda, and R.J.C.t.r. Kurzrock, *Molecular landscape of prostate cancer: implications for current clinical trials.* 2015. **41**(9): p. 761-766.
350. Huret, J.-L., et al., *Atlas of Genetics and Cytogenetics in Oncology and Haematology in 2013.* Nucleic Acids Research, 2013. **41**(Database issue): p. D920.
351. Wang, L., et al., *Hexokinase 2-mediated Warburg effect is required for PTEN-and p53-deficiency-driven prostate cancer growth.* Cell reports, 2014. **8**(5): p. 1461-1474.
352. Heselmeyer-Haddad, K.M., et al., *Single-cell genetic analysis reveals insights into clonal development of prostate cancers and indicates loss of PTEN as a marker of poor prognosis.* The American journal of pathology, 2014. **184**(10): p. 2671-2686.
353. Hilton, J., *Role of aldehyde dehydrogenase in cyclophosphamide-resistant L1210 leukemia.* Cancer research, 1984. **44**(11): p. 5156-5160.
354. Friedman, H.S., et al., *Cyclophosphamide resistance in medulloblastoma.* Cancer research, 1992. **52**(19): p. 5373-5378.
355. Sreerama, L. and N.E. Sladek, *Cellular levels of class 1 and class 3 aldehyde dehydrogenases and certain other drug-metabolizing enzymes in human breast malignancies.* Clinical Cancer Research, 1997. **3**(11): p. 1901-1914.
356. Abdullah, L.N. and E.K.-H. Chow, *Mechanisms of chemoresistance in cancer stem cells.* Clinical and translational medicine, 2013. **2**(1): p. 3.
357. Rodriguez-Torres, M. and A.L. Allan, *Aldehyde dehydrogenase as a marker and functional mediator of metastasis in solid tumors.* Clinical & experimental metastasis, 2016. **33**(1): p. 97-113.
358. Honoki, K., et al., *Possible involvement of stem-like populations with elevated ALDH1 in sarcomas for chemotherapeutic drug resistance.* Oncology reports, 2010. **24**(2): p. 501-505.
359. Di, C. and Y. Zhao, *Multiple drug resistance due to resistance to stem cells and stem cell treatment progress in cancer.* Experimental and therapeutic medicine, 2015. **9**(2): p. 289-293.
360. Vasiliou, V. and D.W. Nebert, *Analysis and update of the human aldehyde dehydrogenase (ALDH) gene family.* Human genomics, 2005. **2**(2): p. 138.
361. Vasiliou, V., et al., *Eukaryotic aldehyde dehydrogenase (ALDH) genes: human polymorphisms, and recommended nomenclature based on divergent evolution and chromosomal mapping.* Pharmacogenetics and Genomics, 1999. **9**(4): p. 421-434.
362. Marchitti, S.A., et al., *Non-P450 aldehyde oxidizing enzymes: the aldehyde dehydrogenase superfamily.* Expert Opin Drug Metab Toxicol, 2008. **4**(6): p. 697-720.
363. Sladek, N.E., *Human aldehyde dehydrogenases: potential pathological, pharmacological, and toxicological impact.* J Biochem Mol Toxicol, 2003. **17**(1): p. 7-23.
364. Stewart, M.J., K. Malek, and D.W. Crabb, *Distribution of messenger RNAs for aldehyde dehydrogenase 1, aldehyde dehydrogenase 2, and aldehyde dehydrogenase 5 in human tissues.* J Investig Med, 1996. **44**(2): p. 42-6.
365. Yanagawa, Y., et al., *The transcriptional regulation of human aldehyde dehydrogenase I gene. The structural and functional analysis of the promoter.* J Biol Chem, 1995. **270**(29): p. 17521-7.
366. Vasiliou, V., A. Pappa, and T. Estey, *Role of human aldehyde dehydrogenases in endobiotic and xenobiotic metabolism.* Drug metabolism reviews, 2004. **36**(2): p. 279-299.
367. Alnouti, Y. and C. Klaassen, *Tissue distribution, ontogeny, and regulation of aldehyde dehydrogenase (Aldh) enzymes mRNA by prototypical microsomal enzyme inducers in mice.* Toxicological sciences: an official journal of the Society of Toxicology, 2008. **101**(1): p. 51-64.
368. Koppaka, V., et al., *Aldehyde dehydrogenase inhibitors: a comprehensive review of the pharmacology, mechanism of action, substrate specificity, and clinical application.* Pharmacological reviews, 2012. **64**(3): p. 520-539.

369. Muzio, G., et al., *Aldehyde dehydrogenases and cell proliferation.* Free Radical Biology and Medicine, 2012. **52**(4): p. 735-746.
370. Pors, K. and J.S. Moreb, *Aldehyde dehydrogenases in cancer: an opportunity for biomarker and drug development?* Drug discovery today, 2014. **19**(12): p. 1953-1963.
371. Vasiliou, V. and D.W. Nebert, *Analysis and update of the human aldehyde dehydrogenase (ALDH) gene family.* Hum Genomics, 2005. **2**(2): p. 138-43.
372. Black, W.J., et al., *Human aldehyde dehydrogenase genes: alternatively spliced transcriptional variants and their suggested nomenclature.* Pharmacogenet Genomics, 2009. **19**(11): p. 893-902.
373. Marchitti, S.A., et al., *Non-P450 aldehyde oxidizing enzymes: the aldehyde dehydrogenase superfamily.* Expert opinion on drug metabolism & toxicology, 2008. **4**(6): p. 697-720.
374. Vasiliou, V., et al., *Aldehyde dehydrogenases: from eye crystallins to metabolic disease and cancer stem cells.* Chemico-biological interactions, 2013. **202**(1): p. 2-10.
375. Mitsubuchi, H., et al., *Biochemical and clinical features of hereditary hyperprolinemia.* 2014. **56**(4): p. 492-496.
376. Mills, P.B., et al., *Genotypic and phenotypic spectrum of pyridoxine-dependent epilepsy (ALDH7A1 deficiency).* 2010. **133**(7): p. 2148-2159.
377. Ehlers, C.L. and I.R.J.A.J.o.P. Gizer, *Evidence for a genetic component for substance dependence in Native Americans.* 2013. **170**(2): p. 154-164.
378. Deak, K.L., et al., *Analysis of ALDH1A2, CYP26A1, CYP26B1, CRABP1, and CRABP2 in human neural tube defects suggests a possible association with alleles in ALDH1A2.* 2005. **73**(11): p. 868-875.
379. Dupé, V., et al., *A newborn lethal defect due to inactivation of retinaldehyde dehydrogenase type 3 is prevented by maternal retinoic acid treatment.* 2003. **100**(24): p. 14036-14041.
380. Steinmetz, C.G., et al., *Structure of mitochondrial aldehyde dehydrogenase: the genetic component of ethanol aversion.* 1997. **5**(5): p. 701-711.
381. Yoshida, A., I.-Y. Huang, and M.J.P.o.t.N.A.o.S. Ikawa, *Molecular abnormality of an inactive aldehyde dehydrogenase variant commonly found in Orientals.* 1984. **81**(1): p. 258-261.
382. Farrés, J., et al., *Effects of changing glutamate 487 to lysine in rat and human liver mitochondrial aldehyde dehydrogenase. A model to study human (Oriental type) class 2 aldehyde dehydrogenase.* 1994. **269**(19): p. 13854-13860.
383. Champion, K.M., et al., *Identification of a heritable deficiency of the folate-dependent enzyme 10-formyltetrahydrofolate dehydrogenase in mice.* 1994. **91**(24): p. 11338-11342.
384. Sato, W., et al., *Hepatic gene expression in hepatocyte-specific Pten deficient mice showing steatohepatitis without ethanol challenge.* 2006. **34**(4): p. 256-265.
385. Sauer, S., et al., *Enzymatic and metabolic evidence for a region specific mitochondrial dysfunction in brains of murine succinic semialdehyde dehydrogenase deficiency (Aldh5a1−/− mice).* 2007. **50**(4): p. 653-659.
386. Chambliss, K., et al., *Molecular characterization of methylmalonate semialdehyde dehydrogenase deficiency.* 2000. **23**(5): p. 497-504.
387. Lassen, N., et al., *Multiple and Additive Functions of ALDH3A1 and ALDH1A1 CATARACT PHENOTYPE AND OCULAR OXIDATIVE DAMAGE IN Aldh3a1 (-/-)/Aldh1a1 (-/-) KNOCK-OUT MICE.* 2007. **282**(35): p. 25668-25676.
388. Rizzo, W.B.J.M.g. and metabolism, *Sjögren–Larsson syndrome: molecular genetics and biochemical pathogenesis of fatty aldehyde dehydrogenase deficiency.* 2007. **90**(1): p. 1-9.
389. Xu, Q., et al., *Association study of an SNP combination pattern in the dopaminergic pathway in paranoid schizophrenia: a novel strategy for complex disorders.* 2004. **9**(5): p. 510.
390. Kamoun, P., B. Aral, and J.J.B.d.l.A.n.d.m. Saudubray, *A new inherited metabolic disease: delta1-pyrroline 5-carboxylate synthetase deficiency.* 1998. **182**(1): p. 131-7; discussion 138-9.
391. Baumgartner, M.R., et al., *Hyperammonemia with reduced ornithine, citrulline, arginine and proline: a new inborn error caused by a mutation in the gene encoding Δ1-pyrroline-5-carboxylate synthase.* 2000. **9**(19): p. 2853-2858.
392. Marcato, P., et al., *Aldehyde dehydrogenase: its role as a cancer stem cell marker comes down to the specific isoform.* Cell Cycle. **10**(9): p. 1378-84.
393. Prockop, D.J., et al., *Evolving paradigms for repair of tissues by adult stem/progenitor cells (MSCs).* J Cell Mol Med. **14**(9): p. 2190-9.
394. Nauta, A.J. and W.E. Fibbe, *Immunomodulatory properties of mesenchymal stromal cells.* Blood, 2007. **110**(10): p. 3499-506.

395. Hess, D.A., et al., *Selection based on CD133 and high aldehyde dehydrogenase activity isolates long-term reconstituting human hematopoietic stem cells.* Blood, 2006. **107**(5): p. 2162-9.
396. Corti, S., et al., *Identification of a primitive brain-derived neural stem cell population based on aldehyde dehydrogenase activity.* Stem Cells, 2006. **24**(4): p. 975-85.
397. Zhou, P., et al., *Human progenitor cells with high aldehyde dehydrogenase activity efficiently engraft into damaged liver in a novel model.* Hepatology, 2009. **49**(6): p. 1992-2000.
398. Ibrahim, A.I., et al., *Expression and regulation of aldehyde dehydrogenases in prostate cancer.* 2018. **4**: p. 2.
399. Russo, J., et al., *4-(N,N-dipropylamino)benzaldehyde inhibits the oxidation of all-trans retinal to all-trans retinoic acid by ALDH1A1, but not the differentiation of HL-60 promyelocytic leukemia cells exposed to all-trans retinal.* BMC Pharmacol, 2002. **2**: p. 4.
400. Luo, P., et al., *Intrinsic retinoic acid receptor alpha-cyclin-dependent kinase-activating kinase signaling involves coordination of the restricted proliferation and granulocytic differentiation of human hematopoietic stem cells.* Stem Cells, 2007. **25**(10): p. 2628-37.
401. Al-Hajj, M., et al., *Prospective identification of tumorigenic breast cancer cells.* Proc Natl Acad Sci U S A, 2003. **100**(7): p. 3983-8.
402. Fillmore, C.M. and C. Kuperwasser, *Human breast cancer cell lines contain stem-like cells that self-renew, give rise to phenotypically diverse progeny and survive chemotherapy.* Breast Cancer Res, 2008. **10**(2): p. R25.
403. Ponti, D., et al., *Isolation and in vitro propagation of tumorigenic breast cancer cells with stem/progenitor cell properties.* Cancer Res, 2005. **65**(13): p. 5506-11.
404. Sheridan, C., et al., *CD44+/CD24- breast cancer cells exhibit enhanced invasive properties: an early step necessary for metastasis.* Breast Cancer Res, 2006. **8**(5): p. R59.
405. Rollins-Raval, M.A., et al., *ALDH, CA I, and CD2AP: novel, diagnostically useful immunohistochemical markers to identify erythroid precursors in bone marrow biopsy specimens.* Am J Clin Pathol. **137**(1): p. 30-8.
406. Ginestier, C., et al., *ALDH1 is a marker of normal and malignant human mammary stem cells and a predictor of poor clinical outcome.* 2007. **1**(5): p. 555-567.
407. Ucar, D., et al., *Aldehyde dehydrogenase activity as a functional marker for lung cancer.* 2009. **178**(1-3): p. 48-55.
408. Carpentino, J.E., et al., *Aldehyde dehydrogenase–expressing colon stem cells contribute to tumorigenesis in the transition from colitis to cancer.* 2009. **69**(20): p. 8208-8215.
409. Wang, L., et al., *Prospective identification of tumorigenic osteosarcoma cancer stem cells in OS99-1 cells based on high aldehyde dehydrogenase activity.* 2011. **128**(2): p. 294-303.
410. Rasheed, Z.A., et al., *Prognostic significance of tumorigenic cells with mesenchymal features in pancreatic adenocarcinoma.* 2010. **102**(5): p. 340-351.
411. Charafe-Jauffret, E., et al., *Aldehyde dehydrogenase 1–Positive cancer stem cells mediate metastasis and poor clinical outcome in inflammatory breast cancer.* 2010. **16**(1): p. 45-55.
412. Kennedy, K.A., S. Rockwell, and A.C. Sartorelli, *Preferential activation of mitomycin C to cytotoxic metabolites by hypoxic tumor cells.* Cancer research, 1980. **40**(7): p. 2356-2360.
413. Rasheed, Z.A., et al., *Prognostic significance of tumorigenic cells with mesenchymal features in pancreatic adenocarcinoma.* J Natl Cancer Inst. **102**(5): p. 340-51.
414. Sun, S. and Z. Wang, *ALDH high adenoid cystic carcinoma cells display cancer stem cell properties and are responsible for mediating metastasis.* Biochem Biophys Res Commun. **396**(4): p. 843-8.
415. Su, Y., et al., *Aldehyde dehydrogenase 1 A1-positive cell population is enriched in tumor-initiating cells and associated with progression of bladder cancer.* Cancer Epidemiol Biomarkers Prev. **19**(2): p. 327-37.
416. Bortolomai, I., et al., *Tumor initiating cells: development and critical characterization of a model derived from the A431 carcinoma cell line forming spheres in suspension.* Cell Cycle. **9**(6): p. 1194-206.
417. van den Hoogen, C., et al., *High aldehyde dehydrogenase activity identifies tumor-initiating and metastasis-initiating cells in human prostate cancer.* Cancer Res. **70**(12): p. 5163-73.
418. Croker, A.K., et al., *High aldehyde dehydrogenase and expression of cancer stem cell markers selects for breast cancer cells with enhanced malignant and metastatic ability.* J Cell Mol Med, 2009. **13**(8B): p. 2236-52.
419. Mirabelli, P., et al., *Extended flow cytometry characterization of normal bone marrow progenitor cells by simultaneous detection of aldehyde dehydrogenase and early*

*hematopoietic antigens: implication for erythroid differentiation studies.* BMC Physiol, 2008. **8**: p. 13.
420. Storms, R.W., et al., *Isolation of primitive human hematopoietic progenitors on the basis of aldehyde dehydrogenase activity.* Proc Natl Acad Sci U S A, 1999. **96**(16): p. 9118-23.
421. Pearce, D.J. and D. Bonnet, *The combined use of Hoechst efflux ability and aldehyde dehydrogenase activity to identify murine and human hematopoietic stem cells.* Exp Hematol, 2007. **35**(9): p. 1437-46.
422. Marcato, P., et al., *Aldehyde dehydrogenase activity of breast cancer stem cells is primarily due to isoform ALDH1A3 and its expression is predictive of metastasis.* Stem Cells. **29**(1): p. 32-45.
423. Minn, I., et al., *A red-shifted fluorescent substrate for aldehyde dehydrogenase.* Nature communications, 2014. **5**: p. 3662.
424. Dollé, L., et al., *Next generation of ALDH substrates and their potential to study maturational lineage biology in stem and progenitor cells.* American Journal of Physiology-Gastrointestinal and Liver Physiology, 2015. **308**(7): p. G573-G578.
425. Chute, J.P., et al., *Inhibition of aldehyde dehydrogenase and retinoid signaling induces the expansion of human hematopoietic stem cells.* Proc Natl Acad Sci U S A, 2006. **103**(31): p. 11707-12.
426. Tallman, M.S., et al., *All-trans-retinoic acid in acute promyelocytic leukemia.* N Engl J Med, 1997. **337**(15): p. 1021-8.
427. Ginestier, C., et al., *Retinoid signaling regulates breast cancer stem cell differentiation.* Cell Cycle, 2009. **8**(20): p. 3297-302.
428. Moreb, J.S., et al., *Retinoic acid down-regulates aldehyde dehydrogenase and increases cytotoxicity of 4-hydroperoxycyclophosphamide and acetaldehyde.* J Pharmacol Exp Ther, 2005. **312**(1): p. 339-45.
429. Moreb, J.S., et al., *RNAi-mediated knockdown of aldehyde dehydrogenase class-1A1 and class-3A1 is specific and reveals that each contributes equally to the resistance against 4-hydroperoxycyclophosphamide.* Cancer Chemother Pharmacol, 2007. **59**(1): p. 127-36.
430. Duester, G., F.A. Mic, and A. Molotkov, *Cytosolic retinoid dehydrogenases govern ubiquitous metabolism of retinol to retinaldehyde followed by tissue-specific metabolism to retinoic acid.* Chem Biol Interact, 2003. **143-144**: p. 201-10.
431. Zhao, D., et al., *Molecular identification of a major retinoic-acid-synthesizing enzyme, a retinaldehyde-specific dehydrogenase.* Eur J Biochem, 1996. **240**(1): p. 15-22.
432. Appel, B. and J.S. Eisen, *Retinoids run rampant: multiple roles during spinal cord and motor neuron development.* Neuron, 2003. **40**(3): p. 461-4.
433. Donato, L.J. and N. Noy, *Suppression of mammary carcinoma growth by retinoic acid: proapoptotic genes are targets for retinoic acid receptor and cellular retinoic acid–binding protein II signaling.* Cancer research, 2005. **65**(18): p. 8193-8199.
434. Vezina, C.M., et al., *Retinoic acid induces prostatic bud formation.* Developmental Dynamics, 2008. **237**(5): p. 1321-1333.
435. Aboseif, S.R., et al., *Effect of retinoic acid on prostatic development.* The Prostate, 1997. **31**(3): p. 161-167.
436. Duester, G., F.A. Mic, and A.J.C.-b.i. Molotkov, *Cytosolic retinoid dehydrogenases govern ubiquitous metabolism of retinol to retinaldehyde followed by tissue-specific metabolism to retinoic acid.* 2003. **143**: p. 201-210.
437. Elizondo, G., et al., *Retinoic acid modulates retinaldehyde dehydrogenase 1 gene expression through the induction of GADD153-C/EBPbeta interaction.* Biochem Pharmacol, 2009. **77**(2): p. 248-57.
438. Leid, M., P. Kastner, and P. Chambon, *Multiplicity generates diversity in the retinoic acid signalling pathways.* Trends in biochemical sciences, 1992. **17**(10): p. 427-433.
439. Donovan, M., et al., *The cellular retinoic acid binding proteins.* The Journal of steroid biochemistry and molecular biology, 1995. **53**(1): p. 459-465.
440. Delva, L., et al., *Physical and functional interactions between cellular retinoic acid binding protein II and the retinoic acid-dependent nuclear complex.* Molecular and cellular biology, 1999. **19**(10): p. 7158-7167.
441. Glass, C.K. and M.G. Rosenfeld, *The coregulator exchange in transcriptional functions of nuclear receptors.* Genes & development, 2000. **14**(2): p. 121-141.
442. Zhang, Y. and D. Reinberg, *Transcription regulation by histone methylation: interplay between different covalent modifications of the core histone tails.* Genes & development, 2001. **15**(18): p. 2343-2360.

443. Dilworth, F.J. and P. Chambon, *Nuclear receptors coordinate the activities of chromatin remodeling complexes and coactivators to facilitate initiation of transcription.* Oncogene, 2001. **20**(24): p. 3047.
444. Rhinn, M. and P. Dollé, *Retinoic acid signalling during development.* Development, 2012. **139**(5): p. 843-858.
445. Black, W. and V. Vasiliou, *The aldehyde dehydrogenase gene superfamily resource center.* Hum Genomics, 2009. **4**(2): p. 136-42.
446. Penzes, P., X. Wang, and J.L. Napoli, *Enzymatic characteristics of retinal dehydrogenase type I expressed in Escherichia coli.* Biochim Biophys Acta, 1997. **1342**(2): p. 175-81.
447. Rexer, B.N., W.L. Zheng, and D.E. Ong, *Retinoic acid biosynthesis by normal human breast epithelium is via aldehyde dehydrogenase 6, absent in MCF-7 cells.* Cancer Res, 2001. **61**(19): p. 7065-70.
448. Lohnes, D., et al., *Developmental roles of the retinoic acid receptors.* J Steroid Biochem Mol Biol, 1995. **53**(1-6): p. 475-86.
449. Rivera-Gonzalez, G.C., et al., *Retinoic acid and androgen receptors combine to achieve tissue specific control of human prostatic transglutaminase expression: a novel regulatory network with broader significance.* Nucleic Acids Res. **40**(11): p. 4825-40.
450. Pasquali, D., C. Thaller, and G. Eichele, *Abnormal level of retinoic acid in prostate cancer tissues.* The Journal of Clinical Endocrinology & Metabolism, 1996. **81**(6): p. 2186-2191.
451. Trump, D.L., et al., *A phase II trial of all-trans-retinoic acid in hormone-refractory prostate cancer: a clinical trial with detailed pharmacokinetic analysis.* Cancer chemotherapy and pharmacology, 1997. **39**(4): p. 349-356.
452. Oldridge, E., et al., *Retinoic acid represses invasion and stem cell phenotype by induction of the metastasis suppressors RARRES1 and LXN.* Oncogenesis, 2013. **2**(4): p. e45.
453. Chen, M.-C., et al., *Retinoic acid induces apoptosis of prostate cancer DU145 cells through Cdk5 overactivation.* Evidence-Based Complementary and Alternative Medicine, 2012. **2012**.
454. Tang, X.-H. and L.J. Gudas, *Retinoids, retinoic acid receptors, and cancer.* Annual Review of Pathology: Mechanisms of Disease, 2011. **6**: p. 345-364.
455. Vinogradov, S. and X. Wei, *Cancer stem cells and drug resistance: the potential of nanomedicine.* Nanomedicine, 2012. **7**(4): p. 597-615.
456. Harris, A.L., *Hypoxia--a key regulatory factor in tumour growth.* Nature reviews. Cancer, 2002. **2**(1): p. 38.
457. Greijer, A., et al., *Up-regulation of gene expression by hypoxia is mediated predominantly by hypoxia-inducible factor 1 (HIF-1).* The Journal of pathology, 2005. **206**(3): p. 291-304.
458. Shiraishi, A., et al., *Hypoxia promotes the phenotypic change of aldehyde dehydrogenase activity of breast cancer stem cells.* 2017. **108**(3): p. 362-372.
459. Zhong, H., et al., *Overexpression of hypoxia-inducible factor 1α in common human cancers and their metastases.* Cancer research, 1999. **59**(22): p. 5830-5835.
460. Su, Y., et al., *Aldehyde dehydrogenase 1 A1–positive cell population is enriched in tumor-initiating cells and associated with progression of bladder cancer.* Cancer Epidemiology and Prevention Biomarkers, 2010. **19**(2): p. 327-337.
461. Januchowski, R., K. Wojtowicz, and M. Zabel, *The role of aldehyde dehydrogenase (ALDH) in cancer drug resistance.* Biomedicine & Pharmacotherapy, 2013. **67**(7): p. 669-680.
462. Sládek, N.E., et al., *Cellular levels of aldehyde dehydrogenases (ALDH1A1 and ALDH3A1) as predictors of therapeutic responses to cyclophosphamide-based chemotherapy of breast cancer: a retrospective study.* Cancer chemotherapy and pharmacology, 2002. **49**(4): p. 309-321.
463. Jenuwein, T. and C.D. Allis, *Translating the histone code.* Science, 2001. **293**(5532): p. 1074-1080.
464. Grunstein, M., *Histone acetylation in chromatin structure and transcription.* Nature, 1997. **389**(6649): p. 349.
465. Kim, H.-J. and S.-C. Bae, *Histone deacetylase inhibitors: molecular mechanisms of action and clinical trials as anti-cancer drugs.* American journal of translational research, 2011. **3**(2): p. 166.
466. Backs, J. and E.N. Olson, *Control of cardiac growth by histone acetylation/deacetylation.* Circulation research, 2006. **98**(1): p. 15-24.
467. Yang, M. and J.Y. Park, *DNA methylation in promoter region as biomarkers in prostate cancer.* Methods Mol Biol. **863**: p. 67-109.
468. Baylin, S.B. and J.G. Herman, *DNA hypermethylation in tumorigenesis: epigenetics joins genetics.* Trends Genet, 2000. **16**(4): p. 168-74.

469. Smiraglia, D.J. and C. Plass, *The study of aberrant methylation in cancer via restriction landmark genomic scanning.* Oncogene, 2002. **21**(35): p. 5414-26.
470. Yang, M. and J.Y. Park, *DNA methylation in promoter region as biomarkers in prostate cancer.* Cancer Epigenetics: Methods and Protocols, 2012: p. 67-109.
471. Pasquali, D., C. Thaller, and G. Eichele, *Abnormal level of retinoic acid in prostate cancer tissues.* J Clin Endocrinol Metab, 1996. **81**(6): p. 2186-91.
472. Touma, S.E., et al., *Retinoid metabolism and ALDH1A2 (RALDH2) expression are altered in the transgenic adenocarcinoma mouse prostate model.* Biochem Pharmacol, 2009. **78**(9): p. 1127-38.
473. Kim, H., et al., *The retinoic acid synthesis gene ALDH1a2 is a candidate tumor suppressor in prostate cancer.* Cancer Res, 2005. **65**(18): p. 8118-24.
474. Kim, H., et al., *The retinoic acid synthesis gene ALDH1a2 is a candidate tumor suppressor in prostate cancer.* Cancer research, 2005. **65**(18): p. 8118-8124.
475. Trasino, S.E., E.H. Harrison, and T.T. Wang, *Androgen regulation of aldehyde dehydrogenase 1A3 (ALDH1A3) in the androgen-responsive human prostate cancer cell line LNCaP.* Exp Biol Med (Maywood), 2007. **232**(6): p. 762-71.
476. Shames, D.S., et al., *A genome-wide screen for promoter methylation in lung cancer identifies novel methylation markers for multiple malignancies.* PLoS Med, 2006. **3**(12): p. e486.
477. Attard, G., et al., *A novel, spontaneously immortalized, human prostate cancer cell line, Bob, offers a unique model for pre-clinical prostate cancer studies.* The Prostate, 2009. **69**(14): p. 1507-1520.
478. BERTHON, P., et al., *Functional expression of sv40 in normal human prostatic epithelial and fibroblastic cells-differentiation pattern of nontumorigenic cell-lines.* International journal of oncology, 1995. **6**(2): p. 333-343.
479. Horoszewicz, J., et al., *The LNCaP cell line--a new model for studies on human prostatic carcinoma.* Progress in clinical and biological research, 1980. **37**: p. 115.
480. Stone, K.R., et al., *Isolation of a human prostate carcinoma cell line (DU 145).* International journal of cancer, 1978. **21**(3): p. 274-281.
481. Kaighn, M., et al., *Establishment and characterization of a human prostatic carcinoma cell line (PC-3).* Investigative urology, 1979. **17**(1): p. 16-23.
482. Chaproniere, D.M. and W.L. McKeehan, *Serial culture of single adult human prostatic epithelial cells in serum-free medium containing low calcium and a new growth factor from bovine brain.* Cancer research, 1986. **46**(2): p. 819-824.
483. Huang, H.-L., et al., *Trypsin-induced proteome alteration during cell subculture in mammalian cells.* 2010. **17**(1): p. 36.
484. Moreb, J.S., et al., *The enzymatic activity of human aldehyde dehydrogenases 1A2 and 2 (ALDH1A2 and ALDH2) is detected by Aldefluor, inhibited by diethylaminobenzaldehyde and has significant effects on cell proliferation and drug resistance.* Chemico-biological interactions, 2012. **195**(1): p. 52-60.
485. O'Neill, A.J., et al., *Characterisation and manipulation of docetaxel resistant prostate cancer cell lines.* Molecular cancer, 2011. **10**(1): p. 126.
486. Frame, F.M., et al., *Mechanisms of growth inhibition of primary prostate epithelial cells following gamma irradiation or photodynamic therapy include senescence, necrosis, and autophagy, but not apoptosis.* 2016. **5**(1): p. 61-73.
487. Quent, V.M., et al., *Discrepancies between metabolic activity and DNA content as tool to assess cell proliferation in cancer research.* 2010. **14**(4): p. 1003-1013.
488. Birnie, R., et al., *Gene expression profiling of human prostate cancer stem cells reveals a pro-inflammatory phenotype and the importance of extracellular matrix interactions.* Genome biology, 2008. **9**(5): p. R83.
489. Ju, Z., et al., *Effects of 5-Aza-2'-deoxycitydine and trichostatin A on expression and apoptosis of ALDH1a2 gene in human bladder cancer cell lines.* Zhonghua wai ke za zhi [Chinese journal of surgery], 2010. **48**(5): p. 378-382.
490. van den Hoogen, C., et al., *The aldehyde dehydrogenase enzyme 7A1 is functionally involved in prostate cancer bone metastasis.* Clinical & experimental metastasis, 2011. **28**(7): p. 615-625.
491. Frame, F., et al., *HDAC inhibitor confers radiosensitivity to prostate stem-like cells.* British journal of cancer, 2013. **109**(12): p. 3023.
492. Chazotte, B.J.C.S.H.P., *Labeling cytoskeletal F-actin with rhodamine phalloidin or fluorescein phalloidin for imaging.* 2010. **2010**(5): p. pdb. prot4947.

493. Smith, P.J., M. Wiltshire, and R.J.J.C.p.i.c. Errington, *DRAQ 5 Labeling of Nuclear DNA in Live and Fixed Cells.* 2004. **28**(1): p. 7.25. 1-7.25. 11.
494. Chazotte, B.J.C.S.H.P., *Labeling mitochondria with fluorescent dyes for imaging.* 2009. **2009**(6): p. pdb. prot4948.
495. Rodrigues, Â., et al., *Biopsy sampling and histopathological markers for diagnosis of prostate cancer.* 2014. **14**(11): p. 1323-1336.
496. Kim, H.-J. and S.-C.J.A.j.o.t.r. Bae, *Histone deacetylase inhibitors: molecular mechanisms of action and clinical trials as anti-cancer drugs.* 2011. **3**(2): p. 166.
497. Eckschlager, T., et al., *Histone deacetylase inhibitors as anticancer drugs.* 2017. **18**(7): p. 1414.
498. Matak, D., et al., *Colony, hanging drop, and methylcellulose three dimensional hypoxic growth optimization of renal cell carcinoma cell lines.* 2017. **69**(4): p. 565-578.
499. McMahon, K., et al., *Characterization of changes in the proteome in different regions of 3D multicell tumor spheroids.* Journal of proteome research, 2012. **11**(5): p. 2863-2875.
500. Li, T., et al., *ALDH1A1 is a marker for malignant prostate stem cells and predictor of prostate cancer patients' outcome.* Laboratory investigation; a journal of technical methods and pathology, 2010. **90**(2): p. 234.
501. Yan, J., et al., *Aldehyde dehydrogenase 3A1 associates with prostate tumorigenesis.* British journal of cancer, 2014. **110**(10): p. 2593.
502. Milone, M.R., et al., *Proteomic analysis of zoledronic-acid resistant prostate cancer cells unveils novel pathways characterizing an invasive phenotype.* Oncotarget, 2015. **6**(7): p. 5324.
503. Zekri, J., M. Mansour, and S.M.J.J.o.b.o. Karim, *The anti-tumour effects of zoledronic acid.* 2014. **3**(1): p. 25-35.
504. Chen, K., Y.-h. Huang, and J.-l. Chen, *Understanding and targeting cancer stem cells: therapeutic implications and challenges.* Acta Pharmacologica Sinica, 2013. **34**(6): p. 732.
505. Kakarala, M., et al., *Targeting breast stem cells with the cancer preventive compounds curcumin and piperine.* Breast cancer research and treatment, 2010. **122**(3): p. 777-785.
506. Agrawal, N., et al., *RNA interference: biology, mechanism, and applications.* Microbiology and molecular biology reviews, 2003. **67**(4): p. 657-685.
507. Davidson, B.L. and P.B. McCray Jr, *Current prospects for RNA interference-based therapies.* Nature reviews. Genetics, 2011. **12**(5): p. 329.
508. Rao, D.D., et al., *siRNA vs. shRNA: similarities and differences.* Advanced drug delivery reviews, 2009. **61**(9): p. 746-759.
509. Hamilton, A.J. and D.C. Baulcombe, *A species of small antisense RNA in posttranscriptional gene silencing in plants.* Science, 1999. **286**(5441): p. 950-952.
510. DJIKENG, A., et al., *RNA interference in Trypanosoma brucei: cloning of small interfering RNAs provides evidence for retroposon-derived 24–26-nucleotide RNAs.* Rna, 2001. **7**(11): p. 1522-1530.
511. Allison, S.J. and J. Milner, *RNA Interference by Single-and Double-stranded siRNA With a DNA Extension Containing a 3' Nuclease-resistant Mini-hairpin Structure.* Molecular Therapy-Nucleic Acids, 2014. **3**.
512. Cullen, B.R., *RNAi the natural way.* Nature genetics, 2005. **37**(11): p. 1163-1165.
513. Le, Y., et al., *The nuclear RNase III Drosha initiates microRNA processing.* nature, 2003. **425**(6956): p. 415.
514. Lee, Y., et al., *MicroRNA maturation: stepwise processing and subcellular localization.* The EMBO journal, 2002. **21**(17): p. 4663-4670.
515. Yi, R., et al., *Exportin-5 mediates the nuclear export of pre-microRNAs and short hairpin RNAs.* Genes & development, 2003. **17**(24): p. 3011-3016.
516. Malumbres, M. and M.J.N.r.c. Barbacid, *Cell cycle, CDKs and cancer: a changing paradigm.* 2009. **9**(3): p. 153.
517. Kitazumi, I. and M.J.T.F.j. Tsukahara, *Regulation of DNA fragmentation: the role of caspases and phosphorylation.* 2011. **278**(3): p. 427-441.
518. Niklaus, M., et al., *Expression analysis of LC3B and p62 indicates intact activated autophagy is associated with an unfavorable prognosis in colon cancer.* 2017. **8**(33): p. 54604.
519. Chan, F.K.-M., K. Moriwaki, and M.J. De Rosa, *Detection of necrosis by release of lactate dehydrogenase activity*, in *Immune Homeostasis*. 2013, Springer. p. 65-70.
520. Chen, M.-H., et al., *ALDH1A3, the major aldehyde dehydrogenase isoform in human cholangiocarcinoma cells, affects prognosis and gemcitabine resistance in cholangiocarcinoma patients.* Clinical Cancer Research, 2016. **22**(16): p. 4225-4235.

521. Rodriguez, L.G., X. Wu, and J.-L. Guan, *Wound-healing assay.* Cell Migration: Developmental Methods and Protocols, 2005: p. 23-29.
522. Shao, C., et al., *Essential role of aldehyde dehydrogenase 1A3 (ALDH1A3) for the maintenance of non-small cell lung cancer stem cells is associated with the STAT3 pathway.*
523. Yu, C., et al., *ALDH activity indicates increased tumorigenic cells, but not cancer stem cells, in prostate cancer cell lines.* in vivo, 2011. **25**(1): p. 69-76.
524. Kakizuka, A., et al., *Chromosomal translocation t (15; 17) in human acute promyelocytic leukemia fuses RARα with a novel putative transcription factor, PML.* Cell, 1991. **66**(4): p. 663-674.
525. Coyle, K., et al., *Retinoid signaling in cancer and its promise for therapy.* J Carcinog Mutagen S, 2013. **7**: p. 16-18.
526. Seruga, B., A. Ocana, and I.F. Tannock, *Drug resistance in metastatic castration-resistant prostate cancer.* Nature reviews Clinical oncology, 2011. **8**(1): p. 12-23.
527. Moretti, A., et al., *Crystal structure of human aldehyde dehydrogenase 1A3 complexed with NAD+ and retinoic acid.* Scientific reports, 2016. **6**.
528. Moreb, J.S., et al., *Heterogeneity of aldehyde dehydrogenase expression in lung cancer cell lines is revealed by Aldefluor flow cytometry-based assay.* Cytometry Part B: Clinical Cytometry, 2007. **72**(4): p. 281-289.
529. Marcato, P., et al., *Aldehyde dehydrogenase 1A3 influences breast cancer progression via differential retinoic acid signaling.* Molecular oncology, 2015. **9**(1): p. 17-31.
530. Li, X., et al., *Aldehyde dehydrogenase 1A1 possesses stem-like properties and predicts lung cancer patient outcome.* Journal of Thoracic Oncology, 2012. **7**(8): p. 1235-1245.
531. Flahaut, M., et al., *Aldehyde dehydrogenase activity plays a Key role in the aggressive phenotype of neuroblastoma.* BMC cancer, 2016. **16**(1): p. 781.
532. Wang, S., et al., *ALDH1A3 correlates with luminal phenotype in prostate cancer.* Tumor Biology, 2017. **39**(4): p. 1010428317703652.
533. Casanova-Salas, I., et al., *MiR-187 targets the androgen-regulated gene ALDH1A3 in prostate cancer.* PloS one, 2015. **10**(5): p. e0125576.
534. Mao, P., et al., *Mesenchymal glioma stem cells are maintained by activated glycolytic metabolism involving aldehyde dehydrogenase 1A3.* 2013. **110**(21): p. 8644-8649.
535. Kurdyukov, S. and M.J.B. Bullock, *DNA methylation analysis: choosing the right method.* 2016. **5**(1): p. 3.
536. Wojdacz, T.K., A. Dobrovic, and L.L.J.N.p. Hansen, *Methylation-sensitive high-resolution melting.* 2008. **3**(12): p. 1903.
537. Das, P.M., et al., *Chromatin immunoprecipitation assay.* 2004. **37**(6): p. 961-969.
538. Martins, R.P., et al., *Tracking chromatin states using controlled DNase I treatment and real-time PCR.* 2007. **12**(4): p. 545.
539. DeAngelis, J.T., W.J. Farrington, and T.O.J.M.b. Tollefsbol, *An overview of epigenetic assays.* 2008. **38**(2): p. 179-183.
540. Moreb, J.S., et al., *Retinoic acid down-regulates aldehyde dehydrogenase and increases cytotoxicity of 4-hydroperoxycyclophosphamide and acetaldehyde.* 2005. **312**(1): p. 339-345.
541. van den Hoogen, C., et al., *The aldehyde dehydrogenase enzyme 7A1 is functionally involved in prostate cancer bone metastasis.* Clin Exp Metastasis. **28**(7): p. 615-25.
542. McKenna, D.J., et al., *Current challenges and opportunities in treating hypoxic prostate tumors.* 2018. **4**: p. 2.
543. Lee, J., et al., *Tumor stem cells derived from glioblastomas cultured in bFGF and EGF more closely mirror the phenotype and genotype of primary tumors than do serum-cultured cell lines.* Cancer cell, 2006. **9**(5): p. 391-403.
544. Izadpanah, R., et al., *Long-term in vitro expansion alters the biology of adult mesenchymal stem cells.* Cancer research, 2008. **68**(11): p. 4229-4238.
545. Jones, P.A., et al., *De novo methylation of the MyoD1 CpG island during the establishment of immortal cell lines.* Proceedings of the National Academy of Sciences, 1990. **87**(16): p. 6117-6121.
546. Frame, F.M., et al., *Harvesting human prostate tissue material and culturing primary prostate epithelial cells*, in *The Nuclear Receptor Superfamily*. 2016, Springer. p. 181-201.
547. Torrecilla, J., et al., *Lipid nanoparticles as carriers for RNAi against viral infections: current status and future perspectives.* BioMed research international, 2014. **2014**.
548. Jackson, A.L. and P.S.J.N.r.D.d. Linsley, *Recognizing and avoiding siRNA off-target effects for target identification and therapeutic application.* 2010. **9**(1): p. 57.
549. Muzio, G., et al., *Aldehyde dehydrogenases and cell proliferation.* 2012. **52**(4): p. 735-746.

550. Hanahan, D. and R.A. Weinberg, *Hallmarks of cancer: the next generation.* cell, 2011. **144**(5): p. 646-674.
551. Rasheed, Z.A., et al., *Prognostic significance of tumorigenic cells with mesenchymal features in pancreatic adenocarcinoma.* Journal of the National Cancer Institute, 2010. **102**(5): p. 340-351.
552. Thiery, J.P., *Epithelial-mesenchymal transitions in tumour progression.* Nature reviews. Cancer, 2002. **2**(6): p. 442.
553. Reya, T., et al., *Stem cells, cancer, and cancer stem cells.* nature, 2001. **414**(6859): p. 105.
554. Moitra, K., *Overcoming multidrug resistance in cancer stem cells.* BioMed research international, 2015. **2015**.
555. Vinogradov, S. and X.J.N. Wei, *Cancer stem cells and drug resistance: the potential of nanomedicine.* 2012. **7**(4): p. 597-615.
556. Stewart, G.D., et al., *The relevance of a hypoxic tumour microenvironment in prostate cancer.* 2010. **105**(1): p. 8-13.
557. Cojoc, M., et al., *Aldehyde dehydrogenase is regulated by β-catenin/TCF and promotes radioresistance in prostate cancer progenitor cells.* 2015.
558. Marcato, P., et al., *Aldehyde dehydrogenase: its role as a cancer stem cell marker comes down to the specific isoform.* 2011. **10**(9): p. 1378-1384.
559. Friedman, R.C., et al., *Most mammalian mRNAs are conserved targets of microRNAs.* Genome research, 2009. **19**(1): p. 92-105.
560. Kwak, P.B., S. Iwasaki, and Y. Tomari, *The microRNA pathway and cancer.* Cancer science, 2010. **101**(11): p. 2309-2315.
561. Casanova-Salas, I., et al., *miRNAs as biomarkers in prostate cancer.* Clinical and Translational Oncology, 2012. **14**(11): p. 803-811.
562. Casanova-Salas, I., et al., *Identification of miR-187 and miR-182 as biomarkers of early diagnosis and prognosis in patients with prostate cancer treated with radical prostatectomy.* The Journal of urology, 2014. **192**(1): p. 252-259.
563. Singh, S., et al., *Acetaldehyde and retinaldehyde-metabolizing enzymes in colon and pancreatic cancers*, in *Biological Basis of Alcohol-Induced Cancer*. 2015, Springer. p. 281-294.
564. Xiong, Z. and P.W.J.N.a.r. Laird, *COBRA: a sensitive and quantitative DNA methylation assay.* 1997. **25**(12): p. 2532-2534.
565. Bartrons, R., J.J.J.o.b. Caro, and biomembranes, *Hypoxia, glucose metabolism and the Warburg's effect.* 2007. **39**(3): p. 223-229.
566. Rademakers, S.E., et al., *Molecular aspects of tumour hypoxia.* Molecular oncology, 2008. **2**(1): p. 41-53.
567. Das, A.B., P. Loying, and B. Bose, *Human recombinant Cripto-1 increases doubling time and reduces proliferation of HeLa cells independent of pro-proliferation pathways.* Cancer letters, 2012. **318**(2): p. 189-198.
568. Russo, J., et al., *Identification of 4-(N, N-dipropylamino) benzaldehyde as a potent, reversible inhibitor of mouse and human class I aldehyde dehydrogenase.* Biochemical pharmacology, 1995. **50**(3): p. 399-406.
569. Balber, A.E., *Concise review: aldehyde dehydrogenase bright stem and progenitor cell populations from normal tissues: characteristics, activities, and emerging uses in regenerative medicine.* Stem Cells, 2011. **29**(4): p. 570-575.
570. Luo, M., et al., *Diethylaminobenzaldehyde is a covalent, irreversible inactivator of ALDH7A1.* ACS chemical biology, 2015. **10**(3): p. 693-697.

# Appendices

## Appendix I

| Sample name | Cell type | Code | Date | Diagnosis | Operation | Patient Age | PSA |
|---|---|---|---|---|---|---|---|
| PEY006/09 p3 | WP | 1 | 24/3/10 | BPH | TURP | - | - |
| PEY011/09 p2 | WP | 2 | 24/3/10 | Ca 3+5 on hormones | TURP | - | - |
| PEY012/09 p4 | WP | 3 | 24/3/10 | BPH | TURP | - | - |
| PEY013/09 p1 | WP | 4 | 24/3/10 | BPH | TURP | - | - |
| PEY021/09 p1 | WP | 5 | 24/3/10 | Ca 4+4 on hormones | TURP | - | - |
| PEY030/09 | WP | 8 | 24/3/10 | BPH | TURP | - | - |
| PEY047/09 | WP | 9 | 24/3/10 | BPH | TURP | - | - |
| PEY029/09 | WP | 10 | 24/3/10 | BPH | TURP | - | - |
| PEY025-26/09 | WP | 11 | 24/3/10 | BPH | TURP | - | - |
| PEY046/09 | WP | 12 | 24/3/10 | BPH | TURP | - | - |
| PE434 p10 | WP | A | 3/6/09 | Gl8/9 cancer | RP | 59 | - |
| PE569 p5 | WP | B | 3/6/09 | Gl8 (3+5) cancer | RP | 67 | - |
| PE665 p4 | WP | C | 3/6/09 | Gl7 (3+4) cancer | RP | 53 | - |
| PE665 p7 | WP | D | 3/6/09 | Gl7 (3+4) cancer | RP | 53 | - |
| PE671 p3 | WP | E | 3/6/09 | Gl7 (3+4) cancer | RP | 62 | - |
| PEH016/09 p4 | WP | F | 3/6/09 | Gl7 cancer | RP | - | - |
| PEY023/09 p1 | WP | G | 20/5/09 | BPH | TURP | 88 | - |
| PEY008/06 p1 | WP | H | 3/6/09 | 3+3 cancer | TURP | 65 | - |

**WP = whole population**

## Appendix II

| Sample name | Cell type | Code | Date | Diagnosis | Operation | Patient Age |
|---|---|---|---|---|---|---|
| PEH030/10 p2 | CB | 13 | 22/7/10 | Normal | Cystectomy | - |
| PEH030/10 p2 | TA | 14 | 22/7/10 | Normal | Cystectomy | - |
| PEH030/10 p2 | SC | 15 | 22/7/10 | Normal | Cystectomy | - |
| PEH030/10 p4 | CB | 16 | 22/7/10 | Normal | Cystectomy | - |
| PEH030/10 p4 | TA | 17 | 22/7/10 | Normal | Cystectomy | - |
| PEY033/10 p1 | CB | 19 | 22/7/10 | BPH | TURP | 84 |
| PEY033/10 p1 | TA | 20 | 22/7/10 | BPH | TURP | 84 |
| H020/09 p5 | CB | 22 | 22/7/10 | Ca 3+4 | RP | - |
| H020/09 p5 | TA | 23 | 22/7/10 | Ca 3+4 | RP | - |

**CB = committed basal cells, TA = transit amplifying cells, SC = stem cells**

## Appendix III

| Sample name | Cell type | Date | Diagnosis | Operation | Patient Age |
|---|---|---|---|---|---|
| PEH030/10 p2 | CB | 20/3/10 | Normal | Cystectomy | 48 |
| PEH030/10 p2 | TA | 20/3/10 | Normal | Cystectomy | 48 |
| PEH030/10 p2 | SC | 20/3/10 | Normal | Cystectomy | 48 |
| PEH030/10 p4 | CB | 20/7/10 | Normal | Cystectomy | 48 |
| PEH030/10 p4 | TA | 20/7/10 | Normal | Cystectomy | 48 |
| PEY033/10 p1 | CB | 20/7/10 | BPH | TURP | 68 |
| PEY033/10 p1 | TA | 20/7/10 | BPH | TURP | 68 |
| PEY033/10 p1 | SC | 20/7/10 | BPH | TURP | 68 |
| H020/09 p5 | CB | 21/7/10 | Gl7 Ca 3+4 | RP | - |
| H020/09 p5 | TA | 21/7/10 | Gl7 Ca 3 + 4 | RP | - |

## Appendix IV

| Sample | Diagnosis | Operation | Patient Age | PSA |
|---|---|---|---|---|
| H398/14 | BPH | TURP | 66 | - |
| H405/14 | BPH | TURP | 82 | 8.7 |
| H415/15 | BPH | TURP | 74 | 0.61 |
| H523 RM | Cancer | RP | 66 | 3.8 |
| H507/14 LM | Cancer Gl7 (3+4) | RP | 68 | 9.9 |
| H507/14 RB | Cancer Gl7 (3+4) | RP | 68 | 9.9 |
| H554 LB | Cancer | RP | 68 | 9.4 |
| H554 RM | Normal | RP | 68 | 9.4 |

**RM = right middle, LM = left middle, RB = right base, LB= left base**

## Appendix V

| Sample | Diagnosis | Operation | Patient Age |
|---|---|---|---|
| YO29/09 | BPH | TURP | 91 |
| YO40/10 | BPH | TURP | 67 |
| YO60/10 | BPH | TURP | 73 |
| YO25/09 | BPH | TURP | 84 |
| 665 | Gl7 (3+4) cancer | RP | 53 |
| H035/11 (RA,RM,LA,LM) | Gl7 (3+4) | RP | - |
| H041/11 (RA, RB, LA, LB) | Gl7 (3+4) | RP | 66 |

**RA = right apex**

**RM= right middle**

**RB = right base**

**LA = left apex**

**LM = left middle**

**LB = left base**

## Appendix VI

| Sample | Diagnosis | Operation | Patient Age | PSA |
|---|---|---|---|---|
| H157/12 Rb | Cancer Gl7 | RP | 69 | 14 |
| H157/12 Lb | Cancer Gl7 | RP | 69 | 14 |
| H158/12 | BPH | TURP | 64 | 0.81 |
| H159/12 | BPH (evidence of PIN) | TURP | - | - |